

Lehrstuhl für Steuerungs- und Regelungstechnik
Technische Universität München

Mobile Robot Locomotion in Human Populated Environments: A Social Situation

Daniel Maximilian Carton

Vollständiger Abdruck der von der Fakultät für Elektrotechnik und Informationstechnik
der Technischen Universität München zur Erlangung des akademischen Grades eines

Doktor-Ingenieurs (Dr.-Ing.)

genehmigten Dissertation.

Vorsitzender: Prof. Dr.-Ing. Gerhard Rigoll

Prüfer der Dissertation:

1. Prof. Dr.-Ing. Dirk Wollherr
2. Prof. Dr.-Ing. Verena Nitsch

Die Dissertation wurde am 19.12.2016 bei der Technischen Universität München eingereicht und durch die Fakultät für Elektrotechnik und Informationstechnik am 18.04.2017 angenommen.

Foreword

This thesis summarizes my research conducted at the Chair of Automatic Control Engineering, LSR, of the Technische Universität München, Germany. I hold many pleasant memories about my time at the LSR, where I found an encouraging working environment among highly talented researchers. Here, I want to express my gratitude to all the people that influenced my work and supported my endeavors.

First of all, I want to thank my adviser Prof. Dr.-Ing. Dirk Wollherr for motivating me to “climb the walls” that I would face. Besides, I want to thank Prof. Dr.-Ing/ Univ. Tokio Martin Buss for creating this extraordinary working environment.

Further I must send special thanks to the secretaries and the technical staff of LSR. Without the support of Larissa Schmid and Mrs. Werner I would not have found my path of virtue. Mr. Jaschik, Mr. Weilbach, Mr. Lowitz and Mr Stöber appertains my respect for their tireless and proficient help in case of any hardware issues. This work is also indebted to the efforts that the sys-admins expended on the IT infrastructure.

I am especially grateful to all my colleagues who made my time at LSR amazingly eventful. The support to tackle any circumstance that live has to offer made this team unique. Still I must particularly thank certain individuals for their tremendous help. Thanks to the team that formed around the IURO project, Chris, Rod, Sheraz, Barbara and Annemarie for the many weeks, evenings and nights that we revolved around our robot. Special thanks to Annemarie for being the initiator of my research path and for helping me out during turbulent times. Thank you Daniel Althoff, Marion Leibold and Sebastian Albrecht for teaching me the path of optimal control. Moreover, I want to thank the people that have significantly contributed to this work and its results: Annemarie Turnwald, Wiktor Olszowy, Dominik Meinzer, Verena Nitsch and Antonia Glaser. Thank you all for your input, your help and your support as well as your proofreading that made this thesis “readable”. Thanks to all the participants of my studies that patiently walked the IURO laboratory up and down. My thesis was also supported and influenced by the excellent work of my students Julian Heuser, Robert Lauer, Simon Schilling, Florian Groß, Damian Mrowca and Manxiu Zhan.

Beyond that, I want to express my immeasurable gratitude to my family for their support, their encouragement and for taking so much weight off of my shoulders that originated from other sources than my research work. Special thanks to my brother for fixing my physiological condition which enabled me to stay focused.

And finally I want to thank my significant other for being so indefinitely patient and loving which eventually enabled me to walk the bumpy road and climb the last wall.

Wolfersdorf, August 2016

Daniel Carton

In deep memory of my beloved mother.

Contents

1	Introduction	1
1.1	Challenges and Goals	3
1.2	Contributions and Outline	6
2	Mobile Robot Locomotion in a Social Context	9
2.1	Optimal Control based Trajectory Planning for Robot-to-Human Approach	9
2.1.1	Classification within the State-of-the-Art	13
2.1.1.1	Mobile Robot Path Planning	13
2.1.1.2	Socio-Contextual Aspects in Motion Planning	13
2.1.1.3	Robot-to-Human Approach Methods	15
2.1.2	Problem Description	16
2.1.2.1	Optimal Control Framework	16
2.1.2.2	Integrating Social Context in Trajectory Planning	18
2.1.3	Methodology for Readable and Socially Compliant Robot-to-Human Approach	19
2.1.3.1	Socio-Contextual Constraints	20
2.1.3.2	On-line Implementation for Dynamic Environments	22
2.1.3.3	Robot Trajectories and Control for the Experimental Evaluation	25
2.1.4	Experimental Evaluation	26
2.1.4.1	Pilot-Study on Robot-to-Human Approach of a Standing Person	27
2.1.4.2	Comparative Robot-to-Human Approach Study with a First-Person View	28
2.1.4.3	Comparative Robot-to-Human Approach Study with a Third-Person View	30
2.1.5	Results	32
2.1.5.1	Pilot-Study on Robot-to-Human Approach of a Standing Person	32
2.1.5.2	Comparative Robot-to-Human Approach Study with a First-Person View	34
2.1.5.3	Comparative Robot-to-Human Approach Study with a Third-Person View	37
2.1.6	Discussion	40
2.2	Effectiveness of Human-Like Locomotion in Cooperative Navigation	42
2.2.1	Classification within the State-of-the-Art	44
2.2.1.1	Human-Human Interaction during Locomotion	44
2.2.1.2	Human-Robot Interaction during Locomotion	45

2.2.2	Problem Description	46
2.2.2.1	Cognitive Theories of Human Locomotion	46
2.2.2.2	Control Theoretic Locomotion Model	48
2.2.2.3	Correlations to Human-Robot-Interaction	51
2.2.3	Experiments on Human-Human and Human-Robot Avoidance	52
2.2.3.1	Transfer of Human-Human to Human-Robot Interaction	53
2.2.3.2	Experiment Setup	54
2.2.3.3	Experimental Method	55
2.2.3.4	Experiment Procedure	56
2.2.3.5	Intruder Concept	56
2.2.4	Results	58
2.2.4.1	Human-Human Avoidance	58
2.2.4.2	Human-Robot Avoidance	61
2.2.4.3	Human-Human and Human-Robot Avoidance Comparison	65
2.2.5	Discussion	66
2.3	Summary	67
2.4	Conclusions	68
3	Towards Behavioral and Dynamic Models for Trajectory Prediction	70
3.1	Human Behaviors for Locomotion Prediction	70
3.1.1	Classification within the State-of-the-Art	73
3.1.1.1	Motion Prediction	74
3.1.1.2	Optimal Control based Prediction	74
3.1.1.3	Behavioral Models for Human Locomotion	75
3.1.1.4	Cognitive Models for Human Locomotion	76
3.1.2	Problem Description	77
3.1.2.1	Cognitive Architecture for Human Locomotion	77
3.1.2.2	Non-linear Model Predictive Control based Locomotion Prediction	79
3.1.2.3	Planning Horizon in NMPC Locomotion Prediction	81
3.1.3	Experimental Exploration of the Human Planning Horizon	84
3.1.3.1	Experiment Design	84
3.1.3.2	Measuring Parameters of the Planning Horizon	85
3.1.3.3	Triggering Adaptations of the Planning Horizon	85
3.1.3.4	Setup of a Virtual Environment	86
3.1.3.5	Pilot-Study for Parameter Definition	88
3.1.3.6	Hardware Setup	89
3.1.3.7	Participants	90
3.1.3.8	Experimental Procedure	90
3.1.4	Main Experiment Results	90
3.1.4.1	Qualitative Data Evaluation	90
3.1.4.2	Statistical Data Evaluation	98
3.1.5	Discussion	104
3.2	Dynamic Model for Human Velocity Prediction	106
3.2.1	Classification within the State-of-the-Art	107

3.2.2	Problem Description	108
3.2.2.1	Periodicity in Human Locomotion Velocity	109
3.2.2.2	Inverse Optimal Control for Parameter Estimation	110
3.2.3	Dynamic Model for Human-Like Velocity Profiles	112
3.2.4	Simulation Results	116
3.2.5	Discussion	118
3.3	Summary	119
3.4	Conclusions	120
4	Human Trajectory Data Analysis for Identifying Situational Behaviors	121
4.1	Introduction	122
4.2	Classification within the State-of-the-Art	124
4.3	Problem Description	125
4.4	Methodology for Trajectory Data Analysis	126
4.4.1	Trajectory Smoothing	127
4.4.2	Analysis of Trajectory Sets	130
4.4.2.1	Confidence Intervals for Trajectory Data	131
4.4.2.2	Pivot Analysis for Path Data	132
4.4.2.3	Gaussian Processes for Path Data	134
4.4.2.4	Autoregressive Moving Average Model for Path Data	136
4.5	Simulation Results	137
4.5.1	Spline based Analysis Framework	138
4.5.2	Gaussian Process based Method	140
4.5.3	Autoregressive Moving-Average Model based Method	140
4.6	Discussion	146
4.7	Summary	147
4.8	Conclusions	147
5	Summary	149
6	Conclusions	151
	Bibliography	154

Notations

Abbreviations

2-dimensional	2d
3-dimensional	3d
ACE	Autonomous City Explorer
ARMA	Autoregressive Moving-Average
ARMAX	Autoregressive Moving-Average with Exogenous Input
ANOVA	Analysis of Variance
CI	Confidence Interval
COM	Center-of-Mass
GCV	Generalized cross validation
GP	Gaussian Process
GPML	Gaussian Processes for Machine Learning framework
HRI	Human Robot Interaction
IOC	Inverse Optimal Control
IURO	Interactive Urban Robot
IQR	Inter-Quartile Range
KLD	Kulback-Leibler Divergence
MPC	Model Predictive Control
NMPC	Nonlinear Model Predictive Control
OC	Optimal Control
Pivot	Statistically independent population used for comparison
PTPRS	Penalized Thin-Plate Regression Spline
interferer	An informed agent in an experiment that disturbs the moving subject
intruder	An informed agent in an experiment that disturbs the moving subject
DTW	Dynamic Time Warping
PPF	Pixel-Per-Frame progress of a virtual object
FPS	Frames Per Second
DeKiFeD	Desktop Kinesthetic Feedback Device
DoF	Degree of Freedom
SD	Standard deviation
Hz	Hertz
p	p-value

Conventions

Scalars, Vectors, and Matrices

Scalars are denoted by lower case letters in italic type. *Vectors* are denoted by boldface lower case letters in italic type, as the vector \mathbf{u} is composed of elements u_i . *Matrices* are denoted by upper case letters in italic type, as the matrix M is composed of elements M_{ij} (i^{th} row, j^{th} column).

u_1	Scalar
\mathbf{u}	Vector
U	Matrix
U^T	Transpose of \underline{X}
U^{-1}	Inverse of \underline{X}
\dot{x}	First derivative
\ddot{x}	Second derivative
$f(\cdot)$	Scalar function
$L(\cdot)$	Length of a path
\bar{x}	Arithmetic mean of x
\tilde{x}	Mean representation of x

Symbols

General

Φ	Set of 2d rotations
\mathcal{S}^1	Manifold defined from set of 2d rotations
$\mathbf{SE}(2)$	Special Euclidean group
$\mathbf{SO}(2)$	Special Orthogonal group of 2d rotations
\mathcal{W}	Configuration space for 2d motions
\mathbf{u}	Input vector of the OC problem
\mathbf{x}	State vector of the OC problem
$\bar{\mathbf{u}}$	Open-loop input vector in the NMPC problem
$\bar{\mathbf{x}}$	Predicted state in the NMPC problem
$\bar{\mathbf{u}}_i$	Predicted state in the finite dimensional NMPC problem
\mathbf{u}^*	Optimal input vector of the OC problem
$\bar{\mathbf{u}}^*$	Optimal input vector of the NMPC problem
\mathcal{U}	Admissible set of controls
\mathcal{X}	Admissible set of states
\mathbf{u}_{\min}	Minimum for controls in admissible set
\mathbf{u}_{\max}	Maximum for controls in admissible set
\mathbf{x}_{\min}	Minimum for states in admissible set
\mathbf{x}_{\max}	Maximum for states in admissible set
$J(\cdot)$	Objective or Cost function for OC or NMPC Problem

$\phi(\cdot)$	Runtime cost
$\vartheta(\cdot)$	Terminal cost
θ_i	Weights of the cost functionals
$f(\mathbf{x}(t), \mathbf{u}(t), t)$	Dynamic model
$g(\cdot)$	Equality constraints
$h(\cdot)$	Inequality constraints
$b(\cdot)$	Boundary values
T_P	Prediction horizon in NMPC
T_C	Control horizon in NMPC
δ	Time-step in NMPC
p^x	Position in x-dimension
p^y	Position in y-dimension
p_R^x	Robot position in x-dimension
p_H^x	Human position in x-dimension
p_R^y	Robot position in y-dimension
p_H^y	Human position in y-dimension
\mathbf{p}	Pose in 2d space
\mathbf{p}_R	Robot pose in 2d space
\mathbf{p}_H	Human pose in 2d space
\mathbf{p}_S	Starting pose in 2d space
\mathbf{p}_G	Goal pose in 2d space
φ	Orientation in 2d space
ω	Rotational velocity
a^ω	Rotational acceleration
φ_R	Robot orientation in 2d space
φ_H	Human orientation in 2d space
v	Velocity in 2d space
a^v	Acceleration in 2d space
\mathcal{C}	Experimental conditions
H_0	Null Hypothesis
$H_{0,X}$	Null Hypothesis for proposition X
H_1	Alternative Hypothesis
$H_{1,X}$	Alternative Hypothesis for proposition X
ξ	Trajectory
ξ^t	2d discrete planar trajectory with time information
ξ^{xy}	Geometric data of a 2d discrete planar trajectory
$\xi_{n,C}^t$	2d discrete planar trajectory from a distinct condition
$\xi_{n,C}^{xy}$	Geometric data of a trajectory from a distinct condition
$\xi_{n,C}^v$	Velocity data of a trajectory from a distinct condition
$\bar{\xi}$	Arithmetic mean of a trajectory
$\tilde{\xi}$	Mean representation of a trajectory
Ξ	Set of trajectories
Ξ^t	Set of 2d discrete planar trajectories with time information
Ξ^{xy}	Geometric data from a set of trajectories

Ξ_C^t	Set of trajectories from a distinct condition
Ξ_C^{xy}	Geometric data of a trajectory set from a distinct condition
Ξ_C^v	Velocity data of a trajectory set from a distinct condition
t	Continuous time
$t(k)$	Discretized time
τ	Time variable for integration in NMPC problem
T	A certain time period
n	Index for the number of subjects
N	Number of Subjects
k	Discretized time index
K	Maximum for discrete time index
m	Discretization index
M	Maximum for discretization index
z	Model input
q	Model output

Sec. 2.1 Optimal Control based Trajectory Planning for Robot-to-Human Approach

v_R	Velocity of the robot
\bar{v}_R	Average velocity of the robot along the trajectory
v_H	Velocity of the human
$B(\lambda)$	Bézier curve
λ	Bézier curve parameter
$\mathbf{b}_{0,1,2,3,4}$	Control point of a Bézier curve
$\mathbf{e}_{\text{left,right}}$	Sensed edge of an obstacle
$\eta_{1,2}$	Weights for the deformation of a Bézier curve
κ	Curvature of a trajectory
κ_{\min}	Minimum curvature of a trajectory
κ_{\max}	Maximum curvature of a trajectory
v_d	Desired velocity for a robot
$v_{R,\min}$	Minimum robot velocity
$v_{R,\max}$	Maximum robot velocity
ω_{\min}	Minimum rotational velocity
ω_{\max}	Maximum rotational velocity
\mathcal{E}	Expectation of a human with respect to his observations
\mathcal{G}	Set of reachable goals in 2d space
G	Observed or expected goal pose in 2d space
S	Observed starting pose in 2d space
R	Observed or expected current pose in 2d space
\mathcal{R}	Readability
\mathcal{S}	Social Acceptance
d_{RH}	Distance to a human where the robot starts decelerating
$d_{RH,\min}$	Minimum approach distance between robot and human
α	Angle between human and robot orientation
R_α	2d Rotation by α

r_{safe}	Safety radius around discrete position on trajectory
t_{enter}	Time the robot enters the safety radius of a position
t_{leave}	Time the robot leaves the safety radius of a position
$\mathbf{p}_R(\text{col})$	Position for the robot where a collision is possible
$\mathbf{p}_R(\text{end})$	Position for the robot where the collision zone ends

Sec. 2.2 Effectiveness of Human-Like Locomotion in Collaborative Navigation

$d_{\Xi}(\cdot, \cdot)$	Distance measured between two trajectory sets
p_{Ξ}	p-value for the comparison of trajectory sets
(d_c)	Cohen's d

Sec. 3.1 Human Behaviors for Locomotion Prediction

$Q_{x,\text{LQ}}$	Diagonal weighting matrix for the states in NMPC
$Q_{u,\text{LQ}}$	Diagonal weighting matrix for the controls in NMPC
$r_{x,\text{LQ}}$	Reference vector for the states in NMPC
$r_{u,\text{LQ}}$	Reference vector for the controls in NMPC

Sec. 3.2 Dynamic Model for Human Velocity Prediction

ξ_{measured}	Measured trajectory
ξ_{model}	Synthesized trajectory
ξ_{measured}^v	Measured velocity profile
ξ_{model}^v	Synthesized velocity profile
L_{model}	Total path lengths for measured trajectory
L_{measured}	Total path lengths for synthesized trajectory
$d_{\text{vel}}(\cdot)$	Distance for path data
$d_{\text{pos}}(\cdot)$	Distance for velocity data
$d_{\text{sum}}(\cdot)$	Overall distance
x_{EL}	x-direction of the Ellipse coordinates
z_{EL}	z-direction of the Ellipse coordinates
x_{W}	x-direction of the World coordinates
z_{W}	z-direction of the World coordinates
$x_{\text{el,W}}$	x-position of the ellipse center in World coordinates
$z_{\text{el,W}}$	z-position of the ellipse center in World coordinates
$\dot{x}_{\text{el,W}}$	Ellipse center velocity in x-direction of the World coordinates
$\dot{z}_{\text{el,W}}$	Ellipse center velocity in z-direction of the World coordinates
a_{el}	Width of the ellipse
b_{el}	Length of the ellipse
ρ_{el}	Inner angle of the ellipse
ι_{EL}	x-position on the ellipse border in Ellipse coordinates
κ_{EL}	z-position on the ellipse border in Ellipse coordinates
ι_{W}	x-position on the ellipse border in World coordinates
κ_{W}	z-position on the ellipse border in World coordinates
R_{W}	Position on the ellipse border in World coordinates

\dot{R}_W	Velocity of a point on the ellipse border in World coordinates
ϱ_{el}	Time variant rotation angle of the rolling ellipse
$\dot{\varrho}_{el}$	Rotational velocity of the rolling ellipse
n_{el}	Normal to any point on the ellipse
$E_2(\cdot)$	Elliptical integral of the second kind
L_{el}	Lagrange equation of the second kind
T_{kin}	Kinetic energy of the system
V_{pot}	Potential energy of the system
J_{el}	Inertia of the rolling ellipse
g	Gravity constant
m_{el}	Mass of the ellipse
Q_{el}	Generalized forces in world coordinates

Chap. 4 Human Trajectory Data Analysis for Identifying Situational Behaviors

\mathcal{D}_Ξ	Distribution of distances
λ_{PTPRS}	Penalization term for the penalized thin-plate spline
w	Index for the control points
W	Maximum index for the control points
ω_w	Control points for a penalized thin-plate regression spline
\mathcal{W}	Set of control points
γ_w	Regression coefficients
f_r	Radial basis kernel
E_{PTPRS}	Energy function
α_{PTPRS}	Significance level
$(\bar{\mu}_1, \bar{\mu}_2)$	Sample means of two populations
(s_1^2, s_2^2)	Estimated variances of two populations
\mathbf{z}_{GP}	Input for a Gaussian Process
\mathbf{q}_{GP}	Output for a Gaussian Process
\mathbf{z}_*	Evaluated input points in a Gaussian Process
$f_{GP}(\mathbf{z}_{GP})$	Function specified as a discrete vector for a GP
\mathbf{f}_*	Function values for the vector function of a GP
$\mathcal{GP}(m(\mathbf{z}_{GP}), \text{cov}(\mathbf{z}_{GP}, \mathbf{z}_*))$	GP
$m(\cdot)$	Mean function
$\text{cov}(\cdot)$	Covariance function
$\mathbb{E}[\cdot]$	Expectation value
ϵ_{GP}	Additive Gaussian noise
σ_N^2	Variance of the Gaussian noise
$\log p(\mathbf{q}_{GP} \mathbf{z}_{GP})$	Marginal likelihood
s_f^2	Standard deviation in the matern-type covariance function
ell	Hyperparameter of the matern-type covariance function
$\mathcal{N}_0(\mu_0, \Sigma_0)$	Normal distribution with mean and variance
l^{-1}	Lag operator
n_a	Degree of the AR model (number of poles)
n_b	Dimension of the affecting input (number of zeroes)

n_c	Degree of the MA model (number of noise terms)
n_k	Defines the dead time in an ARMAX model
\mathbf{q}_{ar}	Output of an Autoregressive model
$a_{1,\dots,k-n_a}$	Output coefficients of an Autoregressive model
ϵ_{ar}	White noise term of an Autoregressive model
c_{ar}	Constant scalar in an Autoregressive model
$A(l^{-1})$	Autoregressive model in matrix structure
\mathbf{q}_{ma}	Output of a Moving-Average model
$c_{1,\dots,k-n_c}$	Noise coefficients of a Moving-Average model
c_{ma}	Constant scalar in a Moving-Average model
$C(l^{-1})$	Moving-Average model in matrix structure
\mathbf{z}_{arma}	Exogenous inputs for an ARMAX model
\mathbf{q}_{arma}	Output of an ARMAX model
b_{1,\dots,n_b}	Input coefficients of an ARMAX model
$B(l^{-1})$	Matrix structure of the exogenous inputs

Abstract

Seamless integration of mobile robots into human populated environments is a key challenge for robotics. Researchers envision robots to leave specifically tailored environments in order to closely cooperate with humans in shared workspaces. In order to integrate seamlessly in these environments, robots require the ability to interact nonverbally and to perform predictable motions that do not interfere with the actions of nearby humans. Both tasks are achievable by a robot that plans appropriate trajectories. These trajectories must convey the intentions of the robot and concurrently prevent interference with other agents, meaning humans and robots. Clearly, both tasks also require the accurate prediction of human locomotion. These abilities are crucial for the seamless integration of robots in shared environments.

The goal of this work is to approach this robot locomotion problem by integrating human behaviors and other social aspects within trajectory planning and prediction methods. The developed approaches should allow robots to successfully initiate interaction with humans, to minimize disturbances of planned trajectories and to enhance their prediction accuracy. Thereby, social aspects and human behaviors are incorporated in according methods to achieve an improvement in the performance of robot locomotion and prediction.

The methods are generally based on optimal control and model predictive control theory. Within these frameworks, objective functions are proposed that realize the inclusion of social aspects and features of human-like locomotion. Obtained models are evaluated within user studies, where subjects rate the locomotion behavior of the robot or perform collaborative locomotion tasks. In order to derive human behaviors, subjects are also recorded during goal directed locomotion. The trajectory data is then examined to identify distinct situational behaviors, that are applicable in locomotion or prediction models. Therefore, this thesis also provides a framework for trajectory data analysis that allows to compare data from different experimental conditions.

For robot locomotion the externalization of intention by employing features of human-like motion is shown to raise success in nonverbal interaction initiation. Thus, humans feel more addressed and understand more quickly that the robot intends to interact. Clear intentions further diminish disturbances and raise social acceptance for the robot. Apart from positive apperception, human-like robot locomotion is shown to reduce the locomotion planning effort for human agents in a shared workspace. The reason are the more reliable mutual predictions for humans and robots due to clear intentions. Prediction methods are anticipated to benefit from the inclusion of human behaviors within control theoretic models for human locomotion. Understanding the human motion planning process will help to increase prediction accuracy. Thereby, models that accurately reproduce human trajectories further improve the predictions. The developed framework for data analysis integrates data variance into qualitative trajectory comparison. This procedure is complemented by a specifically adjusted hypothesis test, which provides the quantitative analysis. The framework allows for statistically feasible evaluations of the data and thus enables the identification of situational human locomotion behaviors.

Considering social context and human behaviors within robot locomotion, is capable of increasing the acceptance towards robots and their ability to approach, avoid and predict humans. The results presented in this thesis demonstrate that both aspects are beneficial for the seamless integration of robots in human populated environments.

Zusammenfassung

Die Integration von Robotern in eine Umgebung mit Menschen, ist eines der Schlüsselprobleme in der Robotik. Das Ziel ist, dass Roboter nicht nur in speziellen Umgebungen sondern in einem gemeinsamen Arbeitsraum mit Menschen kooperieren. Dies setzt einige grundlegende Fähigkeiten für Roboter voraus. Diese müssen eigenständig Interaktionen initiieren und sich Fortbewegen ohne andere Beteiligte, also Menschen oder Roboter, zu beeinträchtigen. Beides verlangt, dass Roboter entsprechende Trajektorien planen können. Zum einen müssen diese Trajektorien den Roboter in Interaktionsreichweite bringen, zum anderen darf dabei niemand in seiner Fortbewegung gestört werden. Zudem ist es für beide Aufgaben nötig die Bewegungen von Menschen vorherzusagen. Alle drei Fähigkeiten sind erforderlich, damit sich mobile Roboter nahtlos in unsere Umgebung einfügen können.

Zu dieser Problemstellung werden in der vorliegenden Arbeit Lösungsansätze diskutiert, die soziale Aspekte und menschliche Verhaltensweisen in die Fortbewegung des Roboters und in Prädiktionsverfahren integrieren. Die entwickelten Methoden sollen es Robotern erlauben sich Menschen für Interaktionen zu nähern, Störungen für andere zu vermeiden und die Prädiktionsgenauigkeit verbessern. Die berücksichtigten sozialen Aspekte und menschlichen Verhaltensweisen tragen dabei zur Verbesserung dieser Fähigkeiten bei.

Hier entwickelte Methoden bauen grundsätzlich auf der Theorie von Optimalsteuerung oder Modell-Prädiktiver Regelung auf. In diesem Rahmen werden Kostenfunktionen konstruiert, die soziale Aspekte und Eigenheiten menschlicher Fortbewegung berücksichtigen. Diese Modelle werden anschließend in großen Probandenstudien evaluiert, wobei sich die Versuchspersonen mit dem Roboter in einem Raum bewegen und dessen Verhalten bewerten. Die Bewegungen von Probanden werden zudem aufgezeichnet, um Modelle menschenähnlicher Fortbewegung zu entwickeln. Die Trajektorien werden anschließend untersucht, um situationsbedingte Verhaltensweisen festzustellen, die in Fortbewegungs- oder Prädiktionsmodellen Verwendung finden. Daher wird in der vorliegenden Arbeit auch ein Prozess zur Analyse von Bewegungsdaten entwickelt, der es erlaubt die Daten verschiedener experimenteller Szenarien statistisch zu vergleichen. Die entwickelte qualitative Analyse von Bewegungsdaten bezieht speziell die Varianz der Daten mit ein. Dieses Verfahren wird durch einen Hypothesentest zur quantitativen Analyse vervollständigt.

Menschenähnliche nonverbale Übermittlung von Intentionen durch einen Roboter erhöht dessen Erfolg Interaktionen zu initiieren, da Menschen dessen Bestreben schneller verstehen. Zudem verhindern klare Intentionen eine gegenseitige Beeinträchtigung bei der Fortbewegung und erhöhen die soziale Akzeptanz. Neben der positiveren Wahrnehmung verringert die menschenähnliche Fortbewegung den Planungsaufwand für Andere in der Umgebung. Der Grund dafür ist eine erhöhte Zuverlässigkeit gegenseitiger Vorhersagen. Die Berücksichtigung menschlicher Verhaltensweisen innerhalb von Regelungstechnischen Modellen wird zudem einen großen Nutzen für Methoden zur Bewegungsvorhersage haben. Dazu müssen der Prozess menschlicher Bewegungsplanung genauer untersucht und detaillierte Modelle des menschliche Bewegungsapparats herangezogen werden.

Werden sozialer Kontext und menschliches Verhalten bei der Fortbewegung von Robotern berücksichtigt, verbessert sich ihre Akzeptanz, ihre Fähigkeit sich Menschen zu nähern, ihnen auszuweichen und ihre Bewegungen vorherzusagen. Beide Aspekte sind demnach grundlegend bei der Integration von Robotern in von Menschen genutzte Umgebungen.

1 Introduction

A long term vision in robotics is the realization of intelligent and highly autonomous robots that seamlessly cooperate and interact with humans in shared environments. First steps are made towards this vision as for example autonomous robots have left the constricted industrial settings and are available for consumers to take on simple household tasks. Yet, adaptivity, intelligence, and interaction capabilities are still too limited to allow for the envisioned seamless cooperation. Besides, the currently tackled tasks are solvable by a single independent system, which excludes the need for abilities to interact or cooperate with humans. Hence, a future step in robotics research must be the integration of intuitive interaction and cooperation capabilities.

Cooperation and interaction are diverse terms that cover a large variety of actions and tasks. Thereby, cooperation means the joint solving of tasks by pro-actively utilizing the individual capabilities. Covered tasks are for example: joint manipulation, physical or haptic contact, and action in shared workspaces in general [113, 119]. In addition, the concept of cooperative navigation was recently introduced, which attempts to model the effects of mutual reactions during locomotion [176]. Strongly connected to cooperation are interaction abilities [73]. Yet, interaction also occurs between agents that do not work on a common task. As soon as an environment is shared, interaction comes into play as a subconscious process for information exchange. It facilitates direct communication or tasks like seamless cooperative navigation. Interaction occurs on many different levels such as physically, through haptic coupling, verbally in conversations and nonverbally during cooperative manipulation or locomotion in shared environments. Cooperation is often facilitated by nonverbal interaction because intentions are conveyed more clearly and allow for more reliable mutual predictions. In fact, the externalization of intentions is shown to increase the effectiveness of collaborative task execution [31, 51, 170].

This thesis is concerned with the interrelation of nonverbal interaction and cooperative navigation in a social context. Especially socially acceptable locomotion in shared spaces and the integration of mutual expectations and reactions is in the focus. For instance, two humans do not need to negotiate verbally in order to avoid collisions during locomotion. This ability of nonverbal intention conveyance would be required by robots to perform equally in such cooperative tasks. A wide research field is developed around the goal to find according factors that facilitate the seamless integration of robots into shared environments. This work pursues this ambition and concentrates on factors that are elicited in social contexts during locomotion. Apart from nonverbal interaction, it is thus examined how cooperative navigation benefits from social acceptance of humans towards robots [147]. In fact, with the acceptance the perceived safety and comfort are raised, which positively affects cooperation [110].

The aspired cooperative locomotion through nonverbal interaction and the seamless integration of robots into shared environments pose important aspects in many envisioned

applications. For example, recent ambitions push the development of parcel services or automated e-commerce warehouses which employ mobile robots. Although these are reasonable applications for currently available mobile robots, a large variety of problems must still be overcome especially with respect to human-robot interaction. For moving seamlessly through a shared environment a mobile robot needs to be cooperative, interactive, compliant with the social context and able to predict human motions. In general, pedestrians or workers should not be disturbed or confused by the actions of the robot. Therefore, the robot must move in a way that humans understand the purpose and intention behind the motions and can easily predict where the robot is going. The robot itself has to be capable of predicting the human in order to adapt its own motion accordingly. From the goal of seamless cooperative robot locomotion in dynamic environments, the research objectives of this thesis are derived: the incorporation of social context into trajectory synthesis, human-like locomotion that enables robots to interact nonverbally and the enhancement of human locomotion prediction based on behavioral models.

The elaborated factors and developed models of this thesis are used to enhance existing optimal control or model predictive control approaches, which only implicitly consider the influence of social context. For a robot to appear sociable and aware of social context, it must follow sociological models that define human interaction on a nonverbal level. Optimal control or model predictive control yield frameworks for trajectory planning and prediction, where the investigated social aspects and human behaviors are realizable as objective functions and constraints. The investigation of applicable factors requires the analysis of trajectory data from human subjects. Thus, new analysis methods are developed here and existing approaches are modified in order to obtain reliable tools.

This thesis addresses the three areas sketched above as follows. For robot locomotion an optimal control framework is outlined that aims to plan intuitively comprehensible and socially acceptable trajectories. Specific objective functionals and constraints are proposed and evaluated to enhance these factors. The experimental setup analyses the performance of a mobile robot in nonverbal interaction initiation with respect to the proposed trajectory features. In the experiments the method is applied for robot-to-human approaches. Subject ratings lead to conclusions about the effectiveness of the proposed human-like trajectories for approaching standing and walking persons.

The overall benefit of social compliance and human-like robot locomotion is investigated in a second user study. Based on a control theoretic definition of effort for human locomotion, a user study shows that humans react similar to humans and robots. Results confirm that humans even expect a non-human-like robot to behave human-like. A comparison of human-human and human-robot avoidance behaviors indicates that planning effort for users diminishes if robots comply with this expectation.

The essential ability for mobile robots to predict the movements of dynamic obstacles is also considered with respect to social behaviors. Derived from literature a modeling problem is found where the human behavior during obstacle avoidance is not reproducible with the considered optimal control approaches. As model predictive control appears to find more reliable solutions, this particularity is approached in an extensive experiment. The focus is set on the investigation of the human planning horizon which is assumed to change in complex environments. Results point towards a specific human behavior,

where the planning horizon is reduced to consider only the most immediate obstacle, while deviations from the initial global optimum occur. The integration of these behaviors into prediction algorithms is assumed as beneficial for their accuracy.

For further enhancement of model based human locomotion prediction, a new dynamic model is proposed in this thesis. It tackles a common problem with the modeling of human velocity profiles. Current approaches consider trapezoidal shapes as typical for human velocity profiles. However, this is only an approximation, which is achieved by heavily smoothing recorded data. Measurements actually show a sinusoidal shape, which originates from the pendulum like gait of human beings. The progress made towards a solution for this problem is described in this work.

Developments in the area of human-like trajectory planning and prediction require the analysis and evaluation of recorded trajectory data. When social aspects and human behaviors are investigated the statements must be justified by statistically feasible analyses. Therefore, methods for trajectory data analysis are proposed and evaluated. A pre-processing and a qualitative analysis is supported by a spline based modeling of human locomotion data. Confidence intervals for the mean of the data-set are derived and allow for a statistically feasible qualitative comparison. For quantitative results a comparative analysis is described that examines the distinction of observed similarities or differences. The performance of both approaches is compared to adapted state-of-the-art methods in order to show the advantages and disadvantages of a statistics based method.

In summary, the main contributions discussed in the following are nonverbal interaction initiation with socio-contextual constraints and human-like robot locomotion, the exploration of the benefits of socially motivated locomotion in shared environments, the investigation of the human planning horizon, a new dynamic model for human locomotion prediction and methods for the analysis of recorded human locomotion data. The results of this thesis are expected to contribute to the advancement of seamless human-robot cooperation within future robotic applications.

1.1 Challenges and Goals

The raised topics of robot locomotion in a social context, human locomotion prediction and trajectory data analysis involve many open research questions. This section outlines current challenges within these areas and points out problems that are addressed by the methods proposed in this thesis.

Robot Locomotion in a Social Context Robot locomotion is a widely developed field but still poses a large variety of challenges. Especially human populated environments are still problematic for most algorithms. On the one hand, many situations can lead to the 'freezing robot' problem [174]. On the other hand, a variety of situations with a distinct social context and according requirements emerge when sharing an environment with humans. Both challenges are tackled in literature by the incorporation of human behaviors and models in navigation approaches. The problem of the 'freezing robot' is addressed by approaches for collaborative navigation [174, 176]. Within this concept a mobile robot should consider that a human being also yields in order to find a free path

in a crowded environment. Similar assumptions hold for collision avoidance, where approaches like the social forces model [77] allow the estimation of a path even in densely packed situations. A fundamental assumption amongst all these models is that each agent behaves equally during locomotion and therefore has equal expectations of all other agents regarding their locomotion behavior [176]. This supposition is necessary to enable mutual prediction because agents use equal means to externalize their intention during locomotion [71]. Transferred to mobile robots, however, this assumption does often not apply as they do not necessarily look and behave human-like. Moreover, it is not clear whether humans really expect robots to act accordingly. This question is generalizable to robots in arbitrary socio-contextual situations in human environments. For example side-by-side walking, waiting in a line, mutual avoidance, approaching of a person for interaction initiation and in general the navigation in shared environments, all require specific behaviors to comply with the expectations of the surrounding social situation [92]. Enabling robots to comply with these expectations and to integrate seamlessly in shared environments therefore involves many challenges. Planned robot trajectories must integrate according social aspects to comply with a specific social context. For a seamless integration the trajectories must be predictable for human agents and clearly display the intention of the moving robot. Important norms, expectations, behaviors, and other particularities need to be identified at first in complex studies with humans and then applied to robots. The importance of finding these parameters lies within the fact that a trajectory is then more capable of externalizing intention on a nonverbal level [49]. Given that appropriate aspects are found, trajectories may be planned that resemble a solution space where intention conveyance and acceptance are maximized [7, 92]. Besides, social acceptance raises perceived safety towards the robot which further enhances its interaction initiation capabilities [110].

This work proposes solutions for the named challenges. Human-like features like smooth velocity profiles, smooth path shape or torso orientation are features of trajectories which affect the named aspects and are thus proposed and evaluated in this work. The mentioned trajectory features are investigated in their effectiveness to externalize the purpose of a motion and raise social acceptance. According parameters and behaviors are integrated into an optimal control based motion planning framework by means of objective functions and constraints. A methodology and experimental results are described, that generalize to non-human-like robots and other platforms. Notably, the results indicate major differences to the field of manipulator motions which is extensively explored in literature [49–51, 192].

Prediction of Human Locomotion Trajectories An essential information for robot locomotion planning is the future position of all agents within the environment. Only this allows for planning of collision free and efficient trajectories. The choice of appropriate social behaviors for a robot also depends on this information. For example, a robot that yields appropriately or approaches a walking person requires an estimate of the future position and speed of its counterpart. The challenge in locomotion prediction is the necessary accuracy of this estimate. For highly efficient navigation and especially for tasks like robot-to-human approaches, high accuracy is crucial. Learning based approaches and filters, which are widely used for tracking and prediction, give a distribution over possible positions which is then accounted for in navigation algorithms. Since an exact trajectory

of a human is desired for prediction, optimal control methods are in the focus of this thesis [14, 18, 121]. In comparison to approaches from Machine Learning, optimal control based methods entail distinct challenges that need to be addressed. The main focus is still accuracy and generalizability to arbitrary environments and situations. Current approaches do not cover larger deviations from the modeled behavior. Therefore, a goal is to identify weaknesses in these approaches and propose new objective functions or constraints to account for them. Accordingly, data acquisition and the identification of related behaviors is necessary. In addition, the underlying dynamic models that are applied for modeling humans offer room for improvements. Many recent methods rely on the unicycle model, which imposes many simplifications regarding human locomotion [14, 18, 121].

In this thesis specific accuracy problems of optimal control based locomotion prediction approaches are determined. First methods and evaluation results are provided as basic solutions towards these problems. Thus, the cognitive process of human locomotion planning and an enhancement of the unicycle model are investigated. From literature only indications towards the investigated behavior and model could be acquired [13, 71, 94, 169].

Analysis of Locomotion Data Identification of behaviors is currently mostly based on plotting the data and interpreting observable particularities. Qualitative evaluation can be subjective and affected by pre-processing. Simple geometric averaging does thereby not represent trajectory data well and is sensitive to noise and outliers. Literature, however, does not supply an appropriate set of methods for evaluating trajectory data. In fact, to progress with the aforementioned challenges, analyzing this data is essential.

Human locomotion data is typically recorded within motion capture systems. From pre-processing the noisy 2d or 3d trajectories, position and velocity data is obtained. A typical problem that is encountered is the application of appropriate smoothing algorithms which is briefly discussed in this thesis. Another critical trait of this data is the missing alignment. Recordings often comprise data from various subjects in different experimental scenarios. Therefore, each trajectory is of different length and a common alignment is usually not possible. Apart from the particular problems regarding the raw data, differences within individual trajectories complicate the identification of common behaviors. Evaluating a set of trajectories obtained from varying persons which is expected to follow a distinct behavior is thus a complex problem. Hence, in trajectory analysis the preprocessing of data and the evaluation of observed particularities pose challenges when a generalizable method is desired. Distance measures such as Dynamic Time Warping or Hausdorff [32, 195] only yield a scalar value with no descriptive meaning. A comparison to a common baseline is necessary whereas distance values are still ambiguous. The occurrence of a specific observation must be statistically feasible since particularities may originate from experimental characteristics instead of human behavior.

Due to the shortcoming of applicable methodologies in literature, a representation for human locomotion data is presented in this work. It allows for smoothing, mean calculation and poses a basis for qualitative as well as quantitative evaluation methods. State-of-the-art methodologies from other areas are adapted for a comparison and to evaluate the reliability of the developed approach.

1.2 Contributions and Outline

This thesis makes several contributions to the state-of-the-art in the areas: socio-contextual aspects for robot locomotion, behavioral and dynamical models for human locomotion prediction and methods for trajectory analysis and behavior identification. These three areas also delineate the structure of this work.

Socio-Contextual Constraints for Robot Locomotion After the introduction in Chap. 1 the advances in optimal control based locomotion planning under socio-contextual aspects are presented in Chap. 2. The main sections 2.1 and 2.2 discuss two aspects of the problem and propose various applications.

Within the first Sec. 2.1 the contributions towards optimal control based robot locomotion planning are depicted. It analyzes formative features of trajectories that support the capability of mobile robots to initiate interaction by conveying their intentions nonverbally during locomotion. Furthermore, the effect of socio-contextual aspects on human comfort and social acceptance of the robot is examined. Initiating interactions on a nonverbal level and the compliance with social context are necessary skills for robots that should seamlessly integrate in shared environments. Related literature covers similar observations for manipulator motions [49, 50], but neglects the differences to locomotion. The proposed trajectory features and social aspects are evaluated and applied in a robot-to-human approach scenario with standing and moving persons, which has large implications on human-robot collaboration. It is shown how readable locomotion that considers socio-contextual aspects enables a robot to comply with human expectations and serves as a basis for cooperative navigation in shared environments. The trajectory features, that are derived from human locomotion, significantly improve nonverbal interaction capabilities of robots and thereby support the predictions of nearby agents. The presented results generalize to a large variety of applications where human-robot interaction during locomotion is required.

The subsequent Sec. 2.2 continues the topic of locomotion within a social context. Here, the benefits of robot locomotion which is compliant with human expectations are addressed. The reason for this analysis is that social aspects in locomotion are mostly considered to affect the positive perception of robots, e.g. acceptance and perceived safety. Yet, it is shown in this thesis how the readability of the robot reduces the motion planning effort for a nearby human being. Two extensive studies are set up for this purpose where human-human and human-robot collision avoidance behaviors are examined. The comparison of experiment conditions and the comparison of the results of both studies confirm that humans actually expect a non-human-like robot to behave human-like. The compliance with expectations therein allows the human subject to resolve a collision situation with low effort. Effort is defined as the energy expenditure on controls when correcting path and velocity, which is derived from the assumption that humans can be considered as optimal control systems. The definition of distinct benefits of comprehensible motion has only been investigated for arm motions in [51]. Thus, this contribution gives an answer to the question whether the integration of social norms, human-like behaviors and the consideration of intention conveyance are useful in future robotic systems.

Behavioral and Dynamic Models for Human Locomotion Prediction In Chap. 3 the prediction of human locomotion is accounted for. Prediction is an essential requirement for robot locomotion as it allows for collision avoidance and it is also important for social compliance since appropriate reactions require a robot to understand its environment. A large variety of algorithms is used for motion prediction spanning from machine learning to control approaches [55, 56, 154, 193]. This thesis focuses on optimal control approaches for prediction as they yield continuous trajectories. As prediction accuracy depends on the used dynamic models and on the applied objective functions, this work investigates new models and parameters. Specifically, human inspired models and parameters are considered to enhance prediction in specific situations.

Section 3.1 gives an introduction to the problem of human locomotion behaviors in case of disturbances. The distinct inaccuracies of optimal control approaches are analyzed in detail. From the review of related work it becomes clear that humans change their planning behavior when the initially followed optimal trajectory is disturbed. However, existing methods are not capable of reproducing the human behavior for recovery from an interference. Therefore, an experimental setup is proposed that gives insight into the cognitive process of human trajectory planning. Specifically the applied planning horizon is examined within this experiment, which is assumed to change with respect to the situation. The experiment explores whether humans shorten their planning horizon when an obstacle has to be passed in a complex virtual scenario. Results from this study yield fundamental conclusions about human avoidance behaviors which have not been tackled in the state-of-the-art. The findings are used to clarify whether current optimal control approaches, that are based on boundary value problems, should consider a shorter horizon or a model predictive control structure to reproduce human behavior.

In Sec. 3.2 the accuracy problem is further considered with respect to a human inspired dynamic model. The introduction and the review of related work explain a deficiency of the commonly used unicycle model which is tackled in this section. This thesis contributes a new model for human locomotion that is proposed to address the inaccuracies of human velocity modeling. In fact, the unicycle model produces a smooth velocity profile while recordings of human gait reveal a sinusoidal shape. Inverse optimal control approaches, such as [14, 121], smooth recorded data and neglect a distinct property of human walking. The contribution in this field is a model that is capable of reproducing a trajectory and the recorded velocities without the need for averaging or smoothing.

Spline based Analysis of Human Trajectory Data In Chap. 4 methods for the analysis of recorded human trajectory data are presented and compared. Section 4.4 describes a newly developed method based on statistical theories and spline models. During an extensive literature review, no suitable method could be found that allowed for lossless smoothing, calculation of confidence intervals or the quantitative comparison of trajectory data. Accordingly, a method is contributed based on penalized spline regression. Trajectories are smoothed and a mean for sets of trajectories is acquired using a penalized thin-plate spline model. With bootstrapping a method is formed that allows to compute confidence intervals for the mean of the data. These are used for the qualitative comparison of recorded data and the identification of behavioral differences. A quantitative

comparison is obtained with a comparative analysis based on trajectory distance measures. This comprehensive analysis framework poses a contribution that is applicable to a wide variety of problems and research fields.

In Sec. 4.6 the aforementioned contribution is compared to methods from robotics disciplines that are applicable to achieve similar conclusions but without the potential to obtain a statistically significant statement. The goal is to model the trajectory data and compare these results instead of purely analyzing the data for differences and similarities. Such models yield the advantage of trajectory synthesis and classification. More specifically Gaussian processes and Autoregressive Moving-Average models with exogenous input (ARMAX) are consulted for this purpose. This thesis contributes an approach to analyze trajectory data using Gaussian processes and the Kulback-Leibler Divergence. Additionally, an approach using ARMAX models is examined and evaluated.

In Chap. 5 the thesis and its results are summarized. Conclusions are drawn from the discussion of the results and contributions in Chap. 6.

2 Mobile Robot Locomotion in a Social Context

The incorporation of social and human-like behaviors is recently emphasized within mobile robot locomotion. These behaviors are required to support the seamless integration of mobile robots into environments which they share with humans. Human-like behaviors allow robots to externalize their intentions, which is important when they act in close proximity to humans. Considering social aspects additionally improves the acceptance towards a moving robot.

The first part of this chapter, which was previously published in [1], is dedicated to interaction initiation during locomotion. The efficiency of human-robot cooperative task completion benefits from seamless interactions. Robots that act in a shared environment with humans, can improve the initiation of such interactions by externalizing the intention of accompanying motions. Especially within robot locomotion the ability to convey intentions nonverbally is beneficial for mutual collision avoidance and the reduction of interferences. The following section examines the influence of specific trajectory features on the performance of a wheeled mobile robot in conveying its intention nonverbally during locomotion. The named correlations are investigated in the social context of robot locomotion for a pro-active robot-to-human approach. An optimal control framework is outlined for planning according trajectories that integrate mentioned features. Results of a subject study show that features for human-like trajectories are highly effective in conveying intentions and meeting the subject's expectations towards robot locomotion.

In the second part, another distinct benefit of these behaviors is demonstrated, which goes beyond positive apperception. The results were previously published in [3]. It is shown that human-like robot locomotion reduces the planning effort for all agents within a shared environment. This effect is revealed in an experiment that compares human locomotion during avoidance of an oncoming human or wheeled robot. The experiment confronts subjects with full and partial knowledge about the situation and shows that extra effort to handle the uncertain case is prevented by human-like behavior and intention conveyance. The study indicates that locomotion planning affords less effort from subjects if the mutual trajectory prediction is facilitated by robots that externalize intentions and comply with human-like behaviors.

2.1 Optimal Control based Trajectory Planning for Robot-to-Human Approach

Current trends in robotics research push the development of applications that involve human-robot collaboration. This comprises, for example, the joint execution of cooperative manipulation tasks as well as locomotion in shared environments. The consequential ambition is to replicate the human ability of seamless collaboration without verbal in-

formation exchange. An equally seamless human-robot cooperation can be facilitated by improving human-robot interaction and especially the initiation of interactions on a non-verbal level [31, 134]. The aspects that support nonverbal interaction initiation thereby differ based on the faced task and the social context. This section focuses on nonverbal interaction initiation with a mobile robot and elaborates this ability in the context of locomotion for a robot-to-human approach. This locomotion task enables a mobile robot to get into range for further verbal or physical interaction. The objective is to identify aspects within robot locomotion that positively influence the ability of an approaching robot in initiating this interaction nonverbally [149]. According robot locomotion trajectories must be able to quickly and clearly externalize the intention of the robot to the desired interaction partner. Uninvolved agents thereby benefit from clearly conveyed intentions as it enables them to avoid interferences.

Indeed, an interaction begins “with the attempt to recognize the intention of the temporal counterpart” meaning that “a mutual understanding has been established between both parties that interaction is intended” [27]. Therefore, an interaction begins on a non-verbal level and can be canceled by either party at this stage or confirmed to be engaged in. Transferred to an approaching robot, it is necessary to convey the intention to interact with a person to allow him/her to accept or decline collaboration. Success in interaction initiation is further increased when technical systems employ social norms, following the “Media Equation Theory” by Reeves and Nass [104, 125, 147].

The inherent capability of motions to nonverbally communicate intent or purpose is subject of various works [5, 7, 49, 50, 170]. The definition of this capability is named readability or legibility in conjunction with predictability. These terms define how well a person understands the purpose of a motion performed by another person or robot. This work adopts readability as a term that combines legibility and predictability.

In order to successfully react to another agent, the counterpart’s intention must be clear. Here, the impact of motion readability must be considered. Readability renders motions intuitively comprehensible [149] and diminishes disturbances for humans since their predictions become more reliable. Readable locomotion is thereby an action that meets the expectations [52, 68, 109] of an observing agent [43].

Thus, in order to improve the nonverbal interaction initiation capability of a robot-to-human approach motion, readability and social acceptance must be enhanced. Both are typically optimized by human-like motion [7, 170], which appears natural and predictable to humans. Therefore, humans understand the intention of a robot more easily if it employs human-like behaviors, as suggested by Breazeal et al. [31]. The hypothesis about the effectiveness of human-likeness for nonverbal communication is adopted and validated for robot locomotion in this section.

Transferred to an approaching robot, this imposes particular requirements on the trajectory planning problem for robot-to-human approach motions. The robot locomotion must be perceived as natural [149], comfortable [149] and adhere to social norms [104] in order to facilitate the nonverbal intention conveyance. Thus, the objective of this work is to investigate the effect of human-like trajectory features on these aspects.

For planning intuitively readable and socially acceptable approach trajectories this section expands optimal control methods by soft and hard constraints to model human-like

locomotion features and socio-contextual aspects. Planned motions are then expected to clearly externalize their purpose to the desired interaction partner.

One may suggest that familiarization and habituation affect predictability of robot motions and render human-likeness unnecessary. This is explored by Dragan et al. for manipulator motion in [50]. They conclude that naturalness mainly contributes to the predictability, whereas familiarization has only little effect. Thus, an appropriate approach motion that communicates this intention nonverbally should be inspired by features of human-like locomotion.

In this work motions are referred to as human-like if they exhibit certain formative features like a smooth path and velocity. This abstraction is employed since the used robotic platforms are wheeled. For a bipedal humanoid robot human-like locomotion comprises far more aspects, up to the point where it is supposed to walk exactly like a human. Human-likeness or anthropomorphism is proposed to be a concept with varying interpretations [152]. Although a common definition exists of what a person perceives as human-like [52, 152], the associated literature does not define unique parameters for human-like robot locomotion. Formative features vary depending on the respective task and whether arm motion or locomotion is considered [68]. Current approaches replay recorded human trajectories, imitate stereotypical behaviors of humans (e.g. a sidestep to indicate intended walking direction) or concatenate according locomotion primitives [52, 79, 111]. This work draws on basic features from literature that enhance the naturalness of motions [52] such as path shape and smoothness, smooth velocity profiles, constrained jerk, constrained acceleration, limited curvature and velocity limits for safety and sociability [18, 79, 160]. In addition, socio-contextual boundaries that positively affect readability and social acceptance are adopted from experiments in literature [9, 15, 22, 181], for example: specific constraints for approach speed, appropriate human-robot distance or positioning in the field of view.

The effect of specific trajectory features on readability and social acceptance of the robot-to-human approach motion is evaluated within two subject studies. The following section will demonstrate how pro-active robot-to-human approaches that employ these constraints perform better in conveying the right intention without creating an obtrusive or obliging situation. Since readability of a motion is enhanced if it is perceived as natural or human-like [170], the perceived naturalness is employed as a measure for the performance of an approach [7, 38]. Social acceptance is not directly measured as it is influenced by a more complex variety of aspects as described by the SOAC-questionnaire [120]. It is assessed by the indirect measure of the sensation of comfort [149]. The sensation of comfort contributes to the social acceptance of a robot as it is defined in literature [95, 96, 109]. Throughout this work the term social acceptance is used to describe behaviors that render actions more comfortable, produce less disturbances or that adhere to common norms [149].

In the first experiment results from a pilot-study are extended which only covered the influence of the path shape. The robot uses different trajectories to approach a subject, which then rates its perception of each trial. This experiment investigates the hypothesis that dedicated human trajectories and trajectories with human-like features are perceived as more natural and thus more readable compared to motions that lack these aspects. In addition, the presumption is examined that basic features of human-like trajectories are

sufficient for a high naturalness perception. In particular, a path must be smooth and constrained in curvature, while the robot orientation declines towards the person.

A second experiment is designed as an online-video study and evaluates the same approach trajectories from a third-person view and towards a walking human. Participants are presented with video sequences that show a robot executing each one of the approach trajectories. The videos randomly show the full approach or only a defined excerpt. Subjects are then asked to guess the intention of the observed robot that approaches the person. This analyzes the performance of an approach motion to convey the intention to third parties. The hypothesis is that readable approach motions convey their intention within a shorter sequence.

Existing works on robot-to-human approach mainly focus on aspects like relative positioning, final distance or approach direction [9, 85, 97, 153, 173, 181]. The integration of social aspects in motion planning [149] and their effects on human-robot interaction are subject to ongoing research. Findings from literature on the topic of legibility for arm motions [49] do not generalize to arbitrary motions [192]. For locomotion only the influence of certain stereotypical human behaviors is analyzed so far [111]. These results are adopted as a basis in the following and many aspects are transferred to locomotion.

This section experimentally examines the effect of further trajectory features on the perceptibility of the intention of a mobile robot that initiates interaction nonverbally during robot-to-human approach. Instead of copying human motion, trajectories are optimized with respect to readability and social acceptance. The features are derived from human-like locomotion and are expected to enhance the conveyance of the robot intention. In particular, the evaluated locomotion trajectories for the social context of a robot-to-human approach feature a smooth path with constrained curvature, while the robot torso orientation declines towards the person.

By comparing the Bezier curve based approach [7, 42] with a human inspired method and a non-human-like trajectory, the distinct features are evaluated in their effectiveness to support nonverbal interaction initiation. Experimental results show that features adopted from human locomotion significantly affect the apperception and the intention externalization capability of mobile robot trajectories. This improves the ability of a mobile robot to succeed in interaction initiation on a nonverbal level.

The demonstrated methods and results are easily generalizable to a variety of platforms and applications. Integrated on a robotic platform the evaluated method facilitates the ability to approach walking persons by applying optimal control based planning in conjunction with motion prediction methods. Thereby, the incorporated features and socio-contextual constraints for human-like locomotion enhance the robot ability to succeed in nonverbal interaction initiation. As an example, models for mutual collision avoidance [176] require that all concerned agents behave equally or act in accordance with certain behavioral patterns. The proposed approach enables a moving robot to comply with the expected behaviors. Consequentially, disturbances for nearby humans are diminished. Applied to a shared workspace, for example in an industrial setting, robots are able to integrate seamlessly into the work-flow. Collaborating humans may be less concerned about collisions with the robot due to the clear externalization of intentions. This raises efficiency while cognitive load declines [35, 51] and leads to higher perceived safety [110].

This section is structured as follows: In Subsec. 2.1.1 literature regarding readability, robot-to-human approach and socially acceptable navigation is discussed. Subsec. 2.1.2 formalizes the raised problem. The following subsections 2.1.3 and 2.1.4 describe the details of the implemented optimal control method and the conducted experiments comparing the different trajectories. Results and their interpretation with respect to the posed hypothesis are presented in Subsec. 2.1.5. A short summary and discussion is given in Subsec. 2.1.6.

2.1.1 Classification within the State-of-the-Art

Motion planning is a wide field of research with a large variety of methodologies and approaches. This work draws upon this field, but a complete overview of the related work is beyond its scope. The following points out basic literature and further discusses works that are dedicated to the problem of integrating social aspects and human-like behavior within mobile robot locomotion.

2.1.1.1 Mobile Robot Path Planning

Works by Latombe [114] and LaValle [115] are often referred to as groundwork for motion planning. Recent methods and approaches are summarized in [72]. Many of the standard algorithms are also applied in [187], which focuses on shortest/fastest path search, neglecting any influence of path shape.

With respect to the posed problem of approaching humans, some works tackle similar problems. Masehian et al. [118] intercept a target and avoid static and moving obstacles by evaluating the set of all collision free directions. The approach proposed here resembles this method but also considers social acceptance parameters. Optimizing Bézier curve parameters for this purpose is adopted from Choi et al. [40, 42]. The authors show many trajectory properties that are satisfied by Bézier curves, which are useful for human-like motion generation.

Reaching an appropriate final pose at about the same time as a moving target person requires movement prediction. Besides, the planned trajectory needs to take crossing passers-by into account. In [28] authors realize motion prediction for humans using Gaussian-Mixture-Models. Another probabilistic approach is shown in [64] where Partially Observable Markov Decision Processes are employed. Statistical data association combined with a particle filter predict motions in [154]. A grid model containing motion probabilities is shown in [172]. Prediction of future poses based on Kalman filtering is described in [55, 168]. In favor of its computational efficiency, a Kalman filter is also implemented here, assuming humans to be walking on a straight line and at constant velocity.

2.1.1.2 Socio-Contextual Aspects in Motion Planning

Ongoing research in the field of motion planning is more and more concerned with the integration of social aspects [149, 156]. Where models used to only focus on trajectory synthesis and obstacle avoidance, current approaches consider all agents within the scene, their mutual reactions and the influence of socio-contextual aspects.

In [31] and [170] it is shown that human-like behaviors improve readability and social acceptance. Both works focus on the enhancement of human-robot collaboration for task completion or information exchange. The hypothesis about the effectiveness of human-likeness for nonverbal communication is adopted and validated for robot locomotion in this section. Literature does not give a common definition of human-likeness for robot motion. Typical features and limits that render robot locomotion human-like as well as quantitative metrics to define human-likeness (comprising trained classifiers or comparison with results from optimization methods) are still subject to research [68]. In order to define acceptable ranges and generalizable formative features of human-like motions further extensive studies that compare wide ranges of motions are required [68]. Therefore, current approaches are mainly based on replays of recorded motions or the synthesis of stereotypical motions with respect to the task [52, 79, 111]. The work at hand abstracts human-likeness with respect to the used robotic platform. For example, the locomotion of a wheeled robot may be considered human-like if it comprises certain formative features like a smooth path.

In [49] the modeling of legibility and predictability within an optimal control framework for robot arm motions is addressed. The authors explore the effect of path shape on the legibility and predictability of arm motions. Furthermore, the effect of exaggeration regarding the trajectory curvature is explored. Zhao et al. [192] build upon the previous work confirming mentioned aspects. An important statement is that the model by Dragan et al. works well for a scenario with two targets but may be confusing for cluttered scenes. They further show significant influence of the motion and orientation of the end-effector for this environment. These results also motivated this work to analyze similar effects within robot locomotion. In [108] legibility is proposed as a metric for the perceived value of a robot together with a study setup to measure the effect. This work is extended in [111] giving an overview of factors that influence the legibility of robot motion. Notably, it is emphasized that the moving robot needs to be visible, meaning that readable locomotion is only effective when conducted right in front of a human. Lichtenthaler et al. propose to measure legibility based on questionnaires within user studies. Legibility is measured by asking whether the robot motion meets the subject’s expectation and whether it is surprising. These factors are similar to naturalness and sensation/comfort as proposed in this work. The presented experiments are also in line with [111] in multiple ways. Video based study setups are used along with common user-robot studies. Generally, literature agrees on the mentioned factors and their generalizability but, as pointed out in [111] as well, contradicting results are found with respect to study setups resembling varying environments. Accordingly, results from studies regarding arm motions might not apply in the same way to interactive navigation problems. This section contributes to the state of the art with evaluations of specific trajectory features for locomotion and extends previous work by an elaborate comparative analysis. Factors mentioned in literature that enhance nonverbal cooperation are taken as a basis for the experiments.

In order to incorporate suitable socio-contextual aspects, studies on human locomotion behavior are necessary. Ground work in this area is posed by Edward Hall [75], who introduces human proxemics. His theory suggests four spaces: public, social, personal and intimate space. For interaction with a stranger the social space is chosen by humans. However, as shown in [9] and [181] robots are allowed to enter the personal space. The

theory of proxemics is further expanded to various situations in [36, 76, 161, 162]. In [30, 185, 186] experiments with pedestrians passing each other are conducted resulting in a basic insight into social norms affecting pedestrian behavior. Especially the minimization of energy expenditure and the importance of mutual influence within human locomotion affects the choice of applied concepts in this work. Approaching humans with a robot to initiate an interaction is studied in [97, 173, 180, 181] analyzing comfortable human-robot distances. In [188] and [9] approach directions, approach speeds and parameters for moving persons are considered. Particularly the parametrization of the final approach pose is an important aspect in these works that was integrated in the subsequent experiments. A number of publications show the effectiveness of the social rules that were defined in the mentioned studies. The effect of intuitively comprehensible robot motions, specifically regarding path shape, and the validation of the effect of social norms was shown in [7]. This work uses the results from mentioned studies and further contributes with its findings and evaluations to this set of parameters.

2.1.1.3 Robot-to-Human Approach Methods

Approaching moving persons with a robot is shown in [153] and [85], whereas the socio-contextual aspects of the robot trajectory are not considered. Approaching humans to ask for help and information is also the subject of [67]. Here, the authors consider straight approaches at different speeds and angles. They explore socio-contextual constraints regarding the approach speed in combination with the final approach pose shifting to the side or back. For measuring social acceptance questionnaires contained the factors sociability and perceived intelligence. Approaching humans for interaction is also tackled in [88] with a focus on certain behaviors. Applied to a shopping mall assistant, the system estimates the intention of a person and behaves accordingly in order to start a nonverbal interaction. A guiding robot that pro-actively approaches humans and persuades them to keep following is presented in [133]. The authors propose that the approach motion should be natural and suggest splines as a solution. Yet, the optimization of intention conveyance and human-like motions are not considered. In [22] the influence of gaze on the readability of a goal directed motion is studied. Different approach scenarios are tested in human-human and human-robot studies. Indeed, the influence of the trajectory parameters is not considered as the used motions are replays of recorded human trajectories. Different control strategies for human interception are evaluated in [58]. As a metric the authors choose human-likeness and compare the model output with recorded path data from humans. Due to the focus on interception motions, an application to robots for a socially compliant approach is not considered. A learning based approach is shown in [20]. Human locomotion data is recorded and converted into a multivariate Gaussian attractor model. The detailed consideration of readability and social acceptance is thereby avoided. The authors mention related features of human locomotion such as the tendency to quickly enter the field of view of the target person. All these methods represent elaborate solutions to the robot-to-human approach problem. Specific features of the approach trajectory are, however, only marginally considered. Indeed, nonverbal communication or the effect of readability and social acceptance are often neglected. Copying human locomotion thereby implicitly considers these aspects.

There are various other tasks for social navigation showing how socio-contextual aspects vary with the robot task. Sisbot et al. [159] and Kessler et al. [89] present human aware motion planners exploiting the effects of proxemics but no further constraints or social norms. The legibility of avoidance behaviors is discussed in [101] and [5]. In [122] side-by-side walking and its social aspect are examined. Person-following builds the social context of [70]. Joining a group for interaction is presented in [17]. The method proposed in [15] integrates social constraints into a probabilistic collision avoidance framework that needs preliminary knowledge about the environment. Collision avoidance on a mutual level also benefits from the results of this work. Typical reactive collision avoidance algorithms like the velocity obstacle [143, 155, 184] model objects individually and neglect the mutual influence. This leads to situations where no collision-free trajectory is found resulting in the “freezing robot” problem. Considering mutually influenced avoidance allows to overcome this problem. Approaches that model mutual collision avoidance, for example [176], rely on the idea of nonverbal intention conveyance and readability. These methods assume that every agent has a model of every other agent. This is assumable for a robot that acts and navigates readable as it is proposed here.

2.1.2 Problem Description

Present work focuses on enhancing the ability of an autonomous mobile robot to initiate nonverbal interaction by improving the readability and social acceptance of its locomotion. This proposition is examined based on the trajectory planning problem for robot-to-human approaches. The following section elaborates on the problem in terms of human-like locomotion planning and subsequently formalizes the role of readability and social acceptance within the proposed optimal control framework.

2.1.2.1 Optimal Control Framework

A robot may be considered as a rigid body that can translate and rotate on a 2d plane. The set of 2d rotations $\Phi = [0, 2\pi)$ is defined as the manifold \mathcal{S}^1 . The space for translation and rotation is a special Euclidean group $\mathbf{SE}(2)$ that is homeomorphic to $\mathbb{R}^2 \times \mathbf{SO}(2)$ with the special orthogonal group of 2d rotations $\mathbf{SO}(2)$. So the configuration space \mathcal{W} corresponds to the special euclidean group $\mathbf{SE}(2)$ and is defined as $\mathcal{W} = \mathbb{R}^2 \times \mathcal{S}^1$, see [115]. A robot pose or configuration is therefore represented by $[p_R^x, p_R^y, \varphi_R]$. For the depicted problem, a robot executes a planar trajectory $\xi \in \mathcal{W}$ describing its change of pose $[p_R^x(t), p_R^y(t), \varphi_R(t)]$ in 2d space over time $t = 0, \dots, T$.

For an approach motion, the robot at its current pose $\mathbf{p}_R(t) = [p_R^x(t), p_R^y(t), \varphi_R(t)]$ starts off at a pose $\mathbf{p}_S(0) = [p_S^x(0), p_S^y(0), \varphi_S(0)]$ and travels to a specified pose $\mathbf{p}_G(T) = [p_G^x(T), p_G^y(T), \varphi_G(T)]$ with relative angle α in front of the target person at $\mathbf{p}_H(T) = [p_H^x(T), p_H^y(T), \varphi_H(T)]$, see Fig. 2.1. Considering the approach of a moving person, \mathbf{p}_G is the optimal approach pose with respect to required time T and path length $L(\cdot)$ within a set of approachable goals \mathcal{G} . The set \mathcal{G} depends on the path prediction for the target person, which is presumably a line, and on the socio-contextual constraints for appropriate interaction positions. The admissible time-frame $[0, T]$ and the positions for an approach also depend on the velocity of the target person v_H , which is assumed to be constant. This

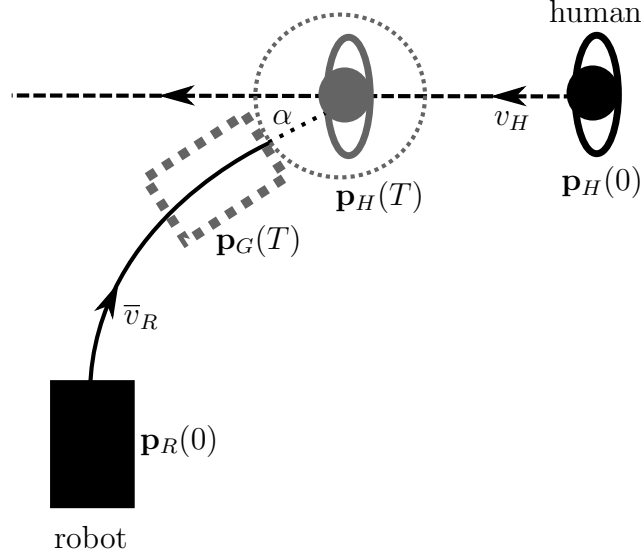


Fig. 2.1: Illustration of the human approach problem where a robot intercepts a walking person by following a trajectory that adheres to specific constraints

leads to a time constraint for the approach:

$$T = \frac{L(\mathbf{p}_H(T) - \mathbf{p}_H(0))}{v_H} = \frac{L(\boldsymbol{\xi})}{\bar{v}_R},$$

where \bar{v}_R is the mean velocity of the robot and $\mathbf{p}_H(0)$ is the pose of the person when the approach starts. For a successful interception of a walking person, the trajectory $\boldsymbol{\xi}$ and the position of the target person $\mathbf{p}_H(T)$ need to be chosen to meet this constraint.

For planning a human-like locomotion trajectory, optimal control methods are applied solving a constrained non-linear optimization problem [14, 121]. Solutions are found by applying direct methods to the non-linear programming problem. The problem of generating an optimal approach trajectory is representable as a two-point boundary value problem with additional non-linear constraints. Since the various constraints are complex and subject to change, a direct method is preferred [137].

An optimal control input from the admissible set $\mathbf{u}^*(t) \in \mathcal{U}$ (e.g. torque, acceleration, velocity) is desired that moves the robot from its initial to the calculated goal position within the time-frame $[0, T]$:

$$\mathbf{u}^*(t) = \underset{\mathbf{u}(t)}{\operatorname{argmin}} J(\mathbf{u}(t), \mathbf{x}(t), t),$$

minimizing a cost function J with runtime cost ϕ weighted by θ_i and terminal cost ϑ :

$$J(\mathbf{x}(t), \mathbf{u}(t), T, \theta_i) = \vartheta(\mathbf{x}(0), \mathbf{x}(T), T) + \theta_i \int_0^T \phi(\mathbf{x}(t), \mathbf{u}(t), t) dt,$$

subject to the equality constraints:

$$\begin{aligned}\dot{\mathbf{x}}(t) &= f(\mathbf{x}(t), \mathbf{u}(t), t) \\ g(\mathbf{x}(T), T) &= 0, \\ \mathbf{x}(0) &= \mathbf{x}_0 \\ T &\text{ free,}\end{aligned}$$

the inequality constraints:

$$h(\mathbf{x}(t), \mathbf{u}(t)) \leq 0,$$

and the boundary values:

$$b(\mathbf{x}(0), \mathbf{x}(T)) = 0.$$

The states $\mathbf{x}(t)$ are defined by the dynamic model used for the robot $f(\mathbf{x}(t), \mathbf{u}(t), t)$ which describes a unicycle as proposed in [121] and [14]:

$$\dot{\mathbf{x}}(t) := \frac{d}{dt} \begin{pmatrix} p_R^x(t) \\ p_R^y(t) \\ \varphi_R(t) \\ v_R(t) \\ \omega_R(t) \end{pmatrix} = \begin{pmatrix} v_R(t) \cos(\varphi_R(t)) \\ v_R(t) \sin(\varphi_R(t)) \\ \omega_R(t) \\ u_1(t) \\ u_2(t) \end{pmatrix}$$

The problem posed here is also solvable by replaying human motions, by fitting an appropriate curve into the given environment or by simply PD-controlling the robot to the goal position. Optimal control is chosen, however, as a framework that allows to plan the robot locomotion in detail while specifying certain boundaries that are then strictly followed. This framework further allows to define the crucial trajectory parameters and features more precisely with ongoing experiments.

2.1.2.2 Integrating Social Context in Trajectory Planning

The approach motion of the robot needs to convey the intention by moving readably and in accordance with social norms. Otherwise, a person might not be aware of the situation and not commence an interaction or even decline a conversation if the robot disregards the social context. The conveyance of intention through nonverbal communication within human behavior is described by two processes for action interpretation [43]:

- Action-to-Goal inference: humans try to predict the result of an action (e.g. approach target) given their observation history
- Goal-to-Action inference: humans try to predict the characteristics of an action (e.g. trajectory shape) given their knowledge of the goal

Accordingly, readability is a crucial attribute for socially compliant robot locomotion as it supports Action-to-Goal inference. In addition, readability leads to motions that are expected following Goal-to-Action inference. Given that the intention of a motion is clear due to its readability, the incorporation of social norms further supports Goal-to-Action

inference since the robot meets expectations and avoids obtrusiveness. Following [49], the observed trajectory ξ_{S-R} for an approach motion needs to be readable and lead to the expectation \mathcal{E} of an approach with a goal $G \in \mathcal{G}$.

$$\mathcal{E}(\xi_{S-R}) = G$$

Ideally, the target person quickly understands the intention and the started interaction leads to an expected meeting point G and a trajectory ξ_{R-G} .

$$\mathcal{E}^{-1}(G) = \xi_{R-G}$$

Hence, with better readability this process finishes faster and more successfully. Following this, the features of the robot trajectory are adapted by a set of equality $g(\cdot)$ and inequality constraints $h(\cdot)$, boundary values $b(\cdot)$ and Mayer-Terms $\phi(\cdot)$ or $\vartheta(\cdot)$. The constraints are designed to influence factors that are observable by humans: acceleration $a_R(t)$, velocity $v_R(t)$, path shape $(p_R^x(t), p_R^y(t))$, orientation $\varphi_R(t)$, curvature κ and positioning with respect to $\mathbf{p}_G(T)$ and α . The goal is to find constraints that alter the trajectory attributes and improve the perceived readability \mathcal{R} :

$$\operatorname{argmax}_{\mathbf{u}(t), c_1(\cdot), c_2(\cdot)} \mathcal{R}(\mathbf{u}(t), v_R(t), \omega_R(t), \mathbf{p}_R(t), \varphi_R(t), \kappa),$$

and social compliance \mathcal{S} :

$$\operatorname{argmax}_{\mathbf{u}(t), c_1(\cdot), b(\cdot), c_2(\cdot)} \mathcal{S}(\mathbf{u}(t), v_R(t), \omega_R(t), \mathbf{p}_G(T), \varphi_R(t), \alpha),$$

where $c_1(\cdot) = (g(\cdot), h(\cdot))$ and $c_2(\cdot) = (\phi(\cdot), \vartheta(\cdot))$. Constraining these parameters leads to a solution subspace among all feasible trajectories Ξ between $\mathbf{p}_S(0)$ and $\mathbf{p}_G(T)$ that favors readability and social acceptance. Readability \mathcal{R} and social acceptance \mathcal{S} are related to human perception and therefore not expressed analytically. Optimal values are found within user studies where subjects rate observed robot locomotion according to suitable measures. Appropriate values are achievable through human-like locomotion as described in literature, for example: minimum jerk, smooth velocity progression, smooth paths and proxemics theory. By comparing human-like motions to simplified constrained motions, experiments will reveal the fundamental features that are sufficient for maximizing naturalness and eventually readability.

2.1.3 Methodology for Readable and Socially Compliant Robot-to-Human Approach

Optimal control as a framework allows to model aspects of locomotion that increase readability and social acceptance as socio-contextual constraints and boundaries for the resulting trajectory. Readability \mathcal{R} enhancement and social compliance \mathcal{S} is realized within equality $g(\mathbf{x}(T), T)$, inequality $h(\mathbf{x}(t), \mathbf{u}(t))$ and soft constraints as well as boundary values $b(\mathbf{x}(0), \mathbf{x}(T))$ imposed on controls, velocities, path, pose and orientation.

2.1.3.1 Socio-Contextual Constraints

For readability \mathcal{R} the locomotion must seem natural and smooth without exaggerated accelerations or velocities. Therefore, the shape of the path and the introduction of suitable control limits are discussed in the following. A path $(p^x(t), p^y(t))$ may be constrained to follow a subspace solution like a Bézier curve $B(\lambda)$. Bézier curves are planar curves $B : \lambda \rightarrow \mathbb{R}^2$ where $\lambda = \{\lambda \in \mathbb{R} | 0 \leq \lambda \leq 1\}$ which feature a smooth shape and low computational cost. Another advantage of Bézier curves is their continuous differentiability, which is especially useful to concatenate re-planned paths in dynamic environments [7]. A disadvantage of these curves is the missing linear mapping from time t to position $B(\lambda) = (p^x(\lambda), p^y(\lambda))$ or the parameter λ . This mapping from time t to the curve parameter λ , such that $B(\lambda(t)) = (p^x(\lambda(t)), p^y(\lambda(t)))$, is acquired through arc-length parametrization, see [115]. This parametrization maps the partial length of the curve to a λ value. Given the smooth path of the Bézier curve, the curvature κ needs to be constrained $\kappa_{\min} \leq \kappa \leq \kappa_{\max}$ to meet the exaggeration problem described in [50].

In order to obtain the typical trapezoid shape of the velocity profile $v_R(t)$, a constraint may be defined that keeps the robot at a desired velocity v_d . In the experiments this velocity is defined to be $v_d = 0.5 \text{ m/s}$.

$$\int_0^T \phi_{v_d}(v_R(t)) dt = \theta_{v_d} \int_0^T (v_R(t) - v_d)^2 dt$$

Efficiency is a characteristic attribute of human motion, enforcing the need for constraints on time, energy and path length:

$$\begin{aligned} \int_0^T \phi_t dt &= \theta_t \int_0^T 1 dt \\ \int_0^T \phi_u(\mathbf{u}(t)) dt &= \theta_u \int_0^T (u_1^2(t) + u_2^2(t)) dt \\ \int_0^T \phi_L(p_R^x(t), p_R^y(t)) dt &= \theta_L \int_0^T B(\lambda(t)) dt \end{aligned}$$

This minimizes the jerkiness of the locomotion and avoids sudden reorientation. The maximum rotational velocity of the robot is constrained due to design conditions and to meet the expectations of people such that $\omega_{\min} \leq \omega_R(t) \leq \omega_{\max}$. Indeed, the Bézier curve handles this since the robot orientation $\varphi_R(t)$ is defined along the path leaving only the forward velocity to be planned. In practice it is beneficial to skip the planning of the robot orientation since this reduces the complexity of the problem. The robot may be simply controlled to always face the next way-point of the trajectory. The orientation $\varphi_R(t)$ at time t enforced by the Bézier curve has the following structure:

$$\varphi_R(\lambda(t)) = \left. \frac{\dot{p}_R^y(\tau)}{\dot{p}_R^x(\tau)} \right|_{\tau=t}.$$

Due to findings in recent literature, which analyzes human-like behavior for goal-directed locomotion [18], moving sideways is not considered in the proposed model. Yet, the com-

parison method of [121] considers the subtle side-way motions that humans use to correct their orientation towards the goal as an important aspect. Therefore, this type of locomotion is considered in the evaluations in order to assess whether naturalness is increased or even decreased. Mombaur et al. [121] define the robot orientation as a weighted Lagrange-term which increases with the difference between the robot orientation and the necessary orientation for the robot to face the human. The desired Bézier curve should decrease the deviation between the actual robot orientation $\varphi_R(t)$ and the final orientation $\varphi_G(T)$ constantly. The reason is a result of previous studies where the locomotion was considered less natural when the robot slightly turned away at the beginning [7]. A simple constraint is feasible that decreases over time and pulls the robot orientation towards the human. Correctly weighted, this constraint also helps to correct deviations in the final pose.

$$\int_0^T \phi_\varphi(\varphi_R(t))dt = \theta_\varphi \int_0^T (\varphi_G(T) - \varphi_R(t))^2 dt$$

More strict in the sense of [121] would be the following constraint ϕ_m , which penalizes a deviation of the robot orientation away from its goal. However, the proposed approach only uses the above constraints since this problem changes drastically as soon as gaze control is added in a later stage.

$$\int_0^T \phi_m dt = \int_0^T \left[\text{atan} \left(\frac{p_G^y(T) - p_R^y(t)}{p_G^x(T) - p_R^x(t)} \right) - \varphi_R(t) \right]^2 dt$$

Constraints enhancing the social acceptance \mathcal{S} mainly influence the positioning of the robot like the final pose $\mathbf{p}_G(T)$ for the approach, the limits for controls u_1, u_2 , and limits for the velocities $v_R(t), \omega_R(t)$ [9, 68, 110, 160]. Very quick reorientation due to high rotational acceleration for example is a capability of robots which is not expected by humans and may induce negative sensation. A robot that rushes towards a person is another example tackled by these constraints. This results in the following inequality $h(\mathbf{x}(t), \mathbf{u}(t))$, runtime $\phi(\mathbf{x}(t), \mathbf{u}(t), t)$ and terminal constraints $\vartheta(\mathbf{x}(0), \mathbf{x}(T), \mathbf{u}(0), \mathbf{u}(T), T)$.

The goal pose constraint $\mathbf{p}_G(T)$ must comply with a set of boundary values that define a position in front of the person at $\mathbf{p}_H(T)$, in the field of view and at a minimum euclidean distance $d_{RH,\min}$ to the person. The relative angle α to the target person is another important factor in the social context. Robot-to-human approaches from behind for example are known to produce low social acceptance [158]. For calculating a goal position, the heading of a walking person is estimated and the goal set in accordance with α and $d_{RH,\min}$:

$$\begin{pmatrix} p_G^x(T) \\ p_G^y(T) \end{pmatrix} = R_\alpha \begin{pmatrix} \cos(\varphi_H(T)) \\ \sin(\varphi_H(T)) \end{pmatrix} d_{RH,\min} + \begin{pmatrix} p_H^x(T) \\ p_H^y(T) \end{pmatrix},$$

where R_α is a rotation in two dimensions by α . The velocity must not be too high or too low such that $v_{R,\min} \leq v_R(t) \leq v_{R,\max}$ and the robot must decelerate when getting close to the target person:

$$\int_0^T \phi_v(p_R^x(t), p_R^y(t), v_R(t))dt = \theta_v \int_0^T \frac{v_R(t)}{d_{RH}(t)} dt,$$

where $d_{RH}(t) = \|(p_R^x(t), p_R^y(t))^T - (p_H^x(t), p_H^y(t))^T\|_2$. The free choice of constraints raises the question of how convergence is affected. Criteria that exactly define how attributes of constraints influence the convergence are subject to elaborate mathematical analysis, which is beyond the scope of this work. Yet, some fundamental aspects need to be considered. The constraints must lead to an admissible set of states and controls that is not empty in order to find a solution. Particularly, the number of equality and active inequality constraints may lead to empty feasible sets. Therefore, the number of equality constraints together with active inequality constraints in the solution point must not exceed the dimension of the optimization problem (rank condition) [189]. Further, the constraint qualification is violated if none of the found minima features linearly independent gradients of all active inequality constraints [189]. In general, state-of-the-art solvers handle these problems and give appropriate warnings. From a problem design perspective and if the focus is on the optimization or the applied solution method, the differentiability and convexity of constraints may require special consideration.

2.1.3.2 On-line Implementation for Dynamic Environments

The following describes an integrated on-line capable system that approximates the developed optimal control problem in Subsec. 2.1.2 by applying a rule based brute force search. This system was published in [7] and found application in the IURO project [4]. It allows to conduct user studies in order to find and confirm effects of parameters or to develop further aspects that affect readability.

For motion planning, Bézier curves are used, since they feature properties which are beneficial for human-likeness and thus readability as well [60]. Firstly, the starting point \mathbf{b}_0 and the endpoint \mathbf{b}_3 of a Bézier curve are freely controllable. For the robot-to-human approach, these points are fixed to the robot and the goal position and change since both move. Secondly, tangents at \mathbf{b}_0 and \mathbf{b}_3 , that connect \mathbf{b}_0 , \mathbf{b}_1 and \mathbf{b}_2 , \mathbf{b}_3 , allow for the definition of the final position and orientation. Thirdly, as the k -th derivative of a Bézier curve is still continuous [41], the curve has continuous curvature. Accordingly, trajectories are consistent continuations of each other if their respective starting and ending point are the same. This is the case when continuous on-line re-planning is applied. Lastly, due to the k -fold differentiability [41] Bézier curves supply smoothness and continuous jerk. The maximum time-frame for the trajectory construction is given by the fact that a person is only approachable until he/she reaches a distance which the robot is unable to catch up with. While the trajectory origin is always set at the robot position $\mathbf{p}_R(t)$, the final pose depends on the predicted movement (position, speed) for the person. Without loss of generality the person's orientation is thereby assumed to be known.

Given these attributes, a cubic Bézier curve is used for static scenarios, as shown in Fig. 2.2. The parameters of the final approach pose and the initial robot pose define the shape of the trajectory. The robot position controller then follows the curve with a constant velocity.

In a static collision case the degree of the curve is increased to four. Hence, one control point, here \mathbf{b}_2 , pulls the curve away from the obstacle as shown in Fig. 2.3. For example, by checking for discontinuities in a forward-facing laser scan, object dimensions are assessed and extremal points found. Searching for a collision free curve, \mathbf{b}_2 is shifted iteratively.

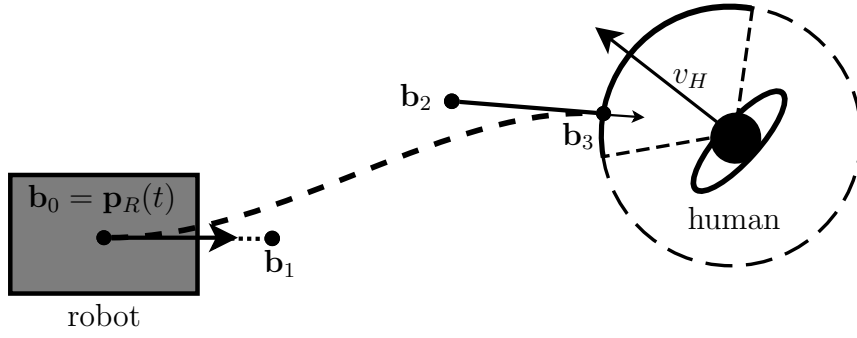


Fig. 2.2: Trajectory formed with Bézier curve of degree three in free space

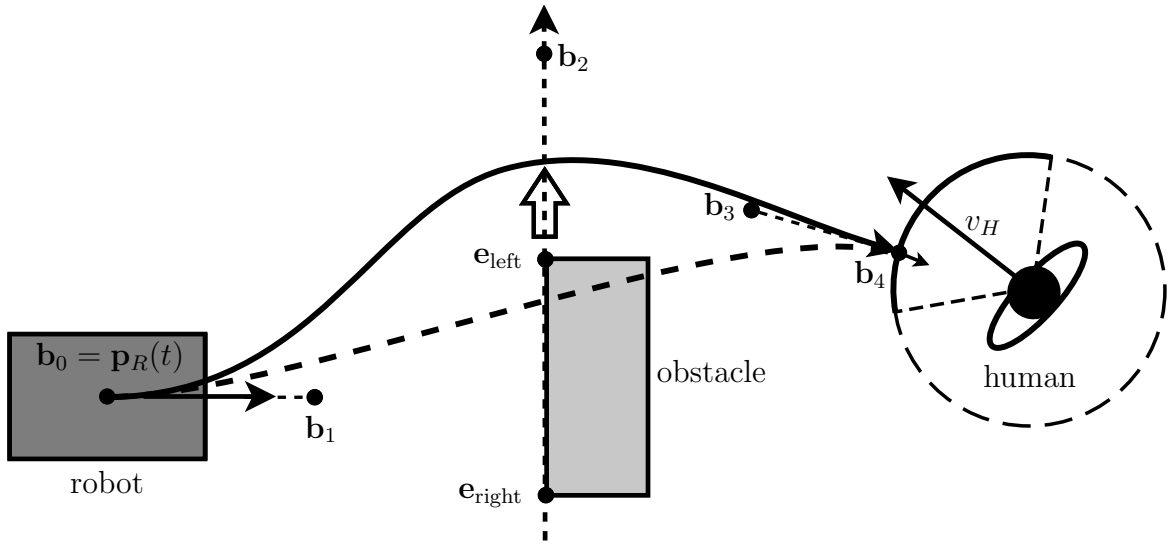


Fig. 2.3: Trajectory formed with Bézier curve of degree four in the static collision case

The control points \mathbf{b}_0 and \mathbf{b}_1 remain on the line defined by the initial orientation. The points \mathbf{b}_3 , \mathbf{b}_4 are still defined by the position of the human $\mathbf{p}_H(t)$ and the goal pose $\mathbf{p}_G(T)$. Therefore, a simple turning on spot never results from this planning process. The positions of the Bézier points may be defined as optimization constraints. For a curve of degree three it follows that:

$$\mathbf{b}_1 = \mathbf{p}_R(t) + \eta_1 \begin{pmatrix} \cos(\varphi_H(0)) \\ \sin(\varphi_H(0)) \end{pmatrix},$$

$$\mathbf{b}_2 = \mathbf{b}_3 + \eta_2 (\mathbf{b}_3 - \mathbf{p}_H(T)),$$

where η_1 and η_2 are arbitrary parameters and $\mathbf{b}_3 = \mathbf{p}_G(T)$ depicts the goal pose that employs social aspects like human-robot distance, positioning in the field of view and preference for sidewise approach. For degree four curves, the constraint on \mathbf{b}_2 and \mathbf{b}_3 is dependant on the obstacle dimension and its extremal points \mathbf{e}_{left} and $\mathbf{e}_{\text{right}}$. Pulling the curve out on the side of \mathbf{e}_{left} leads to the following:

$$\mathbf{b}_2 = \mathbf{e}_{\text{right}} + \eta_3 (\mathbf{e}_{\text{right}} - \mathbf{e}_{\text{left}}),$$

$$\mathbf{b}_3 = \mathbf{b}_4 + \eta_4 (\mathbf{b}_4 - \mathbf{p}_H(T)),$$

where η_3 and η_4 are arbitrary parameters. Given the planned curve, it is discretized in time and space to form a discrete planar trajectory $\xi_R^r(k) = [p_R^x(k), p_R^y(k), \varphi_R(k)]_{k=1, \dots, K}$. The primary velocity profile assumes that maximum speed is possible due to absence of collisions. Deceleration is then necessary nearby the goal pose, as proposed in [9].

The constant velocity profile is adapted to provide a slow down or speed up for avoidance of moving obstacles. At first a safety region with radius r_{safe} is assumed around every discrete position on the trajectory. For a moving obstacle crossing the trajectory, the entrance time t_{enter} and the emission time t_{leave} are calculated by assuming a constant velocity. Based on this concept, the robot executes the trajectory either up to the colliding position $\mathbf{p}_R(\text{col}-1)$ or the position $\mathbf{p}_R(\text{end}+1)$ after the critical point, in order to avoid the obstacle as it leaves the zone or before it crosses. This requires accelerating or decelerating depending on the time the robot may arrive at either position. Generally, holding on to a constant velocity or slight deceleration is preferred over high accelerations, which may lead to a negative sensation for the approached person. Obstacle avoidance therefore follows a human-inspired approach [100]. Figure 2.4 illustrates the concept. Finally the arrival

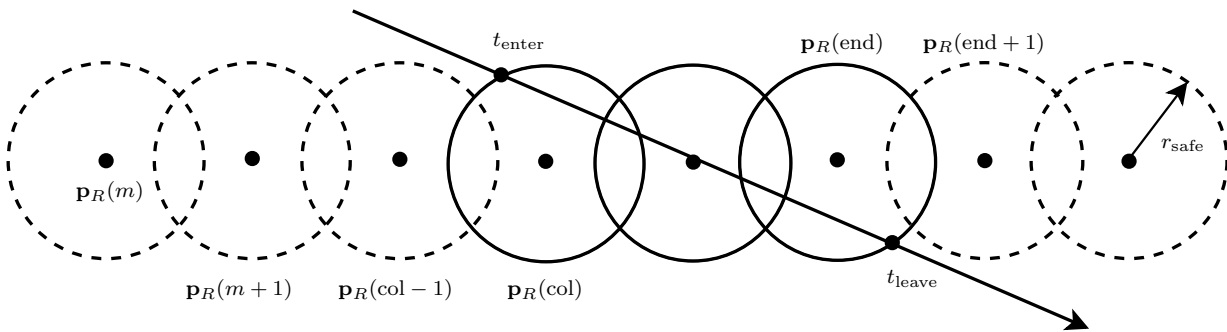


Fig. 2.4: Collision zones around each discrete trajectory position are indicated by circles, while a continuous line around a way-point represents high collision potential

time at each trajectory point is estimated by the distance of two discrete points and the according robot velocity. After that, the velocity profile of the whole trajectory has to be considered in order to assess if the final goal pose is reached in time and the robot arrives simultaneously with the target person. In case the time constraint can not be met, the discrete trajectory needs to be re-planned. This leads to an iterative algorithm capable of adapting the trajectory, velocities and goal positions on-line. The separation of spacial and temporal planning entails that the trajectory shape does not change together with the velocity profiles. This renders the movement even more predictable. The real-time capability further enables the system to adapt in case of tracking errors or dynamic changes in the environment. This is necessary since the algorithm is developed with respect to the IURO project [4], where an autonomous mobile robot is required to approach pedestrians in an urban environment and initiate interactions. The capability of on-line re-planning and adaptation to dynamically changing environments is constrained to a limited number of dynamic obstacles and a certain spatial horizon. Due to this simplification the number of avoidable objects is constrained and the algorithm is thus not complete.

2.1.3.3 Robot Trajectories and Control for the Experimental Evaluation

The described framework is applied to plan the trajectories for the experiments designed in 2.1.4.2 and 2.1.4.3. The control approaches for execution of the four different trajectories are described in the following.

For controlling the mobile robot to follow a planned trajectory, its position and the position of the subject need to be known and tracked. For this purpose a Qualisys Tracking System is used. The system supplies position data of every trackball attached to the person and the robot with a frequency of 204 Hz.

The approach motion that only adopts certain human-like features is described in the previous section and the constraints are described in 2.1.3.1. A Bézier curve yields a smooth path with constrained curvature and predefines the orientation of the robot when it executes the path non-holonomic. Due to the simplified experimental environment in Subsec. 2.1.4, the used curve is defined by the initial robot pose and the pose of the target person. Thus, for optimization the approach defined in [7] is directly applied. The Bézier curve is followed using a control law from literature [98] with position data from the surrounding optical tracking system. As the robot is controlled along the sampled Bézier Curve it elicits a typical human-like velocity profile with a trapezoidal shape. Based on a distance rule (2m distance from the person [9]) it slows down from the 0.5 m/s reference velocity to 0.3 m/s in order to respect social norms.

For representing a human locomotion trajectory the model described by Mombaur et al. [121] is used. This method is implemented using the ACADO Toolkit [12] and the optimization is solved using Multiple-Shooting. It is extended by the constraints on the final approach pose and the limits for controls and velocities in order to raise equal social acceptance as the proposed Bézier method. In order to evaluate the difference between a holonomic movement and a non-holonomic movement, the model provides two trajectories for the experiment, one with and one without the lateral component. This allows for an evaluation of the robot orientation during trajectory execution. Since the Mombaur method plans human trajectories, the velocities feature the intended behavior of constant velocity and smooth deceleration close to the goal pose (trapezoidal shape of the velocity profile). Yet, the drop in velocity begins closer to the end of the trajectory in order to achieve zero velocity at the final pose. The velocities obtained from these optimizations are directly fed into the robot's low-level controllers to follow. Some heuristic tuning of the system enables the robot to realize the planned path.

A movement that does not provide a smooth path, smooth velocity or smooth progress of torso orientation is achieved with a simple straight motion. This behavior follows the idea proposed in [49], where the simple straight reaching motion of a robotic arm is considered as the most predictable motion. For this non-human-like approach motion the robot is controlled to rotate towards its goal in front of the subject, move straight towards this location and finally align to the interaction partner until the angle α is reached.

Parameters that are used in the implementations are shown in Tab. 2.1. The values are transferred from previous works [7] where velocity and stopping distance were rated as appropriate. These parameters were initially adopted from literature discussed in Subsec. 2.1.1. With respect to [173] the stopping distance could now be chosen larger but the used robot is equipped with a touch screen such that it must get into reaching distance.

Tab. 2.1: Constraint parameters used in the experiments

Parameter	Value
v_{\max}	0.5 m/s
v_{\min}	0
ω_{\max}	0.5 π rad/s
ω_{\min}	-0.5 π rad/s
$d_{RH,\min}$	1m
α	$\pm \frac{\pi}{6}$ rad

This feature is kept to meet the requirements that influenced the design of the used robotic platform IURO [4].

The mobile robot that is used for this experiment is shown in Fig. 2.7. The IURO robot has many interactive features such as an emotional display, arms and a touch-screen. As mentioned within related work, directional cues like gaze are sources that humans use to guess the intention of a motion. Therefore, subjects are informed not to pay attention to these cues as they would not act. Subjects are further told to focus on the locomotion of the robot in order to strengthen their attention. Although it cannot be assumed that the appearance of the robot has no influence on the apperception, the effect is expected to be equal for all conditions.

2.1.4 Experimental Evaluation

In order to evaluate the performance of the considered trajectory features and the proposed socio-contextual constraints with respect to readability and social acceptance enhancement, two human-robot experiments are set up in a highly controlled lab environment. Controlling the environment is crucial since environmental factors can not be masked out when running a study for example on a public square. Evaluating the approach within a lab environment further allows to specifically test single factors and ensures comparability by changing only one aspect between conditions. The experiments follow the results of a pilot-study which is described first. In future equivalent studies are aspired on public squares. These prior results will then support the planning of required participant numbers, the consideration of confounders and certainly the complexity of the required technical setup.

The experiments continue the pilot-study and evaluate a wider range of trajectory features and their effect on nonverbal interaction initiation. In terms of readability, the performance of human-like locomotion features is evaluated, that are inherently represented by the attributes of the Bézier curve used here. The described on-line locomotion planner features all mentioned constraints from Subsec. 2.1.3 regarding readability and social acceptance. It is intended to evaluate its performance in comparison with a planner for human locomotion [121] and a simple straight approach motion that is non-human-like, as described in Subsec. 2.1.3.3. Readability of the locomotion is evaluated by rating its naturalness and investigating its intention conveyance capability. The sensation of comfort and thus implicitly the social acceptance is assumed to be equal for all algorithms as they feature equal constraints in this regard.

The experiments evaluate readability as a consequence of the named inference processes defined in 2.1.2.2. Concurrently, the used questionnaires also investigate the social acceptance of the robot-to-human approach. The pilot-study as well as the first experiment provide the subject with the goal of the robot (approaching the subject). Subjects are issued questionnaires and asked for a rating of the approach motion, implying that Goal-to-Action inference $\mathcal{E}^{-1}(G)$ takes place. The second experiment relies on a third-person view using an online-video-study. Subjects are asked to guess the goal of the robot which attempts to trigger the Action-to-Goal inference $\mathcal{E}(\xi_{S-R})$.

2.1.4.1 Pilot-Study on Robot-to-Human Approach of a Standing Person

As a pilot-study for assessing the human perception of the approach behavior, an experiment is set up where a robot moves towards a standing person. Probates are asked to rate the convenience of the robot velocity, the distance where it stops, how natural the motion seems and how comfortable they feel during the approach. The investigated hypothesis $H_{1,A}$ proposes that variations of the robot-to-human approach path are rated differently.

Method The study is carried out with 10 subjects in the age of 21 to 38 years, who are rather experienced in the field of robotics. Country of origin and education level were also part of the questionnaire but no significant influence was found regarding these aspects. Descriptive statistical results are acquired from an analysis of repeated measures using a parametric test (ANOVA).

This user study features a 4×1 within subject design. Subjects rate each robot-to-human approach on a 21 point scale in the categories: speed (too slow ... too fast), stopping distance (too far ... too close), naturalness (very artificial ... very natural) and sensation (very uncomfortable ... very comfortable). The experiment is conducted using the ACE (Autonomous City Explorer) platform [25]. The design of ACE, the predecessor of IURO [4], is less human-like and pleasing, but since only the movement should be in the focus, an elaborate design is not necessary. In order to enforce the focusing on the movement the emotional display is unmounted as well. As free space for an approach is needed and the lab environment was not present at that time, the experiment is set up in the lobby of a public building.

Procedure Subjects are recruited directly at an open public square. If probates are interested in the study, they are led to the nearby study setup and are shown the testing area and the robot. After they agree to participate, an informed consent is issued and further details regarding privacy protection and data security are explained. Prior to the first experiment run, the initial part of the questionnaire has to be filled in. Here, age, country of origin, education level and prior experience with robots are required. Subsequently, the subject is asked to stand on its position and observe the robot approach. The robot is started by an instructor for each of the four different approaches from a position in 4 m distance opposite to the probate. The probate takes three different orientations: facing the robot or $\pm 90^\circ$ looking to the left or right. The according trajectories are shown in Fig. 2.5. Subsequent to each scenario, the probate rates naturalness, approach speed,

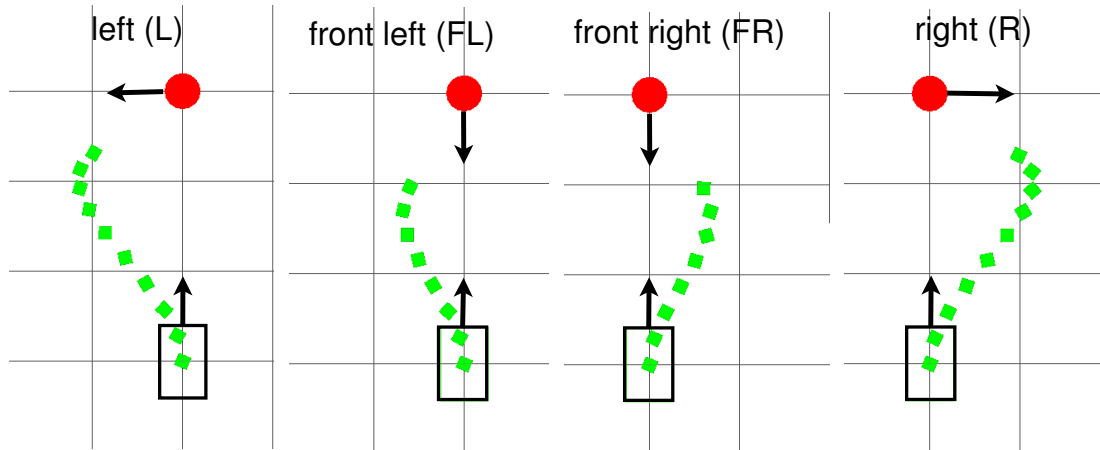


Fig. 2.5: Trajectories executed by the robot during the four different approaches of a static person in the pilot-study

approach distance and sensation on a questionnaire. Randomization of the approach scenario succession is applied to exclude bias effects. After the experiment, each subject is debriefed and thanked for participation.

2.1.4.2 Comparative Robot-to-Human Approach Study with a First-Person View

Under consideration of the results from the pilot-study, the four previously described approach motions are compared in their evaluations. In this follow-up experiment, subjects experience a robot-to-human approach in a laboratory environment. They are provided with the goal of the robot (approaching the subject) and are asked to rate the four described motions, which they will observe. The basic hypothesis is that trajectories with human-like locomotion features are rated as more natural in the social context of an approach. Given the known intention of the robot the process of Goal-to-Action inference defined in 2.1.2.2 as $\mathcal{E}^{-1}(G)$ supports this idea since human-like locomotion is more easily readable and meets the subject's expectation of the motion. Accordingly, subjects rate the naturalness of each observed approach which serves as an indicator for readability. The sensation of comfort is thereby assumed to be equal for all four trajectories. Additionally, subjects rate velocity and stopping distance since these criteria are common for all approach motions and help verifying that the robot performed as expected.

The four trajectories resemble different levels of human-likeness and feature equal constraints regarding social norms. Two hypotheses are therefore established and evaluated. $H_{1,B}$ proposes that trajectories from a human model, with human-like features and without these features achieve different naturalness ratings. $H_{1,C}$ suggests that despite equal approach speeds and final distances, the ratings of velocity, distance and sensation of comfort vary for all trajectories.

The experiment investigates if human and human-like motions perform significantly better than non-human-like motions in enhancing the interaction initiation capabilities of mobile robots. Additionally, the direct comparison between the Bézier based approach and the human locomotion model investigates whether basic human-like features of trajectories are sufficient for an increased readability.

Method This first comparative experiment is carried out with 40 subjects in the age 20-30, who are presented with the four approach motions in a randomized order. Raised data also includes experience of working with robots on a scale from 1 to 5 or the country of origin. However, no significant differences are found related to these factors.

In this user study, subjects are asked to stand at a predefined location and watch the robot approach them. In this 4×1 within-subject design, participants are approached four times with the different locomotion algorithms in a randomized order. The probates are thereby oriented such that the robot is on their right hand side. Subjects are then approached four times with the different locomotion algorithms. After each of the four trials, they are asked to fill in a questionnaire with the four criteria: speed (too slow ... too fast), stopping distance (too far ... too close), naturalness (very artificial ... very natural) and sensation (very uncomfortable ... very comfortable). Subjects rate each robot-to-human approach motion in the four criteria on a 21 point scale (0-10 with intermediate steps). Fig. 2.6 shows the paths that are performed by the robot to reach the person.

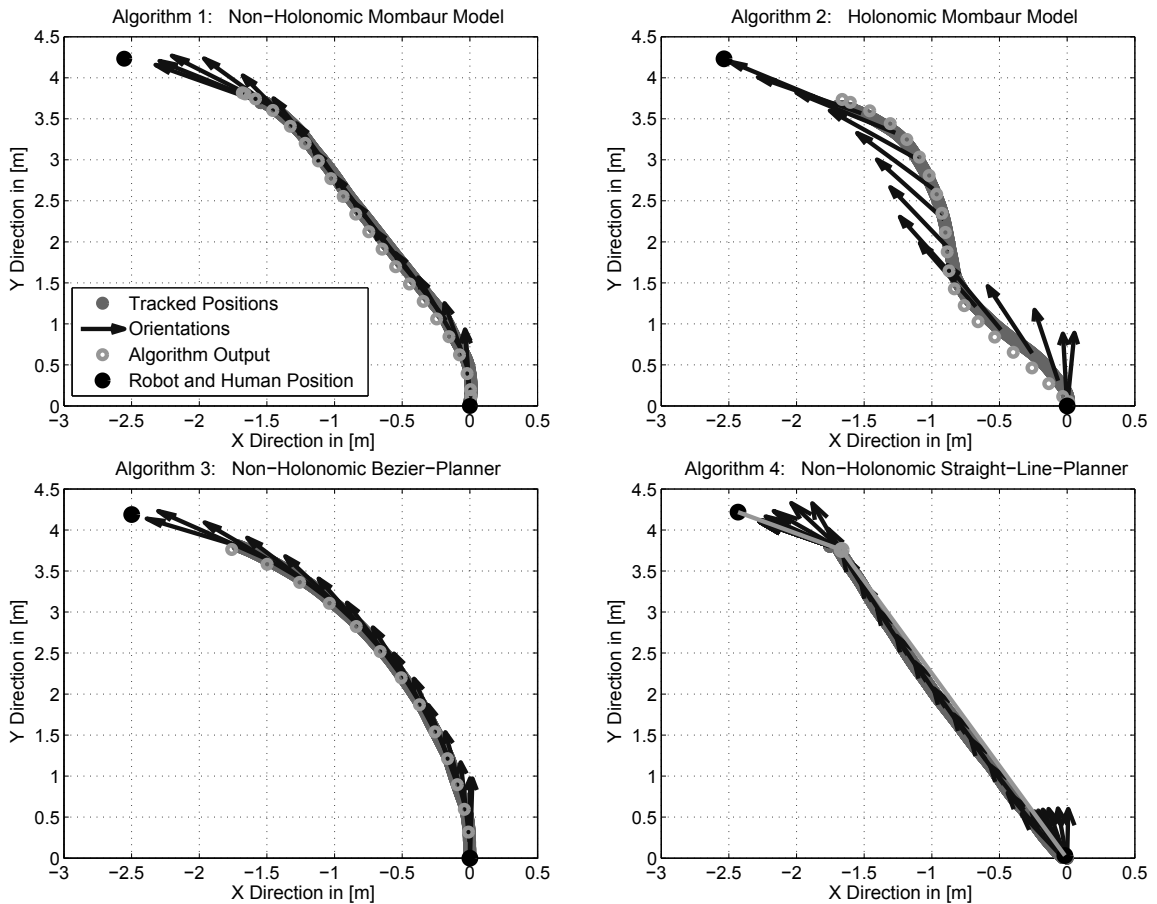


Fig. 2.6: Approach paths compared in the experiment with solid black dots marking the robot and the human position, planned paths shown as light gray rings, tracked paths in dark gray and the robot orientation indicated by black arrows

Calculated paths and the actually tracked paths are shown in light gray (circles/line) and dark gray (solid path) respectively. The tracking accuracy with respect to the robot size is sufficient for the experiment. Perfect accuracy is hardly reachable with respect to

the imperfect platform, the air-pressured tires and the accumulation of tracking errors. The starting position (solid black dot bottom right) of the robot and the position of the person (solid black dot top left) are equal for all trials. The stopping distance to the person is set between $0.75\text{ m} - 1.0\text{ m}$ depending on tracking accuracy and time the robot needs to stop fully. An approach angle of 30° between the person's orientation and the robot's final orientation is set for all motions. The orientation of the robot during trajectory execution is depicted by black arrows along the path. All paths differ in shape and torso orientation of the robot. The non-human-like version, resembled by the straight-line approach, serves as the benchmark for a simple but non-smooth motion.

Procedure Participants of the study were welcomed at the lab and led to the tracking area. They were instructed about the functionality of the tracking system and the robot was presented. The experiment was briefly explained by describing the subject's position and that the robot would approach the subject in different ways. Thereby the participants were reassured that the robot head and emotional display would not act since only the motion should be rated. After this introduction, each subject was asked for an informed consent and further explanations regarding safety, privacy protection and data security were provided. Finally, each subject was equipped with track-balls and given time to ask any further questions. Each participant was then requested to stand at the marked position and watch the robot approach. After each trial the subjects filled in the questionnaire with the four ratings and then positioned themselves on the marked location again. Upon completion of the experiment, every subject was debriefed and thanked for participation.

2.1.4.3 Comparative Robot-to-Human Approach Study with a Third-Person View

Recent findings presented in [167] propose that the point of view (first-person or third-person) matters in the perception of social compliance, such that results should be validated considering different points of view. Thus a third experiment is set up as an online video study where participants are presented with sequences of varying length that show the different approach motions. The method of an online video study is chosen for this purpose as it yields a third-person view and the opportunity of a large range of subjects.

This experiment tackles the question whether the intention of the robot is clearly visible. For each motion the participant has to decide whether the robot intends to approach the person or not. The hypothesis $H_{1,D}$ suggests that the frequency of correct answers differs from chance level for all five shown motions and all observation durations.

This experiment allows for a direct evaluation of the readability of a motion. The third-person view triggers the Action-to-Goal inference described in 2.1.2.2, following $\mathcal{E}(\xi_{S-R}) = G$, asking subjects to infer the goal of the robot given the observed motion. Given that $H_{0,D}$ is rejected and the frequency of correct answers is significantly higher than chance level, it is assumable that the subjects are able to infer the robot intention from its motion. If $H_{0,D}$ is also rejected for shorter sequences that show an approach motion, the result can be interpreted as an indicator for higher readability. Therefore, this study evaluates the conveyance of intention and investigates whether trajectories from a human model, with human-like features or without these features convey the robot intention equally fast.

Results will also give information whether human-like locomotion is advantageous for the anticipatory path planning of uninvolved agents. Given a better readability of natural locomotion, an oncoming pedestrian can adapt its path earlier and completely avoid interference. In the human approach scenario the intention must not only be clear to the approached human but also to anyone in close vicinity to avoid disturbances.

This online experiment allows a person to observe the approaching robot from a third-person perspective and also offers the opportunity to inquire a large range of subjects. Thus a second part was added to the online study where subjects are asked to rate the naturalness of an approach motion. The hypothesis $H_{1,E}$ suggests that trajectories from the human model, with human-like features and without these features achieve varying naturalness ratings when observed by a third-person.

With respect to 2.1.2.2, the experiment triggers a Goal-to-Action inference $\mathcal{E}^{-1}(G) = \xi_{R-G}$ such that human-like trajectories should meet the expectations of a subject more closely. The naturalness ratings are therefore expected to be in line with the lab experiment regarding readability and the performance of the Bézier curve. This experiment also serves as a preliminary study to evaluate how natural and therefore readable the respective robot-to-human approach appears when executed toward a walking person.

Method The third experiment is realized as an online video study. 239 participants were acquired resulting in 202 entirely completed questionnaires. Evaluation of the intention assessment is done with a binomial test against chance level.

Videos of the four approach motions used in the first experiment were recorded with the IURO robot approaching a walking person. A fifth video was then added as a control condition showing the Bézier shaped motion approaching a different position instead of the person. The approached person is chosen to be walking, because a single person standing in the room would directly convey the intuition that he/she must be approached, leading to an inadvertent priming of the subjects.

The recorded sequences of the five videos are each 5s long. The videos (each 5s) were cut into sequences of one, two, three, four and five seconds which leads to 25 video snippets. A participant in this 5×1 within-subject design will see one video of each of the five approach motions in random order whereby the length of the shown sequence is also randomized. Accordingly, the full robot-to-human approach is not always observed.

Subsequently to watching the video snippet, subjects are prompted to answer the question about the robot intention (Does IURO want to go to the person or not?). The correct answer is “to the person” for all motions except the case where the robot approaches another position. The hypothesis is that in case of shorter sequences subjects choose the correct answer (the robot goes to the person) more often if the readability of a motion is higher. Giving only the two answers, allows for a binomial test against the null hypothesis of chance level. Therefore, resulting numbers should be close to chance level for a one second video as people can only guess. The frequency of correct answers should increase with the snippet length, whereas the increase is faster if the approach is more readable.

After answering the question for the robot intention regarding the five video sequences, another five videos are shown to the participant in randomized order. These videos show the full five second versions of the robot-to-human approach trajectories. Subjects are

then asked to rate the naturalness of the approach on a 21 point scale as in the lab study, leading to a 5×1 within-subject design.

Procedure Subjects entering the online questionnaire were at first presented with a welcome note which further informed them about anonymity, privacy protection and data security. A short text then introduces the controls of the online questionnaire and requests the participant to watch each video attentively. Finally, participants were informed about the scenario they will see and the specified goal of the person, see Fig. 2.7.

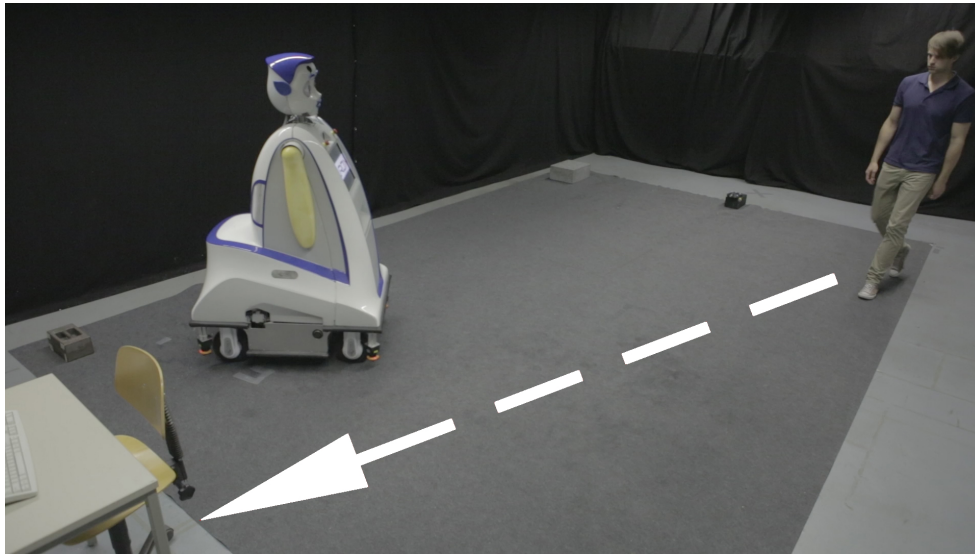


Fig. 2.7: Introductory scene to the video study with the Interactive Urban Robot (IURO) on the left and the person moving to its desk coming from the right

After this introduction they were presented with the randomized choice of video snippets for each robot-to-human approach motion and the stated question below the video. Subsequently to finalizing the first part, subjects were directly presented with the randomly ordered 5s videos asking for a rating of naturalness.

2.1.5 Results

The experimental procedures were approved by the ethics committee of the medical faculty of the Technische Universität München and conformed to the principles expressed in the Declaration of Helsinki. Prior to the experiment, all participants were asked for a written informed consent. None of the subjects had any motor disease or impairment.

2.1.5.1 Pilot-Study on Robot-to-Human Approach of a Standing Person

Results of the piloting experiment are depicted in Fig. 2.8. The velocity ratings are principally optimal with a trend to slow. Figure 2.8 top left shows mean and variance where 0 indicates “too slow”, 50 “optimal” and 100 “too fast”. For the stopping distance (within the personal space) $H_{0,A}$ also holds as it is rated comfortable, showing differences between sidewise and frontal approach. Mean and variance for stopping distance in Fig. 2.8 top

right are scaled from 0 “very uncomfortable” to 100 “very comfortable”. Significant results are found in the naturalness condition, see Fig. 2.8 bottom left. The scaling ranges from 0 “artificial” to 100 “natural”. The outcome shows significant differences comparing left and front right approach with $\sigma_{L,FR} = 0.019$ as well as right and front left/right approach with $\sigma_{R,FL} = 0.046$ and $\sigma_{R,FR} = 0.018$. The left and front left scenario diverge almost significantly with $\sigma_{L,FL} = 0.058$. For these conditions $H_{0,A}$ is rejected, supporting $H_{1,A}$ such that a significant influence of the shape of the approach path is assumed. The mean effect size assuming sphericity is medium to high with $F(3, 27)$, $p < 0.0001$, $\eta^2_{\text{partial}} = 0.586$. According to that, the power of 0.999 indicates that the naturalness condition is a strong benchmark for path shape taking into account the small sample size. Considering comments of the probates, the less natural rating for the frontal approach originates from the fact that the robot slightly turns away and then comes back towards the person, see Fig. 2.5. Probates refer to this movement as “hard to interpret”. The sensation rating is scaled from 0 “very uncomfortable” to 100 “very comfortable” showing a slight difference between frontal and sidewise approaches, as shown in Fig. 2.8 bottom right. Overall, the

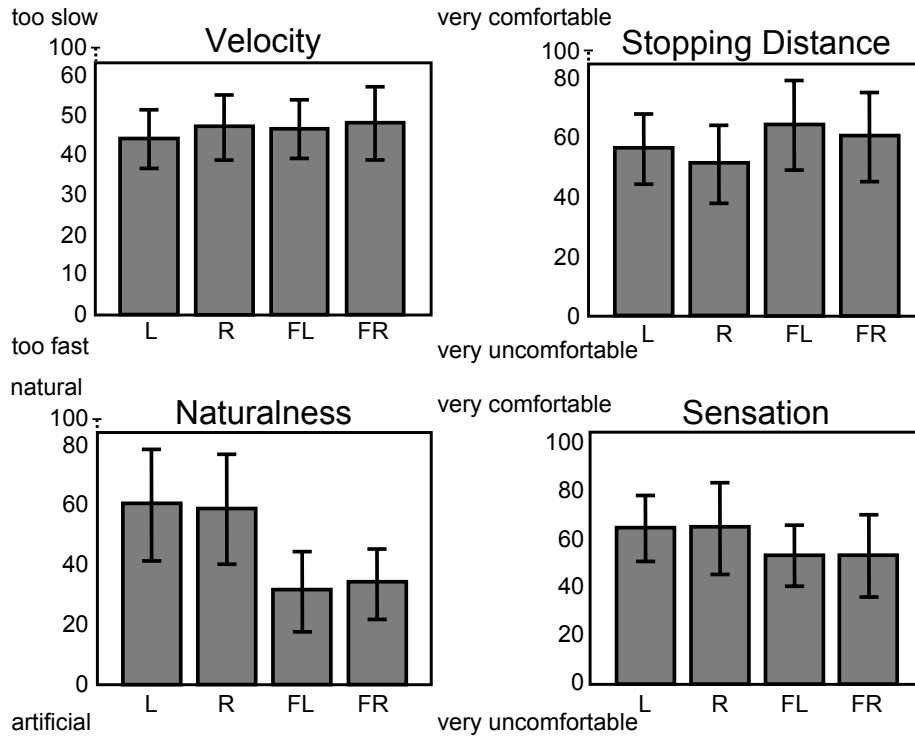


Fig. 2.8: Descriptive statistics with mean and standard deviation. Results are given for the approach directions L=left, R=right, FL=frontal left, FR=frontal right

approach behavior is rated as comfortable and natural, showing that people are not intimidated by the robot. It is obvious that the shape of the trajectory plays an important role in the apperception of the robot locomotion.

Following studies will therefore investigate naturalness and sensation for robot-to-human approach with varying trajectory shapes. The method applied here is then compared to a very simple movement that also allows turning on spot and to a complex optimal control based method for the generation of human locomotion trajectories.

2.1.5.2 Comparative Robot-to-Human Approach Study with a First-Person View

Results of the approach motion ratings for the follow-up first-person study are shown in Fig. 2.9. Since the scale is ordinal and a procedure which is robust against outliers is preferred, the median values are compared instead of the means. Fig. 2.9 shows boxplots for each criterion within each scenario. The notches span $\pm 1.58 \frac{\text{IQR}}{\sqrt{n}}$ where IQR (Interquartile Range) is the difference between the third and the first quartiles and n is the number of observations. This roughly equals a 95% confidence interval for comparing medians [116].

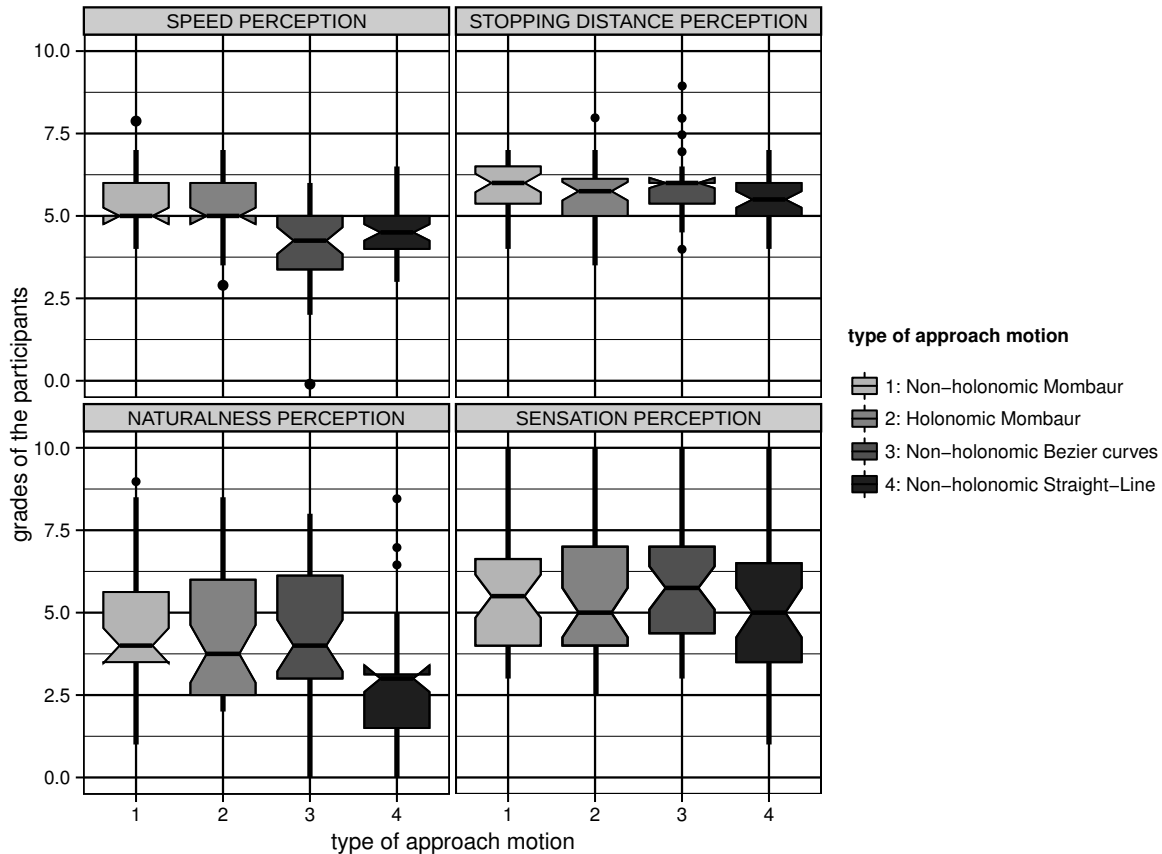


Fig. 2.9: Notched boxplots describing the rating results for speed, distance, naturalness and sensation of each approach path (first-person)

The top left and right plots in Fig. 2.9 show the velocity and distance ratings, which are optimal in the mean value showing variances which are mostly related to individual preference. The Bézier based approach motion is rated as a little too slow. This originates from the parametrization of the distance where the robot starts slowing down which is chosen to be 2 m . Therefore, the average velocity is at 0.45 m/s instead of the 0.5 m/s . The first two approach motions feature this behavior as well without specific parametrization. This leads to the interpretation that the deceleration for the Bézier approach is too drastic. Obviously, the velocity of 0.5 m/s is near optimal with respect to the static setting, the robot design and the fact that the subject is expecting to be approached. For the straight-line approach, velocity is rated too slow as the procedure of turning-driving-turning takes more time than the other motions. The velocity on the straight path is set to 0.5 m/s

as well, yet the turning motion is rather slow with 0.5 rad/s. The re-orientation of the wheels and the acceleration of the robot from a static state creates some delay for this small turn. The bottom left plot shows the naturalness ratings, which are equally high for all three human-like approaches and expectedly low for the simple straight-line motion. Bottom right illustrates the sensation rating, which suggests that all approaches are equally comfortable. Since the parameters for social acceptance (e.g acceleration limits, approach speed, approach angle and final distance) were equal for all four motions, it is concluded that comfort is closely related to social acceptance.

In order to gain more insight into the differences between the four scenarios, they are compared to each other with respect to each criterion. This exploratory analysis based on a Post-Hoc test provides a quantification for the initial assumptions and the results in Fig. 2.9. The most important comparison is conducted for the naturalness criterion between the three human-like and the non-human-like approach motions. Additionally, it is expected that velocity, distance and sensation do not vary significantly between the four motions, since the applied constraints that affect these aspects are similar.

As the confidence intervals in Fig. 2.9 are symmetric and do neither consider multiple testing nor dependencies within the data, a Friedman test is conducted for each criterion [65]. Because the found p-values are below the standard 5% significance level for all criteria except sensation, Friedman Post-Hoc analysis is conducted, with its results shown in Fig. 2.10.

Tab. 2.2 summarizes the quantitative results. Pairs of scenarios with statistically significant differences are shaded gray.

Tab. 2.2: p-values resulting from the Friedman Post-Hoc analysis on the four criteria for all scenario pairs (first-person)

	scenarios	p-value		scenarios	p-value
SPEED	1-2	0.89494	STOPPING	1-2	0.67575
	1-3	0.00000		1-3	0.96180
	1-4	0.00004		1-4	0.09947
	2-3	0.00000		2-3	0.37275
	2-4	0.00116		2-4	0.64516
	3-4	0.35259		3-4	0.02764
	scenarios	p-value		scenarios	p-value
NATURAL	1-2	0.92029	SENSATION	1-2	0.99249
	1-3	0.98886		1-3	0.89891
	1-4	0.00006		1-4	0.65280
	2-3	0.77523		2-3	0.97555
	2-4	0.00100		2-4	0.47610
	3-4	0.00002		3-4	0.24805

Quantifying the increase in readability, the Post-Hoc test shows significant differences for naturalness between the human-like and the non-human-like approach motions. The analysis of the results in Fig. 2.9 and Fig. 2.10 reflects the expected preference of subjects towards trajectories with human-like locomotion features. Thus the $H_{0,A}$ is rejected for

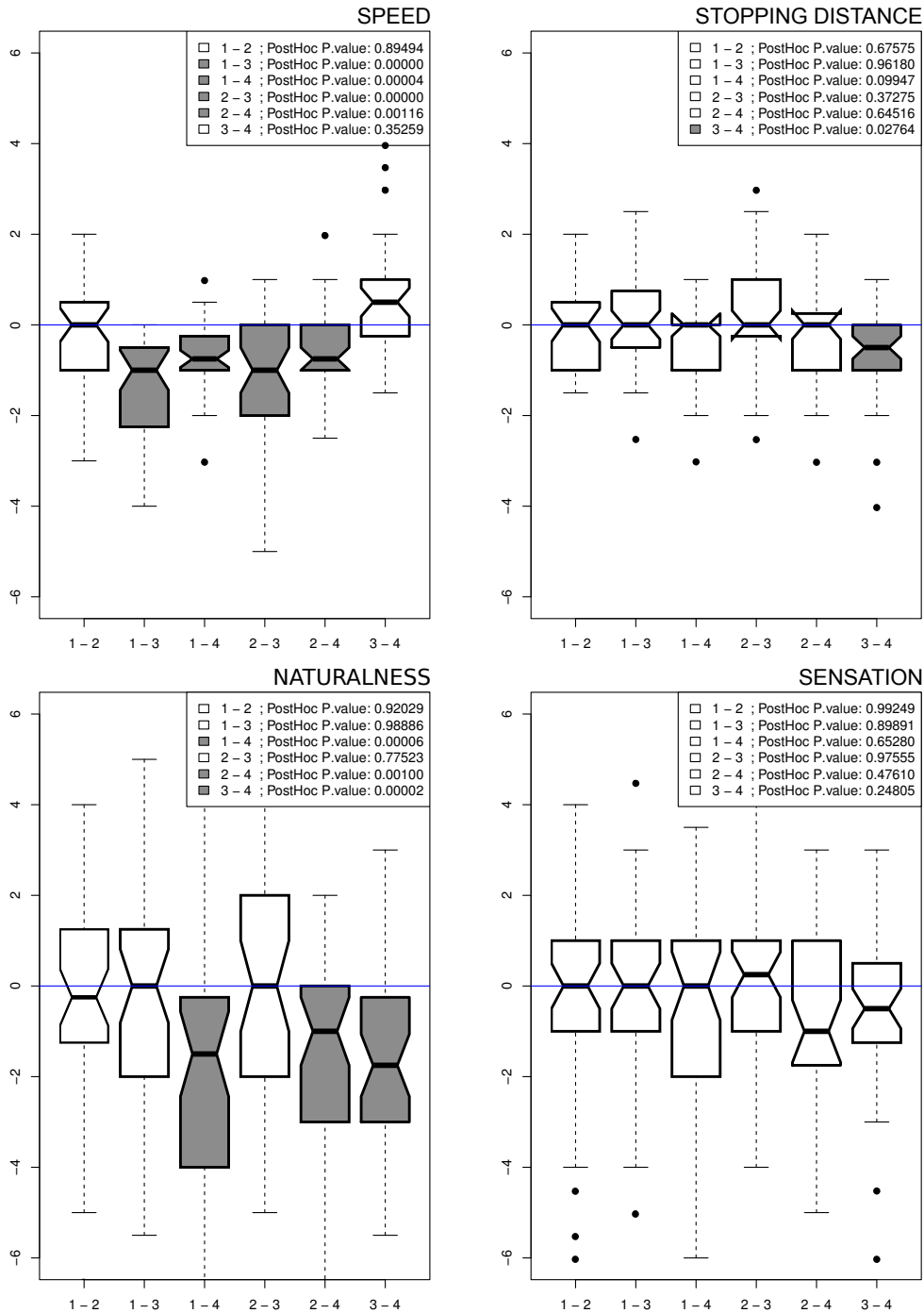


Fig. 2.10: Notched boxplots for the Friedman Post-Hoc analysis on the four criteria for all scenario pairs, where significant differences are shaded gray (first-person)

these pairs and it is concluded that human-like trajectory features have significant influence on the perceived naturalness of locomotion in a social-context. As it was derived from literature, naturalness of a motion should affect readability strongly. This supports the hypothesis that the robot ability to initiate interactions is supported by readable human-like locomotion. Accordingly, the second experiment will build on this result.

The bottom right plot in Fig. 2.10 depicts that sensation did not vary significantly

between the four scenarios. All p-values from the Post-Hoc analysis are above 5% for this criterion. This corresponds to the equality in constraints ensuring equal social acceptance of each approach motion. Hence, $H_{0,B}$ is not rejected. It also suggests that the assumption of similar social acceptance of each approach motion holds, given that comfort correlates with social acceptance [95, 96]. Although the correlation of comfort and social acceptance was established in literature, further studies must revisit this result and run a social acceptance questionnaire in parallel.

The top left plot in Fig. 2.10 confirms the results in Fig. 2.9 regarding the velocities of the different motions. As derived from Fig. 2.9, the Bezier based motion and the straight-line motion are overall rated as slower.

The plot regarding “stopping distance” in Fig. 2.9 does not show any significant deviations, which reflects the equal parametrization of the four approach motions. However, in the case “stopping distance” 3–4 Fig. 2.10 shows p-values contradictory to the median confidence intervals of Fig. 2.9. Analyzing this occurrence, it was found that it results from the different construction of the tests, specifically whether multiple testing is accounted for or not. Generally the Friedman test should be preferred in its propositions.

In conclusion, a robot-to-human approach trajectory modeled with human-like locomotion features is significantly more effective in conveying the expected intention. Since participants were informed about the robot goal, their expectation ξ_{R-G} is met more precisely by human-like locomotion as indicated by the perception of naturalness. The increase in readability can be inferred from the described correlation to naturalness and human-likeness. Yet, the second experiment attempts to further investigate this connection. Furthermore, the human-like features of Bézier curves are similarly effective as the specifically modeled human motion. This implies that the trajectory features introduced by Bézier curves elicit equal readability.

2.1.5.3 Comparative Robot-to-Human Approach Study with a Third-Person View

A one sided Binomial Test with a confidence level of 0.95 is conducted, evaluating the frequency of correct answers (the robot wants to go to the person) to be significantly greater than chance level. The results are shown in Tab. 2.3.

The table rows resemble the snippet length (1s - 5s) of the viewed video and the columns relate to the approach type. The first and second column represent the non-holonomic (Type 1) and holonomic (Type 2) human motions [121], the third is the Bézier shaped motion (Type 3) [7], the fourth is the straight-line approach motion (Type 4) and the fifth is the control condition (Type 5), where IURO does not go to the person (the correct answer here is inverted accordingly). Table 2.3 contains the frequency of correct answers over the sum of all answers (corr./sum), the confidence intervals (conf.) and the p-values for each combination. The acquired data from the online study contained unfinished or canceled questionnaires. However, all answered questions regarding the intention of the robot were used in the shown evaluation. This leads to the differences in the sum of answers among the combinations of videos and snippet lengths.

If a p-value in the table is below the significance level of 0.05, the null hypothesis $H_{0,D}$, that the intention was simply guessed, is rejected. One can see that the control condition is predominantly tagged correctly, which is probably related to the clear orientation of the

Tab. 2.3: Answer frequencies, confidence intervals and p-values from the binomial test against chance level for the question about the robot intention with significant p-values marked gray (third-person)

Video in [s]	Type 1	Type 2	Type 3	Type 4	Type 5
1s					
corr./sum	20/37	13/37	11/49	10/31	45/48
conf.	0.3938	0.2219	0.1313	0.1866	0.8463
p-value	0.3714	0.9765	0.9999	0.9853	<0.0001
2s					
corr./sum	28/43	35/46	29/40	27/49	35/40
conf.	0.5148	0.6354	0.5861	0.4241	0.7550
p-value	0.0330	0.0002	0.0032	0.2841	<0.0001
3s					
corr./sum	43/56	33/46	28/38	14/34	40/43
conf.	0.6565	0.5887	0.5946	0.2688	0.8294
p-value	<0.0001	0.0023	0.0025	0.8853	<0.0001
4s					
corr./sum	35/49	35/43	39/41	20/39	36/41
conf.	0.5899	0.6893	0.8543	0.3714	0.7605
p-value	0.0019	<0.0001	<0.0001	0.5000	<0.0001
5s					
corr./sum	37/43	31/36	34/42	41/54	37/39
conf.	0.7431	0.7299	0.6825	0.6447	0.8472
p-value	<0.0001	<0.0001	<0.0001	<0.0001	<0.0001

robot, away from the person. The one second videos serve mostly for completeness, since it is hardly possible to understand the intention from this short movement. Accordingly, the p-values are well above 0.05. Within the 5s snippets the full motion to the human is shown such that the resulting p-values must be below 0.05. Yet, it is observed that many subjects did not believe that the robot really intended to approach the person. For 2s – 5s the non-holonomic Bézier based motion shows an equal performance as the non-holonomic and holonomic human motion. Even short sequences of the executed trajectories are capable of conveying the intention. The straight-line approach motion does not convey the robot intention unless the full approach is seen in the 5s snippet.

The confidence intervals in Tab. 2.3 support this analysis. Their values are well above 0.5 if the p-value is below 0.05, which further confirms that the answers were not randomly guessed. An exception is the combination of the 2s snippet with the Type 1 motion.

The results depict that it was easier for subjects to understand the robot intention when its locomotion was based on human or human-like features. This holds for a third-person view and the approach of a walking person as confirmed here. The results also support the proposition that basic features of the motion matter most, such as the proposed smoothness of the path. Furthermore, it is shown that the concept of readability is applicable to agents that are not involved in the approach interaction.

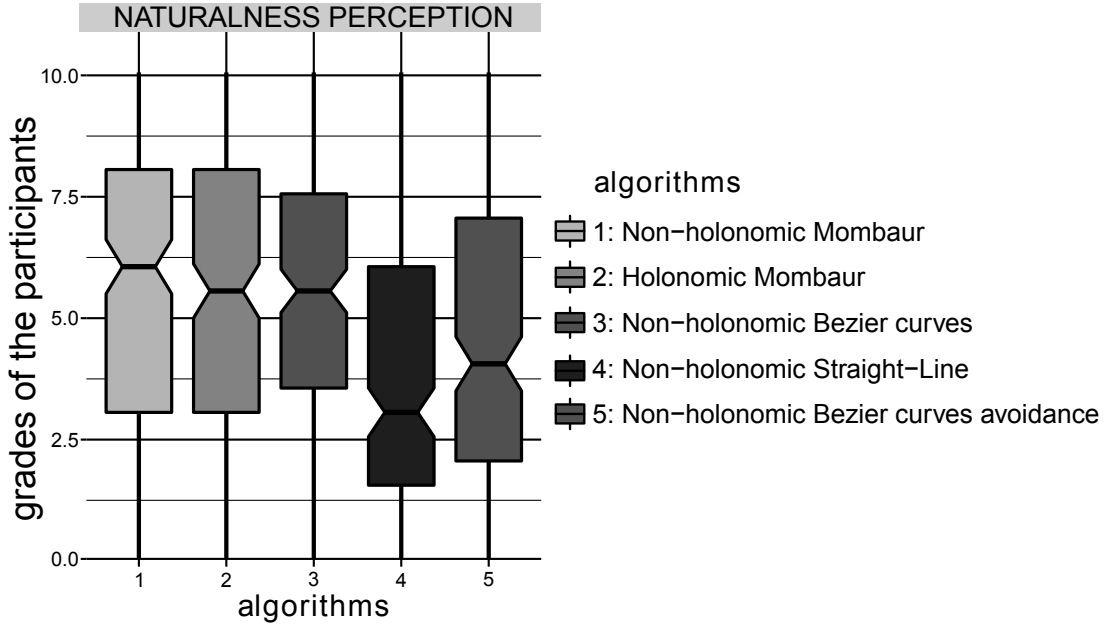


Fig. 2.11: Notched boxplots for the naturalness rating of each approach path (third-person)

Subjects further rated the naturalness of the five conditions shown to them. Fig. 2.11 presents the results again by resembling notched boxplots. Clearly, the online-study setup leads to a larger variance in the ratings. The ratings are in line with the results from the first experiment, showing high naturalness for the three human-like approach motions. In order to investigate the differences between the five scenarios in more detail, a Friedman Post-Hoc analysis is also carried out on the naturalness ratings of the second experiment. This allows for a detailed evaluation of the influence of the human-like trajectory features and enables a comparison to the first experiment. Fig. 2.12 shows the results of this Post-Hoc analysis. The resulting p-values are summarized in Tab. 2.4. Pairs of scenarios with statistically significant differences are shaded gray.

Tab. 2.4: p-values from Friedman Post-Hoc analysis on the naturalness rating (third-person)

	scenarios	p-value
NATURALNESS	1-2	0.6535
	1-3	0.7549
	1-4	4.9e-11
	1-5	1.6e-06
	2-3	0.9998
	2-4	4.6e-07
	2-5	1.3e-03
	3-4	1.6e-07
	3-5	6.6e-04
	4-5	0.4918

The Post-Hoc test reveals that the null hypothesis $H_{0,E}$ may be rejected when comparing the human or the human-like motions with the straight-line approach motion. The human

and human-like motions perform significantly better than the non-human-like motion, as it is visualized in Fig. 2.12 and Tab. 2.4. It is notable that using an approach motion for avoidance seems to be very unnatural to most subjects.

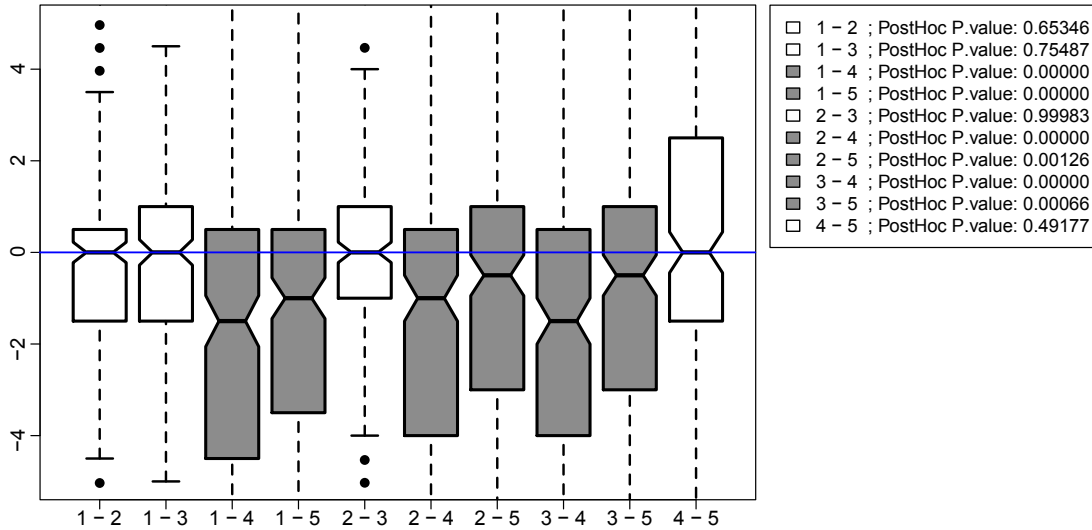


Fig. 2.12: Notched boxplots for the Friedman Post-Hoc analysis on the naturalness rating for all scenario pairs, where significant differences are shaded gray (third-person)

These results support the hypothesis that human-like approach motions are more easily readable than movements without according features. Even short observations of the motions are sufficient to convey the correct intention. When comparing the Bezier based approach with the human locomotion, the results indicate that the basic features of human-like locomotion have a strong influence on the apperception. The integration of sideway motions does thereby not lead to strong deviations between the ratings for human-like locomotion. Obtained results regarding naturalness of robot-to-human approach motions acquired in a lab environment are further shown to hold for a third-person view and the approach of a walking person. Human and human-like locomotion are again rated significantly more natural compared to the non-human-like version. These results show that human-like locomotion features enable a robot to quickly succeed in nonverbal interaction initiation while respecting social context.

2.1.6 Discussion

This section focuses on the problem of nonverbal interaction initiation during locomotion of an autonomous mobile robot. This ability is elaborated in the social context of locomotion for a robot-to-human approach. It is proposed to enhance the readability and social acceptance of the robot locomotion in order to improve its ability to initiate interactions with humans nonverbally. According robot-to-human approach trajectories are generated using optimal control models that are extended by hard and soft constraints to model human-like locomotion features and socio-contextual aspects. The planned locomotion trajectories clearly convey the intention of the robot due to their readability and further increase its social acceptance. This improves the ability of the mobile robot to initiate

interaction on a nonverbal level.

Three user studies particularly investigate the influence of path shape, path smoothness and torso orientation of the robot during locomotion. The pilot-study revealed that the shape of the robot-to-human approach path has significant influence on the apperception of the motion. In the second experiment the pilot study is extended by comparing four distinct approach trajectories. It is shown that human-like locomotion features significantly influence the perceptibility of the robot intention. Within the third experiment participants of an online study are presented with videos of the four approach scenarios featuring a moving target person. This experiment reveals that human-like approach trajectories externalize the intention of the robot within a shorter time horizon and must be assumed as more readable.

This section confirms the hypothesis that readable robot locomotion that incorporates socio-contextual constraints improves the pro-active interaction initiation capability of a mobile robot. The readability of robot locomotion is thereby enhanced by incorporating human-like trajectory features. In order to identify the most important trajectory features, robot-to-human approach trajectories are compared that differ in path shape, path smoothness and robot orientation along the path. Yet, distinctive features of human-like motions may differ depending on the task. The conducted user studies reveal that trajectories with human-like locomotion features appear significantly more natural and thus readable than the non-human-like version. The readable locomotion enhances nonverbal interaction initiation as it appears natural and elicits comfortable sensation while quickly indicating the intention of the motion. Notably, even short observations of the motions are sufficient to convey the correct intention. Readability and social acceptance are defined as dependent on the compliance with human expectations towards the robot intention, given the observed trajectory. The integration of sideways motions does thereby not lead to strong deviations between the ratings for human-like locomotion. Social acceptance, as an important factor in interaction initiation, is enhanced by constraining the robot locomotion with respect to a set of socio-contextual aspects. The posed hypotheses are further shown to hold for a third-person view and the approach of a walking person.

Readable and socially compliant locomotion is modeled using an optimal control framework adding socio-contextual constraints as well as formative features of human-like locomotion. The proposed model, which is based on Bézier curves, performs equally well compared to the human derived models in terms of perceived naturalness, sensation and intention conveyance capability. This validates the assumption that Bézier curves comprise most formative features for human-like locomotion. This result also indicates that the basic features of human-like locomotion have a strong influence on the apperception.

Obtained results are generalizable to a variety of applications and anticipated to apply to mobile robots just as well as to flying or underwater systems. Locomotion in populated urban or industrial environments and tight collaboration with humans are imaginable application scenarios. Clearly, the benefit of diminished disturbance during locomotion due to mutual influence between agents is a capability gained only by robots that move readably and externalize their intention. Future insights into human-like locomotion in social contexts will thus allow for seamless robot navigation in shared environments.

2.2 Effectiveness of Human-Like Locomotion in Cooperative Navigation

With respect to Sec. 2.1, robots are envisioned to leave closed and structured environments like factories and to seamlessly integrate into human populated environments. Accordingly, social aspects have to be considered within all types of behavior. The previous section as well as literature show, that compliance with social aspects increases acceptance, comfort and perceived safety of robots when they share a workspace with humans [7, 9, 110]. Therefore, considering social norms is a recent challenge when planning motions for mobile robots and robotic manipulators. As mentioned before, social aspects are typically accounted for by considering features of human-likeness within robot motion [31]. Along these lines the terms readability, legibility, predictability and anticipation are widely used in this research area. These terms describe the effect, that it is easier for humans to predict and understand the purpose of motions if they are human-like [7, 49, 111].

Despite these facts, there is still a versatile discussion among researchers whether human-like behaviors or human-like locomotion needs to be employed by robots. One argument is that robots are better off behaving and moving “robot-like”, while humans should accustom to the new agents in their workspace. However, habituation effects and familiarization with robot motion are shown to yield a minor effect on collaboration performance, compared to specifically shaped human-like movements [50]. The “Media Equation Theory” [147] and the associated research field of social robotics show, that the performance of human-robot collaboration is improved on many levels when robots employ human-like behaviors and respect socio-contextual aspects [31, 35, 51, 88, 110, 170]. Yet, the benefit of social aspects is still questioned, especially within locomotion.

This section addresses this problem with respect to robot locomotion, which is considered as a form of collaboration in a joint workspace. In this context, the goal is to demonstrate a distinct advantage of socially compliant locomotion, that goes beyond pure apperception as in Sec. 2.1. Thus, it is shown that readability and human-likeness of robot locomotion are effective in reducing the planning effort for all agents that share an environment. In fact, cooperative locomotion greatly benefits from human-like robot behavior, as this strongly facilitates the reliability of mutual predictions. The enhanced predictions allow agents to detect and resolve potential collisions earlier and thereby with less effort.

In the following section it is analyzed how humans react to a non-human-like robot that clearly conveys its intention and complies with human-like behaviors during locomotion. Therefore, humans are considered as optimal control systems which intend to minimize energy consumption and cognitive load [30, 186]. Within optimal control, planning effort is defined as the result of a re-planning process which leads to cognitive load and path adaptations. Adapting a path thereby raises energy cost due to applied controls. Hence, effort is minimized if the initially planned trajectory is not disturbed and no adaptations are necessary. Consequentially, effective locomotion in shared environments implies minimum effort for all agents, which means robots or humans. This is supported by readable human-like robot locomotion since it improves mutual predictions.

The effect that readable locomotion is able to reduce the planning effort for other human agents, is demonstrated in a mutual avoidance experiment. The experiment is designed as a

two-stage study that compares a human-human with a human-robot avoidance experiment. Given a fully observable environment with known paths for all agents, humans are able to follow the minimum effort principle successfully, as they do not need to rely on uncertain predictions. In the experiment it is examined if it is possible for a human to apply this to a partially observable environment as well, given that other agents externalize their intentions nonverbally and thus allow for reliable predictions. This hypothesis is then expanded by assuming that the counterpart may be a robot, which is moving in a natural, human-like and readable way.

The evaluation of this experiment requires methods to analyze sets of locomotion trajectories. This is usually accomplished by a qualitative comparison of the data from different conditions. Within Chap. 4 of this work a method is presented which focuses on integrating data variance into trajectory analysis. The proposed procedure is then expanded by a statistical method for quantitative trajectory analysis. Trajectories are filtered using penalized thin-plate regression splines (PTPRS) and are then compared using standard measures such as Hausdorff distance or Dynamic Time Warping (DTW). The developed “pivot analysis”, which is based on the resulting distance values, then quantifies differences between sets of trajectories from different experiment conditions. These procedures are applied here and analyze whether an observed behavior is generalizable or an incidental occurrence owing to the study setup.

As a main contribution the effect and benefit of readable locomotion applied on a mobile robot is shown in this section. Re-planning effort for human agents and the robot is diminished, since mutual prediction is facilitated. Therefore, collisions are avoided prematurely and smoothly due to clear nonverbal conveyance of intention. Results of the comparative experiment also show, that effort is higher and navigation performance is lowered accordingly, if the robot behavior does not comply with expected human-like behavior. This complements recent findings towards the benefits of legibility in cooperative manipulation tasks [51]. The experiments and the accompanying analysis also confirm that humans expect non-human-like robots to act readable [66] and in accordance with a cognitive model for human locomotion [71]. Works using manipulators in this respect, do not generalize to locomotion well. For data analysis, the methods proposed in Chap. 4 are used and yield confidence intervals for the measured human locomotion data. The presented results address a benefit of readable robot locomotion that was only marginally considered until now. It will support the ambition to model seamless interactive navigation based on human-like behaviors [91, 157, 177]

The proposed insights into the effects of readable locomotion will influence a variety of applications and enable robots to integrate seamlessly into human environments. Furthermore, the results yield a strong argument for the integration of social aspects and human-like behaviors in robot locomotion. Human-robot collaboration shows enhanced performance when nonverbal interaction is considered [35, 51, 88]. Tasks involving cooperative assembling, carrying or simply navigation in a shared environment are improvable. The understanding of human behaviors is further capable of being integrated in prediction and tracking applications [171]. Thereby, knowledge about certain behaviors may increase performance when predicting sudden reactions.

This section is organized as follows: Subsec. 2.2.1 discusses literature related to motion

readability and avoidance. The following Subsec. 2.2.2 gives a detailed problem formulation about the definition of effort. An experiment design is proposed in Subsec. 2.2.3 with the results shown in Subsec. 2.2.4. These are discussed in Subsec. 2.2.5.

2.2.1 Classification within the State-of-the-Art

Avoidance motions have been studied widely by psychologists, sociologists and in robotics. The general goal is to resolve collisions in accordance with a minimum effort principle, meaning as early as possible to keep progressing at an optimal speed and path without the need for re-planning. As this is possible if intentions are clearly externalized, readable locomotion is suggested here as a solution to minimize planning effort. Yet, the positive effects beyond apperception that readability yields, when employed by mobile robots, have rarely been considered by distinct experiments.

2.2.1.1 Human-Human Interaction during Locomotion

Fundamental theories are provided by research regarding the behavior of pedestrians. The underlying concept of readable motion is described by observations made by Erving Goffman during his field studies [71]. The term “externalisation” is used by Goffman to name the use of “overall body-language” to make desired future motions readable and thereby intentions clearer in a nonverbal way. Goffman further elaborates on the theory that humans are constantly “scanning” the area in front where they are going to walk towards and also expect others to do so. Further, the “scanning” is performed in order to perceive nonverbal cues from others to avoid collisions mutually. The result of these processes is described as an automated “coordination of actions” between two persons. Wolff [185] mentions similar observations as Goffman. Pedestrians for example position their head to peek over the shoulder of the person in front, which allows sensing and prediction. He further finds some specific behaviors employed by pedestrians to avoid collisions depending on the density of people in the scene like a “step-and-slide” behavior. Wolff also describes a difference in behavior based on gender with respect to avoidance distance. Personal space plays a side role as it only defines how close people will come when avoiding. Yet, it is interesting when experiments are conducted with a robot. An important work in this area is posed by Edward Hall [75], who introduces human proxemics. His theory is expanded to various situations in follow-up work [36, 76, 161, 162]. In [30, 186] further observations about pedestrian behavior in public space are discussed. Authors give insight into social norms affecting pedestrian behavior. Especially Bitgood et al. elaborate on the fact that humans intend to minimize energy consumption during walking.

With respect to the experiments conducted in this work, literature on avoidance behaviors must be considered. Basten et al. [24] are concerned with the synthesis of human like behavior for virtual characters in computer games but do not transfer the findings to human-robot-interaction (HRI). The described experiment is similar to the setup in this work. Analyses opt to measure “collaboration”, “clearance”, “anticipation” and “synchronisation” by examining the contribution of each agent to the overall avoidance distance, the minimum distance between both agents and the timing of each agent’s path adaptation. The impact of gender and body height is analyzed as well. Realistic collision avoidance

for virtual characters is also studied in [87]. A rule based model for the anticipation of collisions is proposed based on the Time-To-Collision measure. Within their experiments heads-on and right-angle collisions are considered. The method of [127] transfers trajectories into a velocity-curvature space in order to distinguish between straight walk and turns. For classification a feature is acquired within velocity-curvature space by generating a mean from regression and a 95% confidence interval. Models for virtual characters based on experimental results are also in the focus of [138, 141, 151]. The models mainly address interaction between pairs of walking humans and model collision avoidance with fixed rules for orientation and velocity adaptation. A fundamental work for many researchers in the field of human locomotion behavior is provided by Fajen et al. [59]. They propose a constant velocity steering model for avoidance which is derived from human data. The approach is valid for static environments where obstacles may suddenly appear. In [62] the difference between chosen locomotion paths in real and virtual environments is examined. It is shown that humans are well able to project their physical behavior.

Experiments where an interfering but not interacting person (interferer, intruder) crosses a subject's path from the side (usually at 90°) are considered by many researchers [14, 23, 80, 100, 101, 129]. The authors study this case intensively and propose models that are applicable to robots. Focus is set on the avoidance strategies that humans employ within this situation. Typically the occurrence of either velocity or path adaptations is discussed and the reasons for the respective behavior. A definite common principle is hard to define as influential factors are widespread. Some approaches name velocity adaptations as the general behavior [23], whereas others favor a mix of velocity and path adaptations [129]. Readability as a factor to improve collision avoidance behavior is only considered in [100] with a focus on the acceptance of the robot. The reciprocal influence is taken into account in [128] but not with respect to an application in robot locomotion.

2.2.1.2 Human-Robot Interaction during Locomotion

Mobile robot navigation and collision avoidance is a wide research field with a large variety of approaches for obstacle modeling and robot control. Aspects of social navigation and human-like motion behaviors are integrated in many recent navigation algorithms [149]. Kirby et al. [92] propose a framework that integrates socially motivated cost into the robot navigation process. Models for mutual collision avoidance incorporate social aspects and are based on data recorded from walking humans [26, 77, 140, 143, 176, 177, 184]. These methods assume that humans expect robots to follow the socially motivated scheme where motion prediction is based on externalized intentions. However, this assumption is not directly analyzed. Readability as a factor to improve collision avoidance behavior is only considered in [100, 101] with a focus on the acceptance of the robot. Pacchierotti et al. [132] study the comfortable distances for robots to avoid a human in a corridor when resolving a possible heads-on collision situation. The experiment does not reveal how people read the robot motions or whether nonverbal intention conveyance is effective in this situation. Yet, they state that people are expecting cues from the robot to allow for a judgment about the subsequent behavior.

Some works are concerned with the effects and benefits of social or human-like behavior, but without the direct transfer to robot locomotion. In [93] the proposed model may be

understood as an integration of Goffman’s concept into classical human-robot interaction schemes. Authors attempt to leverage the classical HRI model where the robot is simply a task completer. Capabilities for “eliciting” and “reading” behavioral cues regarding the ongoing interaction is shown to be effective in task completion. The proposed model is strongly related to the theory of readability in locomotion, where a robot elicits cues in order to externalize its intention. Dragan et al. [51] show that their interpretation of legibility for robot manipulation tasks enhances collaborative task completion. By comparing purely functional with legible and predictable motions, a reduced task execution time and “more fluent collaboration” is discovered for the legible case. These results as well as the study setup are thereby not applicable to locomotion experiments. The effectiveness of social behaviors is also tackled in [35]. Interactivity and social context (spatial distance) is exploited to enhance task performance. An application for intention estimation from humans and intention externalization by a robot is presented in [88]. Both is used on a shopping mall assistant robot that chooses its own behavior based on its detection results. Appropriate reaction to estimated intentions thereby improves success in interaction initiations for the robot.

Generally, the presented works integrate social aspects into global path or motion planning for robots, to enhance collaboration and robot acceptance. Yet, it is not analyzed if there are further benefits besides the fact that human-robot collaboration is perceived as more convenient [91, 157]. Accordingly, this section demonstrates that the facilitated predictions lead to a reduced motion planning effort for all agents in a shared environment. This implies that human-like, and therefore readable, locomotion will enable robots to seamlessly integrate into shared environments, because collisions are resolved mutually and thus with less effort.

2.2.2 Problem Description

In order to understand the process of human locomotion planning and the expectations of humans towards other agents in the same workspace, some underlying cognitive theories need to be considered. The following further discusses typical human behaviors and underlying principles that define locomotion performance with respect to effort.

2.2.2.1 Cognitive Theories of Human Locomotion

Humans plan and execute their movements following a minimum effort principle [163]. This behavior also applies to locomotion where the shortest and most energy efficient path is commonly chosen [30]. If this path is disturbed, e.g. by another agent, a human will attempt to re-plan its trajectory and choose the most efficient but collision free path. Typical strategies for resolving the collision situations are changing speed and path [80]. Yet, humans try to keep a preferred speed that minimizes their energy consumption [117], so a change in velocity is costly and usually avoided in favor of path adaptations. Progressing with minimum effort in a populated environment is facilitated by mutual reactions between all agents [176]. It requires humans to include other agents into their trajectory planning process by predicting their trajectory and intentions. This behavior is also expected from any other human being in order to facilitate seamless locomotion in a shared environment

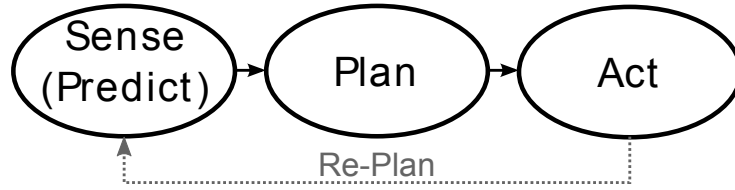


Fig. 2.13: Simplified cognitive process for human trajectory planning derived from [71, 126]

[66]. The underlying cognitive process is described by Goffman [71]. He reports that humans are able to navigate seamlessly and efficiently because they read each others intention. The cognitive model of sense–plan–act [126], see Fig. 2.13, appropriately models Goffman’s observations. It describes how humans repeatedly scan the locomotion of others and integrate the observations into their personal path planning. The work at hand adopts this cognitive model with the addition of a prediction stage between sensing and planning. The prediction step emphasizes that humans must predict the future position of other agents to plan accordingly [80]. Predicting trajectories and intention follows the psychological scheme [43] also described in Sec. 2.1:

- Action-to-Goal inference: humans try to predict the result (e.g. goal) of an action (e.g. locomotion trajectory) given their observation history
- Goal-to-Action inference: humans try to predict the characteristics of an action (e.g. trajectory shape) given their knowledge of the goal

Thus, a human observing another agent’s trajectory ξ_{S-R} (between pose S and R) infers a certain goal G from a set of possible goals \mathcal{G} given his expectation \mathcal{E} :

$$\mathcal{E}(\xi_{S-R}) = G \in \mathcal{G}.$$

If the goal G is known beforehand, a trajectory ξ_{S-G} is inferred based on the situation:

$$\mathcal{E}^{-1}(G) = \xi_{S-G}.$$

Humans expect others to behave similarly and externalize their intention nonverbally to facilitate seamless cooperative locomotion [66]. This assumption is supported by the fact that the minimum effort principle applies to every agent. Following [66], the hypothesis is posed that humans project this interdependence onto robots as well, similarly to the expectation of social behavior [125, 147]. The conception of effort in this work is also derived from these assumptions. Given that the exchange of intentions is successful and the mutual predictions are reliable, potential collisions are resolvable early and without effort. In case of the opposite, both agents must apply strategies to resolve the situation. This is usually accompanied by higher energy costs and thus higher effort, due to sudden movements and velocity adaptations. The following subsection elaborates on this problem from a control theoretic point of view.

2.2.2.2 Control Theoretic Locomotion Model

In order to develop a common definition of effort in locomotion, this work models humans as optimal control systems, similar to [14, 19]. This view complies with literature and reflects the human ambition to minimize effort during locomotion. With respect to a changing or even surprising and non-fully observable environment, applicable models that consider the prediction and planning step repetitively are model predictive control (MPC) approaches. In [14] the locomotion of a human is treated as a receding horizon problem with equal length control and prediction horizon $T_C = T_P$. This problem is recapitulated here with respect to the notation in [16] and simulated using the ACADO Toolkit [12]. The two-point boundary value problem is solved repeatedly each time-step δ using a direct method. The current closed-loop state $\mathbf{x}(t)$ and the closed-loop control $\mathbf{u}(t)$ at the current starting time t are taken into account as the initial boundary. Desired goal position $p_G(T) = (p_G^x(T), p_G^y(T))$ and orientation $\varphi_G(T)$ form the final boundary that the controller uses as set-point. Solving the open-loop optimal control problem yields the predicted state $\bar{\mathbf{x}}(t)$ and the open loop input $\bar{\mathbf{u}}(t)$. The used MPC scheme is illustrated in Fig. 2.14.

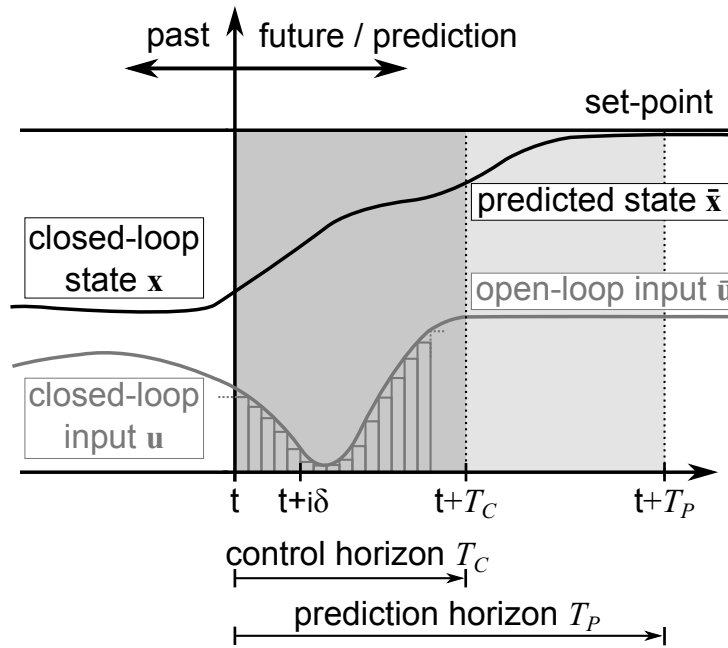


Fig. 2.14: Illustration of an MPC process (inspired by [16])

The dynamic model $\dot{\mathbf{x}}(t) = f(\mathbf{x}(t), \mathbf{u}(t), t)$ with $\mathbf{x}(0) = \mathbf{x}_0$ used in this work, describes a unicycle as proposed in [14, 18, 121], where:

$$\dot{\mathbf{x}}(t) := \frac{d}{dt} \begin{pmatrix} p^x(t) \\ p^y(t) \\ \varphi(t) \\ v(t) \\ \omega(t) \\ a^v(t) \\ a^\omega(t) \end{pmatrix} = \begin{pmatrix} v(t) \cos(\varphi(t)) \\ v(t) \sin(\varphi(t)) \\ \omega(t) \\ a^v(t) \\ a^\omega(t) \\ u_1(t) \\ u_2(t) \end{pmatrix},$$

with constrained states and inputs:

$$\begin{aligned}\mathbf{x}(t) &\in \mathcal{X} \quad \forall t \geq 0, \\ \mathbf{u}(t) &\in \mathcal{U} \quad \forall t \geq 0,\end{aligned}$$

where $\mathbf{x}(t) \in \mathbb{R}^n$ and $\mathbf{u}(t) \in \mathbb{R}^m$. The sets \mathcal{X} and \mathcal{U} are chosen to be both compact and to resemble simple box constraints [16]:

$$\begin{aligned}\mathcal{X} &:= \{\mathbf{x} \in \mathbb{R}^n \mid \mathbf{x}_{\min} \leq \mathbf{x} \leq \mathbf{x}_{\max}\}, \\ \mathcal{U} &:= \{\mathbf{u} \in \mathbb{R}^m \mid \mathbf{u}_{\min} \leq \mathbf{u} \leq \mathbf{u}_{\max}\},\end{aligned}$$

where \mathbf{x}_{\min} , \mathbf{x}_{\max} , \mathbf{u}_{\min} and \mathbf{u}_{\max} are constant vectors. Within Non-Linear Model Predictive Control (NMPC) an optimal control problem with finite horizon is solved repeatedly, optimizing an objective functional J with runtime cost ϕ weighted by θ_i :

$$\underset{\bar{\mathbf{u}}(\cdot)}{\operatorname{argmin}} J(\mathbf{x}(t), \bar{\mathbf{u}}(\cdot); T_C, T_P)$$

with

$$J(\mathbf{x}(t), \bar{\mathbf{u}}(\cdot); T_C, T_P) := \theta_i \int_t^{t+T_P} \phi(\bar{\mathbf{x}}(\tau), \bar{\mathbf{u}}(\tau)) d\tau,$$

subject to equality constraints:

$$\begin{aligned}\dot{\bar{\mathbf{x}}}(\tau) &= f(\bar{\mathbf{x}}(\tau), \bar{\mathbf{u}}(\tau)) \quad \text{with} \quad \bar{\mathbf{x}}(t) = \mathbf{x}(t), \\ \bar{\mathbf{u}}(\tau) &= \bar{\mathbf{u}}(\tau + T_C) \quad \forall \tau \in [t + T_C, t + T_P], \\ T_P &\text{ free,}\end{aligned}$$

inequality constraints:

$$\begin{aligned}\bar{\mathbf{u}} &\in \mathcal{U} \quad \forall \tau \in [t, t + T_C], \\ \bar{\mathbf{x}} &\in \mathcal{X} \quad \forall \tau \in [t, t + T_P],\end{aligned}$$

and boundary conditions:

$$b(\bar{\mathbf{x}}(t), \bar{\mathbf{x}}(t + T_P), \bar{\mathbf{u}}(t), \bar{\mathbf{u}}(t + T_C)) = 0.$$

Repetitive solution of this optimization problem results in the open-loop solution $\bar{\mathbf{u}}^*(\cdot, \mathbf{x}(t), T_P) : [t, t + T_P] \rightarrow \mathcal{U}$ and finally the optimal solution for the closed-loop system as a sequence of open-loop solutions:

$$\mathbf{u}^*(\tau) := \bar{\mathbf{u}}(\tau, \mathbf{x}(t)) \quad \text{with} \quad \tau \in [t, \delta].$$

The resulting “nominal closed-loop system” is:

$$\dot{\mathbf{x}}(t) = f(\mathbf{x}(t), \mathbf{u}^*(t))$$

A direct solution is obtained using a finite parametrization of controls leading to a finite

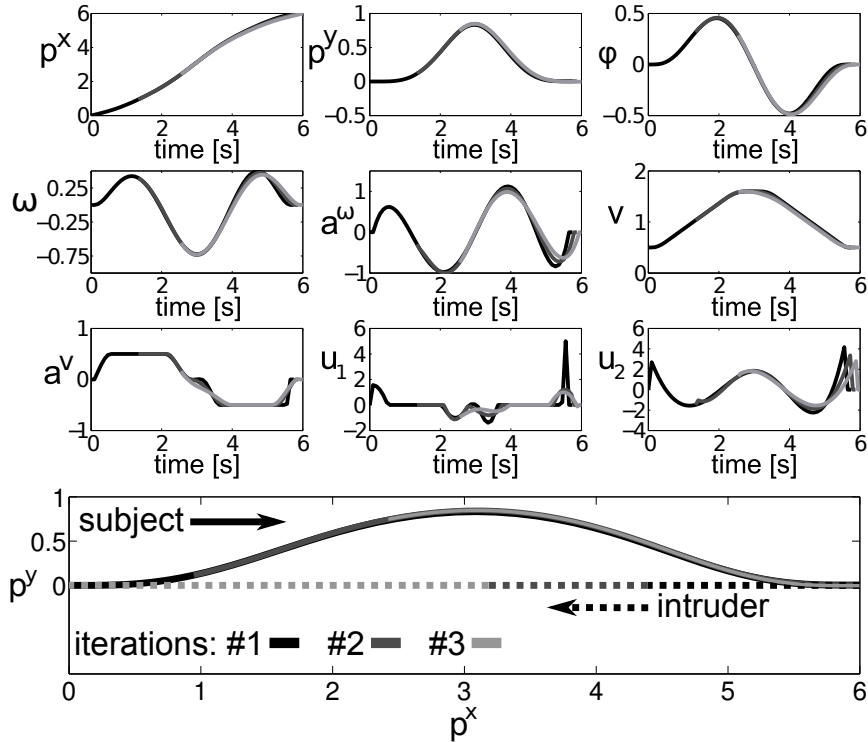


Fig. 2.15: MPC simulation for a fully observable environment. Solid lines represent the prediction for the human, dashed lines represent the interferer path

dimensional dynamic optimization problem. The controls are therefore constant over each sampling interval $M = \frac{T_P}{\delta}$ such that $\bar{\mathbf{u}}(\tau) = \bar{\mathbf{u}}_i$ for $\tau \in [\tau_i, \tau_{i+1})$ with $\tau_i = t + i\delta$. Using a “sequential approach” [16] the control vector $\bar{\mathbf{u}}_i = \{\bar{\mathbf{u}}_1, \dots, \bar{\mathbf{u}}_M\}$ is optimized, leading to:

$$\operatorname{argmin}_{\bar{\mathbf{u}}_i} J(\mathbf{x}(t), \bar{\mathbf{u}}_i, T_P),$$

where only the input vector $\bar{\mathbf{u}}_i$ and $T_P = t + M\delta$ appear. The depicted problem is solvable using direct methods within this MPC framework and allows for the integration of an interfering person. This interferer is modeled as a moving multivariate Gaussian, creating cost in space where it passes [14].

The presented human model enables the definition of a control theoretic view of effort in locomotion. Following simulations consider two situations where the proposed model estimates the reactions of a human when a non-interacting interferer is avoided. The first situation resembles a well predictable behavior of the interferer, whereas the second scenario constitutes a non-predictable behavior of the interfering agent. Simulation results for a human walking on a two-dimensional plane from $(0, 0)$ to $(6, 0)$ together with the non-interacting interferer, that moves from $(6, 0)$ to $(0, 0)$, are shown in Fig. 2.15. The solid lines resemble the predictions for the human and the dashed lines represent the interferer. Colors indicate the results of the three iteration steps. As the ACADO Toolbox does not provide each MPC step, three steps resembling a sample time of $1.2s$ are depicted. The human and the interferer are thereby modeled without a footprint. Figure 2.15 shows that without any changes in the interferer path, all controls and states progress very smoothly.

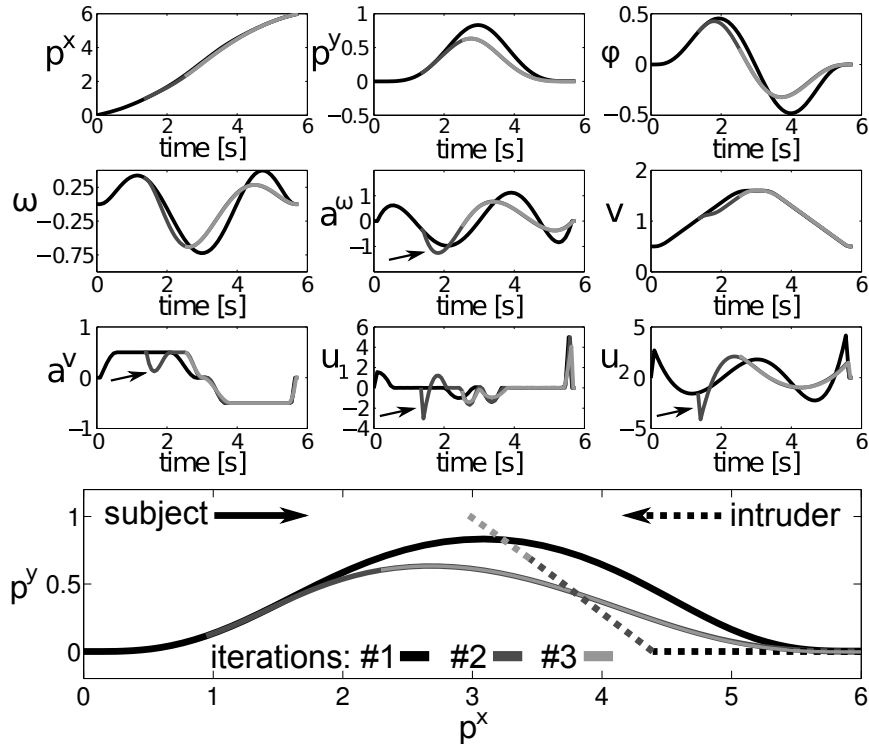


Fig. 2.16: MPC simulation for a partially observable environment. Solid lines represent the prediction for the human, dashed lines represent the interferer path. Arrows indicate high energy expenditure

Notably, the path and velocity are smooth, while the latter follows the typical bell shape. The avoidance of the interfering person is well visible within the resulting trajectory. This simulation resembles a situation where the interferer behaves as expected, thus rendering predictions very accurate. Accordingly, the human is able to reach its goal effortlessly. The opposite is the case, if the counterpart reacts unexpectedly or unreasonably, leading to large deviations from the prediction. More effort in a sense of re-planning and energy expenditure is necessary if the interferer changes its path. Figure 2.16 depicts according simulation results. The interferer path features a sudden change of intention (swerve to the right), which is not predicted in the first planning step. This dissociated behavior of the counterpart leads to a sudden necessity for orientation, velocity and path adaptation. Necessary jumps in the controls and accelerations are marked with arrows. Thus, effort arises from unreliable predictions which lead to re-planning and the required control inputs to resolve the collision situation. The simulations therefore allegorize the posed hypothesis that a robot can contribute to the navigation efficiency of nearby humans if it behaves readably and therefore predictably while concurrently respecting social norms.

2.2.2.3 Correlations to Human-Robot-Interaction

Considering the proposed definition of effort and the cognitive locomotion model, all agents in a shared environment can benefit from clear intentions and reliable mutual predictions. Thus, robots that externalize intentions and comply with human-like behaviors, will strongly facilitate mutual trajectory prediction. Due to the enhanced reliability of the

predictions, locomotion planning for other agents within the environment affords less effort since potential collisions are detected earlier and resolved easily. For the experiments conducted in this work the robot must support the subject’s Goal-to-Action inference $\mathcal{E}^{-1}(G)$. Effort for locomotion planning diminishes if the motion of the robot towards the known goal complies with the prediction ξ_{S-G} of the human.

Readable robot locomotion is achievable by planning human-like trajectories. Yet, literature does not give a common definition of human-likeness regarding locomotion. This work refers to robot locomotion as human-like if it exhibits certain formative features like energy efficiency, suitable velocity profiles, a preference for non-holonomic movement [18] and smooth paths. This abstraction is employed since the robotic platform used within the experiments is wheeled. For a bipedal humanoid robot, human-likeness comprises far more aspects up to the point where it is supposed to walk exactly like a human. Typical approaches for human-like motion generation replay recorded human trajectories or imitate stereotypical behaviors of humans [22, 52, 79, 111]. The aforementioned MPC model or the related approaches in [14, 19, 121], are also capable of providing according trajectories.

Controlling a robot to follow these trajectories requires either a dynamic model of the robot or another controller structure that enables the robot to follow planned velocities and poses. For the MPC model described in this work, the methods in [106] and [107] are concerned with trajectory tracking and stability of similar systems. The robotic platform that is used in the subsequent experiments employs a kinematic model internally to accurately follow provided velocity profiles. Using the precision of a dedicated tracking system, a heuristically tuned PID position controller for each experiment condition allows for accurate trajectory tracking across the experiment.

The following sections are concerned with the statistical analysis of human locomotion trajectory data, which reveals the effectiveness of readable locomotion in decreasing the planning effort for interacting agents. Subsequent experiments will then tackle the question whether this applies to humans and robots equally.

2.2.3 Experiments on Human-Human and Human-Robot Avoidance

The following section describes the experiments which are constructed to reveal the effects of readability in human locomotion and the effectiveness of readable human-like robot locomotion in reducing planning effort. The evaluation of the recorded data-set is conducted using the methods described in Chap. 4.

The conducted studies evaluate the hypothesized behaviors in a collision avoidance experiment, which poses an ideal situation to procreate the necessary environment states. Within four different conditions, subjects must reach a predefined goal and avoid a collision with an interfering agent (intruder). Their counterpart, the intruder, executes the same task but also follows certain prior instructions. With respect to the definitions in Subsec. 2.2.2 this experiment provides a shared environment with a known goal $G \in \mathcal{G}$ for the intruder. Accordingly, the subject applies Goal-to-Action inference and attempts to predict the intruder trajectory $\xi_{S,G}$. Formally, this prediction is enhanced in its accuracy if the intruder externalizes its intention, e.g. the side of avoidance. This allows for the generation of a fully or partially observable environment for the participant. A subject basically walks in a shared environment with an interfering agent (intruder). Thus, the faced

environment is an empty space with one dynamic obstacle, a start and a goal position. The environment may be considered fully observable if the intruder path is previously announced. Partial observability is achieved if the subject has no knowledge about the path of the intruder.

Based on these two situations the effects of readable locomotion are discussed. In the scenario where the subject has full knowledge of all occurrences, a movement with minimum effort and maximum smoothness must be observed, resembling an individual optimum. In comparison to that, the partially observable scenario permits equal behavior as it offers equal conditions but requires the human to rely on its predictions. Given that the predictions are enhanced by readable locomotion of the interfering counterpart, a subject should be able to follow the previously defined optimum closely and effortlessly.

Regarding the measure of effort in human locomotion, experiments and results are based on the assumption of a “maximum-smoothness strategy” employed by humans [23]. In literature smooth paths and “bell-shaped” velocity profiles are defined as typical and desired. Uncertainty or a surprising motion, as an extreme case, lead to deviations from this strategy [23]. The experiments will show that uncertainty leads to re-planning due to prediction errors and therefore to expenditure of energy. Presented evaluation methods visualize these effects as deviations from the smoothness paradigm. Readability and human-likeness are considered as features that reduce uncertainty as motions comply with human expectations. The readable trajectories externalize their purpose more clearly [71] which leads to more reliable predictions and less planning effort for other agents.

2.2.3.1 Transfer of Human-Human to Human-Robot Interaction

The results from the human-human study with a readably moving human intruder are further transferred to a second experiment with a robot as the interfering counterpart. The underlying hypothesis is that a robot is able to achieve the same effect if it shows intent by employing readable locomotion. In order to generate readable locomotion for the experiments with an interfering robot, a mean trajectory from the human interferer of the human-human experiment is replayed. Replaying the mean trajectory further provides stable experimental conditions and comparability across both experiments. The stereotypical motion that is used by the interferer, is copied by the robot using its holonomic motion capabilities. Notably, the used platform is not humanoid but wheeled which may change the perception of its movements. By applying the methods of spline based mean calculation (see Sec. 4.4), the recorded trajectories of the human intruder are averaged and provided to the robot controller. Specific gestures, gaze or animation principles that serve as cues for the robot intention are excluded for both studies.

Similar results in both parts of the study pose a strong argument for the benefit of readable human-like locomotion. Besides, these results also propose that humans apply the same cognitive behavior for planning and prediction (see Subsec. 2.2.2) independent from the agent they share an environment with.



Fig. 2.17: Distribution of trackballs on a subject

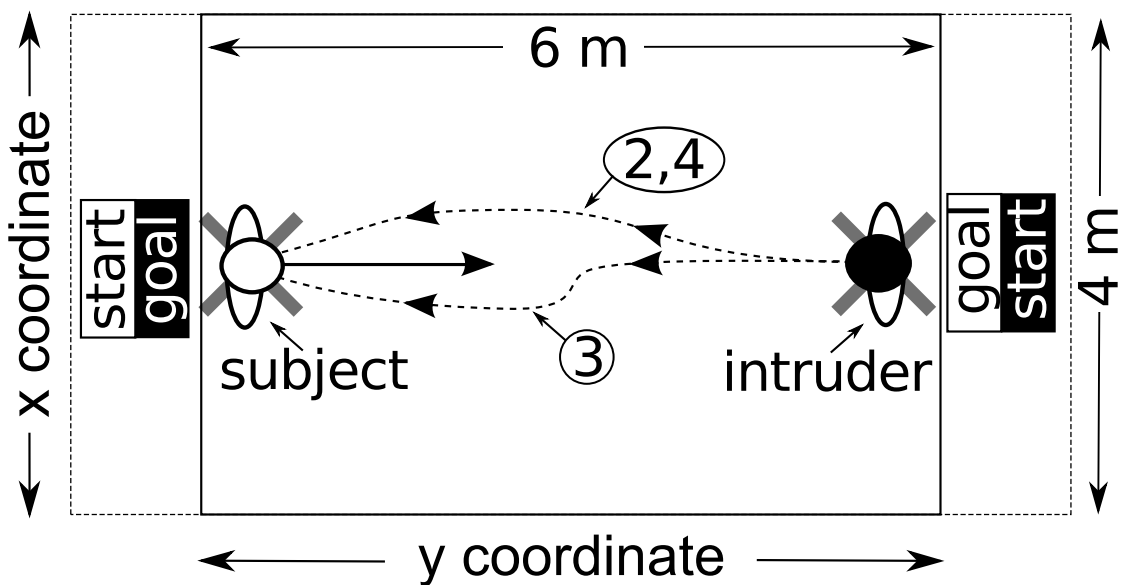


Fig. 2.18: Setup of the study. Numbers illustrate the predefined paths for the intruder in the respective experiment condition. The intruder does not occur in scenario 1 and executes similar paths in scenario 2 and 4

2.2.3.2 Experiment Setup

The experiments are situated in a motion tracking area which is equipped with a Qualisys Tracking System, has clean walls, covered windows and ensures stable conditions for all subjects while canceling external influences. The experiment area has a size of $8m \times 6m$ with ten infrared cameras covering $6m \times 4m \times 2m$. Figure 2.18 illustrates the experimental setup with start and goal positions.

For controlling the mobile robot to follow a trajectory, its position and the position of the subject need to be known and tracked. The system supplies position data of every visible track-ball attached to the person and the robot with a frequency of 204 Hz. Each subject is equipped with tracking balls as shown in Fig. 2.17. The robot carries a fixed structure of 5 track-balls, which allows for position and orientation control.

2.2.3.3 Experimental Method

This 4×1 within subject study features four conditions for each subject, named scenarios subsequently (Sc.1 – Sc.4). Each scenario serves as a part of an overall concept which is the elaborated result of cooperation with social psychologists and statisticians:

- Sc. 1: subject walks to the goal alone as a baseline for straight walking and personal speed
- Sc. 2: subject is told that its counterpart will execute the same task and definitely avoids collisions by swerving to the right
- Sc. 3: subject is told that the previous condition is repeated but the intruder actually disturbs the subject on purpose
- Sc. 4: subject is not given any information except to finish the task

Probands are unwittingly confronted with a special situation in each scenario. Sc. 1 simply generates baseline data for the pivot analysis. Sc. 2 provides the subject with a fully observable environment such that planning and moving with minimum effort and maximum comfort/smoothness is supported. Sc. 3 eradicates the subject’s reliance on prior information and fosters the need to observe and predict the environment in order to succeed in the task. Sc. 4 then implicitly requests the person to “sense” and “predict” the movement of the intruder and to “plan” accordingly.

The baseline scenario is useful for the statistical data analysis. A behavioral baseline is recorded within Sc. 2 which is considered the optimal solution for the supplied experimental condition. The unexpected path of the intruder in Sc. 3 is thereby a critical priming of the subjects. Due to the surprising behavior, the subjects should not rely on any given information for the remaining scenarios but their own observations and predictions. Additionally, Sc. 3 serves as a condition where the prediction step fails. Recorded data gives insight into recovery behaviors and the effect on expended effort considering the necessary forces for sudden path and velocity changes.

Sc 4. is compared to the optimal solution of Sc. 2, to investigate whether readability leads to an equally smooth trajectory, to a similar path shape and accordingly to an equally low planning effort. Therefore, a readable motion is produced by the intruder on purpose. A stereotypical movement is used, as proposed in literature [22, 23, 111], to provide a readable hint towards the chosen side for avoidance (same side as Sc. 2). The interferer takes a slight sideways step to the preferred side as it is typically observed when people resolve collision situations while walking on a sidewalk.

In order to prove the effectiveness and meaningfulness of readability, the recorded trajectories from each scenario need to be compared. As described in the Chap. 4 the subsequent evaluations compare the scenarios using a qualitative method and further apply the proposed approach to these results for a quantification of the found effects. The investigated alternative hypotheses for the experiments are $H_{1,A}$ and $H_{1,B}$, which assume for the human-human and the human-robot experiment that the subject paths of Sc. 2 and 4 are significantly different such that the null hypotheses of equality $H_{0,A}$ and $H_{0,B}$ must be rejected. Thus the effectiveness of readability is supported if the null hypotheses hold.

2.2.3.4 Experiment Procedure

Both experiments are conducted with 40 persons aged 20-35 years, leading to 320 recorded subject trajectories. Experiments are in line with the Helsinki declaration and are reviewed by the ethical committee of TUM Medical Faculty. None of the subjects is allowed to participate in both experiments. The setup of the human-robot study is equal to the human-human study.

A dedicated supervisor leads the experiments and explains all necessary information to each subject. Participants are welcomed at the lab and led to the motion tracking area. The supervisor hands an informed consent to the subject and additionally explains the information verbally. Each subject is advised regarding safety, data security and privacy protection. Afterwards, the purpose of the cameras is described and the trackballs are equipped. As the human intruder must be unknown to the subject, the supervisor must be a different person. During every experiment run only one participant is in the room with the supervisor and the intruder.

The subject is given two tasks for the four experiment conditions: walking from its start-position to the predefined end-position and avoiding collision with its counterpart. Subjects are asked to walk at a comfortable speed but are not given a time constraint. Each subject is further informed about a signal given by the supervisor, which tells the subject to start walking towards its goal. Prior to the first experiment condition with an intruder, the supervisor clarifies that the intruder has the same task but with inverted positions. The counterpart is an informed intruder with certain directives for every experiment condition and acts as a readable dynamic obstacle.

In the second experiment the IURO Robot [4, 7] is used instead of the human intruder. In this case the subject is given equal information and is assured that the robot is moving autonomously and is not tele-operated. Certainly, subjects are not allowed to participate in both studies.

After recording, each subject is debriefed and thanked for participation. The data is later labeled and processed with the software provided by the Qualisys Tracking System. The evaluation with confidence intervals (CI) is conducted using implementations in R.

2.2.3.5 Intruder Concept

Clearly, the trajectories of the intruder play an important role. The human intruder must follow similar paths for each subject and scenario. Besides, the intruder must be unknown to the subjects to avoid socially motivated effects (e.g. acquaintances yield less). Moreover, the intruder does neither interact with the person nor react to the subject's movement. Although, slight adaptations are needed to support the naturalness of the walk. Consistency of the intruder paths is shown using CIs from the recorded data. Figure 2.19 shows the CIs for the paths of the informed intruder in Sc. 2 to 4 (direction bottom to top). Narrow and strongly overlapping CIs for Sc. 2 and 4 imply that the paths were performed similarly for all subjects in both scenarios. This analysis reveals that the intruder started off a little more on the left in Sc. 4 and then pulled to the right with the mentioned movement. The first step of the intruder is always performed with the left leg first, which leads to the impulse to the left in the beginning. CIs are also applicable

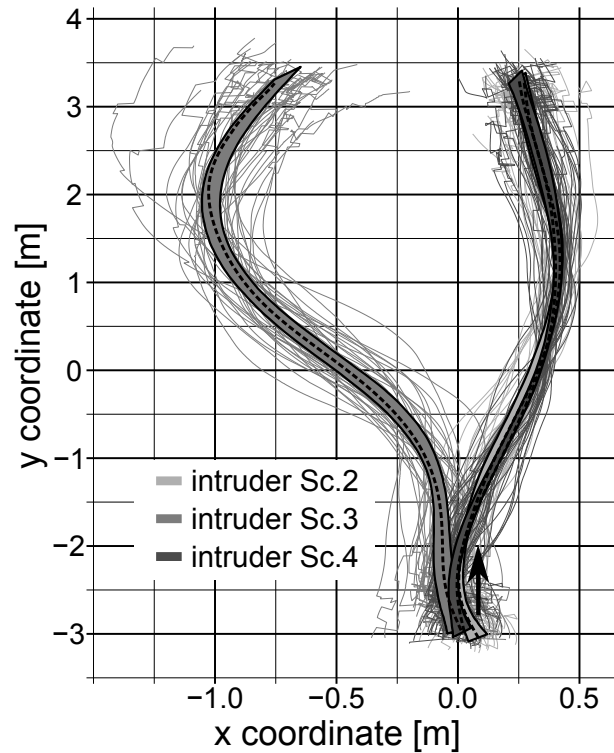


Fig. 2.19: Paths recorded from the human intruder in Sc. 2, 3 and 4. Dashed black lines indicate the paths used for the robot intruder. The arrow indicates the movement direction from bottom to top. Noise at both ends of the paths originates from poor tracking at the borders of the tracking area

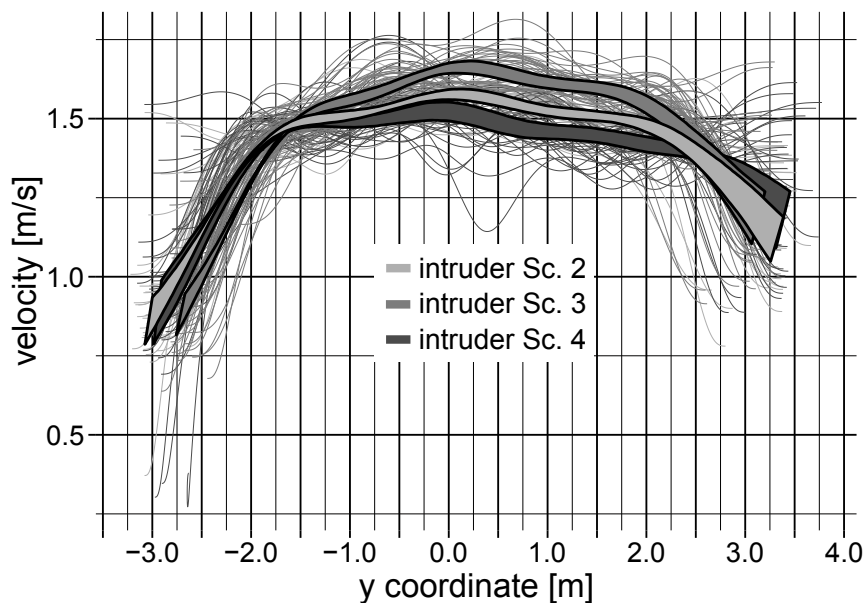


Fig. 2.20: Velocities recorded from the intruder in Sc. 2, 3 and 4. Noise at both ends of the plot originates from poor tracking at the borders of the tracking area

to analyze the velocities which are supposed to be stable across all conditions and for all subjects. Figure 2.20 shows the CIs for the velocities of the informed intruder in Sc. 2 to

4. As previously described, the used robotic platform replays the paths of the intruder at a constant velocity (the robot cannot go faster than 1 m/s) in order to be human-like and to keep experimental conditions stable. Figure 2.19 shows the paths of the robot as dashed black lines which represent a mean inside the CIs.

The results of the interactions of the study participants with the described intruders are shown in the following subsection and are discussed thereafter.

2.2.4 Results

For data evaluation the methods in Sec. 4.4 are applied. Resulting plots show the recorded data together with the CIs. Note, that black arrows within the plots show the walking direction of the intruder or the subjects. Noise at both ends of these plots originates from poor tracking performance at the borders of the tracking area.

2.2.4.1 Human-Human Avoidance

In order to evaluate the effectiveness of readable locomotion, Sc. 2 and Sc. 4 are compared. The paths are similar if the subjects attempt to read the avoidance intention of the intruder in Sc. 4. Figure 2.21 shows the resulting paths of these scenarios. The CIs for the intruder and the subject paths are narrow, supporting the assumption of low variance in the data and stable experimental conditions. Subject paths in Sc. 2 and 4 are qualitatively very similar and the CIs overlap in large parts. The processed data of Sc. 4 reveals that the subjects walk straight for a short duration before they decide to avoid to the right side. A feasible interpretation is that this corresponds to the time needed by subjects to predict the intruder.

In Fig. 2.22 the velocities are analyzed. The velocities are smooth and show overlapping CIs indicating low energy expenditure. An accompanying reduction in velocity with respect to Sc. 2, suggesting hesitation, is not visible in the velocities in Fig. 2.22. In conclusion, subjects move similarly in both scenarios, despite the uncertainty about the intruder behavior in Sc. 4. As the results support $H_{0,A}$ the posed theory is emphasized that readable locomotion must be effective in conveying the avoidance intention and renders the subject's predictions reliable, thus reducing effort.

The conclusions are further supported by the observations of Sc. 3. Resulting subject paths depict the rotational accelerations needed to resolve the collision course due to the surprising movement. Figure 2.23 displays the paths of the intruder and the subject in Sc. 3. The velocity profiles of the subjects further illustrate the effect of diminished planning expenses. Figure 2.24 shows that the surprising change of behavior in Sc. 3 strongly affects the smoothness of the subjects velocity. The readable locomotion hint in Sc. 4, however, leads to smooth walks of all subjects. Judging from the qualitative evaluation the hypothesis about the effectiveness of readable locomotion holds. Paths and velocities in Sc. 4 are similar to the "optimal" solution triggered in Sc. 2 in opposition to $H_{1,A}$. Unexpected changes of the environment, however, lead to significant expenditure of energy in order to resolve the collision situation. For a quantitative comparison of Sc. 2 and 4, the method described in Sec. 4.4 is applied to the path data. Table 2.5 visualizes the results for both distance measures.

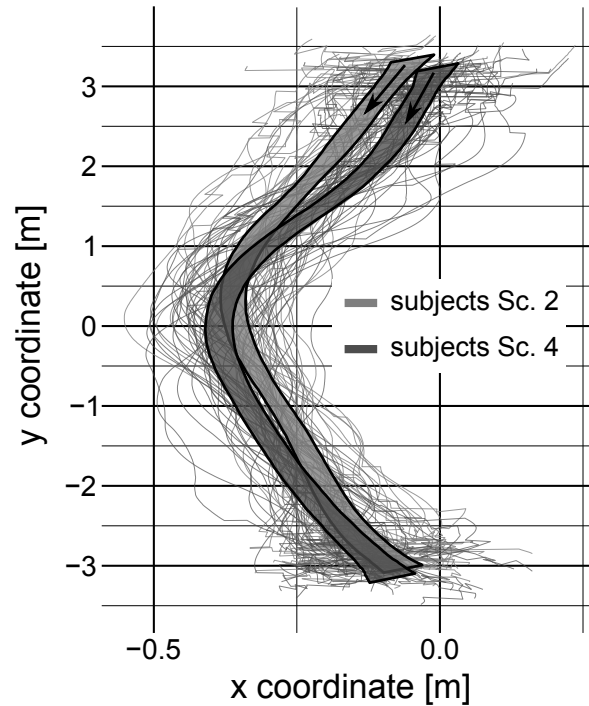


Fig. 2.21: Paths recorded from the subjects in Sc. 2 and 4 in the human-human study

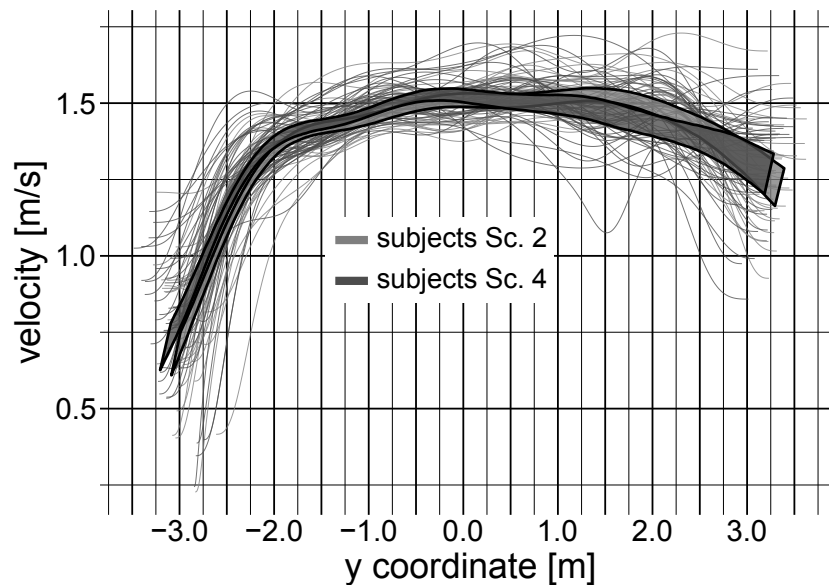


Fig. 2.22: Velocities recorded from the subjects in Sc. 2 and 4 in the human-human study

For the comparison of Sc. 2 and 4 the mean Hausdorff distance amounts to 0.173 m with a standard deviation of 0.086 m . The mean DTW distance yields a value of 0.084 m and a standard deviation of 0.044 m . Comparison using the baselines Sc. 1 and 3 results in the p-values of 0.417 and 0.002 with a d_c of 0.126 and 0.283 for the Hausdorff distance. The use of DTW results in the p-values of 0.867 and 0.003 and in a d_c of 0.028 and 0.285. As expected, the behaviors in Sc. 2 and 4 are very similar with respect to the distance measures. Compared to the straight walk the differences are small, supporting the null

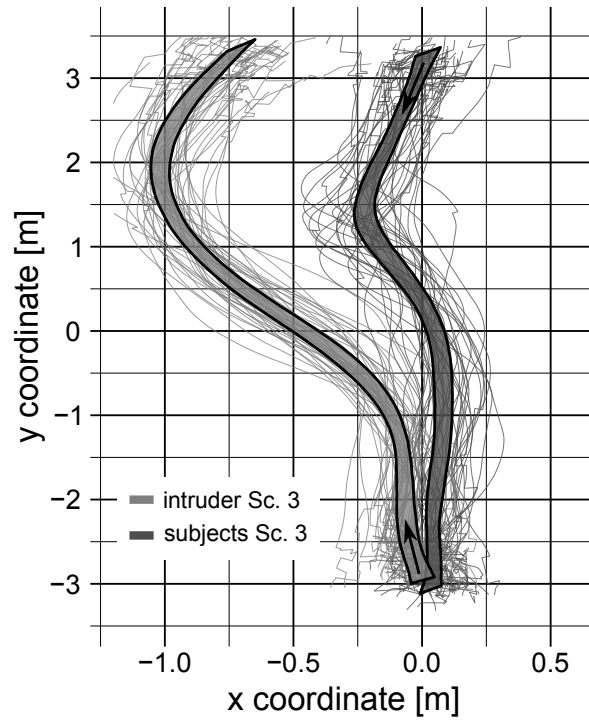


Fig. 2.23: Paths recorded from subjects and intruder in Sc. 3 in the human-human study

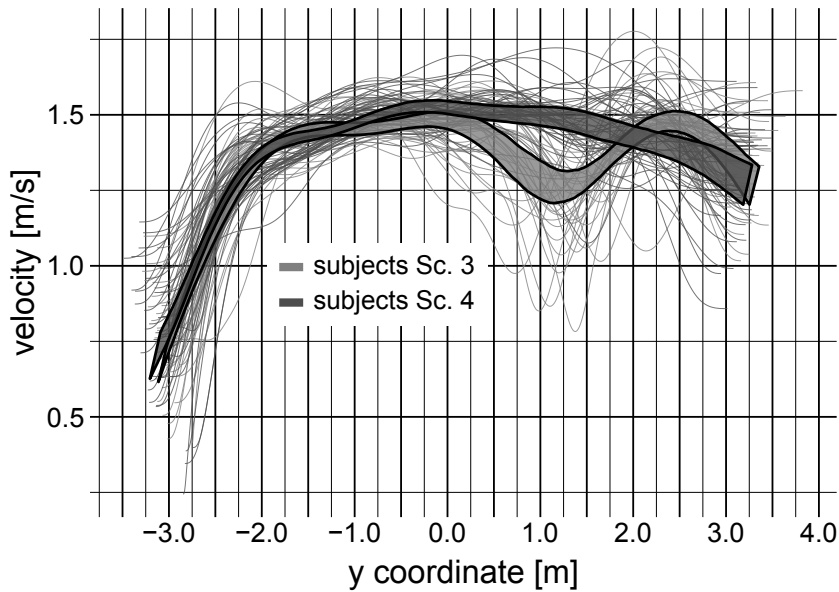


Fig. 2.24: Velocities recorded from the subjects in Sc. 3 and 4 in the human-human study

hypothesis $H_{0,A}$, but the effect is weak. The difference is visible when Sc. 3 is used as a pivot. Resulting p-values lead to a rejection of the null hypothesis $H_{0,A}$ meaning that the paths are not exactly equal. The dissimilarity, however, is small with respect to Cohen's d_c . Overall, the first study shows how strongly readable locomotion influences the performance of cooperative navigation. Consequently, the applicability to a non-human-like robot must be explored in order to investigate if subjects apply the same strategies and react similarly.

Tab. 2.5: Hausdorff and DTW distance based pivot analysis for each scenario pair in the human-human experiment

Sc. pairs	$d_{\Xi}(\cdot, \cdot)$ mean (s.dev.)	pivot Sc. 1 p_{Ξ} (d_c)	pivot Sc. 2 p_{Ξ} (d_c)	pivot Sc. 3 p_{Ξ} (d_c)	pivot Sc. 4 p_{Ξ} (d_c)
$d_{\Xi}(\cdot, \cdot)$ with Hausdorff distance					
1-2	0.304 (0.130)	–	–	0.237 (0.243)	0.000 (1.273)
1-3	0.334 (0.128)	–	0.014 (0.422)	–	0.000 (0.628)
1-4	0.321 (0.141)	–	0.000 (1.191)	0.004 (0.570)	–
2-3	0.375 (0.197)	0.126 (0.231)	–	–	0.000 (1.651)
2-4	0.173 (0.086)	0.417 (0.126)	–	0.002 (0.283)	–
3-4	0.431 (0.204)	0.520 (0.096)	0.000 (1.328)	–	–
$d_{\Xi}(\cdot, \cdot)$ with Dynamic Time Warping					
1-2	0.163 (0.073)	–	–	0.256 (0.197)	0.000 (1.235)
1-3	0.152 (0.064)	–	0.805 (0.041)	–	0.015 (0.359)
1-4	0.161 (0.077)	–	0.000 (1.318)	0.003 (0.506)	–
2-3	0.166 (0.083)	0.290 (0.166)	–	–	0.000 (1.534)
2-4	0.084 (0.044)	0.867 (0.028)	–	0.003 (0.285)	–
3-4	0.191 (0.088)	0.398 (0.132)	0.000 (1.240)	–	–

2.2.4.2 Human-Robot Avoidance

Given the human-human experiment, the question remains open whether readability yields similar effects when transferred to a mobile robot. Hence, following experimental results must clarify if humans react to a mobile robot equally as to a human interferer. Accordingly, Fig. 2.25 shows the resulting paths of Sc. 2 and 4 (subjects move top to bottom). The CIs are narrow, implying low data variance and stable experimental conditions. Both CIs do not overlap as strongly but are considerably close and feature equal shapes.

Despite the fact that the interfering counterpart is a robot and its behavior is not clear in Sc. 4, subjects still move similarly in both scenarios. Velocities shown in Fig. 2.26 further indicate that no delaying was used in order to better predict the robot. In addition, the

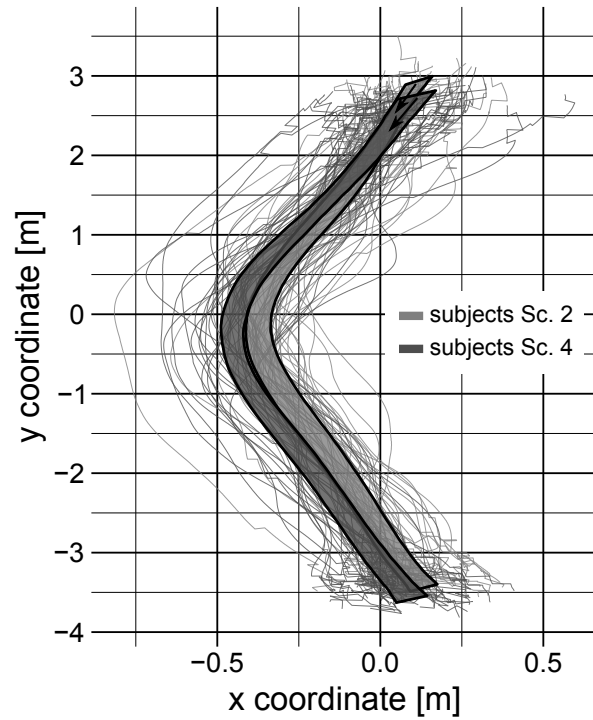


Fig. 2.25: Paths recorded from subjects in Sc. 2 and 4 in the human-robot study

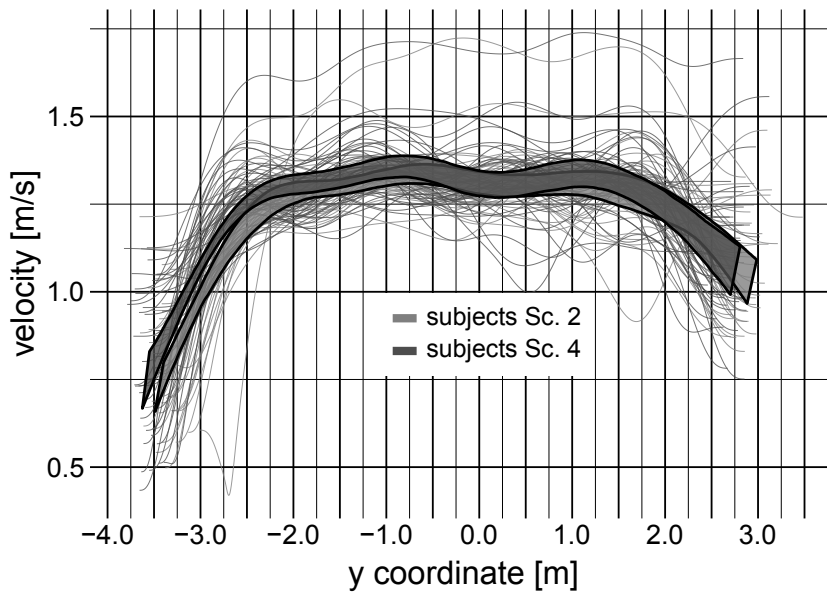


Fig. 2.26: Velocities recorded from subjects in Sc. 2 and 4 in the human-robot study

velocities are very smooth in both scenarios. These results support $H_{0,B}$ and thus the proposition that disturbance and locomotion planning effort is reduced for humans while predictions are enhanced when robots employ readable locomotion patterns. Compared to the human-human study, the CIs show a far shorter delay until the side for avoidance is chosen, but the subjects swerve farther to the side. It is assumed that this is connected to the uncommon encounter of a robot which also has a large footprint of $0.8\text{ m} \times 1.0\text{ m}$.

In order to explore the expended planning effort, the paths and velocities of Sc. 3 are

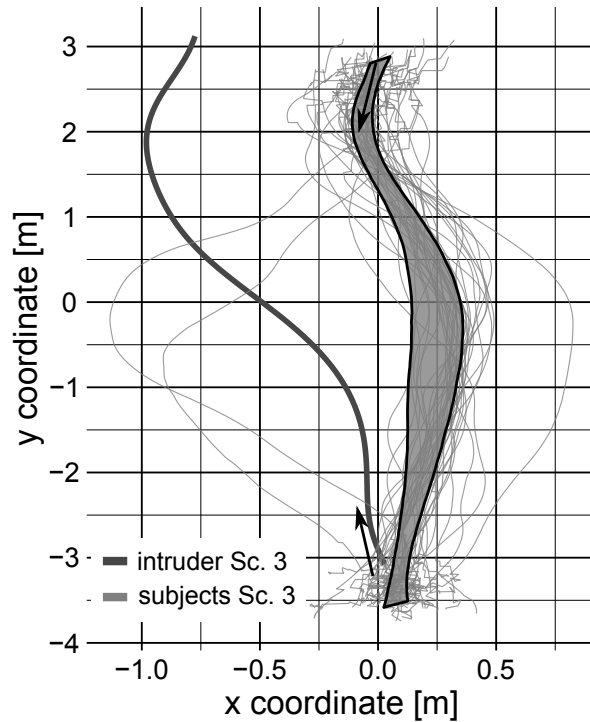


Fig. 2.27: Path of the robot intruder and paths recorded from subjects in Sc. 3 within the human-robot study

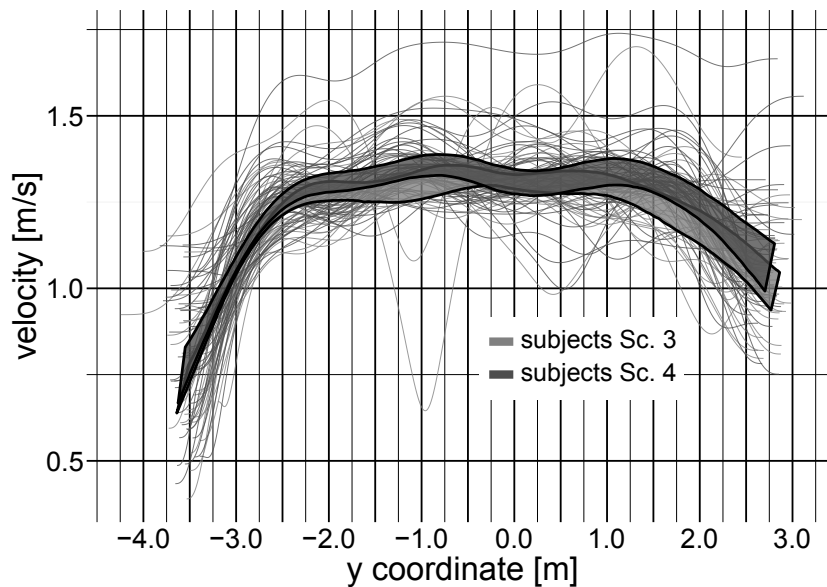


Fig. 2.28: Velocities recorded from subjects in Sc. 3 and 4 in the human-robot study

consulted. An inspection of Sc. 3 in Fig. 2.27 and a comparison of the velocities recorded in Sc. 3 and 4, see Fig. 2.28, reveals that the surprising behavior of the robot in Sc. 3 does not affect the smoothness of the subject's velocity as strongly. Except for some individual cases, subjects do not need to brake. However, the paths in Fig. 2.27 indicate that the avoidance is not resolved early.

The distinct difference to the human-human experiment is the lower speed provided by

Tab. 2.6: Hausdorff and DTW distance based pivot analysis for each scenario pair in the human-robot experiment

Sc. pairs	$d_{\Xi}(\cdot, \cdot)$ mean (s.dev.)	pivot Sc. 1 p_{Ξ} (d_c)	pivot Sc. 2 p_{Ξ} (d_c)	pivot Sc. 3 p_{Ξ} (d_c)	pivot Sc. 4 p_{Ξ} (d_c)
$d_{\Xi}(\cdot, \cdot)$ with Hausdorff distance					
1-2	0.471 (0.168)	– –	– –	0.000 (1.337)	0.000 (1.986)
1-3	0.445 (0.265)	– –	0.000 (1.440)	– –	0.000 (1.287)
1-4	0.518 (0.201)	– –	0.000 (1.937)	0.000 (1.417)	– –
2-3	0.838 (0.319)	0.492 (0.113)	– –	– –	0.000 (2.680)
2-4	0.200 (0.103)	0.036 (0.256)	– –	0.043 (0.129)	– –
3-4	0.881 (0.344)	0.062 (0.308)	0.000 (2.688)	– –	– –
$d_{\Xi}(\cdot, \cdot)$ with Dynamic Time Warping					
1-2	0.237 (0.095)	– –	– –	0.000 (1.065)	0.000 (1.810)
1-3	0.227 (0.142)	– –	0.000 (1.132)	– –	0.000 (0.999)
1-4	0.260 (0.115)	– –	0.000 (1.799)	0.000 (1.131)	– –
2-3	0.398 (0.178)	0.609 (0.083)	– –	– –	0.000 (2.289)
2-4	0.097 (0.055)	0.092 (0.219)	– –	0.157 (0.097)	– –
3-4	0.416 (0.189)	0.098 (0.256)	0.000 (2.287)	– –	– –

the robot. The human intruder provided a walk at an average velocity of 1.5 m/s which is much faster than the maximum of 1 m/s provided by the robot. Yet, given the size of the robot, this speed is perceived as very fast by most subjects. Indeed, the extra time for decision making allows the subjects to avoid the effort of high accelerations. A comparison of both experiments reveals that subjects also walk slower in the human-robot study. Consulting Fig. 2.23 and 2.27 the distance to the intruder when the subjects initiate the avoidance varies between both experiments as well. The distance to the human is around 1 m , but the robot does not get closer than 2 m . Although Sc. 3 does not provoke high effort for the subject, it still fulfills its task to put the subject into a scenario without any prior knowledge. Combined with the results from Sc. 2 and 4 it seems clear that humans attempt to read the robot's intention from its locomotion. As proposed in [66], humans follow the

“sense–plan–act” behavior also when confronted with a robot. Obviously, subjects are thus able to quickly predict the robot intention in Sc. 3. The smooth velocities indicate that the robot is not able to disguise its surprising behavior.

In order to further investigate Sc. 2 and 4, quantitative results are obtained by applying the pivot-method. Table 2.6 visualizes the results of the comparison for both distance measures. For the comparison of Sc. 2 and 4 the mean Hausdorff distance amounts to 0.200 *m* with a standard deviation of 0.103 *m*. The mean DTW distance yields a value of 0.097 *m* and a standard deviation of 0.055 *m*. Comparison using the baselines Sc. 1 and 3 results in the p-values of 0.036 and 0.043 with a d_c of 0.256 and 0.129 for the Hausdorff distance. The use of DTW results in the p-values of 0.092 and 0.157 and in a d_c of 0.219 and 0.097. For the behaviors in Sc. 2 and 4 the null hypothesis $H_{0,B}$ is rejected twice for the Hausdorff distance but not rejected for any pivot with the DTW measure. In all four cases a weak d_c is found. Clearly, this shows that the trajectories from both scenarios are not equal but also not very different. Compared to the CIs this observation appears reasonable. The general shape of the trajectories is similar, which is reflected in the DTW measure. Yet, there are many outliers and the avoidance distance to the robot is larger in Sc. 4. The Hausdorff distance is by definition more sensitive to spatial distance and less to shape similarities.

In fact, the smooth walks of all subjects in Sc. 2 as well as in Sc. 4 and the similarity in shape and distances allow for the conclusion that readability is an effective feature for robot locomotion. Humans treat robots similarly with respect to expectations during cooperative navigation. When sharing an environment with a robot, humans will benefit from clear nonverbal intention conveyance based on readable locomotion.

2.2.4.3 Human-Human and Human-Robot Avoidance Comparison

In order to evaluate if the effectiveness of readability is similar for robots and humans, Sc. 2 and 4 of both studies are compared qualitatively. For the shown data, differences in the alignment are compensated which are caused by variations in the calibration and the setup of the tracking area used for the studies. Fig. 2.29 shows the comparison of the paths and velocities. The CIs show similar avoidance paths and qualitatively similar shapes for both experiments. CIs overlap in large parts but differ in the fact that subjects yield more space to the robot. The velocities for these scenarios show smooth progression of the subjects in both studies, while no deliberate hesitation is visible. Notably, subjects walk slower in the experiment with the likewise slower robot. Therefore, a slightly earlier initiation of the avoidance is visible. Overall, it appears that the subjects are intuitively able to incorporate the robot locomotion into their own prediction and planning. This seamless handling of the situation, while relying only on the prediction, supports the hypothesis that readable human-like locomotion is transferable to a robot. Humans apply their typical motion planning scheme [71] to robots and incorporate externalized intentions. In summary, robots should apply readable locomotion to comply with human expectations and predictions. This behavior is capable of reducing the planning effort for all agents and enables a robot to seamlessly integrate in human environments.

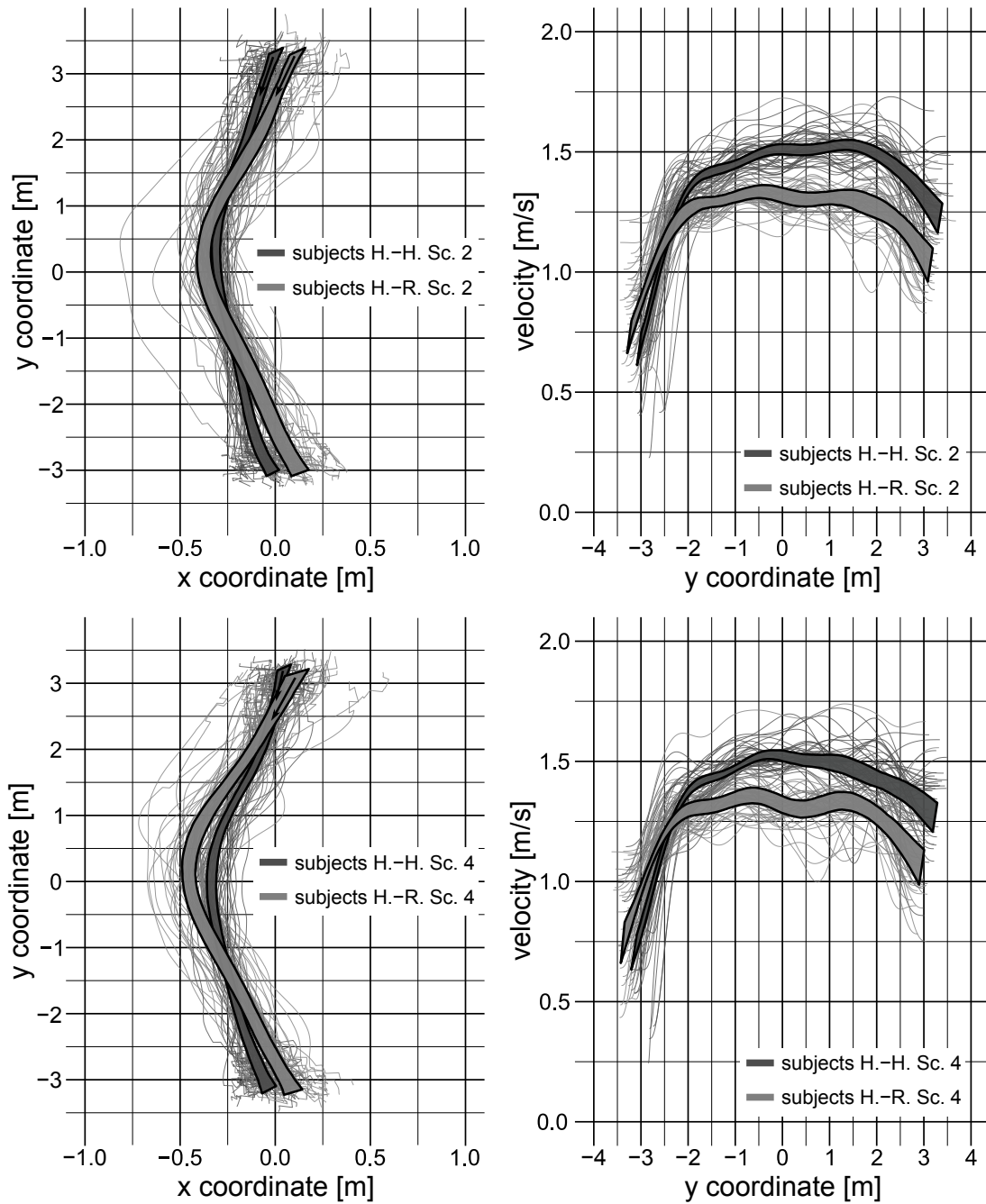


Fig. 2.29: Paths and velocities recorded from subjects in Sc. 2 and 4 in the human-human and human-robot studies

2.2.5 Discussion

Social aspects and the importance of clearly comprehensible intentions find increasing attention in the recent development of motion planners. This section analyzes the effectiveness of the underlying theories for robot locomotion. A literature review shows that this matter is not investigated in detail yet. Therefore, the capability of readable locomotion to support predictions and to reduce the planning effort for nearby agents is demonstrated in a subject study. This result is further transferred to a similar human-robot experiment.

The study confirms that humans apply the same behaviors for locomotion planning when navigating in the vicinity of robots. Given that the robot locomotion is human-like, equal benefits are achieved regarding seamless and effortless cooperative navigation. The experimental results are interpreted using the developed definition of effort, which is based on a model predictive control approach for modeling human locomotion.

Overall, the presented experimental results demonstrate how readable locomotion positively affects the locomotion planning of other agents within the same environment. The conducted mutual avoidance experiments compare various scenarios that put subjects into situations with full and partial knowledge regarding the behavior of the present interferer. It is shown that extra effort to handle the partial knowledge is overcome due to readable locomotion of the interfering human or robot. Although the robot movement is less intuitive to the subjects, the same positive effect on planning effort is visible. The opposite effect is observed in a situation with an unexpected movement of the interferer. Comparing the results from the human-human and the human-robot study reveals, that humans apply similar behaviors when sharing an environment with a human or a non-human-like robot. In fact, using human-like locomotion to enhance the readability of the robot, allows humans to quickly understand its intention and incorporate a reliable prediction into their own planning. This process leads to smooth trajectories for all agents regarding path, velocity and accelerations. Smoothness and the elimination of extra accelerations complies with the human desire for minimum effort. Based on the definition of effort proposed in this section, it is concluded that readability benefits the reduction of planning effort and the seamless integration of robots into human populated environments.

2.3 Summary

This chapter examines the effectiveness of readability and socio-contextual aspects in mobile robot locomotion. Social and human-like behaviors are incorporated in optimal control frameworks and shown to support the seamless integration of mobile robots into environments shared with humans. Behaviors derived from humans allow a robot to convey its intentions during approach or avoidance movements. Respecting social norms additionally improves the acceptance towards the robot.

In this respect the problem of approaching humans with an autonomous mobile robot is considered. By integrating socio-contextual aspects and human-like behaviors into the robot trajectory planning, its readability and social acceptance are enhanced. Thus, its ability to initiate interaction with humans nonverbally is improved. For generating according robot-to-human approach trajectories, an optimal control framework is employed. Therein, hard and soft constraints are used to realize human-like behavior and socio-contextual boundaries. For evaluation, a framework is proposed where multiple trajectory planners are compared based on human apperception. Based on this framework two user studies are conducted that particularly investigate the influence of path shape, path smoothness and orientation of the robot during trajectory execution.

Given the results, the effectiveness of readability and human-like behaviors in robot locomotion is further examined. Readable human-like locomotion is shown to enhance mutual predictions and thereby reduce the planning effort for nearby agents. This effect

is demonstrated in a human-human and a human-robot avoidance experiment. The interpretation of the experimental results is based on a definition of locomotion effort, which is developed using a model predictive control approach for human locomotion prediction. Accordingly, with a human-like robot locomotion behavior, seamless and effortless cooperative navigation is achieved.

2.4 Conclusions

This chapter demonstrates how readability and the incorporation of socio-contextual constraints improve robot locomotion in its ability to pro-actively initiate interactions and to convey intentions for cooperative navigation. The effectiveness of readability and social acceptance is shown for trajectories that comply with human expectations towards the robot. Human-likeness and the consideration of social context are thus defined as essential factors that allow humans to quickly assess the robot intention within nonverbal interaction.

Readable and socially compliant human-like locomotion for robots is modeled using optimal control and model predictive control frameworks. The corresponding constraints are used to represent socio-contextual aspects and formative features of human-like locomotion. A first evaluation compares a simple robot locomotion pattern with models that specifically resemble human trajectory planning in the context of robot-to-human approach. In particular, path shape, path smoothness and robot orientation are considered as trajectory features in the evaluation. The results clearly show that human-like robot locomotion, which comprises the named features, appears significantly more natural and readable than non-human-like movements. A proposed model based on Bézier curves thereby reaches equal performance as the human derived models regarding perceived naturalness, comfort and the intention conveyance capability. Accordingly, trajectories that are based on formative features of human-like robot locomotion can significantly enhance the readability of locomotion and improve nonverbal interaction initiation.

It is further demonstrated how readability affects the locomotion planning of other agents in a shared environment beyond apperception. Based on a developed definition for locomotion planning effort, the shown experiments reveal how readable locomotion reduces the planning effort for all agents. A corresponding mutual avoidance experiment compares different scenarios where subjects have either full or only partial knowledge regarding the behavior of an interfering human or robot. Thereby, readable locomotion allows subjects to overcome collision risks without extra effort within situations where only partial knowledge is available. Obtained results also indicate equal positive effects on planning effort for a robot interferer that applies human-like locomotion. In case the interfering agent performs unexpected and unpredictable movements the opposite effect is observed. A comparison of the conducted experiments with a human and a robot interferer reveals that humans behave similarly for both counterparts. The readable human-like locomotion of a robot enables humans to comprehend its intention and to incorporate a more reliable prediction into their own planning process. This results in smooth paths, velocities and accelerations for all agents. Accordingly, minimum effort is required for planning locomotion trajectories within the shared environment.

The presented results are expected to generalize to different forms of robot locomotion

and various applications. Specific features defining the human-likeness of the locomotion will differ especially with respect to the executed task. Robots that follow the introduced principles and additionally consider the social context will benefit from lower uncertainties within mutual predictions and from more successful interactions. This facilitates the seamless integration of robots into populated environments and supports tight collaborations with humans. Therefore, the reciprocal benefit of readable human-like locomotion yields an essential advantage for robots that act in human populated environments.

3 Towards Behavioral and Dynamic Models for Trajectory Prediction

The seamless integration of mobile robots into shared environments and their close cooperation with humans is not entirely solved by planning specialized trajectories. Focusing on locomotion, sharing an environment means locomotion within traversable areas together with multiple agents like humans and robots. So, the seamless integration of mobile robots into these environments requires them not only to act predictably, but also to accurately predict human locomotion themselves. Only this ability allows robots to avoid collisions while moving effectively and seamlessly. This chapter identifies aspects of human behavior that are considered to improve the performance of optimal control (OC) and model predictive control (MPC) based prediction approaches.

The first part, which was previously published in [2], opts to improve the precision of these methods for collision avoidance situations. Current models are not able to accurately reproduce trajectories observed from specific avoidance maneuvers. It is investigated whether humans adapt their trajectory planning horizon, in order to resolve certain collision situations. According simulation results and the observations found in literature lead to an experiment design that aims to reveal this behavior within human motion planning. Results indicate, that humans employ a shorter planning horizon when moving in a more complex environment. These findings are anticipated to improve the generalizability and accuracy of models used in OC based prediction methods.

In the second part of this chapter, a distinct weakness of recently developed human locomotion models is addressed. State-of-the-art models typically filter oscillations of the human velocity profile that occur due to the pendulum like bipedal walking motion. This smoothing leads to an inaccuracy in the alignment of position over time when the trajectory is reproduced. Therefore, it is proposed to take these oscillations into account by adapting the used dynamic model. The unicycle model serves as a basis for the adaptation, whereby the model of a rolling wheel is exchanged for a rolling ellipse. Within simulations, the elliptical shape leads to a sinusoidal velocity which represents the swinging of the human torso more closely.

3.1 Human Behaviors for Locomotion Prediction

A wide variety of robotic applications has emerged recently and robots start to break into the consumer electronics market. Current trends further aspire mobile robots that deliver packages in cities and move freely in factories or warehouses. These tasks require robots to integrate seamlessly into these environments. When multiple agents, meaning robots and humans, traverse a shared environment in a seamless manner, mutual prediction is a key ability. Therefore, robots must be able to accurately predict human locomotion, in order

to avoid collisions and to seamlessly integrate into these environments.

Numerous approaches for motion prediction are already available. State-of-the-art methods are based on learning approaches or use dynamic models which approximate the human musculoskeletal system. Machine learning methods usually consider fully observable environments with features that determine the motion and thus allow for predictions. These approaches yield a probability for a human to occupy a certain position [193]. Methods based on dynamic models mostly apply OC methods, where specifically designed objective functions lead to trajectories that closely resemble human locomotion [14, 19, 121, 135]. An advantage of the latter approaches is the resulting continuous trajectory, which describes all attributes from positions down to torques. Therefore, this work focuses on these methods due to their accuracy and considers their application in human locomotion prediction.

Yet, efficient and reliable prediction over a large horizon is still an ongoing research topic. Especially the varying collision avoidance behaviors of humans pose a challenging aspect for OC based methods. Current models for human locomotion do not generalize to the wide variety of observed situations and the respective human behaviors. Literature shows, that current models are especially not able to accurately represent the observed trajectories from a moving human that is disturbed by another agent [14, 23]. These disturbances are unexpected events, e.g. due to uncertainty or prediction errors, that influence the agent's path. They lead to specific avoidance or recovery behaviors, i.e. short-term reactions with sudden path or velocity adaptations, and result in suboptimal trajectories. As this is not covered by the models, they are not able to produce a suitable trajectory prediction. Especially, research towards collision avoidance behaviors encounters this problem [14, 23, 80]. It is reported that the applied OC approaches do not resemble the observed behaviors well [14, 23]. Obviously, the objective functionals of the methods, which are usually driven by energy minimization, curvature constraints or velocity adjustments, do not cover these short-term behaviors.

This section addresses this problem and aims to identify human locomotion behaviors that potentially help to enhance prediction algorithms when incorporated and accounted for. Literature already shows, that the consideration of human behaviors can significantly improve the performance of tracking and prediction methods [171]. Specifically OC and model predictive control (MPC) methods are to be improved. The incorporation of the identified behaviors is anticipated to enable a prediction of human locomotion in cases where the initial optimal solution is disturbed.

The particular factor of interest addressed here, is the applied planning horizon of a human. This aspect specifies how far into the future a human plans its motion. For locomotion, this comprises how far a human looks ahead, to what extent he predicts other agents' motions, and whether he plans the full trajectory to the goal or only a few steps ahead [79, 183]. Within recent literature, humans are usually considered to plan an optimal trajectory from their current position to a defined goal. The applied planning horizon covers the whole trajectory, while factors like time, path length and energy expenditure are optimized [19, 49, 121]. However, these methods are not able to reproduce the exact strategy employed by humans, if unpredicted disturbances occur [14, 23, 148]. Therefore, different approaches are found in literature that are applicable as corrective measures: con-

stant re-planning [7, 13], re-planning at specific states [128, 131], integration of intermediate goals [14], or reactive approaches without prior planning [59]. With these approaches, the observed trajectories are reproducible but the underlying human locomotion behavior remains unclear. A detailed model for the human behavior to handle disturbances would thus allow for more accurate predictions. In order to tackle this problem, it must be explored whether humans employ different behaviors within fully observable and partially observable environments. The posed hypothesis is that humans resolve situations like almost collisions, surprising situations or cases of failed prediction by adapting their planning horizon [13]. This behavior could be necessary, since these situations are the result of the human's uncertainty about the exact motions of all other agents within the current environment. Thereby, it is not known how much complexity humans can handle before they start to adapt their planning. A second issue is the fact that the executed trajectory may diverge from an optimal solution and lead to a suboptimal motion [23]. Therefore, it is also of interest if the executed trajectories stay within certain boundaries around the initial optimal solution. These uncertain situations are summarized as "partially observable environments" and it is expected that the hypothesis of an adaptive planning horizon generalizes to most of this collectivity [83]. Within this section, sufficiently complex environments are also assumed as partially observable, because a human being is not able to track more than a certain number of agents at once [83]. In accordance with the posed hypothesis, a human is expected to follow the unique optimal solution, if the environment is "fully observable" and thereby carries no uncertainties. The resulting goal is a specialized experiment, which aims to determine if a shorter planning horizon constitutes a specific human re-planning strategy.

Throughout this section, human locomotion prediction is approached from a control perspective, assuming a human as a dynamic system that optimizes its locomotion with respect to aspects like energy consumption [30]. Based on existing models [14, 121], the prediction problem is formulated within a non-linear model predictive control (NMPC) framework. The influence of the planning horizon is then initially analyzed within simulations. This framework and the respective simulation results are used to illustrate the problem regarding the human planning horizon from a control theoretic point of view. Detailed statements about this human behavior, however, require further evaluations in user studies.

In order to investigate the mentioned aspect, an experiment design is proposed that yields basic insights into the human motion planning process. Indeed, measuring the currently applied planning horizon of a human is challenging. This process is of cognitive nature, such that sensor based approaches are not applicable. The complexity of this process is illustrated by Goffman's theory about interactive human locomotion behavior [71]. On this basis the "sense-plan-act" architecture [126] is established as a cognitive model. It reflects that pedestrians attempt to sense where other humans intend to go and then adapt their own plan to move accordingly. This cognitive model comprises the idea of a planning horizon which starts with sensing and ends with the action. Thus, three distinct tasks define this process: perception of the environment, planning of a path taking into account the predictions of all agents and execution of the trajectory. This point of view also establishes a correlation between the planning horizon and the visual

look-ahead. Clearly, planning further into the future requires humans to gather more visual information and to extend their predictions. In order to experimentally measure this process, the start and end-point are of main interest. Therefore, an experimental setup is proposed that measures the visual focus and the trajectories of subjects that perform movements within a specifically designed virtual environment. The movements are additionally disturbed by other virtual objects to trigger the anticipated avoidance behaviors. Changing the observability and therefore raising the uncertainty is accomplished by altering the complexity of the environment based on the number of obstacles [13]. This experimental design is expected to reveal information about the planning horizon and the accepted deviation of trajectories from distinct optimality criteria.

In summary, an experimental setup is contributed to the state-of-the-art, which allows to investigate adaptations in the human motion planning horizon. Therefore, the experiment assumes that humans can be considered as model predictive controllers with an adaptive prediction horizon. Analyzing how humans adapt their planning horizon, yields the opportunity to improve OC based motion prediction methods by incorporating the identified behavior. Especially the prediction of specific avoidance and recovery motions, which emerge from reactions to high collision risk, is expected to be improved. Aside from that, the theory is investigated whether humans deviate from an optimal solution during an avoidance motion. Thereby, the presumed behavior is a confinement to a convex hull which forms a corridor between the current and the goal location. This would further indicate that complex scenarios are handled with a shorter planning horizon.

Clearly, dynamic environments require a human to re-plan and adapt its locomotion trajectory in case of disturbances. Therefore, knowledge of the way humans adapt their planning horizon will allow robots to predict human motion more accurately in complex situations. Since the planning horizon seems to be strongly connected to collision avoidance behaviors, the varying results towards velocity and path adaptation shown in literature may find more explanation within present work [23, 80]. The results of the proposed study and possible continuations potentially influence future motion prediction approaches, such that a wider variety of human behaviors is accurately representable.

The subsequent section has the following structure: In Subsec. 3.1.1 literature regarding motion prediction and avoidance behaviors is discussed. Subsec. 3.1.2 elaborates the applied cognitive model and formalizes an according NMPC framework. The following Subsec. 3.1.3 describes the experimental design and procedure. Results are shown in Subsec. 3.1.4. After a short summary, the experiments are discussed in Subsec. 3.1.5.

3.1.1 Classification within the State-of-the-Art

The following discusses certain topics in literature which are of relevance to this work. Firstly, a short overview of relevant motion prediction approaches is given. Thereafter, the prediction of human locomotion trajectories based on dynamic models is reviewed. Then works on mutual avoidance behaviors are discussed and weaknesses within the respective models are revealed. Lastly, literature on experimental evaluation of behavioral and cognitive models is accounted for.

3.1.1.1 Motion Prediction

Motion prediction is a wide field applicable to any mobile agent, e.g. humans, cars or robots. The methods are widespread and usually generalize to a large variety of situations. A survey on recent methods applied to autonomous cars is found in [105]. Many prediction algorithms are based on Kalman filtering [21, 55, 154], which does not yield good performance for complex environments. Multiple hypotheses are fused with a Kalman filter in [182], to predict future positions of humans. Here, social aspects are considered to play a crucial role in avoidance and prediction. A very influential work towards prediction of pedestrian locomotion is proposed by Ziebart et al. [193]. Inverse optimal control is applied on top of a Markov decision process to learn the preferred paths of pedestrians with respect to the environment. The approach enables a robot to position itself in a least interfering way or plan its path according to this measure. Incorporation of human behaviors is implicit and generalization to arbitrary environments is possible. Yet, for applications where the accurate trajectory as well as accelerations and torques are necessary, dynamic model based approaches are advantageous. The work of Kuderer et al. [102] is methodologically similar to [193] as it proposes to learn features of the environment in a similar way. Indeed, this work also shows the importance of continuous trajectories and the consideration of velocities as well as accelerations. In accordance to that, this section is concerned with accurate prediction methods based on dynamic models and OC theory.

3.1.1.2 Optimal Control based Prediction

A fundamental fact that influences many prediction algorithms is that humans intend to walk with minimum effort regarding energy and cognitive strain [30, 163, 186]. In a fully observable environment, humans are able to follow this principle successfully. Accordingly, effort is minimal since the initial locomotion plan is not disturbed. On the contrary, to cope with partially observable environments, re-planning and trajectory adaptations are necessary, which cost energy and lead to cognitive load. This is not desirable for a human but certain situations require this flexibility as the experiments will show.

Accurate prediction of human locomotion trajectories using OC and a unicycle model is widely studied [14, 18, 19, 121, 144]. These works propose different objective functions that reduce the solution space to a subset that closely resembles human locomotion trajectories. Thereby, some works focus on minimization of energy, path length and time, whereas others follow specific curvature constraints. In fact, most approaches are developed with the goal of locomotion prediction. An inverse optimal control approach is shown by Mombaur et al. [121]. The method allows to incorporate new objective functionals into a holonomic model and estimates their influence. A similar idea is followed by [14], which applies a different methodology. Albrecht et al. also integrate obstacles into their framework which makes it well applicable to trajectory prediction problems. Indeed, the authors successfully predict a trajectory of a free-space walk, but need to add a re-planning structure based on a distance rule to approximate human data that contains disturbances from an interfering agent. Clearly, the human data shows a behavior that strongly diverges from the OC idea of full observability and a fixed control horizon. In [49, 63], prediction for arm movements based on the same methodology is presented. These approaches also opt to generate

human-like motions and investigate the underlying objectives. In [135] the generation of human locomotion paths is addressed similarly to aforementioned works. Here, the problem is reduced to the path data in order to gain invariance to velocity, although other works consider both aspects to be strongly correlated. The authors reformulate the problem from a constrained into a convex unconstrained least-squares optimization. An adapted inverse optimal control approach is applied that incorporates the discrete Frechét distance and leads to new cost functionals for human locomotion. A comparative evaluation is shown in [136]. In [61] trajectory prediction methods based on OC and spline fitting techniques are compared. Multiple predictions between a current position and all estimated goals are taken into account. Selection of the most likely trajectory is done using minimum curvature variation, path length and execution time. In [79] authors propose that humans plan full trajectories to a goal rather than a series of steps. Subjects varied their foot placement within repetitions of the same path, suggesting that goal-oriented locomotion is related to higher level trajectory planning rather than step planning. Humans are also considered as optimal controllers in [82]. Here, the OC approach is used to predict pedestrian behavior in order to improve building layouts. Bascetta et al. [21] combine the OC procedure with Kalman and particle filters. This enables short term prediction for a human-aware robot cell but only for a single human.

All mentioned approaches consider humans as optimal controllers and aim to identify the composition of objective functions, which are used to predict human locomotion. For this prediction it is assumed that humans always plan trajectories between their current position and a defined goal. This methodology is adopted here, but the attention is also directed to the inherent aspect of the real planning horizon, which is barely addressed. Especially the inaccuracies of OC methods reported in [14, 23] have not been addressed, yet. The results of the work at hand will provide insights into human behaviors which could improve the precision of existing prediction models and methods.

3.1.1.3 Behavioral Models for Human Locomotion

Avoidance behaviors of humans are often investigated in user studies where an interfering but not interacting person (often called intruder) crosses the subjects path from the side [14, 23, 80, 100, 101, 129]. This case is studied intensively, models are proposed and implications to robot navigation are developed. Interest is particularly set on avoidance strategies employed by the human being. Authors repeatedly report either velocity or path adaptations as the reasons for observed trajectories, but a common principle is not defined. Some approaches assume velocity adaptations as the typical behavior [23], whereas others propose the combination with path adaptation as the underlying principle [129]. Rule based behaviors following time-to-collision or minimal-predicted-distance [128, 131], pose another method to model the timing of avoidance movements. These features model the re-planning at specific positions relative to the obstacle.

The disagreement between different studies arises from missing knowledge about underlying parameters and behaviors. Thus the planning horizon is investigated as one important parameter in this regard. Hence, the results presented here yield valuable ideas and insights to clarify this divergence.

Many works are concerned with the general behavior of humans during locomotion.

These approaches often consider humans as simple controllers that change their behavior based on a set of rules. Obstacle avoidance is thereby based on distances rather than a prediction horizon. This rule based behavior resembles a very short planning horizon in contrast to the mentioned OC methods. Some related publications are presented in the following. A fundamental work in the field of human locomotion behavior is provided by [59]. Fajen et al. propose a human inspired constant velocity steering model. Their experiments validate the approach for static environments where obstacles may suddenly appear. Fink et al. [62] evaluate the difference of locomotion paths in real and virtual environments. The results show that humans are able to project their physical behavior. This supports the use of virtual environments for experiments regarding human motion. In [86] a velocity based model for the locomotion behavior of a human crowd is proposed. This model employs the principles of personal space, least effort and time-to-collision. Using a fixed horizon for taking obstacles into account is also proposed in [123]. In relation to a planning horizon, obstacles are considered only within a certain distance and independent of the individual speed. In [142], aspects that influence the use of an open-loop or closed-loop methodology for locomotion control are investigated. This matter is specifically investigated for the absence of visual feedback and for varying velocities. Pham et al. attempt to clarify whether humans use a feedback scheme for locomotion, given they act like a controller. The consideration of closed-loop and open-loop structures shows many parallels to this section.

Behavioral models where humans react to obstacles based on an fixed set of rules, resemble a very short planning horizon. Planning ahead in order to find an optimal solution, as it is the case for OC methods, is not considered. The results of these methods show, that human locomotion behavior is also predictable with a very short horizon. Yet, OC methods yield a better performance when human behavior should be accurately reproduced.

Perception is considered a key indicator for the planning horizon in this work. Some experiments in literature are concerned with the visual look-ahead that humans employ during navigation tasks. Look-ahead during steering around obstacles on a bike in a virtual environment is considered in [183]. Authors analyze how the fixation of near and far obstacles develops during the course and find that fixation goes to the closest obstacle and switches to the next obstacle at a distinct distance. Look-ahead during foot placement on a predefined parcours is the topic of [139]. Results point towards interesting behaviors when the final pose is approached. The influence of the planning horizon of a robot on its apperception is addressed in [100]. It is shown how constant re-planning leads to undesired behavior if the environment is not fully observable or the planning horizon is too short.

Clearly, findings about look-ahead behavior correlate to the planning horizon addressed here. Presented works, however, do not evaluate the correlation of these aspects. Apart from [142], a change in anticipatory horizon is not investigated directly or considered as a critical factor in human behavior.

3.1.1.4 Cognitive Models for Human Locomotion

Human locomotion planning is a cognitive process, which is investigated in the following experiments. The following paragraph depicts literature about cognitive models that are used as a basis for the proposed experiments. Fundamental literature that describes the

considered cognitive processes is posed by Goffman [71] and Reich [148]. Goffman describes the human locomotion behavior as a series of actions. Humans “externalize” their intention (e.g. their goal) nonverbally by stereotypical movements, gaze or heading. Then they try to “sense” what others intend and incorporate this into their own planning process. Finally, under consideration of sensed information and own intentions a trajectory is executed. This sequence is repeated constantly in order to avoid collisions and reach the personal goal. This loop is termed “sense–plan–act” in [148], resembling a typical cognitive control loop used in robotics [126]. A faster model is proposed as “sense–control–act” that reduces the trajectory planning to an adaptive steering to the intended goal position. Apart from that, [148] also poses the question for the correct timing to initiate re-planning. The work at hand yields results towards an answer. Most influential statements towards the human planning horizon are made by Ahmadi et al. The authors of [13] propose to model the cognitive path planning process in the human brain with an MPC approach. They hypothesize that the cognitive load rises with more complex and longer paths to be planned. It is therefore intended to use this assumption for detection of brain diseases. Present work follows this concept closely.

The two cognitive loops proposed in literature obviously favor a long and a short planning horizon. Similar to the different approaches of modeling human locomotion behaviors, this disagreement supports the assumption that this matter is not unanimously defined. Literature in the area of robotics, optimal control, experimental psychology and clinical research has not directly evaluated the applied planning horizon within human locomotion planning as an influential parameter for prediction. The idea of a change in the hypothesized planning horizon is also not further investigated within literature regarding control theoretical models. Therefore, the investigation of the applied planning horizon can contribute to the set of behaviors that are used for human locomotion prediction.

3.1.2 Problem Description

In the following, a model for the planning horizon applied by humans during locomotion is defined. The framework comprises a cognitive process suggested in literature and a control theoretic structure which defines the planning behavior in more detail. Simulations of the planning architecture allow for basic insights into the effects of a varying planning horizon. The results also further motivate the investigation of this aspect.

3.1.2.1 Cognitive Architecture for Human Locomotion

Human behavior during locomotion is described as a repetitive process consisting of: gathering visual information [139], constructing a trajectory to the goal [79] and executing this trajectory. Planning and acting are thereby strongly affected by the human ambition for minimum effort [163]. A descriptive cognitive process, which underlies human motion, is supplied by Goffman [71] and Reich [148]. In Subsec. 2.2.2 of Sec. 2.2 this model is already used as a basis for locomotion. As a different aspect of the model is considered here, the concept is briefly repeated. The cycle of “sense–plan–act” described in [148], see Fig. 3.1, also found application in the early years of robotics [126]. Reich [148] builds upon this model and proposes a “faster” loop: “sense–control–act”. This structure is cognitively less

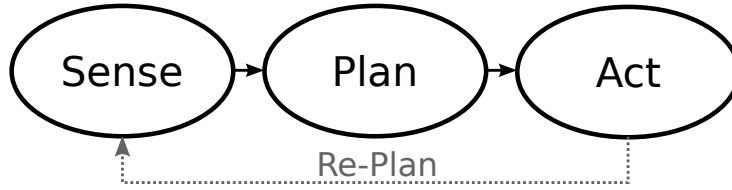


Fig. 3.1: Cognitive Architecture by Goffman and Reich [71, 148]

demanding and allows a human to walk towards its goal while steering around obstacles without the planning or re-planning of a detailed path. A realization of this shorter cycle is described within [59] in Sec. 3.1.1. Both cognitive models are applicable to reproduce human locomotion paths, but the actual human planning horizon and whether this horizon can change, is not yet clarified.

Investigating the human planning horizon requires to measure these subconscious processes in a subject's mind. However, this cognitive loop is neither observable for sensors nor derivable from questionnaires. The described models are therefore an indication of how an experimental setup is able to measure the process. Only input and output information are measurable entities. Following the models, the input consists of visual information and the output is posed by the traversed trajectory.

Accordingly, an experiment needs to be designed that asks a subject to plan and execute a motion in a visually observable environment. Further, in order to trigger changes in the planning horizon, the experiment needs to provide fully and partially observable situations. As mentioned before, the complexity and therefore the observability of a virtual environment is easily adapted by changing the number of obstacles. Thus, the development of the gaze and trajectory data is evaluated, while subjects are presented with various situations. The expectation for simple unobstructed environments is to observe a smooth and immediate movement from a defined start to a defined goal location. Measured sensing data, i.e. gaze, is expected to focus on the goal mostly. On the contrary, a jerky motion is expected for partially observable environments, with stepwise movements (acceleration and braking) and delimited looking ahead. Following this, it is expected that the human planning horizon is proportional to the applied visual anticipation of the person. If the extent of visual anticipation is a precondition for the planning horizon, a correlation to the smoothness of executed motions must be visible. The result of a measurement is a two-dimensional planar trajectory $\xi(t) = [(p^x(t), p^y(t), \varphi(t)) | t = 0, \dots, T]$, where the orientation $\varphi(t)$ is not recorded in subsequent experiments and thus omitted in the following formulations of the problem.

A trajectory ξ describes a change of position over time, between a start point $\mathbf{p}_S = (p_S^x(0), p_S^y(0))$ and an end position $\mathbf{p}_G = (p_G^x(T), p_G^y(T))$. The trajectory ξ and especially the velocity profile $v(t) = \dot{\xi}^{xy} = (\dot{p}^x(t), \dot{p}^y(t))$, are smooth between $\xi(0)$ and $\xi(T)$, if the obstacles are well predictable for the subject. This implies that the trajectory smoothness is proportional to the planning horizon and the visual look-ahead. Given a complex scenario, smoothness is expected to be maintained between an arbitrary starting point and a position close to a predicted obstacle trajectory. It is assumed that smoothness diminishes to a concatenation of movements for more complex environments. Generally, complex situations pose a high level of uncertainty for a human agent. Therefore, the applied planning

horizon is expected to depend on the uncertainty about an environment.

Overall, the cognitive models and literature about human locomotion lead to a set of proportions which are measurable during an experiment: visual anticipation, smoothness of velocity and path, and the complexity of an environment, which correlates with observability and uncertainty [13]. From these factors the applied planning horizon of a human subject is derived. The specific methods for measuring these aspects are explained in detail in the experiment section 3.1.3.

3.1.2.2 Non-linear Model Predictive Control based Locomotion Prediction

For predicting human locomotion a NMPC framework is applied. NMPC resembles the cognitive structure of human motion planning and allows for a variable prediction horizon [13]. In combination with models from literature [14, 121], NMPC yields an adaptive framework for locomotion prediction. Prediction with an NMPC model gives an estimation of the trajectory for the considered situation. As the controls are not applied to a system, the simulation results resemble a model based prediction rather than the controlling of a human. Thus, the following simulations aim to predict the recorded trajectory based on the observation of a system state. Thereby, NMPC poses a model for the human locomotion behavior. The used framework is equal to the formulation of Sec. 2.2, which is based on the notation in [16]. Two different objective functions are applied in order to illustrate their influence. Simulations are conducted with the ACADO Toolkit [12].

Within this NMPC framework the controls are applied over a certain control horizon T_C which is usually shorter than the prediction horizon T_P . The respective objective function $J(\cdot)$, which is evaluated over T_P , is chosen to be a two-point boundary value [14] or a linear-quadratic problem [16]. The problem is then solved with direct methods at every time-step δ . Initial values are formed by the current closed-loop states $\mathbf{x}(t)$ and the closed-loop controls $\mathbf{u}(t)$ at the starting time t . Figure 2.14 in Subsec. 2.2.2 illustrates an NMPC process where T_C is smaller than T_P .

At first, a simple least-squares problem (LSQ) is solved that does not contain the constraints for specific human-like motions as in [14]:

$$\phi(\bar{\mathbf{x}}(\tau), \bar{\mathbf{u}}(\tau)) = Q_{\mathbf{x},\text{LQ}}(\bar{\mathbf{x}}(\tau) - r_{\mathbf{x},\text{LQ}}) + Q_{\mathbf{u},\text{LQ}}(\bar{\mathbf{u}}(\tau) - r_{\mathbf{u},\text{LQ}}),$$

where $Q_{\mathbf{x},\text{LQ}}$ and $Q_{\mathbf{u},\text{LQ}}$ are diagonal weighting matrices and $r_{\mathbf{x},\text{LQ}}$ as well as $r_{\mathbf{u},\text{LQ}}$ are the reference vectors for states and controls. In order to reduce the model complexity and thus calculation times, the dynamic model is defined with inputs on the acceleration level instead of torque level:

$$\dot{\mathbf{x}}(t) := \frac{d}{dt} \begin{pmatrix} p^x(t) \\ p^y(t) \\ \varphi(t) \\ v(t) \\ \omega(t) \end{pmatrix} = \begin{pmatrix} v(t) \cos(\varphi(t)) \\ v(t) \sin(\varphi(t)) \\ \omega(t) \\ u_1(t) \\ u_2(t) \end{pmatrix}.$$

For the initial closed-loop states $\mathbf{x}(t)$ and controls $\mathbf{u}(t)$, a recorded trajectory from the experiments described in Sec. 2.2 is used. Yet, only position, velocity and orientation

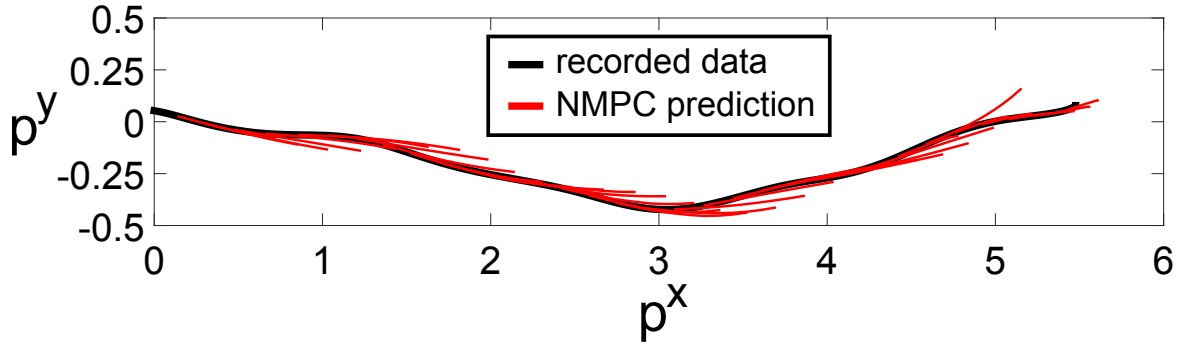


Fig. 3.2: NMPC with LSQ objective function for short-term prediction applied to human locomotion data

are derived from the data. Accelerations are assumed to be 0.0 at the beginning of each prediction step. The NMPC framework is applied to provide short-term predictions based on the mentioned unicycle model. In order to obtain reasonable results, the set-point is determined as the final position of the human (5.0, 0.0). Furthermore, a specific objective functional is added that is evaluated with respect to the final state and enforces a minimum distance to the goal pose constraint [12]. Weights for the states and controls $[\bar{\mathbf{x}}, \bar{\mathbf{u}}] = [p^x(t), p^y(t), \varphi(t), v(t), \omega(t), u_1(t), u_2(t)]$ are set to $\text{diag}(Q_{x,\text{LQ}}) = [100, 1500, 10, 100, 1]$ and $\text{diag}(Q_{u,\text{LQ}}) = [50, 2.5]$. Reference values are set to $r_{x,\text{LQ}} = [5, -0.5, 0, 1.4, 0]$ and $r_{u,\text{LQ}} = [0, 0]$. The references for the states enforce the acceleration towards the goal pose, while a velocity of 1.4 m/s is desired. Since the LSQ problem does not feature a model for an interferer, which is the reason for the avoidance in the used data, a virtual force is generated by setting the p^y reference to -0.5 . Clearly, this is not a generally applicable method, but the modeling of avoidance motions within the LSQ framework poses a problem that is not in the focus of the work at hand. The prediction horizon is set to $T_P = 0.6$ and the control horizon is $T_C = 0.5$, while $\delta = 0.5$. Figure 3.2 shows the prediction results for the LSQ problem applied to recorded data from Sec. 2.2. The short predictions from the NMPC are able to follow the locomotion trajectories well. Although, the trajectory resembles an avoidance movement and the simple model does not include a special cost model for the interferer. Parameters are, however, chosen heuristically and will not generalize to arbitrary trajectories.

For a comparison the NMPC structure of [14] is used. This approach re-plans the OC model at every defined time-step. Thus, a complete trajectory is constructed between the assumed pose $\mathbf{p}_H(t)$ and a goal pose $\mathbf{p}_G(T)$. The approach from Albrecht et al. also features an interferer model and a generalizable cost function. The provided weights of the objective function are adapted heuristically in order to improve the solutions. Prediction horizon and control horizon are set to $T_P = T_C$, since a final pose must be reached with the estimated control. The time for each step is derived from the data, which resembles a trajectory recording of 5.35s. Hence, the OC model is solved with respect to the remaining time-frame between the starting point and the recording time. The starting points are acquired by sampling from the trajectory data. Following simulations only use 10 samples for illustrative purposes. Figure 3.3 shows the results for the trajectory used in Fig. 3.2. The long prediction horizon approximates the recorded trajectory accurately, but requires

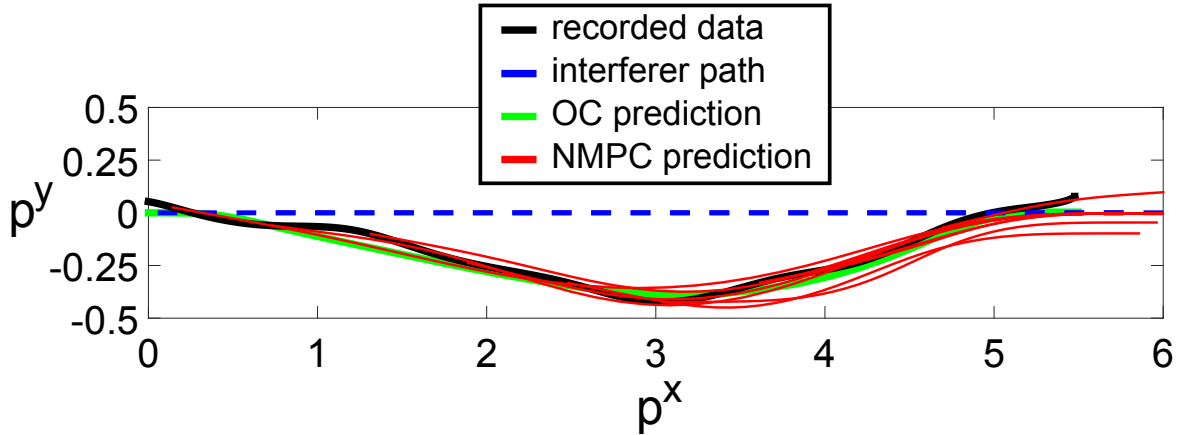


Fig. 3.3: NMPC with OC objective function from [14] applied to human locomotion data

an estimate for the goal pose. Moreover, the path of the interferer must be known for an accurate prediction. This large prediction horizon is advantageous, as for example a robot is able to plan its own motions further into the future. But the necessary prior knowledge limits the applicability of the approach, favoring short term solutions. Eventually, in case of a more complex movement, as it is discussed in the present section, the OC model is not able to follow the quick change of directions.

The presented simulations show that a prediction of a future trajectory is possible when the current state of a walking person is observed and the desired goal is known or estimated. Yet, the problem described in [14, 23], that the OC solution does not resemble the observed avoidance behavior, is not reconstructed here. Reproducing the discussed behavior requires the NMPC to use the last state of the prediction as the current system state. This analysis is provided in the following section.

3.1.2.3 Planning Horizon in NMPC Locomotion Prediction

In this section, the influence of the planning horizon in human locomotion prediction is elaborated. The basic problem is posed by a moving human which is disturbed in his progression by another agent in the same environment. OC methods usually yield accurate prediction results for this situation, if the interfering agent is well predictable. These methods assume a planning horizon that spans the whole trajectory between a start $\mathbf{p}_S(0)$ and an end position $\mathbf{p}_G(T)$. OC thereby follows the theory that humans intend to walk with minimum effort [30]. In a fully observable environment, where the trajectories of all agents are reliably predicted, humans are able to follow this principle. Thus, OC methods will produce reliable predictions. However, many experiments in literature show that humans tend to deviate from this minimum effort behavior [14, 23, 80]. Predictions with OC methods are shown to be unable to reproduce the trajectories observed in these cases. Hence, human locomotion appears to follow different suppositions for some situations. OC based prediction approaches do not generalize to these changes in behavior and therefore need to be improved. Figure 3.4 illustrates the results of these previous investigations. In order to obtain a suitable prediction for such a case, the OC structure is changed to an MPC structure in [14]. This approach basically re-plans the trajectory based on a simple

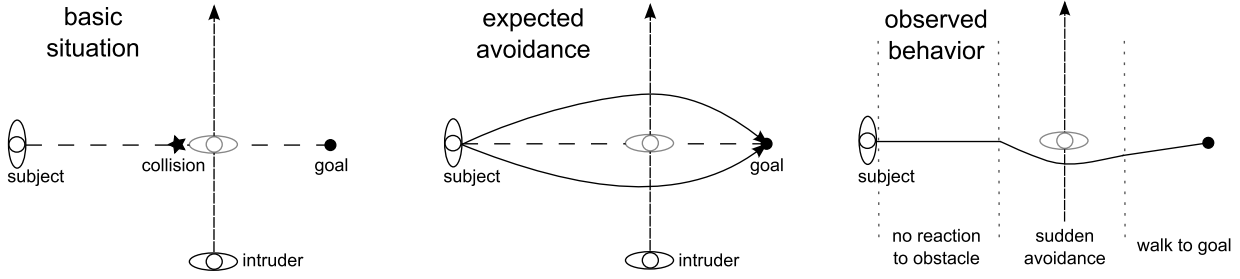


Fig. 3.4: Illustration of an observed deviation from the typical avoidance behavior of humans

distance rule. It appears that humans do not necessarily consider all obstacles from the beginning and apply a shorter planning horizon than the OC methods assume.

Given that even a single obstacle leads to sudden avoidance behaviors, it can be hypothesized that humans change their behavior if they are confronted with uncertainties. For example, unreliable predictions for other agents or high complexity of the environment (e.g. many obstacles) lead to large uncertainties for a human. Surprising behavior of an agent, like a sudden change of direction, may have equal effects. These situations require the flexibility from humans to omit their minimum effort strategy. Here, situations with high uncertainty are summarized as partially observable environments and it is proposed that humans alter their planning horizon to cope with them.

The subsequent simulations investigate this proposition and show that a shorter planning horizon reproduces the observed behavior in [14]. In order to illustrate the problem in more detail, humans are modeled using NMPC, as it is proposed in [14, 79]. This allows to analyze effects of the adaptation of the planning horizon within the modeled human locomotion behavior. For this analysis, the previously defined NMPC model is used. With this NMPC framework as well as the objective function and the constraints from [14], the following simulation results are obtained. These simulations specifically highlight the influence of the planning horizon. An OC solution is therefore compared with the NMPC solution to determine whether the behavior shown in literature is replicated. For the prediction with a human locomotion model, control and prediction horizon have equal length $T_C = T_P$. This is necessary for the incorporation of a goal pose, which is used to constrain the infinitely possible motions to a reasonable set. The two-point boundary value problem is also solved directly at each time-step δ , whereas the initial boundary is formed by the current closed-loop states $\mathbf{x}(t)$ and controls $\mathbf{u}(t)$ at the starting time t . The final boundary is posed by the goal pose $\mathbf{p}_G(T) = (p_G^x(T), p_G^y(T), \varphi_G(T))$ which also serves as set-point. Solving the problem yields state predictions $\bar{\mathbf{x}}(t)$ and the inputs $\bar{\mathbf{u}}(t)$.

The OC method uses a time horizon of $T_P = T_C = 7.2s$ which covers the whole trajectory from the start to the end. For the NMPC the planning horizon is set to $2.4s$. The set-point at $\mathbf{p}_G(T) = (6.0, 0.0)$ is necessary to constrain the solution space of the unicycle model to a reasonable set. Most constraints in the objective function of [14] also depend on this final pose. Thus, it is assumed that the set-point is known, whereas in a prediction scenario this is not the case. Omitting the final pose in order to generate a more generalizable OC based prediction method is not in the focus of this work. Yet, future approaches must take this problem into account in order to generalize to arbitrary situations. Fig. 3.5 illustrates the comparison of the methods. A scenario is considered, where an intruder crosses the

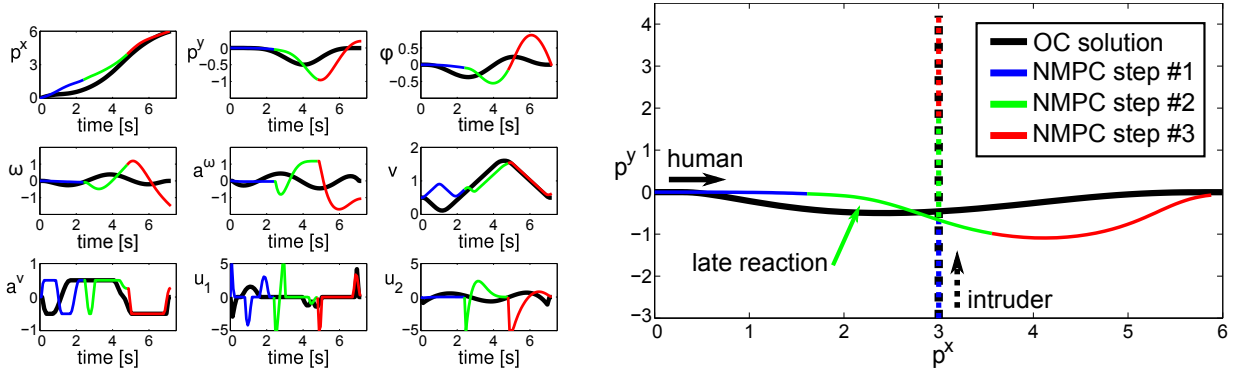


Fig. 3.5: OC solution (black) compared to NMPC solution with the shorter planning horizon (three steps colored). States and controls are subject to time (t). The path of the intruder that disturbs the motion is depicted as a dashed line. The lengths of the lines match the time horizons

human's path at 90 degree and interferes with its intention to walk straight to the goal. The intruder starts its slow walk with 1.0 m/s at a position $(3.0, -3.0)$, which is also three meters away from the crossing point of the straight paths of both agents. A subject has two options in this case, to pass behind or in front of the intruder. With the desired velocity of the human set to 1.4 m/s , see [14], the OC and the NMPC solution let the interfering agent pass first. The black path in Fig. 3.5 is the result of the OC method, which considers a fully observable environment. Clearly, the avoidance maneuver is initiated right from the beginning, because the future positions of the interferer are known. Controls, velocities and states progress smoothly without extensive energy expenditure. The velocity $v(t)$ reveals, that the OC solution brakes and accelerates to let the intruder pass. For comparison, the colored paths show the NMPC result. The obstacle is not considered in the first part (blue) because the planning horizon is reduced. Within the second part (green), the planning horizon reaches the obstacle and a reaction is initiated. State and control plots reveal, that this reaction requires far higher energy expenditure than the OC solution. The velocity plot also indicates the braking, but a smooth progression is not achieved due to the reconsideration of the problem after the first prediction horizon. The last part of the NMPC result (red) predicts a swerve back to the set-point, which shows a smooth progression of states and controls due to the free path. Necessary extra controls when using a shorter planning horizon explain why the OC solution is usually preferred by humans. Yet, these results appear very similar to the observations made within related literature, as illustrated in Fig. 3.4.

The differences in the paths from these simulated situations match the statements of [14, 23], that humans do not strictly follow the OC idea. Within mentioned work, the OC approach shows inaccurate predictions. It is further shown, that humans seem to resolve collision situations with a shorter planning horizon. Presented simulations support this observation. Clearly, humans walk smoothly from start to goal if no information is hidden for them. In case of unexpected events, unreliable predictions or other uncertainties, it appears that humans employ quick adaptations which lead to suboptimal and jerky recovery motions. OC is able to produce a prediction for the optimal trajectory, whereas the NMPC solution is not necessarily optimal but resembles the solution for a shorter

planning horizon. NMPC is further capable of attuning to model inaccuracies and changing environments, e.g. when a dynamic obstacle suddenly stops or its prediction is inaccurate.

Viewing human locomotion as a NMPC framework, allows for the correlation of the human planning horizon with a methodology. As the simulations illustrate, changes of this aspect with respect to environment observability, lead to very different results. Considering the influence of the planning horizon on prediction accuracy, it appears beneficial to investigate this aspect. Accordingly, the properties of the planning horizon that humans employ during locomotion are explored within subsequent experiments.

3.1.3 Experimental Exploration of the Human Planning Horizon

This section describes the experimental design which is developed to tackle the difficulty of measuring the planning horizon employed by humans. The experiment is designed as a study with human subjects that perform a goal directed motion. As mentioned before, measuring a cognitive process is not achievable using sensors. An experiment needs to visualize the aspects that are associated to the process, to eventually allow for conclusions about the underlying planning behavior.

3.1.3.1 Experiment Design

At first, a setup is needed where a subject is required to perform a goal directed motion. A large room equipped with a tracking system or a virtual environment are suitable setups, as they allow to measure the motions. In order to measure changes in the applied planning horizon, the experiment must feature multiple comparable conditions. Thus, a subject will perform the goal directed motion multiple times in varying environments. Generally, the environments will differ in the number of moving obstacles that need to be passed without colliding. Therefore, stable environment conditions must be provided for all subjects to support comparable and unbiased data. This includes that interfering obstacles move equally for all repetitions of the experiment. Within a motion capture area, where subjects walk freely to their goal, moving obstacles are representable by interfering human agents. Providing stable conditions for all subjects is, however, complicated in such a setup. Especially multiple human intruders will hardly be able to walk equally in a concerted way within every trial. A solution would be to use multiple equal robots or other controllable hardware which behaves equally for all subjects. Apart from the excessive effort, safety for the subjects is a major concern. Therefore, virtual environments are considered as they offer measurability and control of all parameters as well as flexibly adjustable complexity. Walking in virtual reality unfortunately requires hardware that is not commonly accessible. Steering a virtual character with a joystick is an unintuitive task and does probably not trigger the respective behaviors in a subject. Hence, an alternative is needed that allows subjects to perform a goal directed motion in a natural and intuitive way. Since the planning of arm motions and locomotion show comparable aspects and are based on similar control theoretic foundations [49, 121], the “Desktop Kinesthetic Feedback Device” (DeKiFeD) is used to record and virtually represent motions [34]. When using this device, subjects perform a natural and intuitive motion with their arm to follow a trajectory which they have planned. The “sense–plan–act” model is triggered as subjects see their progress

as well as obstacles in the virtual representation. In literature, the direct comparison of locomotion and arm motions reveals clear similarities [78, 178]. It was also shown that both motion types are controlled by the same region of the brain [191]. With this substitution, subjects are able to perform goal directed motions and obstacle avoidance in an observable and fully controllable environment.

3.1.3.2 Measuring Parameters of the Planning Horizon

With subjects performing motions in a virtual environment, different conditions can be provided to them in order to elicit changes in their planning horizon. As it is not possible to directly measure the planning horizon, other parameters must be observed to gather interpretable information. As stated in [13], with an increasing complexity of the environment (e.g. dynamic obstacles), cognitive load for locomotion planning will rise and a shorter planning horizon is employed. However, measuring the cognitive load is not sufficient within the proposed study setup, as the increase in cognitive load due to planning may be superimposed by the effort for steering and observing the environment. This issue is tackled by recording other parameters which resemble the planning horizon. With respect to the overall design, gaze tracking offers a direct measurement of the “sense” input to the cognitive process. Under the assumption that the planned trajectory is restricted to the observed part of the environment, a human is expected to look ahead less far if the planning horizon is short. In addition, measuring path and velocity data yields further information about the smoothness of the planned motion. Presumably, subjects will be able to avoid one or two moving obstacles easily, while smooth progression is maintained. But the smoothness of both path and velocity should diminish with a shorter planning horizon in more complex scenarios.

3.1.3.3 Triggering Adaptations of the Planning Horizon

In order to investigate the planning horizon, the experimental conditions must demand a subject to gradually decrease the planning horizon. With respect to Sec. 3.1.2, this decrease must be triggered by increasing the uncertainty for the subject. As mentioned, higher uncertainty is achieved by rendering the environment partially observable due to a rising complexity of the situation. For the virtual environment, this is realized by increasing the number of moving obstacles. A subject is able to track and predict a few obstacles in its way, but with increasing numbers the uncertainty will rise. This way, the gradual influence is realizable and different situations are comparable.

Presumably, subjects attempt to solve the posed motion problem optimally in case of a simple and therefore fully observable environment. This allows for the comparison whether subjects omit the globally optimal solution when a shorter planning horizon is necessary. An optimal solution is defined by the subject’s tasks. The task description defines that the goal position must be reached with least possible collisions, whereas the elapsed time is not of any meaning and the collisions are not counted. In order to solve the posed motion problem optimally, a simple straight motion from the start to the goal position is sufficient. Indeed, the study setup provides an optimal solution in every condition, which allows to move to the goal by a single smooth motion. Owing to the structure of the virtual

environment the opportunity for this optimal path appears periodically, but specifically two seconds after the start of a trial. In correspondence to [130] a human is capable of observing and assessing the environment in less than two seconds. But the subject must be capable of observing and predicting all obstacles in order to find this solution. Note, that owing to the supplied top view, subjects see all obstacles at every time step of their motion planning. Yet, a subject may also move to the goal on a straight line while avoiding collisions step by step.

The hypotheses about the planning horizon and the deviations from an optimal solution are now investigated by measuring the paths, velocities and major gaze fixation areas of each subject. Rising numbers of obstacles are supposed to result in partial observability and a reduction in the planning horizon. Accordingly, fluctuating velocities, lower average look-ahead and deviations from the theoretically optimal path are the expected consequences. Three alternative hypotheses are analyzed in this respect.

- $H_{1,A}$: visual look-ahead diminishes with increasing complexity
- $H_{1,B}$: recorded velocities exhibit diminishing smoothness with increasing complexity
- $H_{1,C}$: deviations from the optimal (shortest) path increase with increasing complexity

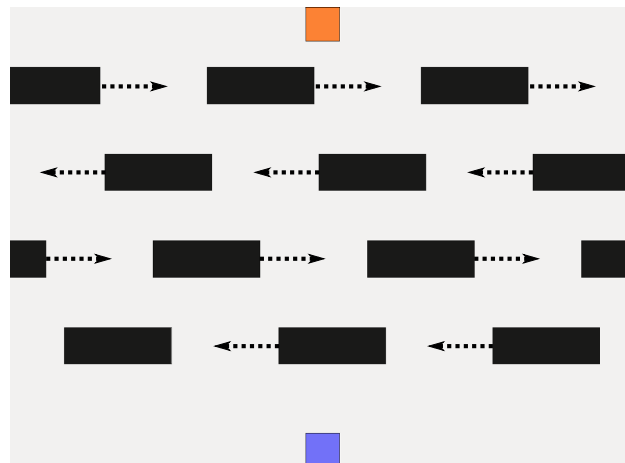


Fig. 3.6: Virtual environment with obstacles in black, start position on the bottom center (pale blue) and the goal position at the top center (pale orange)

3.1.3.4 Setup of a Virtual Environment

Within the virtual environment the smooth and straight motion is defined as the optimal solution baseline. For triggering changes in the planning horizon, a varying number of moving obstructions is integrated. With the rising number of obstacles, complexity and thus uncertainty is increased. The experiment therefore features various scenarios, which are in the following also called “levels of complexity” or “levels”. An example of the virtual environment shown to the participants is illustrated in Fig. 3.6. Its projection is 2 m away from the input device and thus 1.05 m wide and 1.45 m high. All levels have the same starting field, which is always located at the bottom center and printed in a pale blue.

The goal field is adversely at the top center and colored in a pale orange. The marker which is moved by the subject is represented by a dark blue box. All objects are placed on a white background, 1500×1100 pixel in size. At the edges, a virtual force keeps the subjects from leaving the defined workspace. Obstacles are integrated as static and moving blocks. In order to predetermine the motion of the obstacles, they only move straight from left to right or vice versa. Hence, prediction is simple for a subject but becomes complex with an increasing number of these objects. Prior tests revealed that a single obstacle is very easy to circumvent. For multiple obstacles, a subject may simply wait until the straight path is free, because there is no time constraints for the task. By adding multiple obstacles that re-enter the environment, a set of moving gaps is created which makes the task considerably harder. Yet, these “obstacle lines”, see Fig. 3.6, remain easy to pass.

In order to gain data for different situations and with varying complexity levels, a set of ten levels is designed. Confronting subjects with a rising order of complexity probably yields significant effects, when comparing the first and the last level. However, subjects are presented with the levels in randomized order, to cancel out any learning effects. The ten levels have the following structure:

- 01) The first level is an empty field, to test what optimal trajectory subjects choose in this virtual environment.
- 02) The second level contains one static obstacle in the middle of the field, to cause smooth but adjusted paths.
- 03) The third level has one horizontal line of dynamic obstacles moving from right to left with a medium velocity.
- 04) In the fourth level the single line is moving diagonally from bottom right to top left, inspired by [80].
- 05) Two horizontal obstacle lines enter the field from the right on the fifth level, where the first and closer one moves slow and the second one with medium velocity.
- 06) Equal obstacle numbers and speeds appear in the sixth level, yet the second line moves from the left to the right.
- 07) The seventh level is similar to the sixth, but obstacles move diagonally from bottom right to top left and the second line reversely.
- 08) In the eighth level, four obstacle lines are to be passed which move horizontally from the right side to the left. The first line is slow, the second and the fourth line medium and the third line fast.
- 09) Level nine is equal to level eight, but the second and the fourth line move from left to right.
- 10) Complexity is further increased in level ten as lines one and four switch from slow to medium speed, line two slows down from medium to slow speed and line three switches from fast to medium speed, if the subject gets as close as 100 pixels. In addition, line two and three also reverse their movement direction.

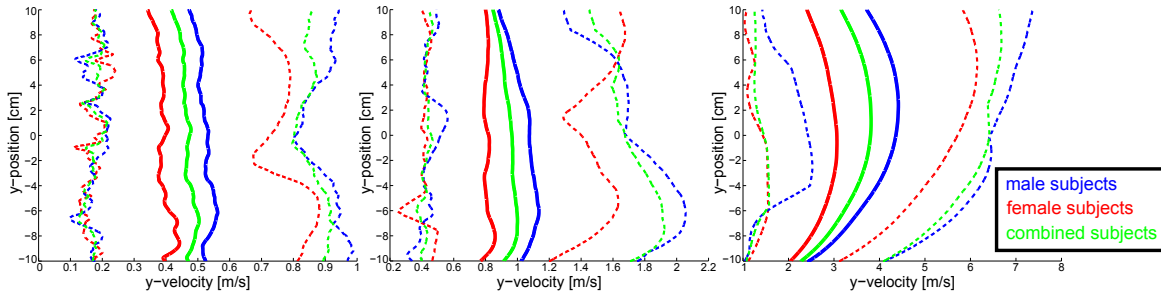


Fig. 3.7: Pilot-study data of the velocities along the y-axis for the individual perception of slow, medium and fast. Red corresponds to data from female participants, blue data from male and green resembles the combined result. Solid lines represent the mean and dashed lines confine the 95% confidence interval

With this last scenario it is intended to observe how subjects manage these 'interruptions' and the inherent uncertainty within their motion planning. The experimental task is performed twice with each level of complexity, hence resulting in a 10 (*complexity*) \times 2 (*trial – run*) within-subjects design. Repetition of the ten levels is important to analyze effects of learning and experience with the handling of the DeKiFeD.

3.1.3.5 Pilot-Study for Parameter Definition

In addition to the varying number of obstacles, different velocities are used as well. The reason is that very slow obstacles are extremely easy to pass, such that a change in planning horizon might not be needed. Thus, the variance in speed and obstacle numbers allows the investigation of the planning horizon more precisely. As the number of trials rises with variability, the velocities are limited to three types, slow, medium and fast. Choosing these qualitative velocities, however, is dependent on human perception. Therefore, a pilot-study is conducted with 21 subjects (12 male and 9 female participants). All subjects are presented with an empty environment and are supposed to move three times from the start to the goal. Participants are only asked to move at slow, medium and fast velocity, which they are allowed to define themselves. Thereby, subject velocities are transformed to progression in pixel-per-frame (PPF) by factors that define the relation of measured data to size and resolution of the visualized environment.

Path and velocity data is collected from 21 subjects in this pilot-study prior to the experiment, in order to define acceptable obstacle velocities. For calculation of the mean velocity along the y-axis, the data is fitted and thereby smoothed with splines. Afterwards, a mean and a 95% confidence interval are calculated, see Fig. 3.7. Women are not significantly slower than men, although the DeKiFeD does require force to be applied. Consequently, data from women and men is evaluated equally. Velocity perception is very individual, leading to a wider range of speeds. Some subjects are four times faster than others, despite equal instructions. The maximum of the combined mean is used for the fast and slow version to define boundaries. Transforming velocities to pixel-per-frame leads to 1 PPF for slow and 7 PPF for fast obstacles. Following this scheme, the medium velocity would be 2 PPF, which is just imperceptibly faster than the slow variant. Therefore, the average over all trials is chosen as a medium velocity, which leads to 3 PPF. Another im-

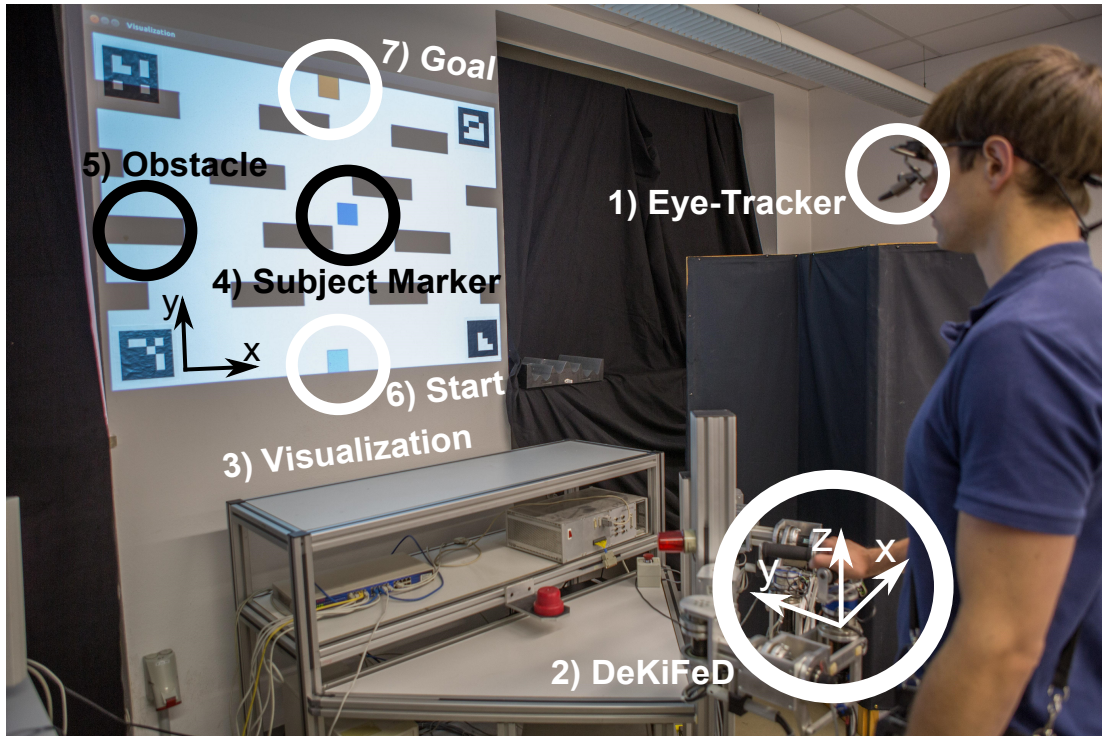


Fig. 3.8: Setup of the experiment where the subject on the right wears the Dikablis Gaze-Tracker (1) while using one part of the DeKiFeD (2) to move the virtual marker (4) through the virtual environment (3). The motion begins at a starting position (6) and ends at the goal (7) while the subject must avoid collisions with the moving obstacles (5)

portant result of the pilot-study is that none of the participants had difficulties in handling the input device. The DeKiFeD supplies an intuitive way of moving the virtual marker and is therefore appropriate to investigate aspects of human motion planning.

With respect to the posed setup, averaging of the recorded velocities results in three values: 1 PPF for slow, 3 PPF for medium and 7 PPF for fast velocity perception. The PPF unit is chosen to resemble the progression of an obstacle over frame-rate, whereas the visualization runs with 50 frames per second (FPS).

3.1.3.6 Hardware Setup

The final hardware setup is shown in Fig. 3.8. Gaze data is recorded with a Dikablis eye-tracker [165]. After calibration the transformations between the eye-tracking device and the observed environment are retrieved. Thus, the recorded focus points are transformable to the image space with the subject's marker position. The subject's trajectory data may then be evaluated with respect to gaze fixation. For recording the arm motions the DeKiFeD is used [34], a four degree of freedom (DoF) interface. It offers three translational and a rotational DoF within a working area of $0.4\text{ m} \times 0.4\text{ m}$. Forces applied by the user are measured with a 6-DOF force-torque sensor (JR3 Inc., Woodland, CA, USA) and transformed into acceleration and velocity of the virtual position marker. The mass of the marker felt by the subjects is set to 3 kg as this proved to be most convenient within prior

studies. By locking the upward facing and the rotational axis, subjects are restricted to move in two dimensions in accordance with the virtual representation.

3.1.3.7 Participants

An opportunity sample of 10 female and 31 male participants, aged 18 to 33 (mean age = 24 yrs., SD = 4 yrs.) took part in the main study, five of whom were left-handed.

3.1.3.8 Experimental Procedure

The experiments were approved by the ethics committee of the Technische Universität München and conformed to the principles expressed in the Declaration of Helsinki. A written informed consent had been obtained from all participants prior to the experiments.

Participants for the experiment were led to the laboratory by a dedicated supervisor. The supervisor then handed an informed consent and provided information regarding safety, data security and privacy protection. After subjects agreed to participate, they were equipped with the eye-tracking system. The headset position and the alignment of eye- and field-camera were adjusted accordingly. With the subject standing at its position, the eye tracking was finally calibrated with respect to eye color and other aspects.

Subjects were then instructed to reach the goal position whilst avoiding any obstacles but that there would be no counting of collisions and no time to beat. Prior to the experiment scenarios, subjects were allowed to familiarize themselves with the handling of the DeKiFeD and the virtual environment. When the respective subject felt comfortable, the experiment started with a random level. The ten scenarios were then to be completed in random order twice resulting in a 10 (*complexity*) \times 2 (*trial – run*) within subject study. Upon completion of the experiment, a questionnaire was issued to every subject. The questions assessed how difficult and exhausting the tasks were perceived to be by the participants. Finally, each participant was debriefed and thanked for participation.

3.1.4 Main Experiment Results

Within the experiments, position and velocity data of 41 subjects is captured at 1 kHz and the corresponding eye-tracking data at 25 Hz. At first, the data is evaluated qualitatively in order to determine the effects of the level complexity. Quantitative statistical evaluation is conducted afterwards to elaborate found indications of changes in the planning horizon.

3.1.4.1 Qualitative Data Evaluation

The following section highlights crucial parts of the recorded data and gives an interpretation of its correlation to the planning horizon. With ten different scenarios and various types of recorded data, showing all the resulting data goes beyond the scope of present work. For example, the scenarios four and seven, which cover diagonally moving obstacles in one and two lines, show very similar results when compared to their counterpart scenarios three and six. Therefore, these results are not illustrated in the following but yield the assurance that a different angle of movement has no exceptional influence. The most relevant gaze data for comparison of behaviors is created in the levels one, two, three,

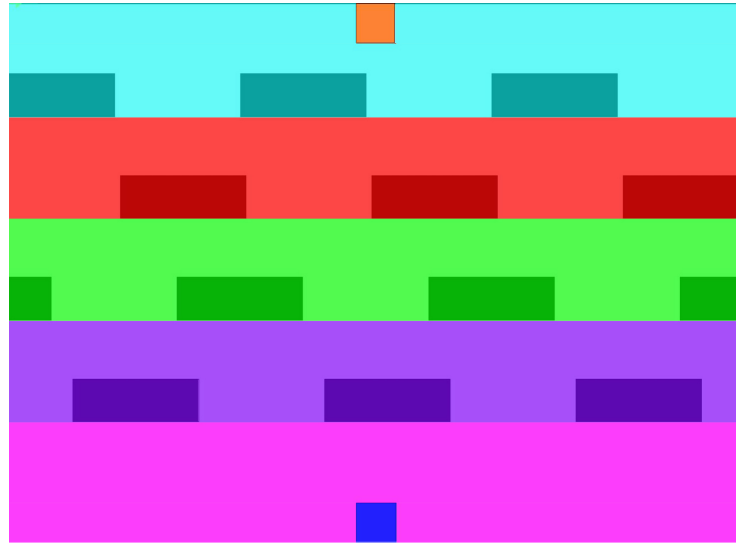


Fig. 3.9: Classification zones for gaze data in a scenario with four obstacle-lines

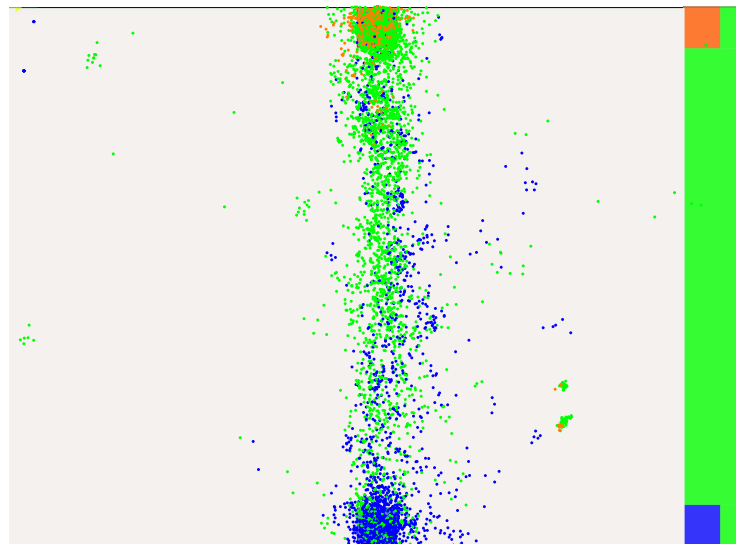


Fig. 3.10: Gaze-points created in level one

six and ten. Across these levels, the complexity is raised significantly with additional obstacles. As mentioned, levels that are not discussed in detail are necessary to investigate side-effects that may have a large influence on the results. However, the effect of inclination and movement direction of obstacle lines is revealed to be mostly negligible.

The subsequent qualitative evaluation considers gaze, path and velocity data, in order to find adaptations in the planning horizon of the human subjects. In order to evaluate gaze data, the virtual environment is divided into areas. One covers the start, another one the goal, and other zones are defined between the spaces start-to-first-obstacle, obstacle-to-obstacle and obstacle-to-goal. Gaze data is then distributed according to these categories such that plots reveal what the subjects focus on while moving in one of the areas. Fig. 3.9 shows the partitioning for a level with four obstacle-lines. The following evaluation also depicts the zones on the side of each gaze-data plot.

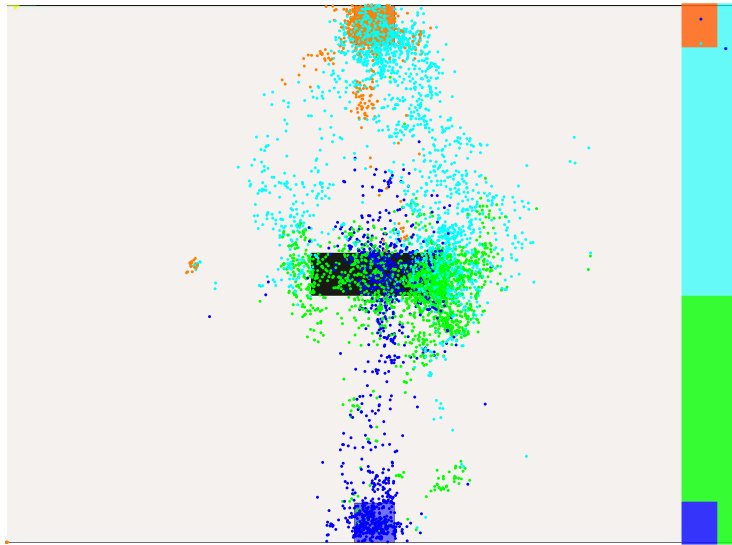


Fig. 3.11: Gaze-points created in level two

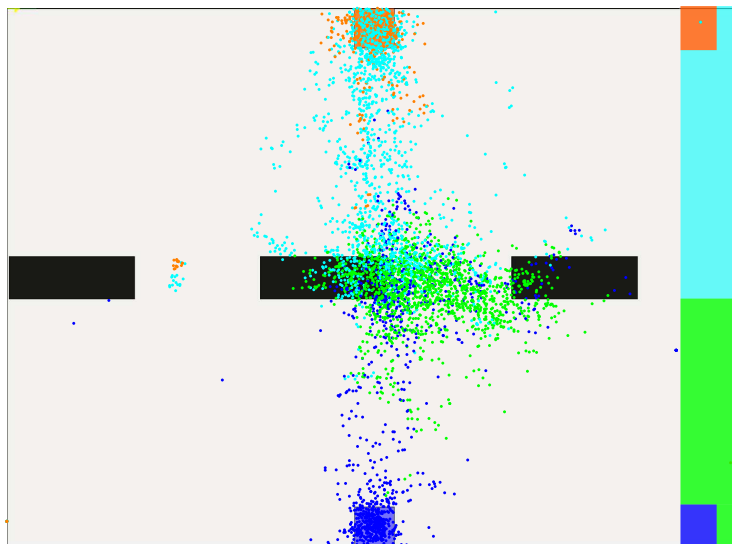


Fig. 3.12: Gaze-points created in level three

Visual Look-ahead In level one, see Fig. 3.10, subjects scan the empty area and then progress to the goal which they focus. The figure shows blue dots for gaze-points created while the subject remained at the start and green dots that represent the gaze during the motion to the goal. Clearly, subjects scan the area in front at first and then progress straight to the goal position. A planning horizon covering the full motion appears reasonable. The few orange dots indicate the gaze data recorded when the subject reaches the goal position. Across all levels it is observable that subjects tend to look back. This is related to the structure of the experiment, because subjects need to move down after each level in order to reset the system and start the next random level. Indeed, the field is free like the first level when subjects reached the goal and need to reposition to the start.

The single static obstacle in level two and the moving obstacle line in level three already receive large parts of the attention. The blue dots in Fig. 3.11 and 3.12 indicate that the

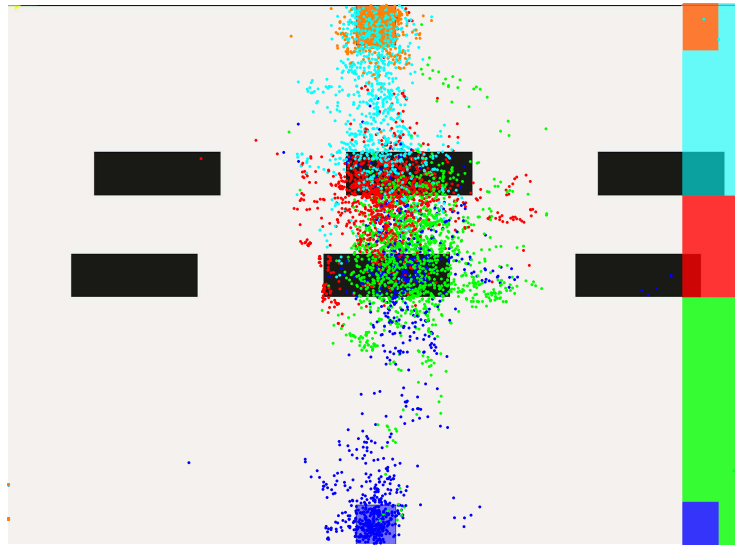


Fig. 3.13: Gaze-points created in level five

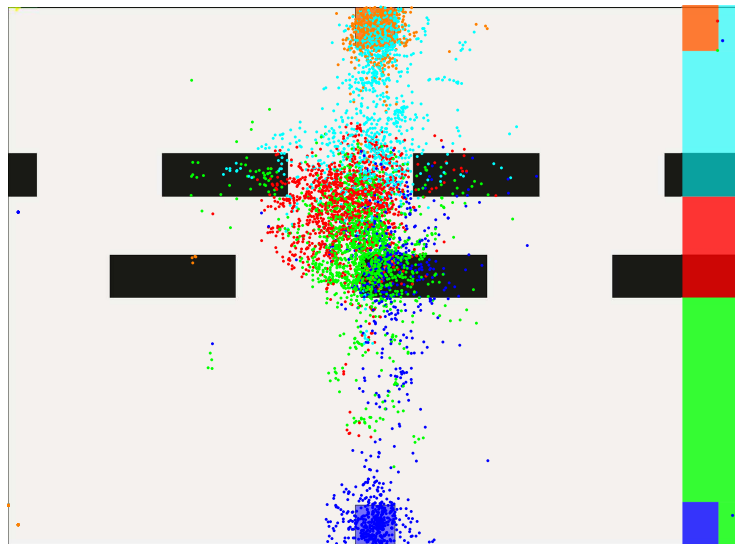


Fig. 3.14: Gaze-points created in level six

scanning of the area ends mostly at the obstacle. Yet, it is possible that the remaining area is processed by the peripheral field of view. The green dots now correspond to the area between the start position and the first obstacle. Most of the gaze is dedicated to the obstacles, although it is not moving in level two. Once the obstacle is reached, gaze slowly shifts to the goal, as the teal dots indicate. Similarly to the problem posed in Subsec. 3.1.2 humans seem to reduce their planning horizon to the most immediate obstacle at first. However, position and velocity data will show that subjects perform very smooth trajectories in level two and are able to stick closely to the optimal straight path in level three. In the following levels, gaze data shows even less look-ahead. Even in the scenarios with only two lines, attention is mostly on the obstacles. Figures 3.13 and 3.14 illustrate this. Red dots now cover the area between the two obstacle lines, all other colors are assigned as before. Notably, the red and green gaze points are mostly between the

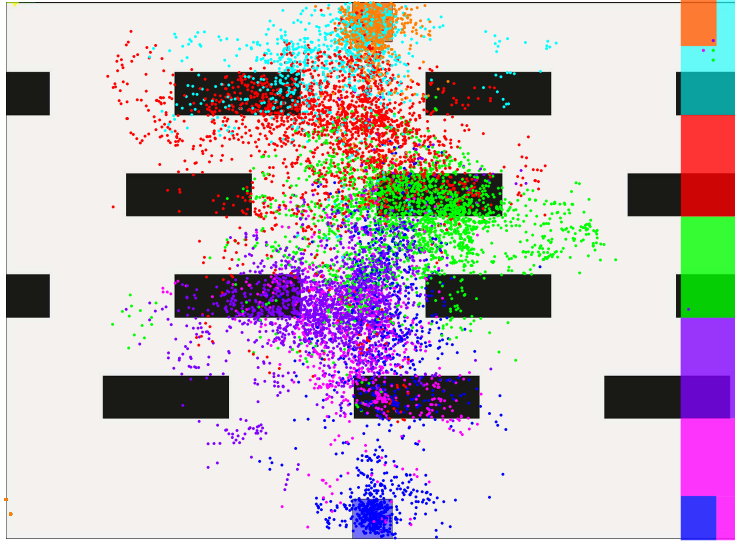


Fig. 3.15: Gaze-points created in level nine

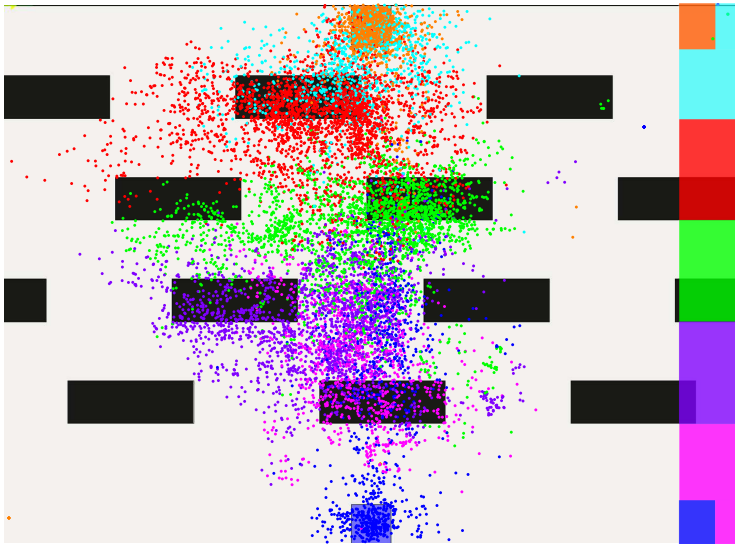


Fig. 3.16: Gaze-points created in level ten

obstacles which are the most immediate at that position. Since the goal or the area past the obstacles is not in the focus, it can be assumed that the planning horizon is constrained to find a solution for passing the obstacles.

These effects become even stronger with four obstacle lines. The color-to-area alignment is now blue-pink-violet-green-red-teal-orange covering the spaces from start to goal. In Fig. 3.15 and 3.16, gaze-points illustrated in pink cover the first two obstacle lines, proposing a larger planning horizon. Violet, red and green dots, however, are again constrained to the areas between obstacles, indicating no further looking-ahead. A comparison of level one and nine or ten respectively suggests that humans do reduce their planning horizon which supports the hypothesis $H_{1,A}$. Yet, this behavior may also be interpreted as a motion towards the most immediate obstacle which is then passed. In fact, further areas might be covered by the peripheral vision of the subject.

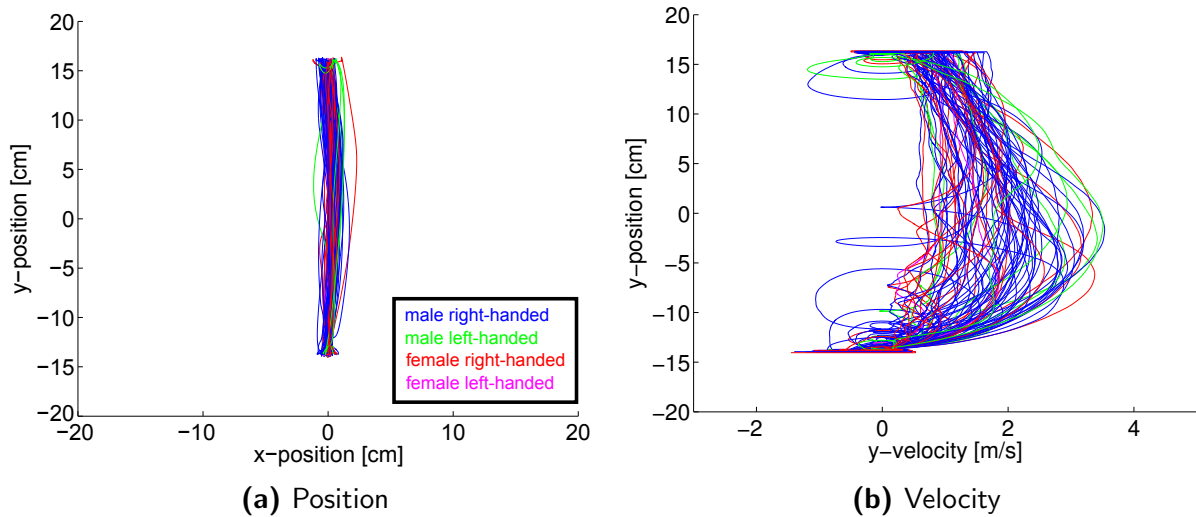


Fig. 3.17: Path and velocity data of level one

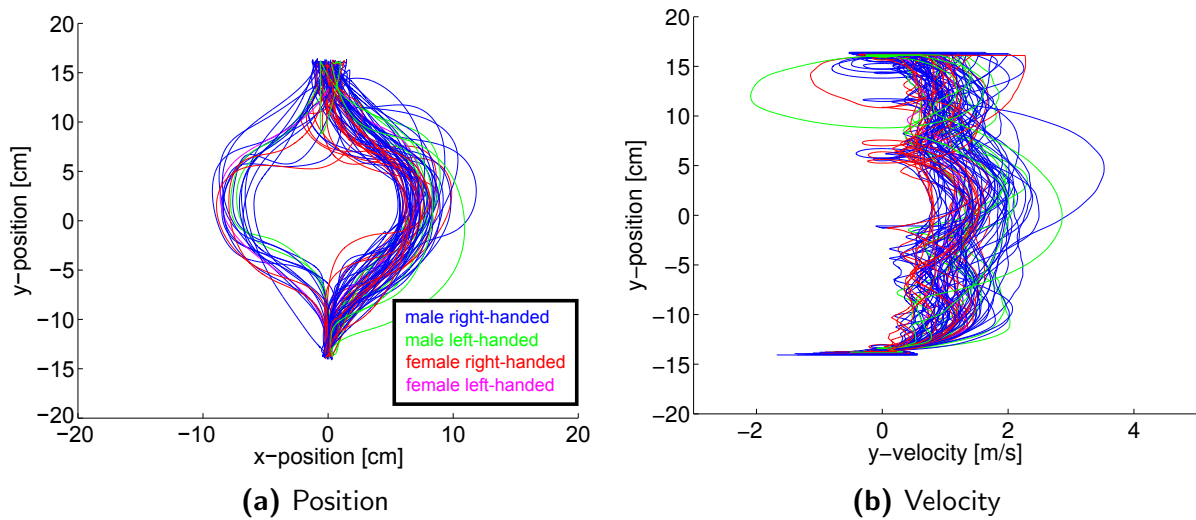


Fig. 3.18: Path and velocity data of level two

Smoothness of Velocity and Deviations from the Optimal Path Therefore, path and velocity data must be considered to gain insight how far the planning horizon reaches. Following plots are color coded such that blue depicts male right-handed subjects, green depicts male left-handed subjects, red depicts female right-handed subjects and pink is used for female left-handed subjects. Handedness, however, does not have any formative influence on the results. Fig. 3.17 shows the position and velocity data of the first scenario. Without any obstructions the path and velocity are smooth and lead directly from start to goal. This supports the proposition that the planning horizon follows the OC idea for this simple level.

The single static obstacle in scenario two is easily circumvented by all subjects with smooth paths, see Fig. 3.18. This argues against the shorter planning horizon. Velocity data shows that subjects brake in front of the obstacle and speed up to go around it. A smooth and continuous progression of the velocity is expected but it appears that the

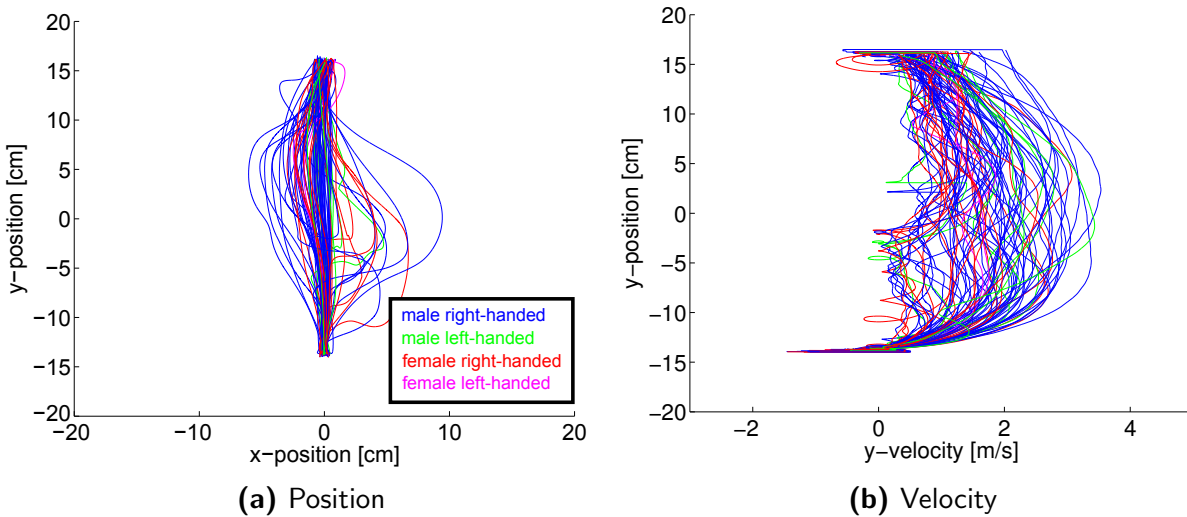


Fig. 3.19: Path and velocity data of level three

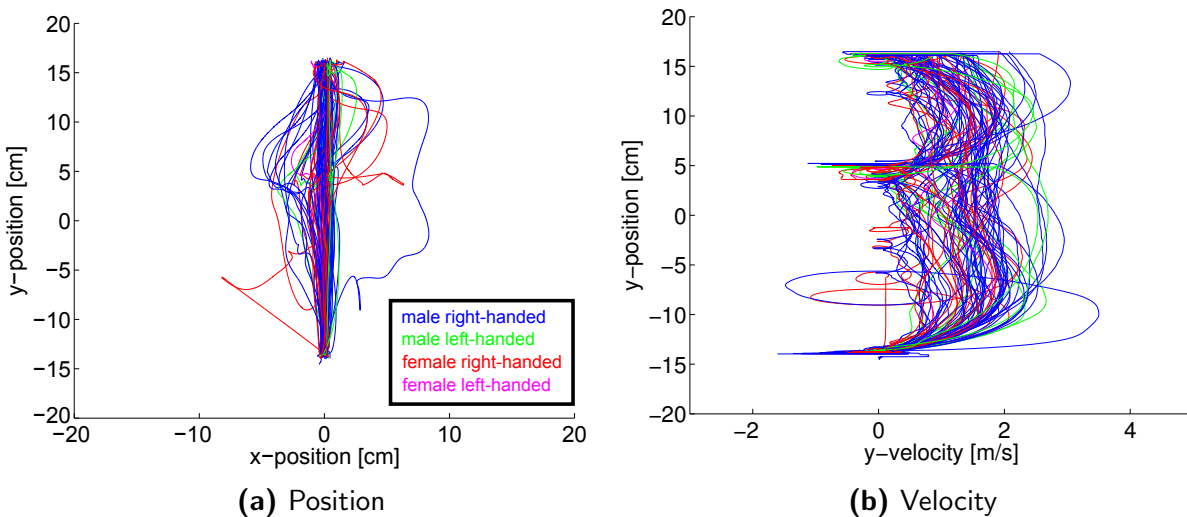


Fig. 3.20: Path and velocity data of level six

planning horizon does not cover the full distance to the goal. Visible loops in the velocities originate from collisions, where the marker is stopped and moves backwards slightly until new speed is gained. In scenario three, see Fig. 3.19, the single obstacle line does also not pose a problem for most subjects. Both path and velocity remain smooth with some visible braking in the velocity plot. This braking combined with the fact that most subjects moved straight towards the obstacle at first, allows for the assumption that some participants relied on a shorter planning horizon. Yet, the majority of the subjects follows the shortest path solution and achieves smooth progression.

For the case of two obstacle lines, velocity and path remain mostly smooth. Figure 3.20 visualizes the data captured in level six. Indeed, as the gaze-points revealed, many subjects are not able to surpass both obstacle lines at once. Their planning horizon seems restricted to the area between the obstacles as the braking in the center of the velocity plot reveals. Yet, the majority of the subjects follows the shortest path and produces smooth velocities.

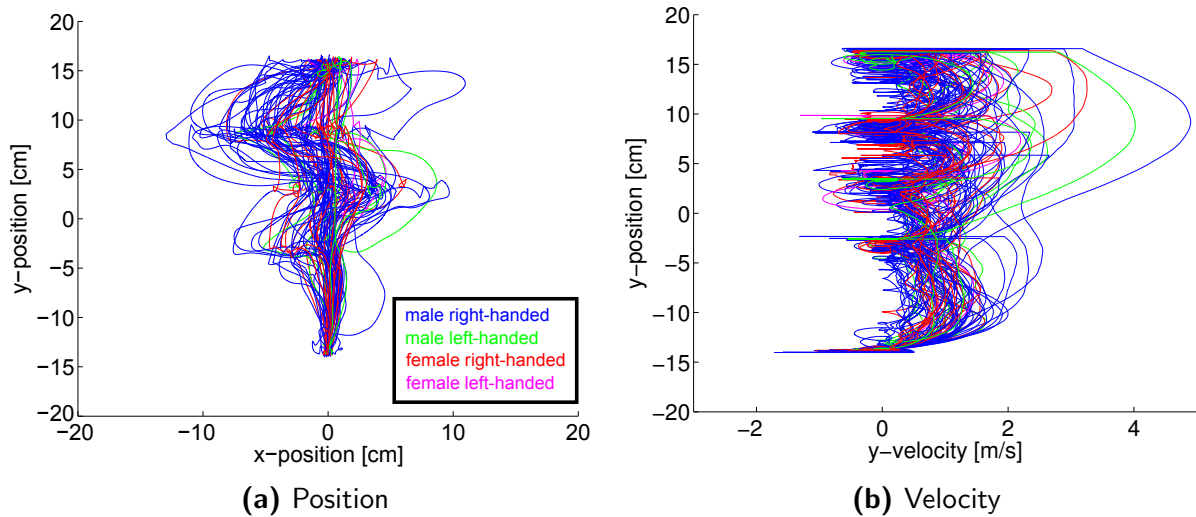


Fig. 3.21: Path and velocity data of level nine

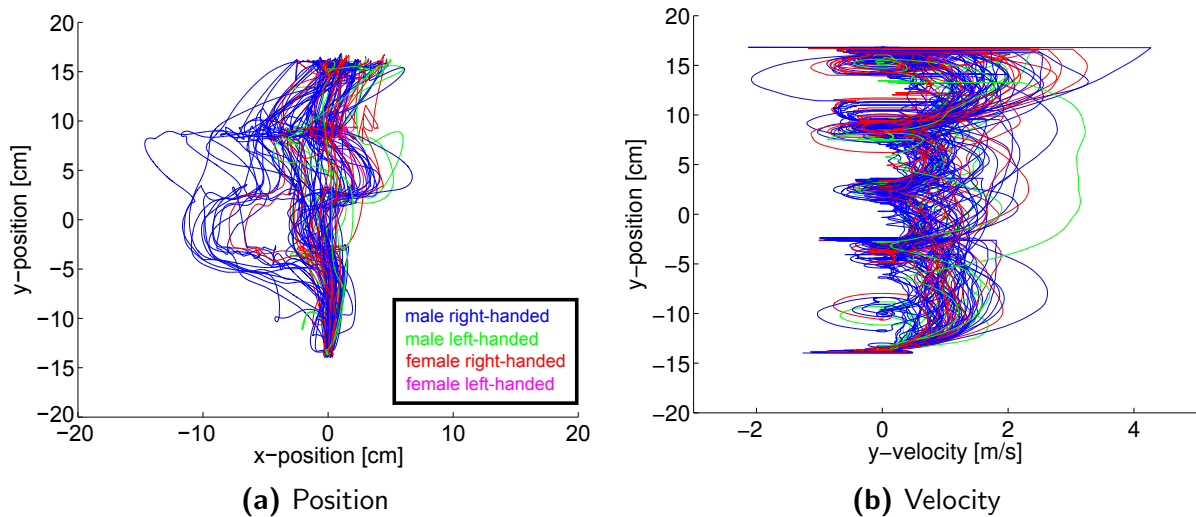


Fig. 3.22: Path and velocity data of level ten

The scenarios nine and ten add another two obstacle rows to the environment. With the added complexity a change in the behavior must be visible, if the hypothesis about the correlation of uncertainty and planning horizon holds. In fact, the data changes drastically as Fig. 3.21 and 3.22 show. With the complexity of the ninth level, subjects are often not able to apply smooth paths. The goal directed motion is therefore reduced to stepwise progression. Path data deviates strongly from the shortest path solution. Velocity data reveals an increase in braking, especially in front of the third and fourth obstacle line. Thus, smoothness of the trajectories is diminished. Taking into account gaze data, the hypothesis holds that subjects are not able to plan a path directly to the goal. Clearly, subjects progress by passing one obstacle line after the other. Indeed, two subjects noticed and used the free optimal path which appears after 2s. If the hypothesis holds that humans reduce their planning horizon within uncertain situations, the observed effects of level nine must intensify if further complexity is added. Thus, in level ten the obstacles additionally

change their velocity and direction of movement. The extra uncertainty actually enhances the mentioned aspects even more, as Fig. 3.22 shows. The velocity data contains increased signs of braking and collisions underpinning $H_{1,B}$. Paths also differ even more from the straight path supporting $H_{1,C}$.

This qualitative data evaluation substantiates the assumption that humans alter their planning horizon in order to cope with complex environments. Subjects focus the most immediate obstacle and pass it before the next obstruction is considered. Further, subjects deviate from the shortest path and omit the global optimum. The velocity data also suggests that the subjects are not able to plan far ahead in complex environments, in order to avoid braking between obstacle lines. In the following, these results are further elaborated by statistical evaluations

3.1.4.2 Statistical Data Evaluation

The statistical evaluation of the acquired data focuses on two distinct parameters. Firstly, the visual look-ahead is considered, where the position of the marker in the virtual environment is compared with the focus of synchronized gaze. Secondly, the velocity profile is analyzed because smooth velocities indicate a continuous motion and thus a large planning horizon or vice versa. Thirdly, the deviation from the inherent optimal path is examined as it yields another indicator for a change in the applied planning horizon.

Visual Look-ahead One indicator for the planning horizon in the experiment is the distance between the human's visual focus of attention and the position of the participant's cursor. In order to ascertain whether the planning horizon changed with increasing complexity of the scene, eye tracking data is evaluated in combination with position data of the participants' cursor. Specifically, the mean distance between participants' visual focus and their cursor position is compared over the different complexity levels. Due to missing data, 10 data-sets are excluded from the analysis, leaving a sample of $N = 31$. Of the 620 remaining values, 25 individual missing values ($= 4.05\%$ of the data-set) had to be replaced by the group mean.

A repeated-measures 10 (*complexity*) $\times 2$ (*trial - run*) ANOVA showed a non-significant¹ run main effect ($F(1, 30) = 0.13, p = .73$), indicating that over all levels of complexity, the distance between the participants' cursor and the point of visual fixation did not vary significantly between the first and second run. The ANOVA further shows a small but significant main effect of complexity on the mean fixation-cursor distance ($F(5.73, 171.86^2) = 4.82, p < .001, \eta p^2 = .14$). Mean values indicate a trend of increasingly smaller distances with increasing level complexity. Post-hoc contrasts to the baseline (level 1) further support $H_{1,A}$ and confirm that the distance is significantly smaller in most complexity levels (with the exception of levels 2 and 5) compared to the visual behavior shown in the fully observable environment in level 1. Mean values, standard errors and the results of the post-hoc contrasts to the baseline (level 1) are summarized in Tab. 3.1.

¹Accepted $\alpha = .05$

²With Greenhouse-Geisser correction.

Tab. 3.1: Means and standard errors for average mean distances between eye fixation and cursor position (in pixels).

	Description	Mean (SE)	Baseline Contrast
Levels of Complexity	1 No objects	300.279 (17.733)	–
	2 1 static object	264.118 (18.731)	$F(1,30) = 2.02,$ $p = .166$
	3 1 obstacle line moving horizontally	244.169 (12.854)	$F(1,30) = 9.01,$ $p = .005^*$
	4 1 obstacle line moving diagonally	250.484 (11.972)	$F(1,30) = 7.63,$ $p = .010^*$
	5 2 obstacle lines moving horizontally in same direction at different speeds	285.741 (24.006)	$F(1,30) = 0.45,$ $p = .510$
	6 2 obstacle lines moving horizontally in opposite directions at different speeds	240.153 (12.529)	$F(1,30) = 10.43,$ $p = .003^{**}$
	7 2 obstacle lines moving diagonally in opposite directions at different speeds	262.189 (16.754)	$F(1,30) = 4.42,$ $p = .044^*$
	8 4 obstacle lines moving horizontally in same direction at different speeds	206.796 (16.055)	$F(1,30) = 18.16,$ $p < .001^{**}$
	9 4 obstacle lines moving horizontally in opposite directions at different speeds	228.984 (25.359)	$F(1,30) = 6.00,$ $p = .020^*$
	10 4 obstacle lines moving horizontally in opposite directions at different speeds with both changing	189.679 (11.858)	$F(1,30) = 25.08,$ $p < .001^{**}$

*sig. at $p < .05$
**sig. at Bonferroni corrected $p < .005$

Smoothness of Velocity Further analyses investigate the effects of scenario complexity on participants' variation of movement velocity. Using Roy's largest root, a repeated-measures MANOVA indicates a significant medium-sized main effect of complexity on velocity variation on x- and y-axis ($\Theta = 2.62, F(9, 351) = 102.02, p < .001, \eta p^2 = .72$). A follow-up ANOVA shows that on both axes, velocity varies significantly between the different complexity levels, which supports $H_{1,B}$. There is also a large and significant multivariate main effect of run ($\Theta = 3.74, F(2, 38) = 70.97, p < .001, \eta p^2$), and a small yet significant interaction effect ($\Theta = 0.18, F(9, 351) = 7.04, p < .001, \eta p^2 = .15$). Considering the mean values, the velocity variation on the x-axis is significantly larger on the first run than the second run, while it is approximately similar between runs on the y-axis.

For levels with higher complexity compared to levels with lower complexity the mean values indicate a tendency towards greater velocity variations on the x-axis, but not on

Tab. 3.2: Means and standard errors for average velocity variation on x-axis (in dm/s).

	Description	Mean (SE)	Baseline Contrast
	1 No objects	.068 (.005)	–
	2 1 static object	.481 (.021)	$F(1,39) = 483.75,$ $p < .001^{**}$
	3 1 obstacle line moving horizontally	.152 (.012)	$F(1,39) = 37.50,$ $p < .001^{**}$
	4 1 obstacle line moving diagonally	.168 (.011)	$F(1,39) = 58.07,$ $p < .001^{**}$
Levels of Complexity	5 2 obstacle lines moving horizontally in same direction at different speeds	.123 (.006)	$F(1,39) = 56.95,$ $p < .001^{**}$
	6 2 obstacle lines moving horizontally in opposite directions at different speeds	.127 (.012)	$F(1,39) = 20.11,$ $p < .001^{**}$
	7 2 obstacle lines moving diagonally in opposite directions at different speeds	.174 (.012)	$F(1,39) = 60.51,$ $p < .001^{**}$
	8 4 obstacle lines moving horizontally in the same direction at different speeds	.283 (.013)	$F(1,39) = 216.36,$ $p < .001^{**}$
	9 4 obstacle lines moving horizontally in opposite directions at different speeds	.292 (.018)	$F(1,39) = 148.69,$ $p < .001^{**}$
	10 4 obstacle lines moving horizontally in opposite directions at different speeds with both changing	.260 (.013)	$F(1,39) = 229.54,$ $p < .001^{**}$
	*sig. at $p < .05$		
	**sig. at Bonferroni corrected $p < .005$		

the y-axis. A noticeable difference is level 2, which contains 1 static object and seems to encourage maneuvers with more extreme x-axis velocities. Post-hoc contrasts to the baseline indicate that the velocity variation on the x-axis is significantly smaller in the baseline condition (level 1) compared to movements in all other levels. On the other hand, velocity variation on the y-axis is significantly larger in the baseline condition compared to the variation observed in levels 2 and 5–10. The results of the baseline contrasts are summarized in Tab. 3.2 and Tab. 3.3.

Deviation from the Optimal Path In order to investigate to what extent the level of complexity affects a deviation from the optimal path, the absolute and mean values of participants' maximum path deviations are examined. Mean values and standard deviations are shown in Tab. 3.4 and 3.5. The mean values indicate, that on average, participants deviate from the optimum path the most in level 2 with one immobile object, followed

Tab. 3.3: Means and standard errors for average velocity variation on y-axis (in dm/s).

	Description	Mean (SE)	Baseline Contrast
	1 No objects	.685 (.034)	–
	2 1 static object	.514 (.026)	$F(1,39) = 42.39,$ $p < .001^{**}$
	3 1 obstacle line moving horizontally	.671 (.039)	$F(1,39) = 0.23,$ $p = .634$
Levels of Complexity	4 1 obstacle line moving diagonally	.702 (.046)	$F(1,39) = 0.27,$ $p < .609$
	5 2 obstacle lines moving horizontally in same direction at different speeds	.623 (.036)	$F(1,39) = 5.05,$ $p < .030^*$
	6 2 obstacle lines moving horizontally in opposite directions at different speeds	.578 (.032)	$F(1,39) = 18.38,$ $p < .001^{**}$
	7 2 obstacle lines moving diagonally in opposite directions at different speeds	.543 (.033)	$F(1,39) = 25.25,$ $p < .001^{**}$
	8 4 obstacle lines moving horizontally at different speeds in the same direction	.559 (.031)	$F(1,39) = 19.87,$ $p < .001^{**}$
	9 4 obstacle lines moving horizontally at different speeds in opposite directions	.504 (.030)	$F(1,39) = 36.58,$ $p < .001^{**}$
	10 4 obstacle lines moving horizontally at different speeds in opposite directions with both changing	.512 (.022)	$F(1,39) = 41.60,$ $p < .001^{**}$
		*sig. at $p < .05$ **sig. at Bonferroni corrected $p < .005$	

by large deviations in levels with four objects. The smallest deviations from the optimum path are observed in the baseline level 1, followed by those levels that contain 1 and 2 objects, with the exception of level 2. Large deviations in level 2 may be attributed to the fact that there are two optimum paths around the object. Overall, a large variance can be observed in the average deviations, whereby the variance seems to increase with the number of objects in the scene.

Repeated measures 10 (*complexity*) \times 2 (*trial – run*) ANOVA reveals a significant main effect of run ($F(1, 40) = 20.55, p < .001$) and complexity ($F(3.73, 149.08) = 42.88, p < .001$), but no significant interaction ($F(4.02, 160.93) = 0.84, p = .50$). With respect to the mean values, the data indicates that participants deviate significantly less from the optimum path when moving through the levels for a second time compared to the first time. Presumably, this can be attributed to a reduced uncertainty. Regarding the complexity, post-hoc comparisons to the baseline level 1 support $H_{1,C}$ and confirm that participants

Tab. 3.4: Means and standard errors for mean deviations from the optimal path (in dm).

	Description	Mean (SE)	Baseline Contrast	
Levels of Complexity	1	No objects	.020 (.002)	–
	2	1 static object	.244 (.006)	$F(1,40) = 1374.62,$ $p < .001^{**}$
	3	1 obstacle line moving horizontally	.061 (.008)	$F(1,40) = 23.19,$ $p < .001^{**}$
	4	1 obstacle line moving diagonally	.078 (.008)	$F(1,40) = 43.98,$ $p < .001^{**}$
	5	2 obstacle lines moving horizontally in same direction at different speeds	.052 (.007)	$F(1,40) = 19.36,$ $p < .001^{**}$
	6	2 obstacle lines moving horizontally in opposite directions at different speeds	.053 (.008)	$F(1,40) = 13.56,$ $p < .001^{**}$
	7	2 obstacle lines moving diagonally in opposite directions at different speeds	.060 (.008)	$F(1,40) = 19.82,$ $p < .001^{**}$
	8	4 obstacle lines moving horizontally in the same direction at different speeds	.170 (.022)	$F(1,40) = 46.71,$ $p < .001^{**}$
	9	4 obstacle lines moving horizontally in opposite directions at different speeds	.107 (.011)	$F(1,40) = 56.68,$ $p < .001^{**}$
	10	4 obstacle lines moving horizontally in opposite directions at different speeds with both changing	.140 (.021)	$F(1,40) = 31.82,$ $p < .001^{**}$
	*sig. at $p < .05$			
	**sig. at Bonferroni corrected $p < .005$			

deviate significantly less in the baseline condition compared to each of the 9 experimental levels (see Tab 3.4). Contrasts further confirm that the deviations are significantly larger in levels with four objects compared to those with only two objects.

Looking at the maximum deviations from the optimum path, a similar pattern is observed, with the largest deviations occurring in level 2, followed by the levels with four objects. The smallest maximum deviations are found in the baseline level, suggesting that participants followed the optimum trajectory when there are no objects to circumvent. On the other hand, with the introduction of further objects, participants increasingly deviated from the optimum path. Again, the variance seems to increase notably with the introduction of four moving objects, suggesting that individual differences effect more variance in the movement with increasing scene complexity, while individual difference are much less notable in the levels with lower scene complexity, in particular the baseline level 1.

Repeated measures 10 (*complexity*) \times 2 (*trial-run*) ANOVA revealed a significant main

effect of run ($F(1, 40) = 26.80, p < .001$) and complexity ($F(3.39, 135.49) = 68.12, p < .001$) on the maximum deviations, but no significant interaction ($F(4.94, 197.64) = 0.65, p = .66$). Looking at the mean values, the data thus indicate that participants deviated significantly less from the optimum path when moving through the levels for a second time compared to the first time. Presumably, this can be attributed to a reduced uncertainty. Regarding the complexity, post-hoc comparisons to the baseline level 1 further support $H_{1,C}$ and confirmed that participants deviated significantly less in the baseline condition compared to each of the 9 experimental levels (see Tab. 3.5). Contrasts further confirmed that the deviations were significantly larger in levels with four objects compared to those levels with only two objects.

Tab. 3.5: Means and standard errors for maximum deviations from the optimal path (in dm).

		Mean (SE)	Baseline Contrast	
Levels of Complexity	1	No objects	.069 (.005)	–
	2	1 static object	.764 (.015)	$F(1,40) = 2422.73,$ $p < .001^{**}$
	3	1 obstacle line moving horizontally	.205 (.023)	$F(1,40) = 31.274,$ $p < .001^{**}$
	4	1 obstacle line moving diagonally	.241 (.025)	$F(1,40) = 42.08,$ $p < .001^{**}$
	5	2 obstacle lines moving horizontally in same direction at different speeds	.162 (.016)	$F(1,40) = 25.98,$ $p < .001^{**}$
	6	2 obstacle lines moving horizontally in opposite directions at different speeds	.178 (.023)	$F(1,40) = 19.10,$ $p < .001^{**}$
	7	2 obstacle lines moving diagonally in opposite directions at different speeds	.240 (.026)	$F(1,40) = 38.35,$ $p < .001^{**}$
	8	4 obstacle lines moving horizontally at different speeds in the same direction	.598 (.062)	$F(1,40) = 67.837,$ $p < .001^{**}$
	9	4 obstacle lines moving horizontally at different speeds in opposite directions	.484 (.038)	$F(1,40) = 110.173,$ $p < .001^{**}$
	10	4 obstacle lines moving horizontally at different speeds in opposite directions with both changing	.456 (.040)	$F(1,40) = 87.193,$ $p < .001^{**}$
		*sig. at $p < .05$		
		**sig. at Bonferroni corrected $p < .005$		

3.1.5 Discussion

This section is concerned with the improvement of human locomotion prediction methods based on the incorporation of human behaviors. Focus is set on optimal control and model predictive control methods due to their ability to generate accurate trajectories. A review of related literature shows, that many recent methods do not generalize to avoidance behaviors that are observed in human locomotion studies. Therefore, the hypothesis is investigated that humans apply a situational strategy for avoidance. Focus is set on the particular behavior of using a shorter planning horizon in order to resolve collision situations which originate from uncertainty about the immediate environment. The influence of the planning horizon is demonstrated within simulations of a non-linear model predictive control based framework for human locomotion prediction. Based on these results, the hypothesis is further investigated within a specifically designed subject study. This experiment measures gaze and trajectory data of subjects that perform a goal directed motion in a virtual environment. Varying conditions in the experiment confront subjects with different states of uncertainty about the environment. If it is free of obstacles, results show that the subjects' gaze scans the whole area between start and goal position. Paths and velocities of the motion are smooth and follow a straight line. With a static obstacle, subjects focus on the obstacle to avoid collisions but still produce smooth trajectories. If the complexity is increased by adding more obstacles, gaze tends to address only the next obstacle to be passed. Most subjects then progress step by step, which leads to observable braking in the velocity data. With respect to the hypothesis, the strong focus on the immediate obstacle indicates a reduction in the planning horizon, while path and velocity data further support this proposition. The statistical evaluations support the findings as they indicate according trends in the data. Evaluation of the mean distance between the marker and the gaze position shows that looking-ahead diminishes when comparing an empty scenario with a very complex scenario. Questionnaires issued to the subjects clarify, that these observations are not a result of an overly demanding task, as it is not rated as particularly difficult or exhausting.

Non-linear model predictive control with a reduced planning horizon resembles more accurately the avoidance movements presented within literature. Simulations illustrate the influence of a changing planning horizon on locomotion prediction. Accordingly, the change in planning horizon is understood as a human behavior and thus investigated in the designed experiment. Results obtained in the experiment validate the control approach and support the integration of this aspect within prediction methods. A detailed model for human motion planning behavior with an adaptive planning horizon is not obtained from the experiment, yet. Changing the planning horizon poses one factor that is not considered in current models, but various other aspects may affect the trajectories similarly. The described behavior should therefore be investigated within more complex studies, where subjects can walk in a three-dimensional environment. Thereby, peripheral vision must be considered as well as the differences due to occlusions that occur during locomotion in populated environments. Additionally, a detailed and systematic analysis of differential effects of obstacle features on the planning horizon remains subject to future investigations.

Empirical and statistical evaluations of the experiment supply strong indications that humans employ varying strategies when avoiding obstacles. The adaptation of the planning

horizon is identified as one distinct method to cope with this problem. This holds under the assumption that gaze fixation and the smoothness of trajectories are determined by the length of the planning horizon. Given these results, modeling the motion planning horizon of humans has a large potential to improve human locomotion prediction methods.

3.2 Dynamic Model for Human Velocity Prediction

As discussed in the previous section, recent research must tackle the problem of accurate prediction of human locomotion trajectories. This is an essential ability for autonomous mobile robots, as it allows them to navigate without collision and integrate seamlessly into human populated environments. Reliable predictions of other agents within a shared environment also support efficient and comfortable collaboration, since almost collisions or surprising movements of robots may induce inconvenience for nearby humans.

For accurate prediction of human locomotion trajectories, models are typically derived from recorded human locomotion data, for example by reinforcement learning or inverse optimal control (IOC). The generated trajectories resemble human locomotion trajectories accurately for a variety of situations. However, a critical problem is often neglected. Human locomotion elicits a pendulum like effect which results in a sinusoidal shape of velocity profiles. Recent publications generally filter the data using a second- or third-order low-pass filter. This is necessary as the recorded data must conform with the applied dynamic model. The common approach to use a unicycle model to represent human locomotion actually requires the velocity to be smooth and flat. In fact, this smoothing affects the data strongly and leads to a wrong association of velocity profile and the recorded position data. Furthermore, this approximation is transported into the model and may lead to larger inaccuracies.

Hence, the goal of this section is to provide a model that does not require a flat velocity profile. In addition, the new model should be integrated into an existing inverse optimal control framework in order to allow for the identification of parameters. Generally, the problem is solvable by applying an accurate bio-mechanical model of a human. However, the complexity of such a model and the large number of individual parameters (e.g. leg length, body height, etc.) will not enable an on-line capable prediction algorithm.

The demonstrated approach is an adaptation of the unicycle model, where the round wheel is exchanged for an elliptical one. This ellipsoid leads to sinusoidal velocities and the simplicity of the model allows for parameter estimation within given frameworks. Equations for a model are thus derived from the mathematical description of a rolling ellipse. Applying Lagrange equations to an undamped rolling motion finally yields the dynamic model. These equations are then used to modify the unicycle model. With inverse optimal control methods from [14] and [121] the model parameters are fit to the recorded data of human locomotion.

Simulation results show that the model produces smooth goal directed trajectories and the characteristic sinusoidal velocity profiles. Yet, the high sensitivity of the model prevents the inverse optimal control method from resulting in accurate parameters such that recorded data is reconstructed accurately. The obtained approximations, however, pose a large step towards a generalizable solution.

A novel velocity model for human-like trajectory generation is proposed and common inverse optimal control methods are adapted to fit parameters for this model. These findings are capable of enhancing existing modeling approaches in order to reconstruct human locomotion data more accurately. Especially prediction and trajectory generation for mobile robots benefit from these results.

This section is structured as follows: related literature is discussed in Subsec. 3.2.1. Subsec. 3.2.2 describes the problem of inaccurate velocity modeling. The Ellipse model is derived in Subsec. 3.2.3. Simulation results are presented in Subsec. 3.2.4. A brief summary followed by a discussion of the results is given in 3.2.5.

3.2.1 Classification within the State-of-the-Art

Modeling human locomotion for prediction is a wide research area and features a large variety of approaches. The previous Sec. 3.1 already discusses this area and briefly summarizes related work. Since this section is specialized on the topic of human-like velocity profiles, the works on prediction are not considered in the following. The distinct focus is set on literature which is concerned with the generation of human locomotion trajectories using optimal control methods and dynamic models. Further, some approaches are briefly examined that are alternatives to the solution proposed here.

For generating human motions, inverse optimal control approaches are recently very popular [14, 18, 19, 121, 144]. These approaches consider recorded human trajectory data as an optimal solution to a goal directed motion. Based on that, an OC model with a specifically designed objective function is used as an underlying model. The goal is to improve the human-like motion generation with this model by identifying the ideal parameters for the OC problem. An approach that is employed in this work as well, is proposed by Mombaur et al. [121]. They split the IOC problem into a bilevel procedure, where a trajectory is generated using the OC model with the current parameters and then compared to the recorded data. An optimization process then adapts the parameters in order to minimize the calculated difference. The result is an OC model that is capable of producing holonomic locomotion trajectories. This basic idea is further developed by Albrecht et al. [14]. Here, the IOC is based on the calculation of the Hamilton-Function. Given that the recorded data is optimal, the parameters of such a trajectory must lead to a minimum within the conditions derived from the Hamiltonian. Therefore, the parameters for the Hamilton-Function must be chosen such that the conditions for a minimum are met considering the data. This approach requires the mathematical examination of the posed problem, which can be extremely complex. Thus the method of [121] is often preferred. The approach by Albrecht et al. [14], however, offers the integration of dynamic obstacles as well. This allows for the prediction of human locomotion trajectories in avoidance situations. Another method in this respect is the minimization of the curvature variation as shown in [19, 39]. These works assume that human locomotion trajectories follow a non-holonomic principle and are well described by curvature constrained models. The parameter optimization for curvature based approaches follows the same concept as described before. Recorded trajectories are assumed as the optimal solution and the model is adapted to follow the data with minimum deviation.

The presented approaches optimize their parameters based on distance measures applied to path and velocity. However, these works rely on a dynamic model, the unicycle model, that is not capable of reproducing the sinusoidal shape of human velocity profiles. The presented works commonly solve this problem by smoothing the velocity data as it is described in Chap. 4. Accordingly, the developed models involve an inaccuracy that leads to a misalignment of time and position considering the comparison of synthesized and

recorded data. In [136] this problem is removed by applying the parameter optimization to path data only. Clearly, the generated velocities can not approximate the sinusoidal characteristic of human velocities accurately. In order to enhance the accuracy of future approaches to this topic, a solution must be found, that allows for modeling these velocities. The following works are considered as applicable methods for this problem.

One method to generate variable sinusoidal velocity profiles is the use of a Van-der-Pol oscillator [164, 194]. An oscillator is applicable to describe the temporal development of the angles in the knee and hip joints of a human. A disadvantage of this approach is the high number of parameters that need to be derived from the data. Thus, an integration into the existing optimization framework of [121] is very challenging. Besides, these parameters are very individual for each person and will not generalize to a larger data-set. As an alternative the approach from [84], the Three-Dimensional Linear Inverted Pendulum Model (3D-LIPM), should be considered. Humans with their upright body constantly apply adjustments to maintain balance, whether standing, walking, or running. This behavior is modeled with an inverted pendulum. By constraining the center-of-mass of a moving human to an arbitrarily defined plane, a three-dimensional movement is transformed to a two-dimensional movement. The resulting dynamics are then expressed as linear motion equations. This model describes bipedal walking in the 2d-plane when only limited knowledge of the dynamics, e.g. the location of the total center-of-mass or the total angular momentum, is given. The model for bipedal walking actually includes the oscillations of the velocity. Yet, it distinguishes between two phases, the single-leg support phase, where the 3D-LIPM applies and a double-leg support phase, where the velocity of the center-of-mass remains unchanged. This two-phased property of the model requires to solve an optimal control problem with a switching behavior. Yet, the goal of this section is not to develop a completely new model, but to improve the framework including the unicycle model. Lastly, the implementation of a highly complex full-body model for a human may be considered [69, 81]. In order to generate highly accurate and natural human locomotion trajectories, this approach must be taken into account. Indeed, the number of parameters and the computational complexity of many models prohibits their application to on-line prediction systems for robots.

This literature review shows, that many methods exist that allow for the modeling of the particularities of human gait. However, their disadvantage is the complexity of the newly formed problem and the missing approaches for parameter estimation. Accordingly, this thesis proposes a model that is able to reproduce human velocity profiles while parameters are derived using inverse optimal control as in [121]. Hence, the goal of improving existing OC based models and their accuracy is maintained with regard to future methodological advancements that may benefit from these findings.

3.2.2 Problem Description

This section elaborates the problem introduced by simplified velocity models within state-of-the-art human locomotion prediction approaches. Firstly, the influence of smoothed velocities is discussed by comparing results from an existing model with recorded data. Secondly, the re-parametrization of the improved model is addressed with an inverse optimal control methodology.

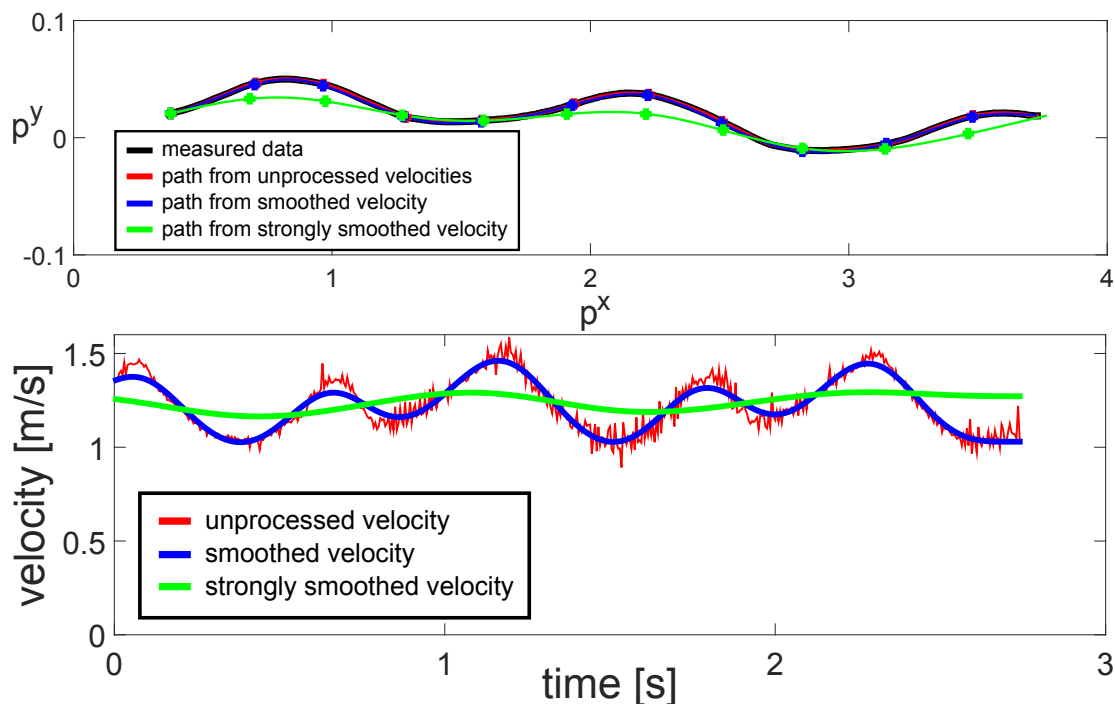


Fig. 3.23: Path and velocity recorded from a subject walking from $(0.0, 0.0)$ to $(0.0, 6.0)$ shown in black. Comparison of the recorded path with the path recovered from the derived velocities and the paths recovered from smoothed velocities

3.2.2.1 Periodicity in Human Locomotion Velocity

Parameters for OC based locomotion models are typically estimated from a defined optimal solution that also poses the modeling goal. For human locomotion prediction, IOC is applied to trajectory data recorded from human subjects. This data is similar to the dataset described in 4.4.1, which is also used in Sec. 2.2. However, the trajectory data for OC models usually covers a wider range of goal directed motions in order to facilitate the generalization of the model. As described in Subsec. 3.2.1, state-of-the-art approaches use smoothed versions of the recorded velocity profiles to prepare the data for the commonly applied unicycle model. In fact, this procedure is found to be a source of inaccuracies in [14] and [136]. This section is concerned with this problem and aims to propose a model that allows for the representation of human velocity profiles. Therefore, the following illustrates the effects in more detail. Fig. 3.23 shows an excerpt of the path and velocity data recorded from a subject that walks $6m$ from $(0.0, 0.0)$ to $(0.0, 6.0)$. Due to limits of the tracking equipment, the first and the last parts of the motion are not recorded or corrupted by noise. The path exhibits the typical sideway swinging of human gait and the velocity profile shows the sinusoidal characteristic. For comparison, Fig. 3.24 shows the results of the Mombaur model [121] for the same start and goal pose. The depicted path is straight as expected, but the velocity profile shows the typical flat trapezoidal shape from using this type of model.

Using a mean or smoothed representation for the velocities is not a disadvantage in practice. It allows for a direct application of the model to wheeled robots that are clearly not able to perform the pendulum-like swinging of human gait. For locomotion predic-

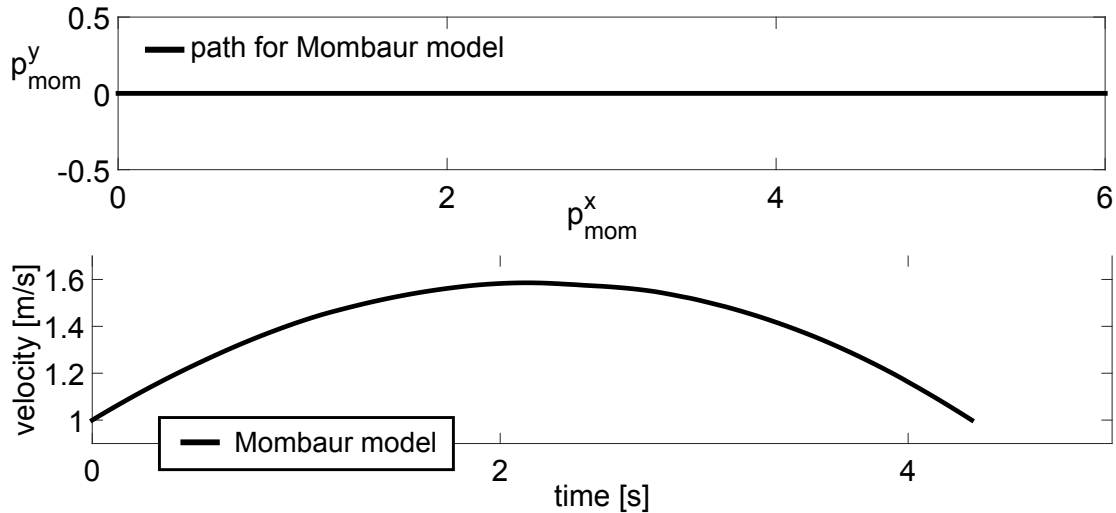


Fig. 3.24: Path and velocity generated with the Mombaur model [121] for locomotion from $(0.0, 0.0)$ to $(0.0, 6.0)$

tion, however, the smoothing transfers inaccuracies into the model. Accordingly, Fig. 3.23 shows three paths: one is the recorded data (black), one is generated from the directly derived velocities (red), one is generated from smoothed velocities (red) and a last path is reconstructed from a velocity that does not contain any swinging due to strong smoothing (green). For the calculation of position from velocity, the recording frequency of 204 Hz provided by the tracking system is used as the sampling time. The three paths are qualitatively similar with deviations that clearly originate from the smoothed velocities. Markers along the paths indicate the position at a specific time that is the same for each path. Notably, the markers point out the inaccuracy that is introduced by smoothing. As the real velocities follow a sinusoidal profile, the markers of the respective path are alternating between being behind and ahead of the smoothed version. This illustrates the problem that smoothing of the velocity profile leads to an inaccuracy within the spatio-temporal alignment of the data. Thus, the comparison of measured and synthesized path data suffers from a misalignment of the data as well. Therefore, this work proposes a model that constitutes an adjustment to the simple unicycle and aims to generate human-like velocity profiles for the current OC approaches.

3.2.2.2 Inverse Optimal Control for Parameter Estimation

Parameter estimation for OC problems has a variety of solution as shown in Subsec. 3.2.1. Since the model proposed in this section will substitute the unicycle model within given OC approaches, the parameters must be adapted. In order to provide suitable parameters based on recorded data, an IOC method is employed. The approach used in this work is adopted from Mombaur et al. [121]. Within their work, a model similar to Subsec. 2.1.2 is used. The applied dynamic model is the common unicycle model with accelerations as inputs $\mathbf{u}^*(t) \in \mathcal{U}$. The parameters θ_i of the objective function are adapted with respect to recorded data, see Fig. 3.25.

This method follows a bi-level approach, where the discrete trajectory $\xi_{\text{model}}(\theta_i, k)$ with

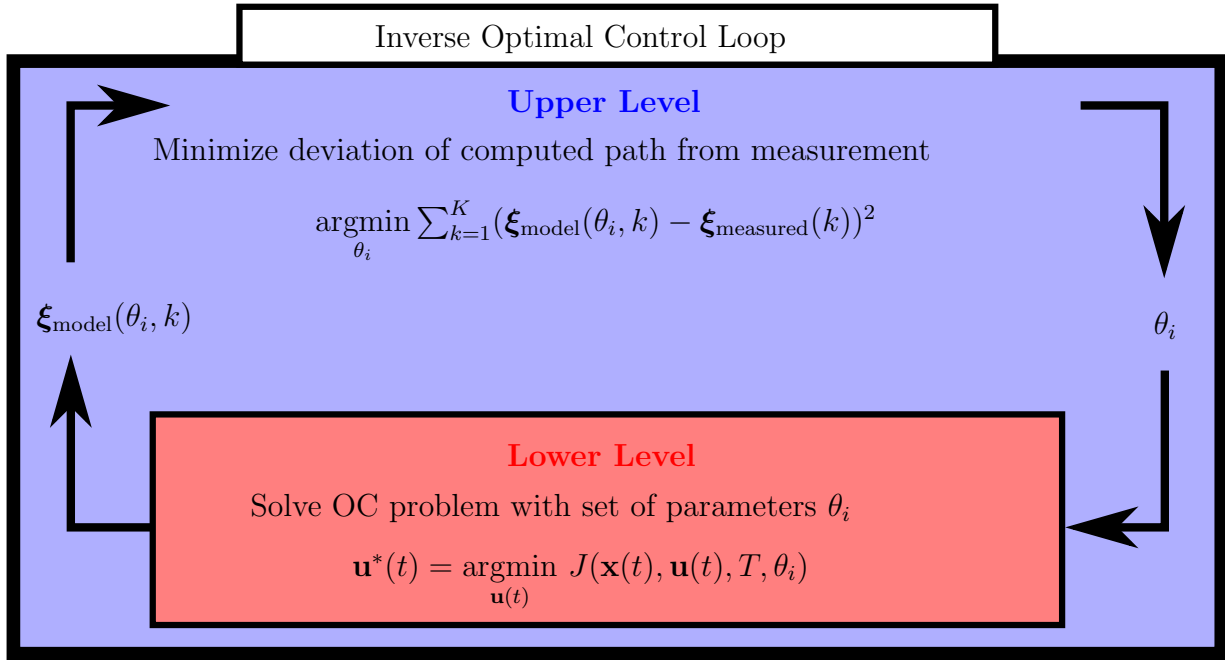


Fig. 3.25: Inverse optimal control loop as bilevel optimization problem as in [121]

$k = 1, \dots, K$ computed in the “lower level” is based on the current parameters θ_i . Within the “upper level” problem a distance between the measured trajectory $\xi_{\text{measured}}(k)$ and the generated trajectory $\xi_{\text{model}}(\theta_i, k)$ is calculated. Mombaur et al. [121] use the general euclidean distance as a metric in the upper level:

$$d(\xi_{\text{measured}}(k), \xi_{\text{model}}(\theta_i, k)) = \sum_{k=1}^K (\xi_{\text{model}}(\theta_i, k) - \xi_{\text{measured}}(k))^2.$$

The goal is the minimization of this distance by adapting θ_i . Clearly, the number of discrete states K within both trajectories must be matched if the applied distance measure is not able to handle different trajectory lengths.

With respect to the distance measures, the problem created by the smoothed velocity profiles is discussed in [14]. Albrecht et al. identify the inaccuracies introduced by this procedure and propose a separation of the distance calculation for path and velocity data as a solution. Different distance metrics are applied within the fitting problem. For positional data the distance:

$$d_{\text{pos}}(\xi_{\text{measured}}^{xy}(k), \xi_{\text{model}}^{xy}(k)) = \sum_{k=1}^{K-1} \left\| \xi_{\text{model}}^{xy}\left(\frac{k}{K-1}L_{\text{model}}\right) - \xi_{\text{measured}}^{xy}\left(\frac{k}{K-1}L_{\text{measured}}\right) \right\|^2$$

is applied, where the path data is re-parametrized by the respective total path lengths L_{model} and L_{measured} . Velocity profiles are compared by:

$$d_{\text{vel}}(\xi_{\text{measured}}^v(k), \xi_{\text{model}}^v(k)) = \sum_{k=1}^K |\xi_{\text{model}}^v(k) - \xi_{\text{measured}}^v(k)|^2$$

The overall distance $d_{\text{sum}}(\boldsymbol{\xi}_{\text{measured}}(k), \boldsymbol{\xi}_{\text{model}}(k))$ is then obtained by summation:

$$d_{\text{sum}}(\cdot) = d_{\text{pos}}(\boldsymbol{\xi}_{\text{measured}}^{xy}(k), \boldsymbol{\xi}_{\text{model}}^{xy}(k)) + d_{\text{vel}}(\boldsymbol{\xi}_{\text{measured}}^v(k), \boldsymbol{\xi}_{\text{model}}^v(k)).$$

Clearly, the used dynamic model does not consider the dynamics of human locomotion as a multibody system with all its internal joint degrees of freedom, but instead it describes the planar motion of the whole system in the 2d plane. Hence, the velocities must be smoothed to be flat as shown in 3.2.2.1. In the following, an adaptation to this model is provided that allows for generation of sinusoidal human-like velocity profiles. This model is proposed as a solution for the mentioned problems with velocity smoothing and poses a step towards a general model for accurate human locomotion trajectory prediction.

3.2.3 Dynamic Model for Human-Like Velocity Profiles

The following concentrates on the posed problem of velocity modeling within the field of OC based human trajectory prediction. As the given OC frameworks offer good results and the ability to find suitable parameters using IOC, the proposed model aims to adjust the unicycle model such that the remaining framework [121] still applies. In order to obtain a more human-like velocity profile, the generated velocity for the existing unicycle model may be constrained to follow the typical sinusoidal shape. The approach proposed in this work, is to exchange the concept of a rolling unicycle by a rolling ellipsoid.

In the following, the equations for an ellipse rolling on the ground are derived. In order to simplify the equations, the motion is restricted to model the case where a human is walking with a constant average velocity. Acceleration and deceleration phases are therefore not considered. Describing an ellipse in a global coordinate frame requires the general parametric form.

At first, the ellipse is described in an ellipse coordinate frame $(x_{\text{EL}}, z_{\text{EL}})$, which originates in the center-of-mass (CoM) of the ellipse at $(x_{\text{el,W}}(t), z_{\text{el,W}}(t))$. The CoM is situated in the world frame $(x_{\text{W}}, z_{\text{W}})$. With $a_{\text{el}} < b_{\text{el}}$ and $\rho_{\text{el}} \in [0, 2\pi]$ every point on the ellipse can be expressed as:

$$\begin{aligned} \iota_{\text{EL}} &= a_{\text{el}} \sin(\rho_{\text{el}}), \\ \kappa_{\text{EL}} &= -b_{\text{el}} \cos(\rho_{\text{el}}), \end{aligned}$$

within ellipse coordinates. Starting with an ellipse in upright position, see Fig. 3.26, the contact point on of the ellipse frame with the ground is obtained by setting $\rho_{\text{el}} = 0$. As the motion of the ellipse is of interest, respectively of its CoM, the ellipse is described in its general parametric form when rotated by an angle $\varrho_{\text{el}}(t)$, which is time-variant as it is changing over time when the ellipse is rolling:

$$\begin{aligned} R_{\text{W}} = \begin{pmatrix} \iota_{\text{W}} \\ \kappa_{\text{W}} \end{pmatrix} &= \begin{pmatrix} x_{\text{el,W}}(t) \\ z_{\text{el,W}}(t) \end{pmatrix} + \begin{pmatrix} \cos(\varrho_{\text{el}}(t)) & -\sin(\varrho_{\text{el}}(t)) \\ \sin(\varrho_{\text{el}}(t)) & \cos(\varrho_{\text{el}}(t)) \end{pmatrix} \begin{pmatrix} \iota_{\text{EL}} \\ \kappa_{\text{EL}} \end{pmatrix} \\ &= \begin{pmatrix} x_{\text{el,W}}(t) + \iota_{\text{EL}} \cos(\varrho_{\text{el}}(t)) - \kappa_{\text{EL}} \sin(\varrho_{\text{el}}(t)) \\ z_{\text{el,W}}(t) + \iota_{\text{EL}} \sin(\varrho_{\text{el}}(t)) + \kappa_{\text{EL}} \cos(\varrho_{\text{el}}(t)) \end{pmatrix}, \end{aligned}$$

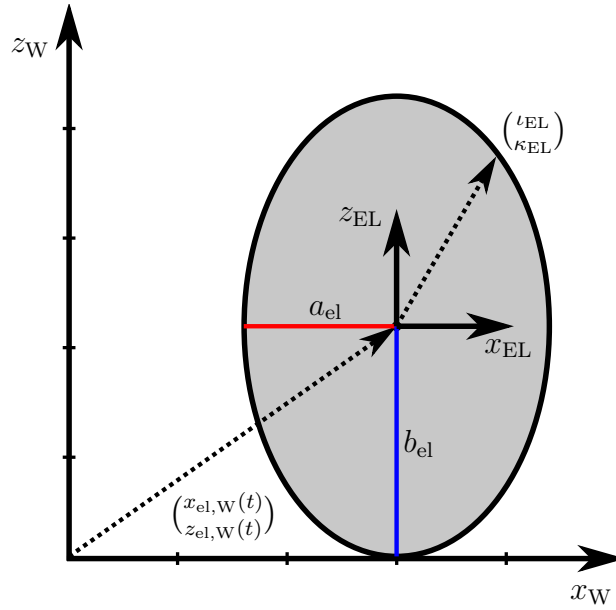


Fig. 3.26: Illustration of the ellipse model for human-like velocity profile generation

where R_W denotes the border of the ellipse in world frame. The velocity of any point on the edge of the ellipse can therefore be calculated by taking the derivative with respect to the time.

$$\dot{R}_W = \dot{\varrho}_{el}(t) \begin{pmatrix} \frac{dx_{el,W}(t)}{d\varrho_{el}(t)} - \iota_{EL} \sin(\varrho_{el}(t)) - \kappa_{EL} \cos(\varrho_{el}(t)) \\ \frac{dz_{el,W}(t)}{d\varrho_{el}(t)} + \iota_{EL} \cos(\varrho_{el}(t)) - \kappa_{EL} \sin(\varrho_{el}(t)) \end{pmatrix},$$

Further, the normal n_{el} to any point on the ellipse is expressed as:

$$n_{el} = \frac{1}{\sqrt{\dot{\kappa}_{EL}^2 + \dot{\iota}_{EL}^2}} \begin{pmatrix} \dot{\kappa}_{EL} \\ -\dot{\iota}_{EL} \end{pmatrix} = \frac{1}{\sqrt{a_{el}^2 \cos^2(\varrho_{el}) + b_{el}^2 \sin^2(\varrho_{el})}} \begin{pmatrix} \frac{b_{el}}{a_{el}} \iota_{EL} \\ \frac{a_{el}}{b_{el}} \kappa_{EL} \end{pmatrix}$$

With this expression a condition for the normal of a point on the edge of the rotated ellipse is derived to be perpendicular to the ground, which means, perpendicular to the x_W -axis.

$$\begin{aligned} 0 &= \left(\begin{pmatrix} \cos(\varrho_{el}(t)) & -\sin(\varrho_{el}(t)) \\ \sin(\varrho_{el}(t)) & \cos(\varrho_{el}(t)) \end{pmatrix} \begin{pmatrix} \frac{b_{el}}{a_{el}} \iota_{EL} \\ \frac{a_{el}}{b_{el}} \kappa_{EL} \end{pmatrix} \right)^T \begin{pmatrix} 1 \\ 0 \end{pmatrix} \\ &= \begin{pmatrix} \frac{b_{el}}{a_{el}} \iota_{EL} & \frac{a_{el}}{b_{el}} \kappa_{EL} \end{pmatrix} \begin{pmatrix} \cos(\varrho_{el}(t)) \\ -\sin(\varrho_{el}(t)) \end{pmatrix} \end{aligned}$$

$$\Rightarrow b_{el}^2 \iota_{EL} \cos(\varrho_{el}(t)) = a_{el}^2 \kappa_{EL} \sin(\varrho_{el}(t)) \quad (3.1)$$

With this result and the relation $1 = \sin^2(\varrho_{el}(t)) + \cos^2(\varrho_{el}(t))$, the condition for the ellipse

rolling on the ground is derived:

$$\begin{aligned}
 0 &= \kappa_W \\
 &= z_{el,W}(t) + \iota_{EL} \sin(\varrho_{el}(t)) + \kappa_{EL} \cos(\varrho_{el}(t)) \\
 &= z_{el,W}(t) \sin(\varrho_{el}(t)) + \iota_{EL} \sin^2(\varrho_{el}(t)) + \kappa_{EL} \cos(\varrho_{el}(t)) \sin(\varrho_{el}(t)) \\
 &= z_{el,W}(t) \sin(\varrho_{el}(t)) + \iota_{EL} \underbrace{\left[1 + \left(\frac{b_{el}^2}{a_{el}^2} - 1\right) \cos^2(\varrho_{el}(t))\right]}_{c_{el}}, \\
 &\Rightarrow \iota_{EL} = -\frac{z_{el,W}(t) \sin(\varrho_{el}(t))}{1 + c_{el} \cos^2(\varrho_{el}(t))}. \tag{3.2}
 \end{aligned}$$

As a last condition the velocity in the ground contact point has to be zero, since the ellipse is rolling without slipping.

$$0 = \dot{R}_W$$

By using the results from 3.1 and 3.2 the kinematics of the CoM of the ellipse are derived. For the z_W direction movement of the CoM, following applies:

$$\begin{aligned}
 0 &= \frac{dz_{el,W}(t)}{d\varrho_{el}(t)} + \iota_{EL} \cos(\varrho_{el}(t)) - \frac{b_{el}^2}{a_{el}^2} \iota_{EL} \cos(\varrho_{el}(t)) \\
 &= \frac{dz_{el,W}(t)}{d\varrho_{el}(t)} + c_{el} z_{el,W} \frac{\sin(\varrho_{el}(t)) \cos(\varrho_{el}(t))}{1 + c_{el} \cos^2(\varrho_{el}(t))} \\
 &\text{with } z_{el,W}(t) = a_{el} \sqrt{1 + c_{el} \cos^2(\varrho_{el}(t))} \\
 &\Rightarrow \dot{z}_{el,W}(t) = \frac{dz_{el,W}(t)}{d\varrho_{el}(t)} \frac{d\varrho_{el}(t)}{dt} = c_{el} \iota_{EL} \cos(\varrho_{el}(t)) \dot{\varrho}_{el}(t). \tag{3.3}
 \end{aligned}$$

The x_W -component of the motion follows:

$$\begin{aligned}
 0 &= \frac{dx_{el,W}(t)}{d\varrho_{el}(t)} - \iota_{EL} \sin(\varrho_{el}(t)) - \kappa_{EL} \cos(\varrho_{el}(t)) \\
 &= \frac{dx_{el,W}(t)}{d\varrho_{el}(t)} + z_{el,W} \\
 &= \frac{dx_{el,W}(t)}{d\varrho_{el}(t)} + a_{el} \sqrt{1 + c_{el} \cos^2(\varrho_{el}(t))} \\
 &\text{with } x_{el,W}(t) = -a_{el} \sqrt{1 + c_{el}} E_2(\varrho_{el}(t), \frac{c_{el}}{1 + c_{el}}) = -b_{el} E_2(\varrho_{el}(t), \frac{b_{el}^2 - a_{el}^2}{b_{el}^2}) \\
 &\Rightarrow \dot{x}_{el,W}(t) = \frac{dx_{el,W}(t)}{d\varrho_{el}(t)} \frac{d\varrho_{el}(t)}{dt} = -a_{el} \sqrt{1 + c_{el} \cos^2(\varrho_{el}(t))} \dot{\varrho}_{el}(t), \tag{3.4}
 \end{aligned}$$

where $E_2(\cdot)$ is the elliptical integral of the second kind (Legendre form). In order to obtain the model dynamics, the gravitational force is taken into account. Additionally, the motion of the ellipse is assumed to be undamped and the overall energy of the system is considered constant. The differential equations of the rolling ellipse model are found using the Lagrange equation of the second kind. The kinetic energy T_{kin} of the system is

described by:

$$\begin{aligned}
 T_{\text{kin}} &= \underbrace{\frac{1}{2} J_{\text{el}} \dot{\varrho}_{\text{el}}^2}_{\text{rotational}} + \underbrace{\frac{1}{2} m_{\text{el}} (\dot{x}_{\text{el,W}}^2 + \dot{z}_{\text{el,W}}^2)}_{\text{translational}} \\
 &= \frac{1}{2} \underbrace{\left(J_{\text{el}} + m_{\text{el}} \left(\left(\frac{dx_{\text{el,W}}(t)}{d\varrho_{\text{el}}(t)} \right)^2 + \left(\frac{dz_{\text{el,W}}(t)}{d\varrho_{\text{el}}(t)} \right)^2 \right) \right)}_{f_{\text{el}}(\cdot)} \dot{\varrho}_{\text{el}}^2(t) \\
 &= \frac{1}{2} f_{\text{el}}(\varrho_{\text{el}}(t)) \dot{\varrho}_{\text{el}}^2(t),
 \end{aligned}$$

where J_{el} is the inertia and m_{el} is the mass of the ellipse. The potential energy of the system is denoted as:

$$V_{\text{pot}} = m_{\text{el}} g z_{\text{el,W}}$$

The Lagrange equation of the second kind leads to:

$$\begin{aligned}
 L_{\text{el}} &= T_{\text{kin}} - V_{\text{pot}} \\
 \Rightarrow \frac{d}{dt} \left(\frac{\partial L_{\text{el}}}{\partial \dot{\varrho}_{\text{el}}(t)} \right) - \frac{\partial L_{\text{el}}}{\partial \varrho_{\text{el}}(t)} &= \\
 f_{\text{el}}(\varrho_{\text{el}}(t)) \ddot{\varrho}_{\text{el}}(t) + \frac{df_{\text{el}}(\varrho_{\text{el}}(t))}{dt} \dot{\varrho}_{\text{el}}(t) + \frac{1}{2} \frac{df_{\text{el}}(\varrho_{\text{el}}(t))}{d\varrho_{\text{el}}(t)} \dot{\varrho}_{\text{el}}^2(t) + m_{\text{el}} g \frac{dz_{\text{el,W}}}{d\varrho_{\text{el}}(t)} &= Q_{\text{el}},
 \end{aligned}$$

where Q_{el} are the generalized forces with respect to the world coordinates. Considering the undamped case, where the ellipse starts rolling with a given initial rotational velocity, Q_{el} is set to 0. This leads to to the solution of the differential equation:

$$\ddot{\varrho}_{\text{el}}(t) = \frac{1}{f_{\text{el}}(\varrho_{\text{el}}(t))} \left(-\frac{df_{\text{el}}(\varrho_{\text{el}}(t))}{dt} \dot{\varrho}_{\text{el}}(t) - \frac{1}{2} \frac{df_{\text{el,W}}}{d\varrho_{\text{el}}(t)} \dot{\varrho}_{\text{el}}^2(t) - m_{\text{el}} g \frac{dz_{\text{el,W}}}{d\varrho_{\text{el}}(t)} \right)$$

Finally, the modified unicycle model is described. The velocity in the dynamic model of [121] is exchanged with the velocity $\dot{x}_{\text{el,W}}$ of the ellipse, leading to the dynamical system:

$$\frac{d}{dt} \begin{pmatrix} x_{\text{el}}(t) \\ y_{\text{el}}(t) \\ \varphi_{\text{el}}(t) \\ \varrho_{\text{el}}(t) \\ \dot{\varrho}_{\text{el}}(t) \\ \omega_{\text{el}}(t) \end{pmatrix} = \begin{pmatrix} -a_{\text{el}} \sqrt{1 + c_{\text{el}} \cos^2(\varrho_{\text{el}}(t))} \dot{\varrho}_{\text{el}}(t) \cos(\varphi_{\text{el}}(t)) \\ -a_{\text{el}} \sqrt{1 + c_{\text{el}} \cos^2(\varrho_{\text{el}}(t))} \dot{\varrho}_{\text{el}}(t) \sin(\varphi_{\text{el}}(t)) \\ \omega_{\text{el}}(t) \\ \dot{\varrho}_{\text{el}}(t) \\ \frac{1}{f_{\text{el}}(\varrho_{\text{el}}(t))} \left(-\frac{df_{\text{el}}(\varrho_{\text{el}}(t))}{dt} \dot{\varrho}_{\text{el}}(t) - \frac{1}{2} \frac{df_{\text{el,W}}}{d\varrho_{\text{el}}(t)} \dot{\varrho}_{\text{el}}^2(t) - m_{\text{el}} g \frac{dz_{\text{el,W}}}{d\varrho_{\text{el}}(t)} \right) \\ u_{\text{el}} \end{pmatrix},$$

subject to:

$$\varrho_{\text{el}}(0) = 0, \quad |\dot{\varrho}_{\text{el}}(0)| > 0.$$

This holds for the undamped case and locomotion on even ground.

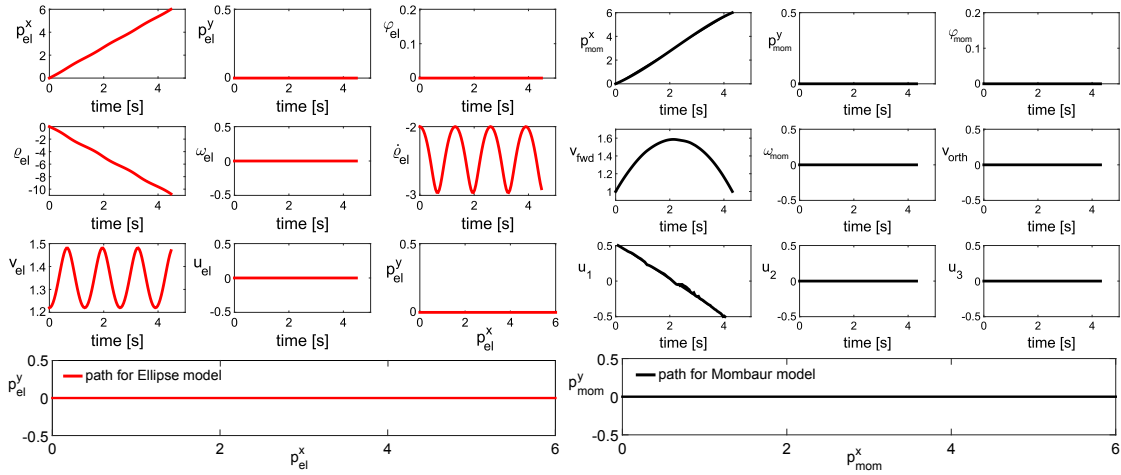


Fig. 3.27: Paths, system states and controls generated with the Ellipse and the Mombaur model for a straight walk

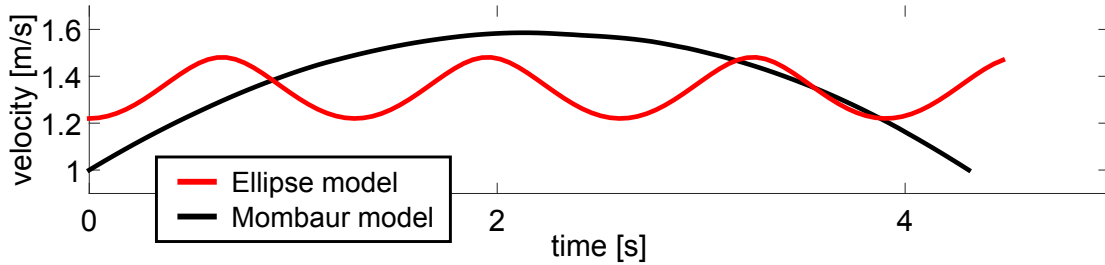


Fig. 3.28: Velocity profiles generated with Ellipse and Mombaur model for a straight walk

3.2.4 Simulation Results

The following compares the performance of the proposed Ellipse model to the recorded data and the results of the Mombaur model [121]. From the IOC a set of parameters is derived resulting in $[a_{el}, b_{el}, m_{el}] = [0.5, 0.61, 80]$. For the human-like path generation, three objective functionals are employed with their weights adapted by the IOC. Derived from [121], the objective function for a motion between $\mathbf{p}_S(0)$ and $\mathbf{p}_G(T)$ is:

$$\begin{aligned}
 J(\mathbf{x}(t), \mathbf{u}(t), T, \theta_1, \theta_2, \theta_3) = & \theta_1 T + \\
 & + \theta_2 \int_0^T u_1^2 dt + \\
 & + \theta_3 \int_0^T \left[\text{atan} \left(\frac{\mathbf{p}_G^y(T) - \mathbf{p}_H^y(t)}{\mathbf{p}_G^x(T) - \mathbf{p}_H^x(t)} \right) - \varphi_{el}(t) \right]^2 dt,
 \end{aligned}$$

where $\mathbf{p}_H(t)$ is the current position and $[\theta_1, \theta_2, \theta_3] = [0.1, 2.5, 5.2]$. In Fig. 3.27 the simulation results for a subject walking 6m from $\mathbf{p}_S = (0.0, 0.0)$ to $\mathbf{p}_G = (0.0, 6.0)$ are illustrated, comparing the Ellipse model and the Mombaur model. The latter uses the parameters from [121], while the ellipse is parametrized as previously described. The velocities for each model are shown in Fig. 3.28. The paths are straight as expected, while the velocity profiles illustrate the difference of the models. With the Ellipse model the characteristic

sinusoidal shape of a human-like velocity profile is reproduced more closely. With parameters derived by IOC, the model is also applicable to generate more general paths. Starting at (0.0, 0.0), Fig. 3.29 shows the results for an end pose (6.0, 0.5) with an orientation of $\varphi_{el} = 0.0$. Figure 3.30 depicts the velocities for the Ellipse and the Mombaur model.

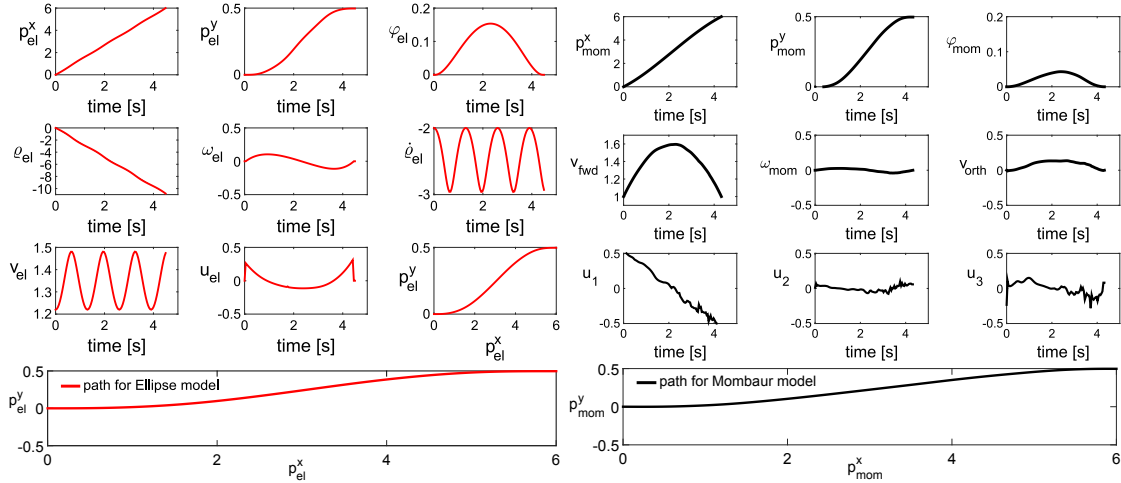


Fig. 3.29: Paths, system states and controls generated with the Ellipse and the Mombaur model for a curved walk

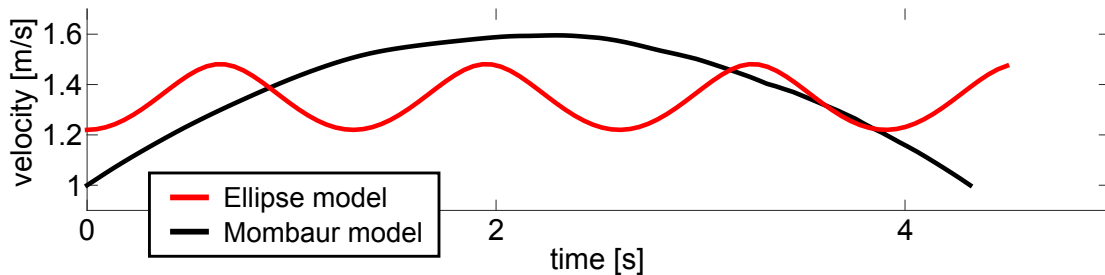


Fig. 3.30: Velocity profiles generated with Ellipse and Mombaur model for a curved walk

By applying the described IOC framework, the parameters are also adapted to reconstruct recorded trajectories from human subjects. Thereby, a higher frequency for the velocity profile is achieved with smaller values for a_{el} and b_{el} . The ratio $\frac{b_{el}}{a_{el}}$ of 1.22 is preserved for a smooth sinusoidal result. Figures 3.31 and 3.32 show the path and velocity data from a person walking with an avoidance motion (black). The reconstruction with the proposed model results in path and velocity shown in red. These results demonstrate the applicability of the model to human locomotion data. The velocities are qualitatively similar to typical human velocity profiles but are not perfectly matched. In fact, IOC supplies a basic adaptation of the initial parameters from [121], but the OC problem suffers from a strong tendency to local minima. With heuristical tuning of the parameters, a well applicable set is found. Finding a global minimum and ideal parameters requires further elaboration of the problem with respect to optimization methodologies. Therefore, the exact matching of path and velocity remains unsolved. Overall, the model poses a step towards solving the problem of velocity modeling described in [14, 136].

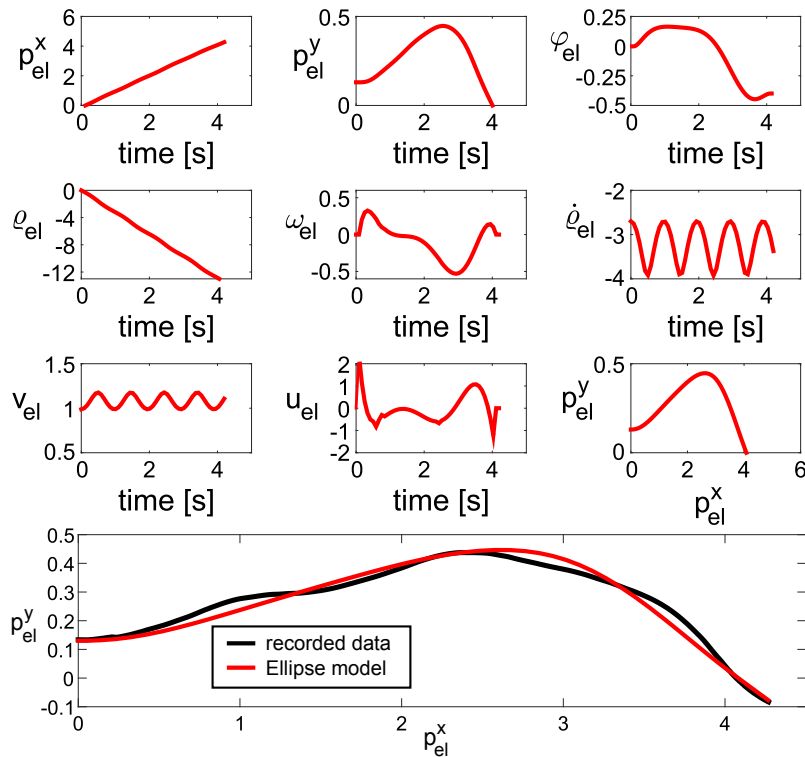


Fig. 3.31: Path and velocity data recorded from a human (black) and reconstructed with the Ellipse model (red)

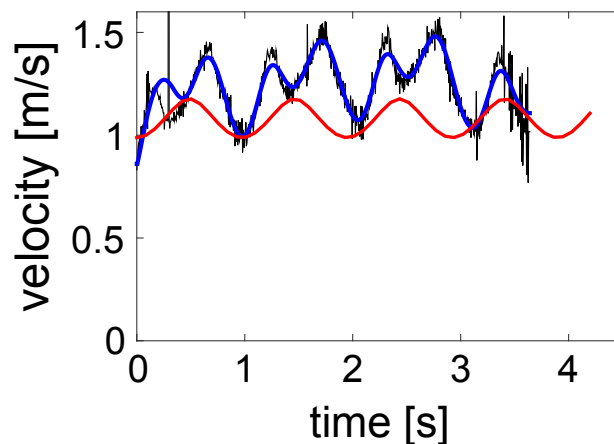


Fig. 3.32: Velocity data recorded from a human (black and blue) and reconstructed with the Ellipse model (red)

3.2.5 Discussion

In this section the problem of velocity modeling for human trajectory prediction is tackled. A literature review reveals that the problem is considered in according works, but a distinct model for the sinusoidal shape of human velocities is not proposed. Current models for human trajectory generation and parameter estimation circumvent the problem by smoothing recorded velocities in order to adapt the data to the used models. This section proposes to exchange the common concept of a unicycle model within an optimal control

framework. By using the dynamics of a rolling ellipse, the sinusoidal shape of human velocity profiles is achieved. The model is based on the kinematics of a rolling ellipse and the dynamics are derived using the Lagrange equation of the second kind. Suitable parameters for the model are found using an inverse optimal control approach from literature, in order to reproduce and thus predict recorded trajectory data. Simulations show the capability of the model to predict human locomotion trajectories with a human-like velocity profile. However, the parametrization exposes the sensitivity of the model as a problem. Good performance is only obtained after a heuristic tuning of the model parameters. From the simulations it follows that the model introduces a high sensitivity to parameter changes and a strong tendency to local minima for the applied optimization method. Although the proposed approach suggests an improvement for existing human locomotion prediction models, its applicability and ability to generalize must be further investigated. Thus the model must be analyzed in more detail and with respect to optimization theory. An according analysis should result in a more robust optimization procedure and more generalizable parameters for the model. Furthermore, the missing representation of an acceleration phase is required for the general applicability of the model to arbitrary human locomotion trajectories and thus prediction approaches. In summary, the model poses an important step towards solving the velocity modeling problem that is reported within related literature. Further mathematical elaboration of the model within an optimal control setting is therefore reasonable.

3.3 Summary

This chapter is concerned with the improvement of human locomotion prediction methods based on the integration of human behaviors. Focus is set on optimal control and model predictive control methods due to their ability to generate accurate trajectories. A review of related literature shows, that many recent methods do not generalize to certain behaviors that are observed in human locomotion studies and filter distinct attributes of human gait.

Therefore, the hypothesis is investigated whether humans adapt their planning horizon when resolving collision situations which originate from uncertainty about the immediate environment. The influence of the planning horizon is demonstrated within simulations of a non-linear model predictive control based framework for human locomotion prediction. Obtained results are then validated within a specifically designed subject study. The empirical and statistical evaluations of the study indicate that smoothness of motions and visual look-ahead diminish with rising uncertainty of the environment, while the deviations from an optimal path increase. These aspects lead to the conclusion that a reduction of the planning horizon resembles a distinct human strategy to resolve sudden collision situations.

Furthermore, the problem of velocity modeling for human trajectory prediction is tackled. Recent models for optimal control based trajectory generation avoid the problem by smoothing recorded velocities. This chapter provides an adaptation of the common unicycle model that enables the generation of more human-like velocity profiles. The proposed model employs the kinematics and the dynamics of a rolling ellipse. Simulation results of velocity profiles show the typical sinusoidal shape of real human trajectory data and verify the applicability of this model to human locomotion prediction.

3.4 Conclusions

A distinct aspect of the cognitive process of human motion planning and a specific attribute within human gait are discussed in this chapter, regarding their potential to increase the accuracy of optimal control and model predictive control based prediction approaches. Simulations reveal the effects on locomotion prediction, which are then further validated within subject studies. The respective results indicate that human locomotion prediction can benefit from the detailed identification of the named factors.

Within the first section, the motion planning horizon of humans is investigated. Results from simulations of a non-linear model predictive control approach expose the influence of the planning horizon on the predicted trajectory. These simulations and the evaluations of a subject study reveal the potential of this aspect to improve human locomotion prediction methods. As similar behaviors are observed in literature, it is assumed that humans resolve uncertainties in their prediction of other agents by reducing their planning horizon. A design of a subject study is derived from these results to further investigate the human motion planning horizon. Subjects perform a goal directed motion and avoid a varying number of obstacles, while their gaze focus and trajectories are measured. An evaluation of the visual focus shows that their looking-ahead diminishes when the scenarios gain complexity. Additionally, deviations in the velocities are visible as subjects brake more often and pass only one obstacle at a time. Furthermore, subjects deviate strongly from an optimal solution, which is simply the shortest path, if the environment is complex. These empirical results are supported by statistical evaluations that confirm the focus of gaze on nearby obstacles, the velocity adaptations and the deviations of the path from an optimal solution. These factors indicate a reduction in the applied planning horizon and thus validate the hypothesis. As the planning horizon poses one distinct aspect of human avoidance behavior, further studies should identify other factors in order to allow for the development of more accurate prediction models.

Another aspect that is not considered within existing prediction models is the sinusoidal shape of human velocity profiles. The second section achieves to model according profiles by exchanging the common unicycle concept with a rolling ellipse. Simulations show the capability of the model to predict human locomotion trajectories with a human-like velocity profile. Suitable parameters are found using an inverse optimal control approach from literature. Yet, high parameter sensitivity and local minima pose a challenge for the proposed model. The model constitutes a step towards solving the problem with velocity modeling that is reported within related literature. Indeed, further mathematical elaboration of the model within an optimal control setting is necessary.

The human trajectory planning horizon and the modeling of human velocity profiles are factors with a high potential to improve human locomotion prediction. Certainly, modeling more aspects of human locomotion behavior will improve the accuracy of future model based locomotion prediction algorithms.

4 Human Trajectory Data Analysis for Identifying Situational Behaviors

As pointed out by this thesis, research in motion planning for mobile robots increasingly focuses on modeling human-like motions and behaviors. Applied to robots, these models help generating motions that are intuitively comprehensible for a human interaction partner. Thereby, human-like motions enhance human-robot collaboration and cooperative navigation in shared environments. The synthesis of human-like motions and behaviors on robots requires accurate models. However, identifying the underlying parameters of such human motion models is a challenging task. These parameters are commonly estimated by a qualitative analysis of measured trajectories or by inspecting the means of respective trajectory sets. Indeed, raw trajectory data as well as the means are often not representative for the data, because measurements are noisy and the amount of generated data is limited. Therefore, a reliable analysis methodology should include a qualitative and a quantitative evaluation in order to assess the significance of observed particularities within the data. For a feasible analysis it is also necessary to minimize loss when filtering the data and to consider data variance especially for qualitative inspection.

The goal of this chapter is to develop methods for qualitative and quantitative trajectory evaluation. The proposed approaches were previously published in [5] and [3]. These methods must consider an according confidence interval for the mean of the data and supply a reliable quantitative analysis. An according framework is proposed for human trajectory data analysis. Penalized splines are applied to smooth single trajectories and to estimate means of trajectory sets, which ensures little distortion of the original data. Based on that, a method is presented that yields a confidence interval for the mean of human motion data. Bootstrapping copes with the unknown distribution and the small size of the data-sets. An analysis based on the estimated confidence intervals takes the variance of the data into account and allows for reasonable conclusions about underlying human motion parameters. This procedure is complemented by a comparative analysis that quantifies differences and analogies within the data. Similarities between two trajectory sets are thereby quantified using distance measures and a paired Welch-test. This framework allows for a statistically feasible qualitative and quantitative analysis of human motion trajectories.

Feasibility of these methods is further evaluated by a comparison to alternative approaches based on Gaussian processes and Autoregressive Moving-Average models. These methods from machine learning and system identification are well established methodologies and applicable to the problem. The comparison reveals that the latter methods provide the advantage of trajectory synthesis but facilitate a less detailed analysis.

4.1 Introduction

Previous chapters discuss the generation of human-like motions as one recent challenge within the research area of motion planning for mobile robots and robotic manipulators. It is identified as an important ability, especially for seamless human-robot interaction. If a robot moves human-like, its intentions are easier to interpret for a human who is collaborating with the robot or walking in its vicinity [31, 170]. Consequently, a human interaction partner feels more comfortable and less disturbed in his own motion planning process [7]. Reinforcement learning and inverse optimal control [14, 48, 103, 121] are used to obtain models of human motion. The performance of such a model is bound to its accuracy of reproducing human-like motions and thus to the accuracy of the inherent parameters. The characteristic parameters that define such a model, are usually obtained in extensive subject studies and are challenging to identify. Within these studies, data is collected by firstly recording human motions, secondly post-processing this data, thirdly analyzing the data and finally applying a modeling method. Eventually, the model is evaluated, for example in a user study, where subjects observe and rate the generated motions.

The post-processing step is often paid little attention, although it is essential to obtain generalizable models since the collected data is naturally corrupted by noise. A fast solution is low-pass filtering of each recorded trajectory. This smoothing method, however, leads to a spatio-temporal misalignment that affects the results in later applications. These effects are similar to the described problem in Subsec. 3.2.2. The obtained and smoothed velocities, for example, produce different paths (e.g. deviation of endpoint) than described by the geometric data, which leads to modeling inaccuracies [166]. With the smoothing method presented here, this problem is avoided.

Apart from that, the data analysis step, which is mainly focused on here, is often regarded as a negligible side task. Indeed, it is essential to analyze recorded data before applying modeling methods. It needs to be verified that the recorded trajectory data represents the expected characteristics (e.g. specific motions) that are to be modeled. Moreover, analysis methods are also applicable for evaluations where the motions of users are recorded while they interact with the system that uses the model. The recorded trajectory sets from different experimental conditions are compared and an evaluation of the data allows for conclusions that confirm hypotheses or support further analyses.

Within literature this topic is mostly uncovered, such that reliable approaches and methods to analyze, compare and evaluate trajectory data are missing. The work at hand depicts methods that are developed to tackle this problem. A framework is proposed that allows for qualitative and quantitative comparison of trajectory data. This allows for statistically feasible analyses of recorded trajectory data with respect to observed model parameters and motion behaviors. The methods are further compared to other parameter identification approaches in order to show their benefits and reliability.

Smoothing trajectories is achieved by using penalized thin-plate regression splines (PT-PRS). This method provides automatically tuned parameters and an accurate fitting of the data. Furthermore, the regression splines also provide a mean for a trajectory set. Comparing trajectory sets qualitatively is commonly based on mean or median trajectories. However, a simple mean calculated from the trajectory data does not reflect its variance.

In order to establish a statistically reasonable graphical comparison of trajectory data, the variance of the data must be part of the analysis. This is achievable with confidence intervals regarding the mean of the trajectory data. A confidence interval is a measure for the reliability of an estimate for a specific feature (e.g. the mean) [45]. The interval is calculated from observations of the respective feature when repeating the experiment that produces it. The according confidence level quantifies the probability for the interval to contain the feature of interest when observing the experiment. The width of a confidence interval with a certain confidence level is proportional to the variance of the data. Note, that the concept of confidence bands is not applied here. As an approximation to the confidence bands, the intervals are calculated point-wise along the data, which is explained in detail in the following sections. Therefore, the term confidence interval applies.

The proposed methodology is further expanded by a statistical method for quantitative trajectory analysis. As literature does not yield a suitable method to compare trajectories and analyze results quantitatively, a new procedure is developed. Trajectories are smoothed as proposed and then compared using standard measures such as Hausdorff distance or Dynamic Time Warping. The developed “pivot analysis”, which is based on the resulting distance values, then quantifies differences between sets of trajectories from different experiment conditions. Together with the qualitative evaluation method, this framework analyzes whether an observed behavior is generalizable or an incidental occurrence owing to the study setup.

In order to prove its reliability and feasibility, this framework is compared to parameter estimation methods from machine learning and system identification. Firstly, Gaussian processes [145] are applied to model the data. The obtained covariances allow for a qualitative comparison by graphically overlaying them. For a quantitative comparison of the trajectory sets, the Kulback-Leibler Divergence is applied to the resulting Gaussian processes. Secondly, a system identification approach [29] is consulted. From the data an ARMAX model is obtained which allows for comparisons by applying any obtained system to the various trajectory sets. These alternative approaches are applied with the same goal of qualitative and quantitative evaluation. Benefits and advantages of the proposed methods are revealed within simulation results.

The contribution presented in the following comprises a generalizable framework for the analysis of human trajectory data. This work applies penalized spline regression to address the mentioned problems. Firstly, it allows for non-parametric smoothing of each trajectory while ensuring little distortion of the original data. Secondly, based on the splines, a method is proposed to calculate a confidence interval for the mean of trajectory sets. By considering the variance of the data, the resulting representation poses a statistically feasible baseline for qualitative trajectory comparison. The method is evaluated on data from a previously shown experiment concerning the readability in human locomotion. This analysis is further improved by a cross-condition comparison method, called “pivot analysis”, developed in this work. The pivot analysis compares trajectory data from one condition to data from another condition and quantifies significant differences. Thus, the comparison of whole sets of trajectories is tackled within this chapter.

The developed approaches generalize to higher dimensionality and arbitrary trajectories. Hence, they are applicable to estimate behaviors and parameters in data from various

experimental settings. The methods complement the state-of-the-art and improve parameter identification and trajectory analysis processes. A facilitated evaluation of obtained models further contributes to more accurate parameters and higher performance of robots that integrate into environments by using human-like behaviors. An enhanced identification process for human behaviors can strongly facilitate the development of reliable and feasible models of human motion. Future work in robot locomotion and human locomotion prediction will also emphasize the integration of social aspects and human behaviors. The aspired aspects and behaviors are thus detectable with the methods proposed here.

This chapter is organized as follows: in Sec. 4.2 literature related to trajectory analysis is discussed and examples of other approaches to the problem are given. The following Sec. 4.3 elaborates the problem in more detail. Subsequently, methods that solve the problem are described in Sec. 4.4. Simulation results are illustrated in Sec. 4.5 and discussed in Sec. 4.6. After a summary in Sec. 4.7, Sec. 4.8 draws the conclusions.

4.2 Classification within the State-of-the-Art

Many of the presented works about human locomotion modeling come across the problem of data smoothing and trajectory analysis. Indeed, this aspect is not focused on and methods for trajectory comparison are not applied. In this thesis, methods for trajectory comparison are required to estimate whether subjects walk similarly in different experimental conditions. Especially the comparison of sets of trajectories is a challenging problem. The following provides a short overview of recent publications within the area of human motion modeling and literature that addresses the problem of trajectory analysis.

In [18] the idea of measuring human trajectories to derive a control model based on the dynamics of a unicycle is formulated. This includes the processing of trajectory data and the inherent problem of data smoothing. Here, a fourth order low-pass filter with heuristically selected parameters is used to remove the noise. In [121] and [14] this idea is adopted and the model expanded by further parameters based on extended experiments. The smoothing of the trajectory data to remove noise, however, remains similar with a 2nd order low-pass. This smoothing procedure is also applied to velocities in [80]. In [80] the arithmetic mean of trajectories and velocities is used to compare sets of trajectories. The authors derive parameters of human locomotion without considering the confidence intervals of the data. The identification of parameters and their effects, based on qualitative analysis of trajectories, is also conducted in [48] and [101]. However, the authors do not consider variance in the data analysis. Su et al. [166] specifically state that model inaccuracies are introduced by data smoothing and the use of a simple arithmetic mean. They investigate the problem of temporal variance within the data and focus on distance measures to compare two trajectories. A method to calculate a mean trajectory and a time alignment on Riemannian manifolds is shown and applied to bird migration data. In [136] multiple prediction methods based on the unicycle model and optimal control theory are compared in their accuracy. The analysis is based on the Frechét and the Hausdorff distance but limited to boxplots showing median and variance for the distances between considered paths.

[37] and [146] also discuss similarity measures for trajectory analysis and [166] addition-

ally addresses the p-value computation. In [32, 37, 74, 124, 146, 179] trajectory comparison and similarity measures are discussed. Distance measures are relevant for the analyses in this work as well but do not directly provide a tool for a significance analysis or a qualitative comparison. Within [99] the authors discuss the problem of trajectory analysis for hurricane data. A suitable solution for human locomotion data is not provided.

The analysis of trajectories using Gaussian processes and ARMAX models is only marginally addressed in literature. However, the classification of motions has many goals in common with the analysis discussed here. In [44] Gaussian process regression is used to model trajectories recorded from subjects in an experimental setup. The variance of some derived parameters and particularities in the predicted trajectories are used to analyze the data and draw conclusions about the behavior of the participants. Yet, comparing different conditions on a qualitative and quantitative basis is not elaborated in this work. Gaussian process regression is used in [54] for tracking and predicting the locomotion of pedestrians. This gives insight on the applicability of Gaussian processes on locomotion data, but the focus is not set on data analysis or behavior identification. In [190] mixtures of ARMA models are used in combination with the EM-Algorithm to cluster data based on the estimated parameters. Clustering is related to the proposed approach as it is based on estimating similarities. The application to human locomotion data is thereby not tackled. Deng et al. [47] propose a similar idea. ARMA models are employed to represent time series as parameter vectors. Machine learning methods are then applied to build a classification framework that recognizes time series based on the trained database. This categorization is similar to the approach for trajectory comparison proposed here. Yet, the classifier requires a database which must be built and annotated at first.

The state-of-the-art does not propose a framework for analysis and comparison of sets of trajectories. An investigation of distinct situational behaviors based on trajectory analysis is therefore not supported. Accordingly, present work proposes methods for qualitative and quantitative evaluation of geometric differences within human trajectories. The methods developed in this thesis are based on penalized regression splines [57] and implemented using the R package `mgcv`. The proposed non-parametric framework is applicable to single trajectories for smoothing and is employed in previous evaluations for the qualitative and quantitative comparison of trajectory sets with respect to variance in the data.

4.3 Problem Description

Human locomotion modeling requires complex models with a large variety of parameters, some of which are still unknown. These parameters define distances, timings or weights that favor one behavior over another. For modeling human-like locomotion these parameters are crucial but difficult to measure. In order to prove their existence and to quantify their influence, researchers design experiments where the effects of such parameters become visible. The effects appear as variations in human trajectory data recorded under different conditions within an experiment. More specifically, the effects can be sudden velocity changes or certain path adaptations.

Conducted in a large room equipped with an optical tracking system, locomotion experiments yield recordings of walking humans. Tracked positions (shoulders, back,

chest, hips) are multiple sequences of discrete 3-dimensional (3d) positions that are merged to resemble the movement of the center-of-mass (COM). This 3d trajectory is then projected to the ground plane resulting in a two-dimensional discrete planar trajectory $\boldsymbol{\xi}^t(k) = (\mathbf{p}^x(k), \mathbf{p}^y(k), \mathbf{p}^t(k))_{k \in \{1, \dots, K\}} \in \mathbb{R}^{3 \times K}$ which describes a change of position $(\mathbf{p}^x(k), \mathbf{p}^y(k))$ over discrete time $t(k)$. The indexing parameter $\mathbf{p}^t(k) = t(k)$ reflects the sequence of K time-steps Δt of the data that is dependent on the tracking frequency $\Delta t = \frac{1}{f} = \frac{1}{204 \text{ Hz}}$ and the length of the recording $T_{\text{rec}} = K\Delta t$. If experiments are repeated with N subjects, the data for one condition \mathcal{C} is a set of trajectories $\Xi_{\mathcal{C}}^t = \{\mathbf{p}_n^x(k), \mathbf{p}_n^y(k), \mathbf{p}_n^t(k)\}_{k \in \{1, \dots, K\}} \in \mathbb{R}^{3 \times K \times N}$ such that $\boldsymbol{\xi}_{n, \mathcal{C}}^t(k) \in \Xi_{\mathcal{C}}^t$ with $n = 1, \dots, N$.

Identifying similar or, in contrast, diverging behaviors across experimental conditions requires the analysis and comparison of trajectory sets $\Xi_{\mathcal{C}}^t$ and according velocity profiles. Qualitative evaluation is able to identify the appearance of named variations between sets $\Xi_{\mathcal{C}}^t$, which validates the experiment design. After analyzing the trajectory data $\boldsymbol{\xi}^t(k)$ qualitatively, it is of interest if found differences or analogies are significant and not just random occurrences. Thus, a method is needed that allows for a quantitative comparison of trajectory sets. Distance measures for trajectories compare one or more dimensions [37, 90] and result in a single scalar for two trajectories. However, from comparing two trajectories, e.g. the mean of a set, it is not possible to judge whether two sets are significantly different from each other. Accordingly, a statistical analysis is required that yields a p-value p_{Ξ} , i.e. a measure of significance, for the null hypothesis H_0 that two sets Ξ_1^t and Ξ_2^t are equal or the alternative hypothesis H_1 that the two sets are not equal. This is interpretable as a test if the two sets are produced by the same process. For the p-value, a probability $P(\cdot)$ is defined, that the distances between two sets $d_{\Xi}(\Xi_1^t, \Xi_2^t)$ are suitable samples or even more extreme results from a given distribution of distances \mathcal{D}_{Ξ} , assuming that H_0 holds. The according right- and left-sided tests are defined as:

$$p_{\Xi, r} = P(\mathcal{D}_{\Xi} \geq d_{\Xi} | H_0)$$

$$p_{\Xi, l} = P(\mathcal{D}_{\Xi} \leq d_{\Xi} | H_0)$$

Literature does not provide elaborated approaches to conduct these qualitative or quantitative analyses of trajectory data. Therefore, the methods provided in this work are developed to solve the depicted problem. The following discusses smoothing of single trajectories $\boldsymbol{\xi}^t(k)$, calculation of a mean representation $\tilde{\boldsymbol{\xi}}^t(k)$ for a set Ξ^t and comparison of sets $\Xi_{\mathcal{C}}^t$ with respect to data variance. Thereby, variance is particularly important for small datasets. This is critical for human locomotion data since datasets are usually small due to the time consuming recording process.

4.4 Methodology for Trajectory Data Analysis

In literature model building from human motion data, e.g. based on reinforcement learning or inverse optimal control methods, is a common topic [14, 49, 103, 121]. Methods that analyze recorded data in order to identify specific behaviors and prove their generalizability are, however, hardly found. Yet, it should be verified qualitatively and quantitatively that the trajectory data used for modeling represents the expected characteristics (e.g. specific

motions). Moreover, when a model is evaluated within a user study, the recorded trajectory sets from different conditions need to be compared. The following methodologies provide this comparison and are applied to investigate the hypotheses posed in this work.

Human locomotion behaviors vary between subjects. Comfortable velocities and path adaptations, for example, are chosen differently among individuals. In addition to that, noise is an important factor when measuring human locomotion. The methods proposed in this work are also applicable for smoothing trajectories with minimum divergence.

Qualitative evaluation of the data allows for conclusions that confirm hypotheses or support further analysis. Comparing trajectory sets qualitatively is commonly based on mean or median trajectories. But a simple mean calculated from the trajectory data does not reflect its variance. In order to establish a statistically reasonable comparison of trajectory data, the variance of the data must be part of the analysis. This is achievable with confidence intervals (CI) for the mean of the trajectory data.

Confidence intervals do not yield quantitative estimates when sets of trajectories are compared. When analyzing experimental data, evaluation of significance is an important step. But state-of-the-art methods are not suitable to provide this for trajectory data. Accordingly, an additional method is developed that applies standard distance measures to the data and analyzes the relations of trajectory sets with a pivot comparison. This allows for statistically feasible statements about correlations of locomotion behaviors which is necessary for the subsequent experiments.

Additionally, two approaches are proposed that are based on existing methods but are adapted to follow the proposed procedures. Gaussian processes and ARMA models are used to acquire similar analysis results. Both methods are applied to compare the analysis results and to support the reliability of the proposed method. Results as well as advantages and drawbacks are therefore examined.

The following firstly depicts how penalized splines are used to model human locomotion data and to avoid problems with low-pass filtering of trajectories. After that, a method for calculating CIs concerning the mean of the path data is presented. This framework is then complemented by the developed pivot analysis. Finally, the machine learning and system identification based procedures are described.

4.4.1 Trajectory Smoothing

Accumulated tracking data is usually noisy and needs to be smoothed before it is used in modeling algorithms. The common approach to apply signal filters requires a frequency analysis or hand tuning of the parameters. Achieved results are usually good because the margin between low frequency oscillations describing the path and high frequency noise is large within trajectory data. However, low-pass filters yield disadvantages: filter parameters are usually selected heuristically and without any in-depth frequency analysis such that they can not adapt to variations in the data. This leads to problems for experiments where more subtle variations in the motion or velocity are of interest. Without proper tuning, important characteristics of the data may be removed. This problem is tackled here using penalized spline regression.

In the conducted experiments a measurement error of approximately $1 - 2 \text{ mm}$ is usually present. At a measurement frequency of 204 Hz, corresponding paths are still very

smooth. Yet, specific measurement errors lead to outliers in the discrete data. More affected by the noise are calculated velocities. This observation is easily explained by the high measurement frequency. In case a trackball is measured 2 mm off its real position, a velocity change of around ± 0.4 m/s occurs, whereas the typical maximum velocity of an adult is around 1.4 m/s. Therefore smoothing the data is inevitable.

Smoothing of a trajectory is achievable through a mean or median calculation [33]. A reliable mean trajectory must represent the tendency of the input data with a minimum error and robustness to outliers. The arithmetic mean $\bar{\xi}_c^t$ of a set of N trajectories with K time-steps is:

$$\bar{\xi}_c^t = \frac{1}{N} \sum_{n=1}^N \xi_{n,c}^t(k) \quad \forall k = 1, \dots, K,$$

where $\xi_{n,c}^t(k) \in \Xi_c^t$ is a single trajectory of the whole set with $n = 1, \dots, N$. With the inherent noise and possible outliers in the data due to measurement errors, the arithmetic mean does not pose a good fit [5]. Smoothing filters, on the other hand, require hand tuning and therefore do not generalize to data from varying experiments. These problems are addressed with penalized thin plate regression splines [57]. PTPRS pose a non-parametric model that generalizes to higher dimensional problems and resembles important properties of locomotion (smoothness, horizontal and vertical swinging) [102]. Necessary parameters are derived from the input data. Especially the automated estimation of the penalization term λ_{PTPRS} is of interest, which is estimated using generalized cross validation (GCV). This adaptive penalization term allows PTPRS to follow subtle variations in the data. In addition, computational properties, like the stability at borders, are superior compared to polynomials. Spline regression is further applicable to a single trajectory for smoothing or to a set to obtain a mean representation. The resulting spline thereby features minimum difference to the original data. When applying the common univariate P-splines within analyses, which use B-spline bases as well, no significant differences were found but for the extra parameters needed.

For path data the fitting is separated for the p^x and p^y dimensions. For fitting the spline the input data \mathbf{z} and the output data \mathbf{q} need to be assigned. Here, the input equals the data point indexing $\mathbf{z}(k) \in \{z(1), \dots, z(K)\}$ and the output resembles one of the axes such that $\mathbf{q}(k) = \mathbf{p}^x(k)$ or $\mathbf{q}(k) = \mathbf{p}^y(k)$. The radial basis function $f_b(\mathbf{z}(k))$ for the PTPRS is:

$$f_b(\mathbf{z}(k)) = \sum_{w=1}^W \gamma_w f_r(\|\mathbf{z}(k) - \omega_w\|),$$

where $\omega_w \in \mathcal{W}$ defines a set of control points for the spline with $w = 1, \dots, W$, γ_w depict the regression coefficients (subject to optimization) and $f_r = r^2 \log r$ is the radial basis kernel with $r = \|\mathbf{z}(k) - \omega_w\|_2$. The number of control points W is equal to the number of data points K for smoothing splines. The fitting is based on a minimization of the following energy function:

$$E_{\text{PTPRS}}(f_b) = \sum_{k=1}^K \|\mathbf{q}(k) - f_b(\mathbf{z}(k))\|^2,$$

for the corresponding data-point sets $\mathbf{q}(k)$ and $\mathbf{z}(k)$. The λ_{PTPRS} -weighted regularization term, which includes the second derivative of f_b , penalizes the trade-off between data fit and smoothness:

$$E_{\text{PTPRS}}(f_b) = \sum_{k=1}^K \|\mathbf{q}(k) - f_b(\mathbf{z}(k))\|^2 + \lambda_{\text{PTPRS}} \int \left(\frac{\partial^2 f_b(\mathbf{z}(k))}{\partial z^2} \right)^2 dz.$$

PTPRS yield a robust mean representation because data is smoothed globally instead of point-wise. Applied to a single trajectory $\xi^t(k)$, a smoothed version $\tilde{\xi}^t(k)$ is obtained. The original data and specific characteristics are closely modeled. Processing a whole set of trajectories Ξ_C^t yields a single mean $\tilde{\xi}^t(k)$.

In order to evaluate the performance of PTPRS for smoothing, two approaches are compared: 4th order Butterworth filters (BF) and PTPRS. One of the motion sequences from the conducted experiments takes around 5s, wherein the avoidance maneuver takes around 1s. The frequency of the tracking cameras is 204 Hz. Hence, the estimated cutoff frequency of the BF must be around 0.01 Hz, because the filter implementation assumes the input data vector to represent time-steps of 1s. In Fig. 4.1 a trajectory is shown that is smoothed using penalized spline regression and two differently adjusted BF for comparison. One can see that the properly tuned BF (0.01 Hz) performs equally well compared to the spline whereas the spline is non-parametric. The wrongly tuned BF (0.005 Hz) removes parts of the characteristic avoidance motion of the subject.

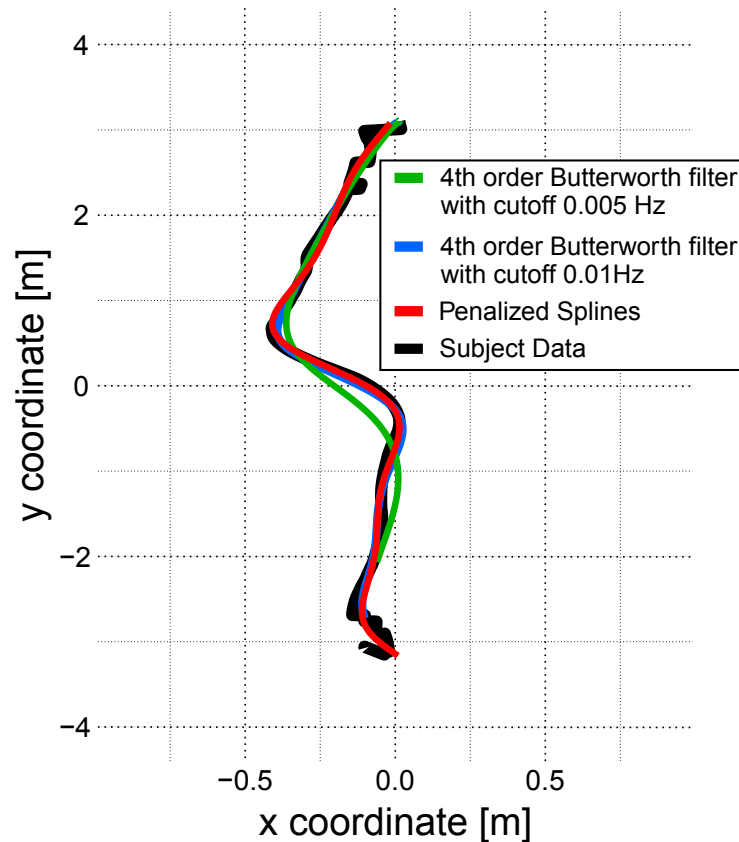


Fig. 4.1: Raw data trajectory (black), low-pass smoothed representation (green and blue with proper and inapt parameters) and spline smoothing (red).

4.4.2 Analysis of Trajectory Sets

Qualitative evaluation enables the analysis whether a set Ξ^t shows the expected variations triggered by experimental conditions. The data ξ^t varies amongst subjects, so an analysis must consider variance in the data when comparing different sets. This applies particularly to small datasets and therefore often to human locomotion data since the recording process is time consuming. Accordingly, a method is needed that meets the requirements for the analysis and allows for a qualitative comparison of multiple sets.

Distance measures, as mentioned in Sec. 4.2, result in a scalar for the comparison of two trajectories. However, from a comparison of two trajectories one can neither judge whether the whole set follows the expected behavior for the experiment nor does the scalar yield an intuition about variance within the set. Alternatively, analyzing exclusively the geometric data of trajectories $\xi^{xy}(k) = (\mathbf{p}^x(k), \mathbf{p}^y(k))_{k \in \{1, \dots, K\}} \in \mathbb{R}^2$ (i.e. paths) also allows for examining qualitatively whether the experiment produces relevant data. For this purpose, paths are plotted super-imposed as in Fig. 4.2. A common approach to analyze tendencies

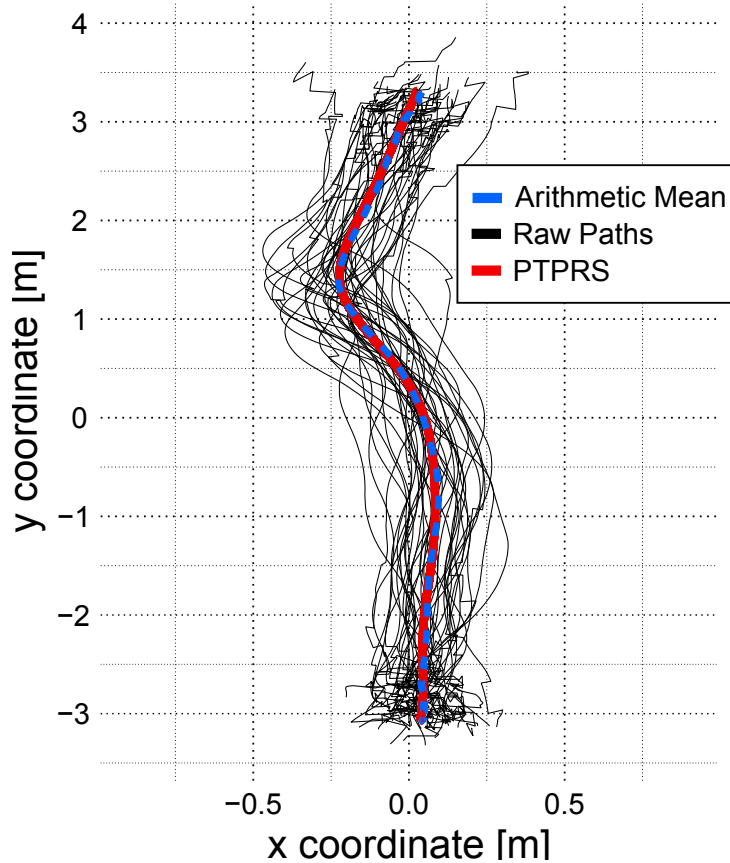


Fig. 4.2: Superimposed paths (black) with point-wise arithmetic mean (blue) and smoothing spline (red). Noise at both ends originates from low tracking performance at the borders of the tracking area.

in superimposed path data are mean or median paths [33]. Note, that the raw paths of a set $\xi_n^{xy}(k) \in \Xi^{xy}$ vary in length, which prohibits a point-wise calculation of a representative mean. Therefore, the length K of all raw paths in the set Ξ^{xy} must be normalized to an

equal value \tilde{K} . The arithmetic mean of a set of N discrete paths with \tilde{K} time-steps is $\bar{\xi}^{xy}$. Fig. 4.2 shows the mean (blue) for the normalized data. Comparing two sets based on one representative like the mean still omits the variance. A mean value calculated from path data may just represent a random sample from the underlying motion generation process. Specifically, the arithmetic mean does not consider the extent of variance within the data. Hence, if two means pose a good example to prove a certain effect, this may be coincidence as the observed occurrence is merely a suitable sample from a distribution with a potentially large variance. Consequently, for a reasonable analysis a confidence interval (CI) of the mean must be considered, to account for the data variance. Then, if the data yields a narrow CI and shows the influence of the tested parameter, the mean may be considered as a strong indicator for the validity of the hypothesis. From this point, further statistical evaluation would be appropriate. Therefore, a method to solve the problem of calculating CIs is proposed in the following.

4.4.2.1 Confidence Intervals for Trajectory Data

This paragraph addresses the CI calculation for the mean of the recorded human walking trajectories. The problem is split into CIs for path and velocity data. A CI is a measure for the reliability of an estimate for a specific feature (e.g. the mean) [45]. The interval is calculated from observations of the respective feature when repeating the experiment that produces it. The according confidence level quantifies the probability for the interval to contain the feature of interest when observing the experiment. The width of a CI with a certain confidence level is proportional to the standard deviation of the data. In this work, inference is conducted to statistically compare means of the given trajectory data. Thereby, the CI refers to the expected value from the unknown distribution of a trajectory set. Note that the concept of confidence bands is not applied here. As an approximation of the confidence bands the intervals are calculated point-wise along the data, which is explained in the following.

A mean path $\tilde{\xi}^{xy}(k)$ is calculated by applying the spline fitting technique to sets Ξ^{xy} of raw path data $\xi_n^{xy}(k)$, see [5]. For this mean a confidence interval is estimated considering the N repetitions of one experiment condition. Assuming the two dimensions $\mathbf{p}^x(k)$ and $\mathbf{p}^y(k)$ as random samples from unknown distributions, the CI is defined between the two endpoints:

$$[U^x(\mathbf{p}^x(k)), V^x(\mathbf{p}^x(k))] \text{ and } [U^y(\mathbf{p}^y(k)), V^y(\mathbf{p}^y(k))],$$

for each sample $k = 1, \dots, K$ and a significance level α_P , by the probabilities:

$$\begin{aligned} P(U^x(\mathbf{p}^x(k)) \leq \mathbf{p}^x(k) \leq V^x(\mathbf{p}^x(k))) &\geq 1 - \alpha_P, \\ P(U^y(\mathbf{p}^y(k)) \leq \mathbf{p}^y(k) \leq V^y(\mathbf{p}^y(k))) &\geq 1 - \alpha_P, \end{aligned}$$

that the intervals:

$$[U^x(\mathbf{p}^x(k)), V^x(\mathbf{p}^x(k))] \text{ or } [U^y(\mathbf{p}^y(k)), V^y(\mathbf{p}^y(k))],$$

contain the mean of the data [57]. As the number of sample points varies across the input sequences, a normalization has to be applied to equalize all lengths to \tilde{K} . Due to the point-

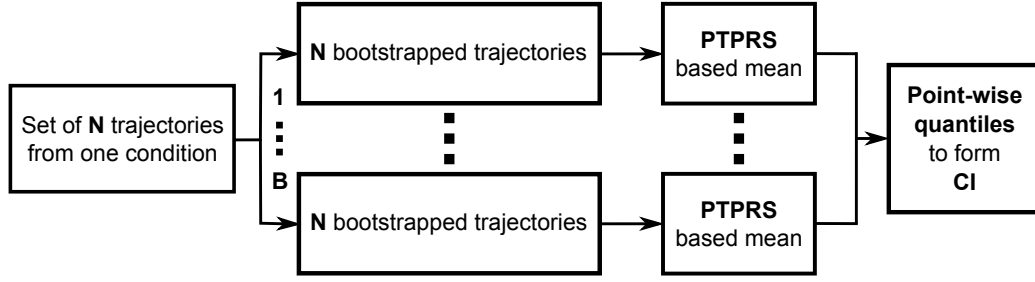


Fig. 4.3: Calculation of CIs for trajectory sets

wise processing, a shorter path would otherwise contribute with less weight in the CI (e.g. a fast person generates less data-points over the same distance). Estimating the variance of a mean for small datasets is possible with bootstrapping [53], i.e. a virtual repetition of the experiment. Bootstrapping is based on data re-sampling and estimates a non-parametric statistical distribution. Given that, a calculation of point-wise empirical quantiles for each dimension $\mathbf{p}^x(k)$ and $\mathbf{p}^y(k)$ is possible. The procedure samples N paths with replacement from the N normalized and non-smoothed paths $\xi_{n,c}^{xy}(k)$ with $k = 1, \dots, \tilde{K}$. From the set of N sampled paths $\hat{\xi}_{n,c}^{xy}$ a mean representation is calculated using PTPRS. This is repeated B times (B is a high number, i.e. 1000) and yields B mean paths $\tilde{\xi}_b^{xy}$ with $b = 1, \dots, B$. Computing the empirical quantile for each index-step $k \in \tilde{K}$ of each dimension from the result, which is a set of $B \times \tilde{K}$ data points in \mathbb{R}^2 , approximates the data variance. These quantiles are used to calculate \tilde{K} point-wise CIs for the mean. CIs are defined as the concatenation of the \tilde{K} point-wise intervals which represent a probability that the unknown mean path is contained. A significance level $\alpha_p = 1 - \sqrt{0.95} \approx 2.53\%$ is employed, to model a two-dimensional 5% significance level. This confidence interval of 5% resembles the interval covered by 95% of the calculated mean paths from the bootstrapping and PTPRS step. Figure 4.3 illustrates the process of CI calculation.

The same process is applicable to calculate CIs for velocity data. This analysis allows for the investigation of velocity variations which are often related to avoidance behaviors. Velocity changes are related to applied controls and therefore indicate energy expenditure. Discrete velocities are derived from $\xi^t(k)$ leading to velocity sequences $\xi^v(k) = (v(k), p^t(k))$ with $k = 1, \dots, \tilde{K}$. Since aligning velocity profiles is non-trivial due to the variations in speed and path across subjects, a different scale is necessary which is equal for all recordings. Owing to the setup of the experiments in this work, all recorded trajectories proceed along the length $-3m \leq \mathbf{p}^y \leq 3m$ as subjects walk from one side of the tracking area to the exact opposite position. Accordingly, velocities are specified with respect to $\mathbf{p}^y(k)$ such that $\xi^v(k) = (v(k), \mathbf{p}^y(k))$. Sets of velocities from each experiment condition $\xi_{n,c}^v(k) \in \Xi_c^v$ are then processed with the same procedure for CI calculation.

4.4.2.2 Pivot Analysis for Path Data

The method proposed for CI calculation allows for a qualitative inspection of the recorded trajectory data, but not for a quantification of the similarity of observed behaviors. Therefore, an according method is needed to identify if locomotion behaviors are similar or significantly different.

Within the aforementioned experiments it needs to be identified whether a subject walks similarly in different experiment conditions. However, a direct comparison of the two generated paths using distance measures only yields a scalar value without a statistical interpretation. The same problem argues against the comparison of the conditions based on their mean representations from PTPRS. Further, permutation tests with distance measures, where all trajectories of two sets are compared to each other, would allow to identify whether two sets are similar. Yet, the result ignores individual differences, as it refers to the general distribution of the trajectory data. Every human walks differently within locomotion experiments, even if the conditions are equal for every subject. Thus, the analysis must focus on the individual subject. Permutation tests also require the statistical independence of the samples. This is not provided here due to specific aspects in some experimental setups which prohibits the randomization of conditions. Accordingly, the pivot analysis is developed where two conditions are compared by their distance to a third condition, called “pivot condition” or “pivot”. Thereby, a distance is calculated for each person separately between each condition and the pivot. This yields two sampled distributions of distances which are statistically independent and consider subject specific characteristics. Given these samples, a statistical evaluation regarding similarity is possible based on a hypothesis test.

During the experiments in Sec. 2.2, which are revisited here, trajectories from N subjects are recorded under four conditions $\mathcal{C} = \{1, 2, 3, 4\}$. The evaluation is based on the null hypothesis H_0 that two conditions produce equal paths. This hypothesis is tested by comparing the two distributions that originate from the distance calculations between the pivot and the two conditions under consideration. The distances for each person between each of the two trajectory sets, e.g. Ξ_2^{xy} and Ξ_4^{xy} , and a pivot set, e.g. Ξ_1^{xy} , are calculated and the two sampled distributions of distances $\mathcal{D}_{\Xi_2,1}$ and $\mathcal{D}_{\Xi_4,1}$ are obtained. Both distributions consist of N values. In order to test H_0 regarding these two distributions the variances must be estimated from the samples, leading to a t-test. With respect to the mentioned statistical dependence and the assumed differences in the variances, a paired Welch-test is necessary. This variant of the t-test evaluates H_0 with respect to the mean and variance of the distance distributions. The developed concept exploits the fact that two paths with a small distance between them also feature similar distances to paths of a baseline or pivot condition. For example, when two paths from the sets Ξ_2^{xy} and Ξ_4^{xy} are compared, resulting in a small distance value, a small difference will be found when comparing the distances of Ξ_2^{xy} to Ξ_1^{xy} with Ξ_4^{xy} to Ξ_1^{xy} .

The procedure to find a similarity between conditions is therefore structured as follows. A mean value and a variance for the distances of the paths from each person between the two conditions, e.g. Ξ_2^{xy} and Ξ_4^{xy} , are calculated. This allows for a first interpretation whether the conditions produce similar paths, given that the mean and variance are relatively low. Mean and variance values for the distances of each condition to the pivot are then compared using the Welch-test. The result are p-values regarding H_0 for each combination with a pivot and for each applied distance measure. By conducting this test with multiple pivots, a bias from relations between the considered conditions and the pivot is excluded. If one of the p-values is below the standard 5% significance level for a given pair of conditions, the null hypothesis (paths are equal) is rejected. In order to avoid a bias of the results

regarding the distance measure, the test is carried out using two different measures. The resulting p-values indicate if two data-sets are similar or significantly different. In order to quantify this significance, the effect size is measured using Cohen's d_c [46].

$$d_c = \frac{|\bar{\mu}_1 - \bar{\mu}_2|}{\sqrt{(s_1^2 + s_2^2)/2}},$$

where $\bar{\mu}_1$ and $\bar{\mu}_2$ represent the sample means, and s_1^2 and s_2^2 are the estimated variances of two populations (trajectories under two different conditions). Considering the data recorded from experiments in this work, a $d_c \approx 0.2$ corresponds to a small, $d_c \approx 0.5$ to a middle and $d_c \approx 0.8$ to a strong difference or similarity. Note, that the value d_c will raise and diminish together with the distance between trajectory sets, due to the difference $|\bar{\mu}_1 - \bar{\mu}_2|$ and that the p-value will shift accordingly.

This approach is not applied to velocity data in the evaluation of the conducted experiments. The reason is that velocities vary strongly among subjects and are not normalized, such that calculated distances are not meaningful.

4.4.2.3 Gaussian Processes for Path Data

For a comparison with CIs and the pivot analysis, Gaussian processes (GPs) are defined with similar goals, as proposed in [145]. The input to the Gaussian process (GP) is \mathbf{z}_{GP} and the output \mathbf{q}_{GP} with a function specified as a discrete vector, $\mathbf{q}_{\text{GP}} = f_{\text{GP}}(\mathbf{z}_{\text{GP}})$, as in [145]. A Gaussian process therefore describes a distribution of functions mapping \mathbf{z}_{GP} to \mathbf{q}_{GP} . Given experimental path data from humans, one can define a process that yields a mean value and a standard deviation for the data pairs $(\mathbf{z}_{\text{GP}}, \mathbf{q}_{\text{GP}})$ at each evaluated input point \mathbf{z}_* . With respect to the previously formulated confidence intervals, a GP is defined for each experiment condition. The input is defined to be $\mathbf{z}_{\text{GP}} = \mathbf{p}_n^y(k)$ and the output $\mathbf{q}_{\text{GP}} = \mathbf{p}_n^x(k)$. With respect to the used trajectory data, this specifies the sideway or avoidance movements in $\mathbf{p}_n^x(k)$ direction as the output and the forward progression in $\mathbf{p}_n^y(k)$ dimension as the input. In general, the mean $m(\cdot)$ and covariance function $\text{cov}(\cdot)$ define a Gaussian process as:

$$\begin{aligned} m(\mathbf{z}_{\text{GP}}) &= \mathbb{E}[\mathbf{z}_{\text{GP}}], \\ \text{cov}(\mathbf{z}_{\text{GP}}, \mathbf{z}_*) &= \mathbb{E}[(f_{\text{GP}}(\mathbf{z}_{\text{GP}}) - m(\mathbf{z}_{\text{GP}}))(f_{\text{GP}}(\mathbf{z}_*) - m(\mathbf{z}_*))], \\ &\Rightarrow f_{\text{GP}}(\mathbf{z}_{\text{GP}}) \sim \mathcal{GP}(m(\mathbf{z}_{\text{GP}}), \text{cov}(\mathbf{z}_{\text{GP}}, \mathbf{z}_*)) \end{aligned}$$

Above definitions consider only position data, whereas this approach is applicable to velocity data $(\dot{\mathbf{p}}_n^x(k), \dot{\mathbf{p}}_n^y(k))$ as well. For the GP regression on the noisy data and subsequent sampling from the resulting posterior, the following applies:

$$\mathbf{q}_{\text{GP}} = f_{\text{GP}}(\mathbf{z}_{\text{GP}}) + \epsilon_{\text{GP}},$$

with the additive Gaussian noise ϵ_{GP} which features a variance σ_N^2 . This leads to the covariance function

$$\text{cov}(\mathbf{q}_{\text{GP}}) = \text{cov}(\mathbf{z}_{\text{GP}}, \mathbf{z}_{\text{GP}}) + \sigma_N^2 I.$$

The joint distribution of the observed values \mathbf{q}_{GP} for the input \mathbf{z}_{GP} and the function values \mathbf{f}_* at the test locations \mathbf{z}_* are given as:

$$\begin{bmatrix} \mathbf{q}_{\text{GP}} \\ \mathbf{f}_* \end{bmatrix} \sim \mathcal{N} \left(0, \begin{bmatrix} \text{COV}(\mathbf{z}_{\text{GP}}, \mathbf{z}_{\text{GP}}) + \sigma_N^2 I & \text{COV}(\mathbf{z}_{\text{GP}}, \mathbf{z}_*) \\ \text{COV}(\mathbf{z}_*, \mathbf{z}_{\text{GP}}) & \text{COV}(\mathbf{z}_*, \mathbf{z}_*) \end{bmatrix} \right).$$

For the prediction of a function value \mathbf{f}_* at the test location \mathbf{z}_* following applies:

$$\begin{aligned} \mathbf{f}_* | \mathbf{z}_{\text{GP}}, \mathbf{q}_{\text{GP}}, \mathbf{z}_* &\sim \mathcal{N}(\bar{\mathbf{f}}_*, \text{COV}(f_*)), \quad \text{where} \\ \bar{\mathbf{f}}_* &\hat{=} \mathbb{E}[\mathbf{f}_* | \mathbf{z}_{\text{GP}}, \mathbf{q}_{\text{GP}}, \mathbf{z}_*] = \text{COV}(\mathbf{z}_*, \mathbf{z}_{\text{GP}}) [\text{COV}(\mathbf{z}_{\text{GP}}, \mathbf{z}_{\text{GP}}) + \sigma_N^2 I]^{-1} \mathbf{q}_{\text{GP}} \\ \text{COV}(\mathbf{f}_*) &= \text{COV}(\mathbf{z}_*, \mathbf{z}_*) - \text{COV}(\mathbf{z}_*, \mathbf{z}_{\text{GP}}) [\text{COV}(\mathbf{z}_{\text{GP}}, \mathbf{z}_{\text{GP}}) + \sigma_N^2 I]^{-1} \text{COV}(\mathbf{z}_{\text{GP}}, \mathbf{z}_*). \end{aligned}$$

The marginal likelihood is computed by:

$$\begin{aligned} \log p(\mathbf{q}_{\text{GP}} | \mathbf{z}_{\text{GP}}) &= \\ &= -\frac{1}{2} \mathbf{q}_{\text{GP}}^T (\text{COV}(\mathbf{z}_{\text{GP}}, \mathbf{z}_{\text{GP}}) + \sigma_N^2 I)^{-1} \mathbf{q}_{\text{GP}} - \frac{1}{2} \log |\text{COV}(\mathbf{z}_{\text{GP}}, \mathbf{z}_{\text{GP}}) + \sigma_N^2 I| - \frac{N}{2} \log 2\pi \end{aligned}$$

In order to define a Gaussian process for human trajectory data, a mean function $m(\cdot)$ and a covariance function $\text{cov}(\cdot)$ must be chosen. The covariance function defines the smoothness of the drawn sample functions as well as the dependency between consecutive observations. Defining a suitable mean and covariance function (and hyper-parameters) that model the observed behavior, such that sampling from the process yields a suitable trajectory, is thus the first problem to be tackled. Human path data $\xi_n^{xy}(k)$ is not the result of a simple linear system. As mentioned before, the correlations are non-linear such that the covariance function needs to be chosen accordingly. In [175] the mean is proposed as a linear function and the covariance as a matern type function for modeling human locomotion trajectories. This approach is adopted here and the hyper-parameters are trained based on the input data, using the framework of [145]. The used mean function $m(\cdot)$ has the following structure:

$$m(\mathbf{z}_{\text{GP}}) = a_{\text{GP}} \mathbf{z}_{\text{GP}} + c_{\text{GP}},$$

where a_{GP} and c_{GP} are parameters that are acquired from the data using learning methods [145]. The covariance function, exemplarily evaluated with \mathbf{z}_{GP} and \mathbf{z}_* is chosen as:

$$\text{COV}(\mathbf{z}_{\text{GP}}, \mathbf{z}_*) = s_f^2 f_{\text{matern}}(\sqrt{5} r_{\text{GP}}) e^{(-\sqrt{5} r_{\text{GP}})},$$

with the distance:

$$r_{\text{GP}} = \sqrt{(\mathbf{z}_{\text{GP}} - \mathbf{z}_*)^T (\text{ell} \cdot I)^{-1} (\mathbf{z}_{\text{GP}} - \mathbf{z}_*)},$$

and the function:

$$f_{\text{matern}}(l_{\text{GP}}) = 1 + l_{\text{GP}} + l_{\text{GP}}^{\frac{2}{3}},$$

where the parameters s_f^2 and ell are determined from the input data.

For evaluation of trajectory data, the GPs of different conditions must be compared. A comparison method must be applied that quantifies the deviations between the processes.

Since gaussian processes describe probability distributions, e.g. \mathcal{N}_0 and \mathcal{N}_1 , the Kulback-Leibler Divergence (KLD) is applicable to the distribution of the output variable \mathbf{q}_{GP} at each input \mathbf{z}_{GP} . For the case of discrete data the KLD for two Gaussian distributions $\mathcal{N}_0(\mu_0, \Sigma_0)$ and $\mathcal{N}_1(\mu_1, \Sigma_1)$ is defined in [145] by:

$$\text{KLD}(\mathcal{N}_0|\mathcal{N}_1) = \frac{1}{2} \log |\Sigma_1 \Sigma_0^{-1}| + \frac{1}{2} \text{tr} \Sigma_1^{-1} ((\mu_0 - \mu_1)(\mu_0 - \mu_1)^T + \Sigma_0 - \Sigma_1) \quad (4.1)$$

These definitions are now applied to the recorded human locomotion data to generate a GP for each experiment condition. By overlaying the confidence interval of the GP, a qualitative comparison of the processes and is possible. The KLD then provides a quantitative evaluation of the comparison.

4.4.2.4 Autoregressive Moving Average Model for Path Data

As a second comparison method a trajectory may be referred to as a time dependent series of data points. For an analysis it is suitable to derive generative models and compare them. With respect to Sec. 4.4.2.1 and 4.4.2.3, models require the definition of an input and an according output. If the accelerations or torques applied by humans are observable, the data considered in this work could be regarded as the output. Indeed, the focus is on the comparison of the generated path data such that the two dimensional data needs to be assigned to input and output. The following is concerned with the analysis of time series using Autoregressive Moving Average Models with exogenous inputs (ARMAX). ARMAX models are used to fit time dependent data sets and result in a linear time-discrete stochastic process. These models are also closely related to discrete linear-time-invariant systems used in control theory [112, 150]. In order to suit the linearity of ARMAX models, the recorded human trajectories are considered as the result of a simple linear system that produces discrete position data with a high frequency. Furthermore, the ideas of Autoregressive and Moving Average models show parallels to the progression of humans. Autoregressive models (AR) propose that the current system output \mathbf{q}_{ar} at discrete time-point k is the result of a linear combination of past outputs $\mathbf{q}_{\text{ar}}(k-1), \dots, \mathbf{q}_{\text{ar}}(k-n_a)$ and an additive white noise term $\epsilon_{\text{ar}}(k)$:

$$\mathbf{q}_{\text{ar}}(k) = c_{\text{ar}} + a_1 \mathbf{q}_{\text{ar}}(k-1) + \dots + a_{k-n_a} \mathbf{q}_{\text{ar}}(k-n_a) \epsilon_{\text{ar}}(k),$$

where c_{ar} is a constant scalar, $a_{1, \dots, k-n_a}$ are output coefficients and n_a is the degree of the AR model. The shift $k-1, \dots, k-n_a$ is typically expressed by a lag operator which is defined as l^{-1} such that $l^{-1} \mathbf{q}_{\text{ar}}(k) = \mathbf{q}_{\text{ar}}(k-1)$. This leads to the following structure with matrix $A(l^{-1})$:

$$A(l^{-1}) \mathbf{q}_{\text{ar}}(k) = c_{\text{ar}} + \epsilon_{\text{ar}}(k).$$

The AR models express the dependence of the current or next position on the past positions. Accordingly, the random part of this progression is captured by Moving Average models (MA). MA models construct the conditional mean of $\mathbf{q}_{\text{ma}}(k)$ from a sum of weighted unconditioned stochastic processes:

$$\mathbf{q}_{\text{ma}}(k) = c_{\text{ma}} + \epsilon_{\text{ma}}(k) + c_1 \epsilon_{\text{ma}}(k-1) + \dots + c_{k-n_c} \epsilon_{\text{ma}}(k-n_c),$$

where c_{ma} is a constant scalar, $c_{1,\dots,k-n_c}$ are the noise coefficients and n_c is the degree of the MA model. With the lag operator and the matrix $C(l^{-1})$ the model is formalized as:

$$\mathbf{q}_{\text{ma}}(k) = c_{\text{ma}} + C(l^{-1})\epsilon_{\text{ma}}(k).$$

By combining AR and MA models, setting $c_{\text{ar}} = c_{\text{ma}} = 0$ and adding exogenous inputs $b_1\mathbf{z}_{\text{arma}}(k - n_k), \dots, b_{n_b}\mathbf{z}_{\text{arma}}(k - n_k - n_b + 1)$, the ARMAX structure is acquired:

$$\begin{aligned} \mathbf{q}_{\text{arma}}(k) + a_1\mathbf{q}_{\text{arma}}(k - 1) + \dots + a_{n_a}\mathbf{q}_{\text{arma}}(k - n_a) = \\ b_1\mathbf{z}_{\text{arma}}(k - n_k) + \dots + b_{n_b}\mathbf{z}_{\text{arma}}(k - n_k - n_b + 1) + \\ \epsilon_{\text{arma}}(k) + c_1\epsilon_{\text{arma}}(k - 1) + \dots + c_{n_c}\epsilon_{\text{arma}}(k - n_c), \end{aligned}$$

where b_{1,\dots,n_b} are the input coefficients. Here, n_b defines the dimension of the affecting input and n_k describes the dead time of the system, meaning the number of input samples \mathbf{z}_{arma} that occur before they affect the output \mathbf{q}_{arma} . With:

$$\begin{aligned} A(l^{-1}) &= 1 + a_1l^{-1} + \dots + a_{n_a}l^{-n_a} \\ B(l^{-1}) &= b_1 + b_2l^{-1} + \dots + b_{n_b}l^{-n_b+1} \\ C(l^{-1}) &= 1 + c_1l^{-1} + \dots + c_{n_c}l^{-n_c}, \end{aligned}$$

the compact form is acquired:

$$A(l^{-1})\mathbf{q}_{\text{arma}}(k) = B(l^{-1})\mathbf{z}_{\text{arma}}(k) + C(l^{-1})\epsilon_{\text{arma}}(k).$$

The compact form reveals the connection to linear time-invariant systems and allows for the following interpretations: n_a is the number of poles, $n_b + 1$ the number of zeroes, n_c the number of noise terms and n_k defines the dead time. In order to model the avoidance behavior within the data, the input data \mathbf{z}_{arma} is chosen to be the $\mathbf{p}_n^y(k)$ dimension and the output data \mathbf{q}_{arma} represents the $\mathbf{p}_n^x(k)$ dimension.

4.5 Simulation Results

In order to estimate the capabilities of the proposed analysis framework, the methods are applied to data recorded in the experiment presented in Sec. 2.2. The data is composed of 160 trajectories from 40 subjects that walk from a start to a goal and thereby avoid a human interferer. Trajectory data describes four conditions called scenarios (Sc.), where in: Sc. 1 the subject walks alone, Sc. 2 the subject knows that the interferer avoids to the right, Sc. 3 the interferer disturbs the subject and in Sc. 4 the subject is supposed to predict the interferer path without prior knowledge. Each scenario provides particularities for the data comparison: Sc. 1 provides simply straight trajectories, Sc. 2 and Sc. 4 should be very similar and Sc. 3 is a very specific avoidance movement. All four conditions are considered in the following, in order to be able to compare them and test the performance of the proposed methods. The pivot method, however, is not specifically evaluated here, since all necessary results are provided in Sec. 2.2 already. Therefore, the following discusses the

reliability and advantages of the methodologies and whether they offer similar performance.

4.5.1 Spline based Analysis Framework

The results for the four scenarios using the PTPRS based analysis framework are shown in the following. Each figure illustrates the paths and a respective CI for the subject and the interferer. In Fig. 4.4 on the left the CI for data from Sc. 1 is shown, where no interferer is present. On the right of Fig. 4.4 the CIs for subject and intruder data from Sc. 2 are illustrated. Figure 4.5 refers to the Sc. 3 and Sc. 4.

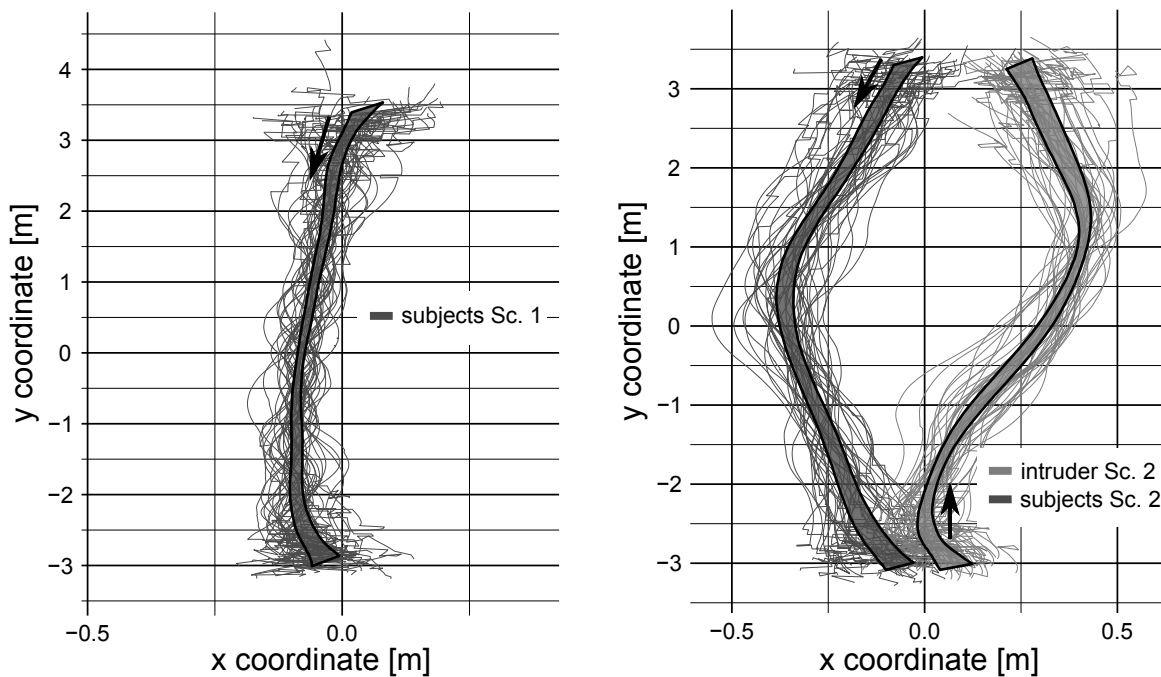


Fig. 4.4: CIs from the PTPRS framework for Sc. 1 and Sc. 2

These CIs only illustrate the processed data whereas the width of the CIs resembles the variance. Clearly, narrow CIs indicate low variance which allows for the conclusion that the subjects behave very similar. The qualitative comparison of the subject data from these scenarios is possible by overlaying different CIs. Within the mentioned experiment of Sec. 2.2 the important fact is that Sc. 2 and Sc. 4 have very similar paths while Sc.3 shows the swerve to the left (from subject view) due to a surprising behavior of the interferer. Therefore, the left side of Fig. 4.6 shows the comparison of the CIs from subjects in Sc. 2 and Sc. 4. It is visible that the CIs are very similar and overlap in large parts. Thus, as a qualitative evaluation the two scenarios seem to produce similar paths. The opposite is observable for Sc. 2 and Sc. 3. Behaviors of the subjects are clearly different with respect to the paths. The CIs shown in Fig. 4.6 on the right, allow for this statement. In order to support the qualitative evaluation with CIs, the method described in 4.4.2.2 is applied. The results are not repeated here, but are to be found in Tab. 2.5 in 2.2.4.1 of Sec. 2.2. For the comparison of Sc. 2 and Sc. 4 the mean distances for Hausdorff and DTW are 0.173 and 0.084 respectively while the combination of Sc. 2 and Sc. 3 produce 0.375 and 0.166. The considerably higher distances are also represented within the significance test.

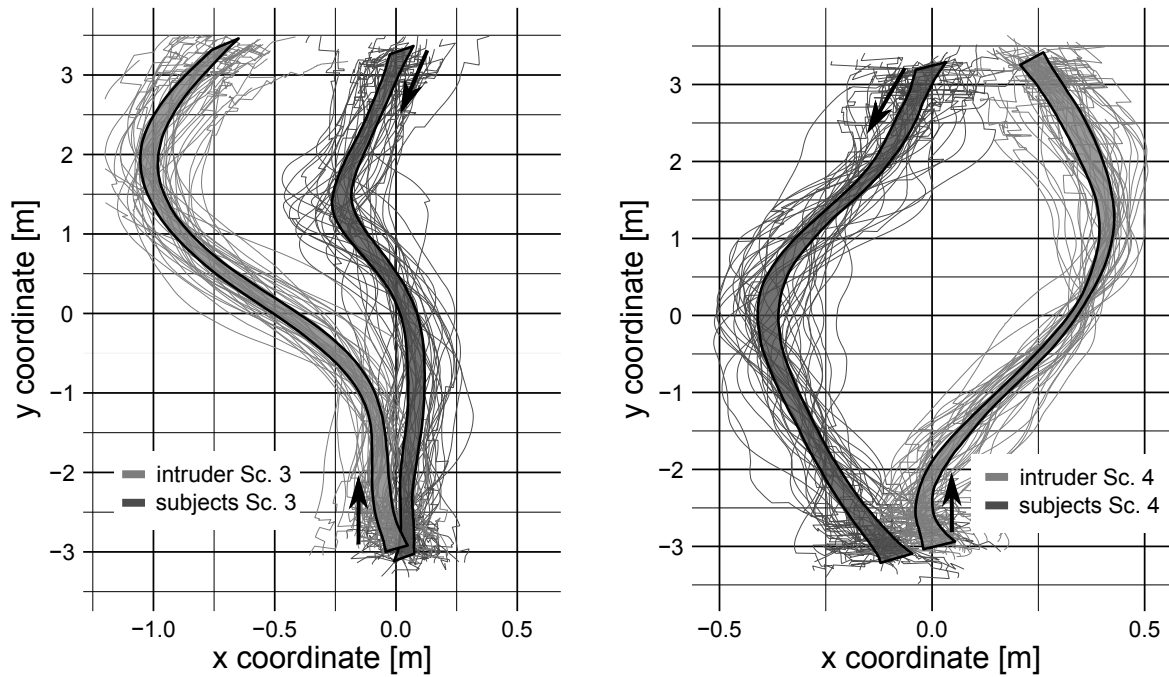


Fig. 4.5: Cls from the PTPRS framework for Sc. 3 and Sc. 4

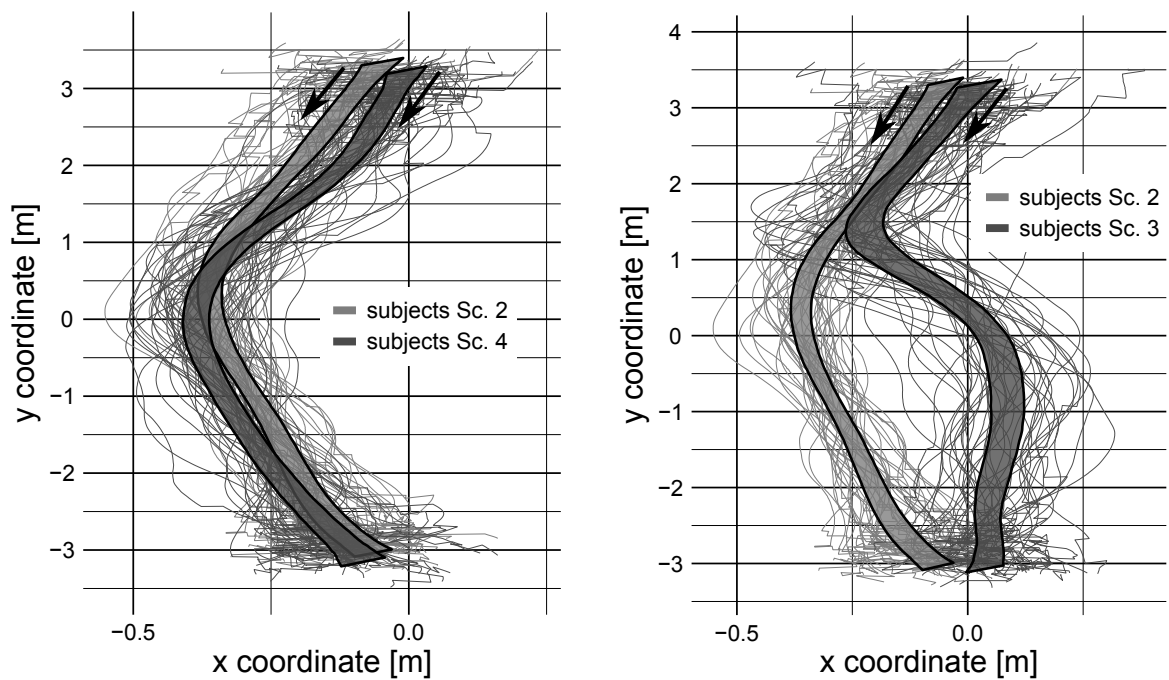


Fig. 4.6: Cls from the PTPRS framework for the comparison of subject data from Sc. 2 and Sc. 3 as well as Sc. 2 and Sc. 4

For both combinations and both distance measures, the pivot of Sc. 1 does not lead to a rejection of the null hypothesis (trajectories are similar in both scenarios). The comparison of Sc. 2 and Sc. 4 via pivot Sc. 3, however, leads to significant differences. For Sc. 2 and Sc. 3 the pivot of Sc. 4 also results in the rejection of the null hypothesis. The important difference, however, is the value of the d_c . For Sc. 2 and Sc. 4 with pivot Sc. 3 the d_c is

in the range of 0.28 which is very low. This means that there is a difference between both scenarios but it is not very strong. When looking at the d_c for Sc. 2 and Sc. 3 with pivot Sc. 4, it reaches a value of over 1.5. This actually indicates that the difference is very high. Therefore, this quantitative analysis supports the qualitative CI evaluation and allows for the conclusion that Sc. 2 and Sc. 4 are quite similar, whereas Sc. 2 and Sc. 3 resemble very different locomotion behaviors.

4.5.2 Gaussian Process based Method

The regression results for the Gaussian process on each scenario are shown next. Simulation results are acquired from the GPML framework in MATLAB[®] [145]. Each figure depicts the path data of the subjects in black, the mean of the GP in red and the confidence interval as a dark gray area. Figures 4.7 and 4.8 show the results for Sc. 1, Sc. 2, Sc. 3 and Sc. 4 respectively.

For the comparison of different scenarios the confidence intervals are to be overlaid. This allows for a qualitative analysis similar to the CIs. Figure 4.9 illustrates the comparison of Sc. 2 and Sc. 4. The result is equal to the CIs meaning that both scenarios are very similar. Comparing Sc. 2 and Sc. 3 also yields the same result as the PTPRS based CIs.

In order to further evaluate the viability of the GP approach, the quantitative method using KLD is examined. Therefore, the GPs for every scenario are compared to each other. Tab. 4.1 displays the resulting values. The KLD distance values confirm the previous results as the value is significantly lower for the comparison of Sc. 2 and Sc. 4 than for all other combinations. Thus, the GPs are capable of supporting a qualitative and a quantitative comparison method for arbitrary trajectory sets.

Tab. 4.1: Values from Kulback-Leibler distance between GPs of Sc. 1 to Sc. 4

Scenario pair	KLD
1-1	0.0000
1-2	15666
1-3	7062
1-4	15098
2-2	0.0000
2-3	30355
2-4	877
3-3	0.0000
3-4	32846
4-4	0.0000

4.5.3 Autoregressive Moving-Average Model based Method

For implementation and simulation of the presented ARMAX models, the “System Identification Toolbox” from MATLAB[®] is used. This toolbox offers an ARMAX fitting algorithm as well as a comparison tool to identify how well a system approximates the

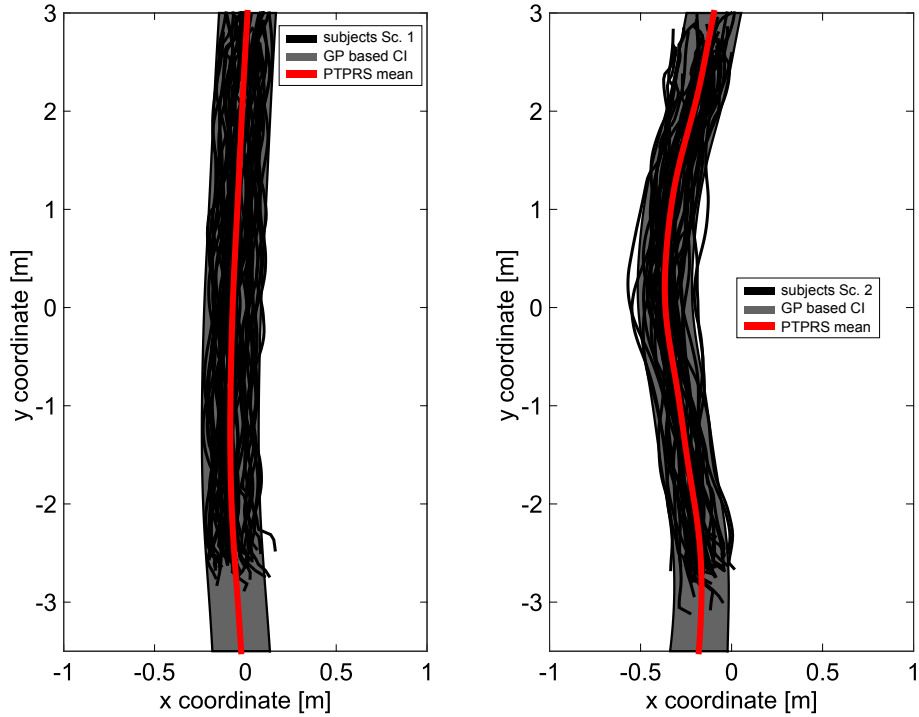


Fig. 4.7: GP for Sc. 1 and Sc. 2

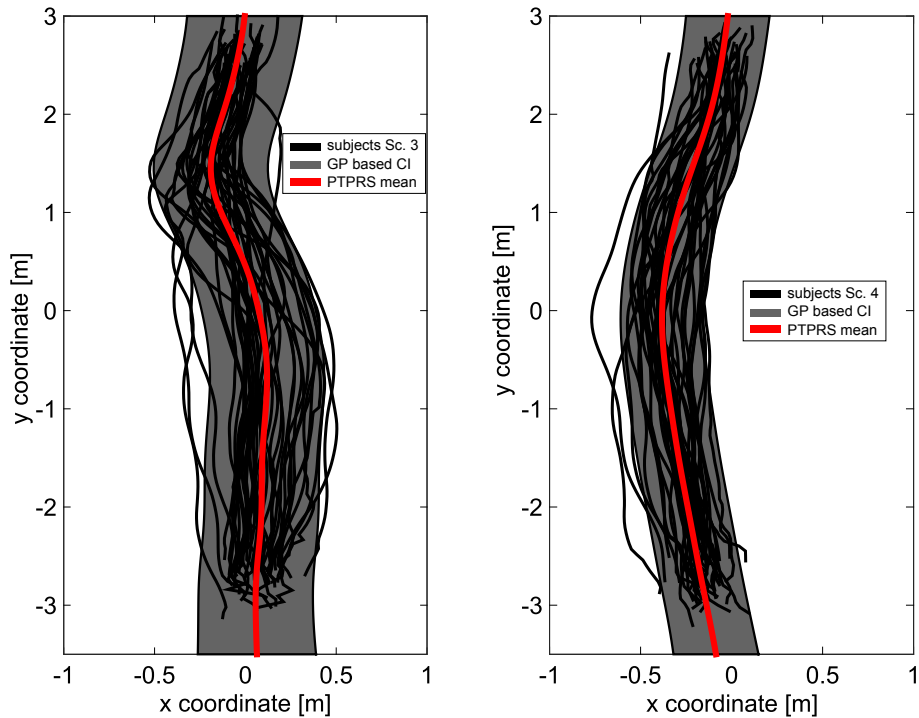


Fig. 4.8: GPs for Sc. 3 and Sc. 4

provided data. ARMAX models are not able to fit multiple trajectories with a single model like a regression method. Rather, one model is obtained per trajectory. Therefore, the method from 4.4.2.1 is applied to the data of each scenario, in order to supply the ARMAX method with a representative model of the recorded data. The Figures 4.10 and

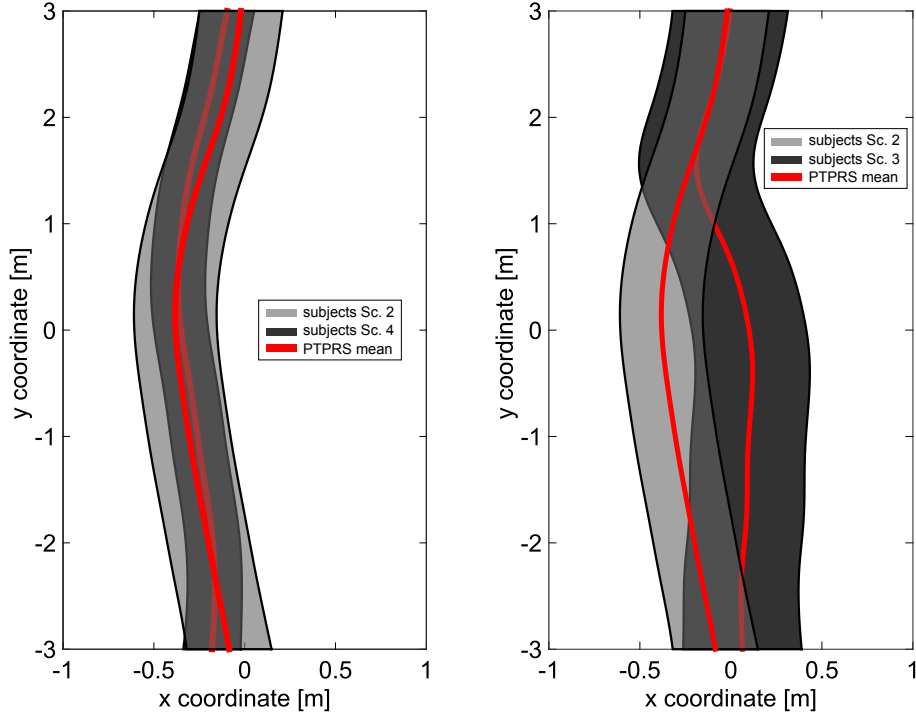


Fig. 4.9: GPs for the comparison of Sc. 2 and Sc. 4 as well as Sc. 2 and Sc. 3

4.11 illustrate the used models with the PTPRS mean in red and the used data in black. An ARMAX model is fit iteratively to the PTPRS representation for each scenario, in order to estimate an optimal set of parameters $[n_a, n_b, n_c, n_k]$. The four resulting sets are $[25, 22, 1, 3]$, $[22, 4, 2, 2]$, $[24, 5, 6, 2]$ and $[23, 10, 4, 2]$, which lead to the following system representations for the four evaluated scenarios:

$$\begin{aligned}
 \text{Sc. 1: } \mathbf{q}_{\text{arma}}(k) + a_1 \mathbf{q}_{\text{arma}}(k-1) + \dots + a_{25} \mathbf{q}_{\text{arma}}(k-25) &= \\
 b_1 \mathbf{z}_{\text{arma}}(k-3) + \dots + b_{22} \mathbf{z}_{\text{arma}}(k-24) + \epsilon(k) + c_1 \epsilon(k-1) & \\
 \text{Sc. 2: } \mathbf{q}_{\text{arma}}(k) + a_1 \mathbf{q}_{\text{arma}}(k-1) + \dots + a_{22} \mathbf{q}_{\text{arma}}(k-22) &= \\
 b_1 \mathbf{z}_{\text{arma}}(k-2) + \dots + b_4 \mathbf{z}_{\text{arma}}(k-5) + \epsilon(k) + c_1 \epsilon(k-1) + \dots c_2 \epsilon(k-2) & \\
 \text{Sc. 3: } \mathbf{q}_{\text{arma}}(k) + a_1 \mathbf{q}_{\text{arma}}(k-1) + \dots + a_{24} \mathbf{q}_{\text{arma}}(k-24) &= \\
 b_1 \mathbf{z}_{\text{arma}}(k-2) + \dots + b_5 \mathbf{z}_{\text{arma}}(k-6) + \epsilon(k) + c_1 \epsilon(k-1) + \dots c_6 \epsilon(k-6) & \\
 \text{Sc. 4: } \mathbf{q}_{\text{arma}}(k) + a_1 \mathbf{q}_{\text{arma}}(k-1) + \dots + a_{23} \mathbf{q}_{\text{arma}}(k-23) &= \\
 b_1 \mathbf{z}_{\text{arma}}(k-2) + \dots + b_{10} \mathbf{z}_{\text{arma}}(k-11) + \epsilon(k) + c_1 \epsilon(k-1) + \dots c_4 \epsilon(k-4) &
 \end{aligned}$$

Results for the fitting of the models to the used PTPRS data are shown in Figures 4.12, 4.13, 4.14 and 4.15. With the optimized parameters, the fitting accuracy is very high, but the models will not generalize very well anymore. Using the comparison methodology for ARMAX models provided by MATLAB[®], the ability of an acquired system to predict the progression of provided data is tested. With the optimized fit to the data, an acquired model will only be able to fit very similar data at a high accuracy. This idea is applied to compare the different scenarios of the experiment. As the hypothesis is that Sc. 2 and

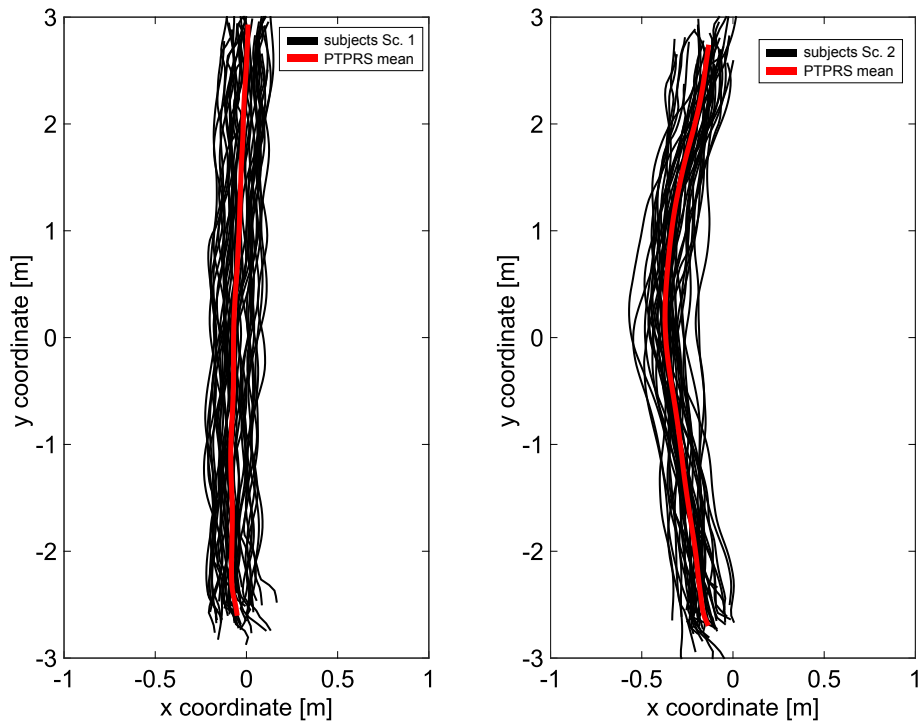


Fig. 4.10: Data for Sc. 1 and Sc. 2 in black with the PTPRS model in red

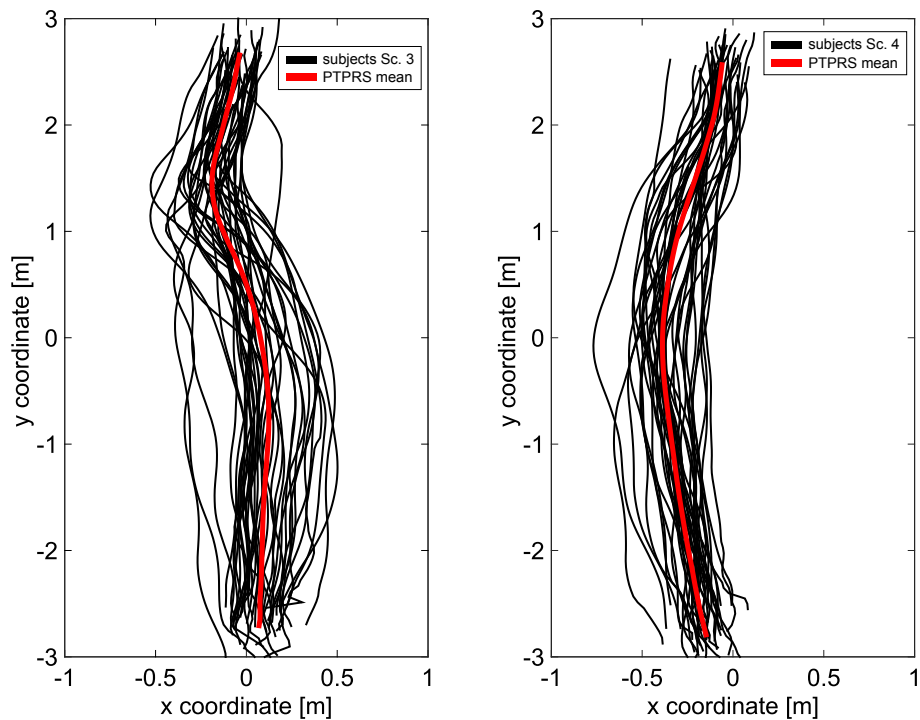


Fig. 4.11: Data for Sc. 3 and Sc. 4 in black with the PTPRS model in red

Sc. 4 are very similar, it is expected that applying the system of Sc. 4 to the data of Sc. 2 and vice versa leads to a good fit. The Figures 4.16, 4.17, 4.18 and 4.19 show the fitting combinations of Sc. 2 and Sc. 4 as well as Sc. 2 and Sc. 3.

Clearly, the fitting of the Sc. 2 and Sc. 4 PTPRS data with the ARMAX system of the

respectively other scenario, confirms the hypothesis and matches the results from the CIs and GPs. The fitting accuracies of over 89% prove the similarity of the data, given that the ARMAX systems do not generalize well. This is visible in the combination of Sc. 2 and Sc. 3. The accuracy is very low and the resulting reconstruction is far off the provided PTPRS data.

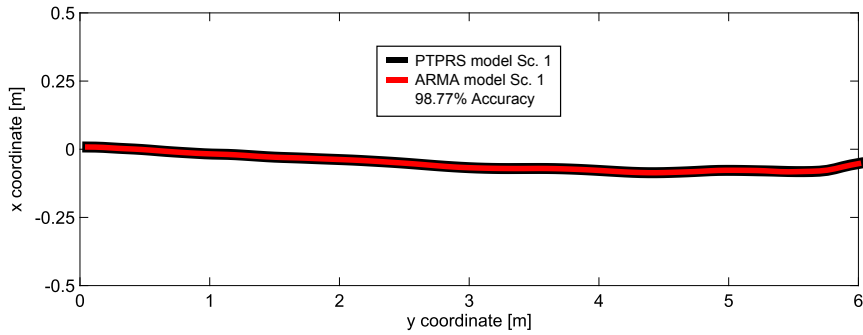


Fig. 4.12: ARMAX fit to PTPRS data for Sc. 1

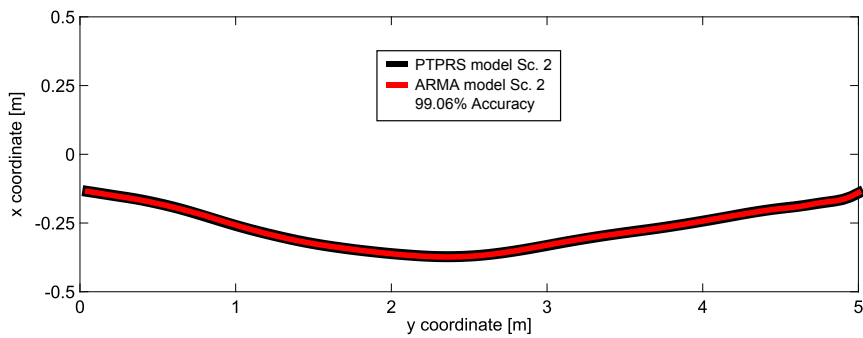


Fig. 4.13: ARMAX fit to PTPRS data for Sc. 2

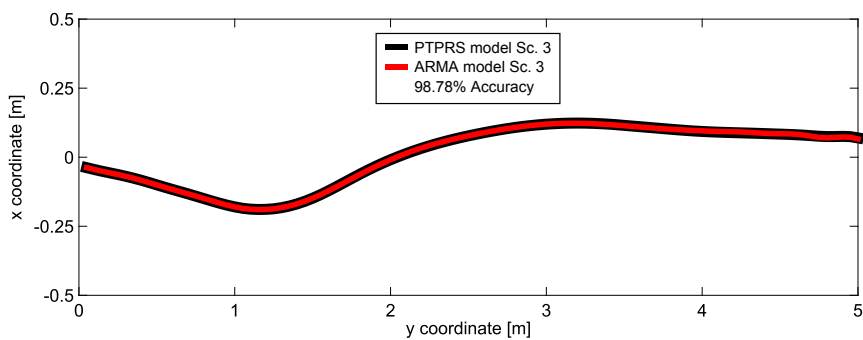


Fig. 4.14: ARMAX fit to PTPRS data for Sc. 3

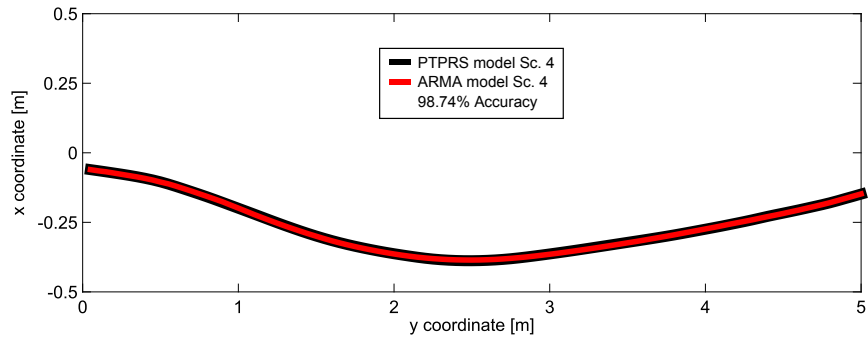


Fig. 4.15: ARMAX fit to PTPRS data for Sc. 4

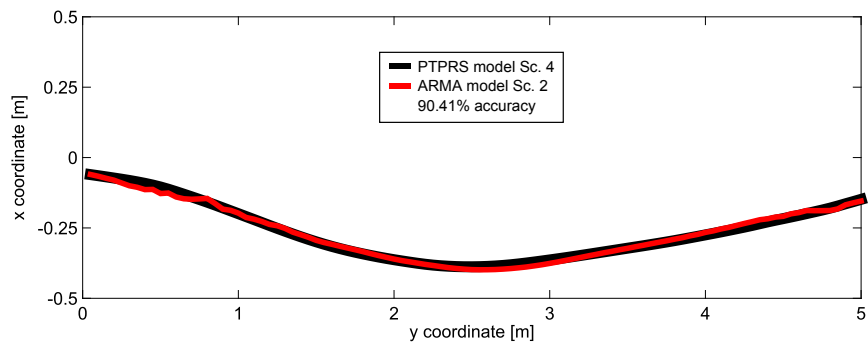


Fig. 4.16: ARMAX model of Sc. 2 applied to PTPRS data for Sc. 4

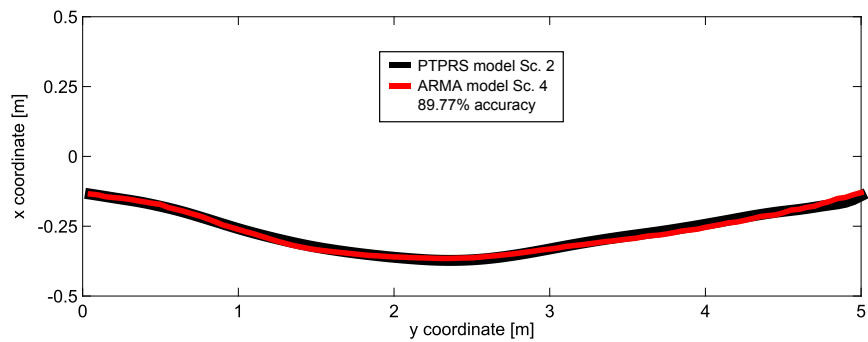


Fig. 4.17: ARMAX model of Sc. 4 applied to PTPRS data for Sc. 2

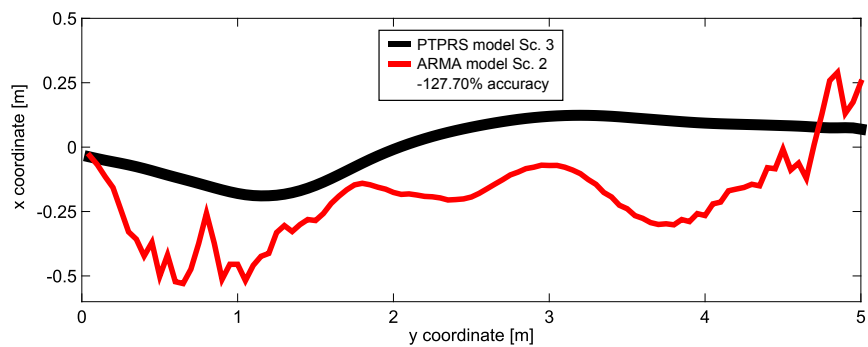


Fig. 4.18: ARMAX model of Sc. 2 applied to PTPRS data for Sc. 3

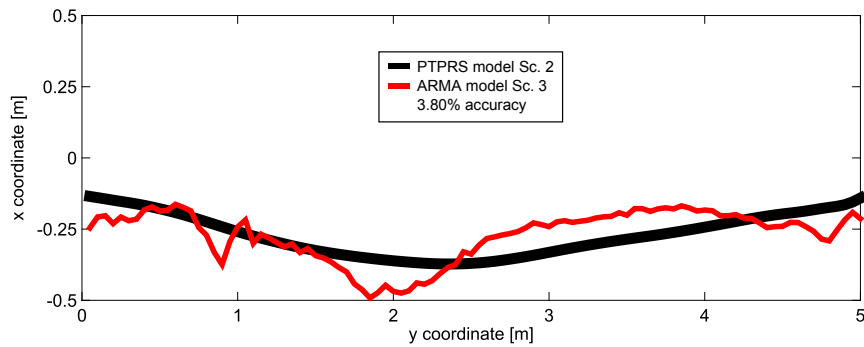


Fig. 4.19: ARMAX model of Sc. 3 applied to PTPRS data for Sc. 2

4.6 Discussion

This chapter presents three methods for the qualitative and quantitative comparison of human trajectory data. All methods meet the requirement to provide a measure for differences or similarities within trajectory data. The methods are also capable of comparing sets of trajectories with respect to similarity. Hence, the goal is to discuss whether a statistics based methodology is advantageous in comparison to established Machine Learning or System Identification approaches. The evaluation of trajectory data from an experiment shown in Sec. 2.2, leads to the same conclusion with every applied method. Thus, the applicability of the methods is clarified. The proposed methods each provide qualitative and quantitative results as well. Therefore, specific problems must be discussed.

Analysis methods based on statistical methods are subject to two distinct disadvantages. Firstly, the procedures require data with specific properties. Although a generalization is possible, the application to variants of the initial data requires adaptations in the methods. Secondly, the data is only analyzed with respect to underlying behaviors. A synthesis, i.e. to generate a trajectory for a robot, is not supported. Additionally, classification of new data is only possible if the framework is extended accordingly.

GPs thereby yield a very well elaborated framework and a transparent measure with the KLD. GPs generalize and scale to arbitrary data, while prediction as well as classification are provided. In this respect, the qualitative evaluation is equal to the PTPRS based CIs in its reliability. However, the disadvantage of the proposed approach is found within the quantitative comparison. The KLD yields an arbitrary value that only gains expressiveness when compared to other conditions that must be different. Unless further developed, the result is not statistically validated and as such more like a qualitative measure. The KLD itself does not allow for a statement whether an effect or a difference is significant. In contrast, the values of the pivot analysis depend on dedicated distance measures that form a distribution of differences which are then compared with statistically reliable methods.

ARMAX models are subject to similar disadvantages. They are applicable to the problem of trajectory analysis and comparison, although the modeling falls short of the ability for directly supporting a regression to the whole data-set. ARMAX models offer the opportunity to synthesize trajectories and to analyze control theoretic attributes like stability. Yet, the results do not provide any statistical assessment. Similar to the GP method, the ARMAX results are useful but not reliable in comparison to a statistical method.

The applications presented in this thesis, however, requires the statistical soundness, such that results for CIs and pivot analysis are preferred. The main advantage of the CI and pivot method is the statistical reliability. Quantitative results from GPs and ARMAX comparisons yield similar assessments but proving that an observation generalizes to the majority of subjects requires statistical examination.

4.7 Summary

In this chapter, the problem of trajectory analysis for human locomotion data is discussed. A literature review reveals that the state-of-the-art does not strictly focus on this problem and thus no generalizable and statistically feasible methods are available. The problem of data recording and processing is elaborated and methods based on penalized thin-plate splines are provided for smoothing and pre-processing. Based on that, the calculation of confidence intervals is presented that allow for qualitative evaluations under consideration of the variance in the trajectory data. For quantitative analysis a method using Hausdorff distance and Dynamic Time Warping is proposed. Both methods are applied successfully for the evaluation of trajectory data in a previously described experiment. In order to elaborate the reliability of the presented framework, a comparison with adapted state-of-the-art methods is provided. Gaussian process regression and Autoregressive Moving-Average models with exogenous inputs are applied to the same trajectory sets. The comparison of the different approaches reveals similar performance. Yet, the requirement of statistical feasibility within experimental evaluations favors the proposed methods over the Gaussian processes and the Autoregressive Moving-Average models.

4.8 Conclusions

This chapter introduces the advantages of spline smoothing over common low-pass filtering used in human motion data processing. The applied approach of penalized thin-plate regression splines outperforms the arithmetic mean or median of a trajectory, considering outliers and noise. Spline fitting combined with bootstrapping further allows for generating confidence intervals over small data-sets. The confidence intervals are a tool that permits statistically reasonable statements when comparing trajectory sets qualitatively as variance in the data is specifically considered. This chapter further proposes a method for quantitative trajectory data analysis. The developed pivot-method allows for a quantitative comparison of trajectory data and evaluates similarities or differences of observed behaviors. A combination of both methods yields statistically feasible statements about the reliability of the observed behaviors in human locomotion data. This framework also scales to data of higher dimensionality and generalizes to arbitrary trajectory data. The analysis shown here, however, is adapted to some specifications of the experimental setup such that generalization demands further elaboration.

The results shown in Chap. 2 are used to discuss the advantages of the proposed framework in comparison to an adaptation of Gaussian processes and Autoregressive Moving-Average models. Specific conditions in the respective experiment are compared to identify

particularities in human locomotion planning. It is shown that the proposed framework provides reliable evaluations for the human-human avoidance experiment. The framework reveals that humans react very similar within two specific conditions. Both alternative approaches provide a similar analysis for the trajectory data and also offer additional opportunities like classification and prediction. Yet, statistical feasibility is only provided by the proposed framework. Therefore, the approach based on penalized thin-plate splines must be preferred for its statistical soundness.

The analysis of recorded sets of trajectories will play a critical role in future research on human and robot locomotion. Affordable systems for full-body tracking should encourage researchers to unveil the particularities of human locomotion behaviors and enable them to provide new models for human aware or human-like robot control. Analyzing human trajectories will become an important prerequisite for future modeling approaches, especially since human-like behaviors will find increasing interest when robots should seamlessly integrate into human populated environments.

5 Summary

This thesis investigates the integration of socio-contextual aspects and human-like behaviors in mobile robot trajectory planning and human locomotion prediction. The effectiveness of these aspects is analyzed with respect to cooperative locomotion in environments shared by humans and robots. Optimal control and model predictive control frameworks are adopted from literature and adjusted to consider mentioned aspects. Subject studies and simulations show the advantages and gained benefits when robots incorporate social norms and human behaviors in their trajectory planning and prediction methods. In order to evaluate the generated trajectories and the behavior of subjects that are confronted with the moving robot, a framework is developed for qualitative and quantitative comparison of trajectory sets.

The first chapter after the introduction is dedicated to the incorporation of social context and human-like motion features within robot locomotion. This aims at the enhancement of clear intention conveyance and an increased social acceptance of the robot. The shown benefits are a more successful interaction initiation on a nonverbal level and a lower effort for cooperative navigation.

Within the first section, focus is set on the problem of robot-to-human approach with an autonomous mobile robot for verbal or physical interaction. Optimal control models are used to generate robot-to-human approach trajectories. Within this framework, socio-contextual constraints are designed that enhance the readability of planned trajectories and increase the social acceptance of the moving robot. Both aspects of the robot locomotion are further improved by applying human-like locomotion features. This step strongly enhances the ability of the robot to initiate interaction nonverbally with humans. Multiple trajectory planners are compared based on human apperception in order to show the effect of the mentioned constraints. In particular, the influence of path shape, path smoothness and torso orientation of the robot during locomotion are evaluated. It is shown that these basic trajectory features contribute largely to the nonverbal interaction initiation capability of a robot and to its social acceptance.

Despite the importance of apperception, the idea of social compliance and human-like locomotion is still questioned in the robotics community. The second section therefore analyzes the effectiveness of human-like robot locomotion within cooperative navigation in a shared environment. It shows the capability of readable locomotion to support predictions and to reduce the planning effort for nearby agents. A definition of effort for locomotion planning is developed based on a model predictive control modeling of human locomotion. The reduction of this effort due to readable locomotion among interacting agents is demonstrated in a human-human experiment and further transferred to a human-robot experiment. The evaluation of both studies confirms that humans assess the intentions of another human or a robot in a similar way. Therefore, human-like robot locomotion allows other agents to quickly understand the robot intention and benefits the seamless

and effortless cooperative navigation.

Since cooperative navigation in a social context requires a robot to integrate the movement of human agents in his planning, human locomotion prediction becomes a crucial task. Chapter three is thus concerned with this problem and aims to investigate human behaviors that are capable of improving predictions when being accounted for. Optimal control and model predictive control methods are focused on, due to their ability to generate accurate trajectories.

In the first section of chapter three it is derived from literature that recent optimal control based prediction methods do not generalize to certain avoidance behaviors that are observed in many human locomotion studies. Hence, a behavioral factor is to be determined that leads to the observed behavior. In particular, the hypothesis is investigated whether humans reduce their planning horizon when collision situations are resolved within uncertain environments. The influence of the planning horizon is demonstrated within simulations of a non-linear model predictive control based framework for human locomotion prediction. Following these results, a subject study is designed that observes human behavior during avoidance in a goal oriented motion task. From the measured gaze and trajectory data a diminishing visual look-ahead and a reduced smoothness of motions is identified which is related to the faced complexity of an environment. These results support the hypothesis that humans adapt their planning horizon to handle the uncertainty in complex environments during avoidance motions.

The second part of chapter three is concerned with the modeling of the velocity profiles for human locomotion prediction. This problem is considered in related work, but a distinct model for the sinusoidal shape of human velocities is not proposed. The aspect is circumvented by smoothing recorded velocities which adapts the data to the used models. Thus, an alternative model to the common unicycle model is proposed, that reproduces the sinusoidal shape of human velocity profiles. The new dynamic model is derived from the kinematics of a rolling ellipse and integrated in an optimal control framework. Simulations indicate the applicability of the model to human locomotion trajectory synthesis, as the resulting velocity profiles show the typical sinusoidal shape of real human trajectory data.

In the fourth chapter, the problem of trajectory analysis for human locomotion data is considered. The state-of-the-art does not provide a generalizable and statistically feasible method for evaluating trajectories and comparing sets from different experimental conditions. Accordingly, data recording and processing is elaborated in this chapter and methods based on penalized thin-plate splines are proposed for smoothing, pre-processing and comparison. The proposed methods for qualitative and quantitative analysis are successfully applied within the thesis. The reliability of the presented evaluation framework is shown by comparison to adapted state-of-the-art methods. Gaussian process regression and Autoregressive Moving-Average models with exogenous inputs are applied to the same trajectory sets and advantages as well as disadvantages are discussed.

6 Conclusions

From the results of this thesis it is concluded that socio-contextual aspects and human-like behaviors can highly contribute to the social acceptance of mobile robot locomotion and the efficiency of cooperative human-robot locomotion in shared environments. The clearly comprehensible intention of the robot facilitates the predictions of other agents, which enables the robot to successfully initiate interactions nonverbally and reduces the effort required by both parties for planning a collision free path. Secondly, the understanding of behaviors that humans employ during locomotion, allows for more accurate predictions in distinct situations. Findings in this area lead to novel or improved prediction models, that are applicable within future methods. These implications are elaborated in the following paragraph with respect to the presented thesis.

The first section of chapter two shows, that human-like robot locomotion in combination with socio-contextual constraints, improves the readability and the nonverbal interaction initiation ability of a mobile robot. This is based on the fact that the readable and socially acceptable robot locomotion complies with human expectations towards the robot intention. Accordingly, human-likeness of trajectories must be considered as a crucial aspect within future planning algorithms. Especially formative features like path shape, path smoothness and torso orientation must be considered. Applications that require seamless navigation in shared environments will benefit from these results. The integrated planning algorithm presented in this thesis enables a mobile robot to approach a moving person autonomously in a dynamic environment. Thereby, optimal control is applied to model socio-contextual constraints as well as formative features of human-like locomotion. The proposed method is compared to models that specifically address trajectory planning for humanoids. Results show that trajectories with human-like features perform equally well compared to human trajectories in terms of perceived naturalness, comfort and intention conveyance capability. This validates the assumption that path shape, path smoothness and robot orientation along the path have significant influence on readability when approaching static or moving persons.

The effectiveness of readable robot locomotion, beyond the positive perception from human agents, is shown in the second section of chapter two. Experimental results demonstrate how readability affects the locomotion planning of other agents within the same environment. The conducted mutual avoidance experiments compare various scenarios where subjects have either full or partial knowledge about the behavior of their counterpart. It is shown that extra effort to handle the uncertain case is easily overcome when the human or robot counterpart employ readable locomotion. Accordingly, the opposite effect is observed when the counterpart performs an unexpected movement. Since readable robot locomotion allows humans to quickly understand its intentions, they are able to incorporate a reliable prediction into their own planning. This leads to smooth trajectories for all agents and complies with the human desire for minimum effort. Based on the proposed definition

of effort, it is concluded that readability benefits the reduction of planning effort and the seamless integration of robots into human populated environments.

These results are generalizable to trajectories of higher dimensionality as well as a variety of applications and platforms. Clearly, distinctive features of human-like motions differ depending on the task. For the presented methods, locomotion in populated urban or industrial environments and collaborative navigation with humans are imaginable application scenarios. The benefit will be a decrease in disturbances between all agents within the environment, due to mutual influence from nonverbal interaction initiation. This is a capability gained only by robots that move readably and externalize their intention.

The applicability of human locomotion behaviors within prediction methods is taken into account in chapter three. Simulations of optimal control and model predictive control models are used to demonstrate the capabilities of these approaches. In this respect, the motion planning horizon of humans is investigated experimentally within the first section. This aspect is considered to be potentially capable of improving human locomotion prediction methods. The designed experiment requires subjects to perform a goal directed motion in a virtual environment, while avoiding collisions with moving obstacles. Results show that subjects apply different avoidance strategies when the complexity of the environment changes. Subjects plan an optimal path and perform smooth and continuous trajectories if they are able to predict each obstacle. An evaluation of the mean distance between the marker and the gaze position indicates that looking-ahead diminishes with rising scenario complexity. Furthermore, subjects deviate more from a given optimal solution if the environment is more complex. These results pose a strong indicator that the adaptation of the planning horizon is one distinct behavior of humans. This holds under the assumption that the length of the planning horizon is a determinant for gaze fixation and trajectory smoothness.

The second part of chapter three is dedicated to the modeling of human-like velocity profiles. With the proposed dynamic model the sinusoidal shape of human velocity profiles is reconstructed successfully. Integration into an optimal control framework and parametrization using inverse optimal control results in human-like trajectories with sinusoidal velocity profiles. However, the simulations expose the sensitivity of the model and its parametrization as a problem. Acceptable performance is only reached after a heuristic tuning of the parameters. The model poses an important step towards solving the velocity modeling problem that is reported within related literature. Thus, further elaboration of the model within an optimal control framework will be necessary.

These results regarding human locomotion prediction reveal a wide range of necessary improvements to optimal control or model predictive control based approaches. The inclusion of human behaviors thereby poses one aspect that is able to provide higher accuracy. More complex dynamic models are a necessary step to precisely reproduce human trajectories. However, prediction in situations with disturbances or other particular circumstances still constitute a main source of errors.

The fourth chapter comprises the developed methods for trajectory processing and evaluation that are applied within mentioned studies. Spline based smoothing provides better performance compared to common low-pass filtering in human motion data processing. Penalized thin-plate regression splines further outperform the calculation of the arithmetic

mean or median for a trajectory, with respect to outliers and noise. Based on that, confidence intervals are calculated for small data-sets using bootstrapping. The confidence intervals provide a statistically reasonable evaluation tool for comparing trajectory sets qualitatively, because variance of the data is taken into account. Furthermore, a method for the quantitative comparison of trajectory sets is proposed. Similarities and differences are identified reliably with this framework, while statistical feasibility is maintained. This framework scales to data of higher dimensionality and is generalizable to arbitrary trajectory data. A comparison to an adaptation of Gaussian processes and Autoregressive Moving-Average models reveals the advantages of the proposed framework. Both alternatives are good measures for the analysis of trajectory data. Yet, statistical feasibility is only provided in the proposed framework.

With respect to recent developments in human motion tracking and the elaborated importance of human-likeness for robots, processing motion data will remain a critical topic. Accurate models of human motion and locomotion already play an important role within many applications, as it is shown in this thesis. Further research towards generalizable and reliable methods for trajectory analysis will thus benefit future methodologies.

Overall this work presents the benefits of incorporating human-like behaviors and social context in robot locomotion and in prediction methods. Conveying intentions in nonverbal interaction and complying with expectations by considering social context allows robots to seamlessly integrate in human environments. In addition, observing these aspects of human behavior will allow robots to enhance their locomotion prediction accuracy. The advantages of these reciprocal effects are thereby only utilized by robots that incorporate readability and social acceptance within their locomotion planning and prediction.

Bibliography

Own Publications

- [1] D. Carton, W. Olszowy, D. Wollherr, and M. Buss, “Socio-Contextual Constraints for Human Approach with a Mobile Robot,” *Int. J. of Social Robotics*, 2017, submitted for 3rd revision.
- [2] D. Carton, V. Nitsch, D. Meinzer, and D. Wollherr, “Towards Assessing the Human Trajectory Planning Horizon,” *PLOS ONE*, vol. 11, no. 12, pp. 1–39, 2016.
- [3] D. Carton, W. Olszowy, and D. Wollherr, “Measuring the Effectiveness of Readability for Mobile Robot Locomotion,” *Int. J. of Social Robotics*, vol. 8, no. 5, pp. 721–741, 2016.
- [4] M. Buss, D. Carton, S. Khan, B. Kühnlenz, K. Kühnlenz, R. de Nijs, A. Turnwald, and D. Wollherr, “IURO – Soziale Mensch-Roboter-Interaktion in den Straßen von München,” *at – Automatisierungstechnik*, 2015.
- [5] D. Carton, A. Turnwald, W. Olszowy, M. Buss, and D. Wollherr, “Using Penalized Spline Regression to calculate Mean Trajectories including Confidence Intervals of Human Motion Data,” in *Workshop on Advanced Robotics and its Social Impacts*, pp. 76–81, 2014.
- [6] M. Van den Bergh, D. Carton, and L. Van Gool, “Depth SEEDS: Recovering Incomplete Depth Data using Superpixels,” in *Workshop on Applications of Computer Vision*, pp. 363–368, 2013.
- [7] D. Carton, A. Turnwald, D. Wollherr, and M. Buss, “Proactively Approaching Pedestrians with an Autonomous Mobile Robot in Urban Environments,” in *Int. Symp. on Experimental Robotics*, pp. 199–214, Springer, 2012.
- [8] D. Carton, A. Turnwald, K. Kühnlenz, D. Wollherr, and M. Buss, “Proactive Human Approach in Dynamic Environments (Video),” in *Int. Conf. on Intelligent Robots and Systems*, pp. 3320–3321, 2012.
- [9] M. Buss, D. Carton, B. Gonsior, K. Kühnlenz, C. Landsiedel, N. Mitsou, R. de Nijs, J. Zlotowski, S. Sosnowski, E. Strasser, *et al.*, “Towards Proactive Human-Robot Interaction in Human Environments,” in *Int. Conf. on Cognitive Infocommunications*, pp. 1–6, 2011.
- [10] M. Van den Bergh, D. Carton, R. de Nijs, N. Mitsou, C. Landsiedel, K. Kühnlenz, D. Wollherr, L. Van Gool, and M. Buss, “Real-time 3D Hand Gesture Interaction with a Robot for Understanding Directions from Humans,” in *Int. Symp. on Robot and Human Interactive Communication*, pp. 357–362, 2011.

-
- [11] U. Klank, D. Carton, and M. Beetz, “Transparent Object Detection and Reconstruction on a Mobile Platform,” in *Int. Conf. on Robotics and Automation*, pp. 5971–5978, 2011.

Cited Publications

- [12] B. Houska, H. J. Ferreau, and M. Diehl, “ACADO Toolkit – An open-source framework for automatic control and dynamic optimization,” *Optimal Control Applications and Methods*, pp. 298–312, 2011.
- [13] M. Ahmadi-Pajouh, F. Towhidkhah, S. Gharibzadeh, and M. Mashhadimalek, “Path Planning in the Hippocampo-Prefrontal Cortex Pathway: An Adaptive Model based Receding Horizon Planner,” *Medical Hypotheses*, vol. 68, no. 6, pp. 1411–1415, 2007.
- [14] S. Albrecht, P. Basili, S. Glasauer, M. Leibold (Sobotka), and M. Ulbrich, “Modeling and Analysis of Human Navigation with Crossing Interferer Using Inverse Optimal Control,” in *Int. Conf. on Mathematical Modelling*, pp. 158–163, 2012.
- [15] A. Alempijevic, R. Fitch, and N. Kirchner, “Bootstrapping Navigation and Path Planning using Human Positional Traces,” in *Int. Conf. on Robotics and Automation*, pp. 1242–1247, 2013.
- [16] G. Allgöwer, T. Badgwell, J. Qin, J. Rawlings, and S. Wright, “Nonlinear Predictive Control and Moving Horizon Estimation – an Introductory Overview,” in *Advances in Control*, pp. 391–449, Springer, 1999.
- [17] P. Althaus, H. Ishiguro, T. Kanda, T. Miyashita, and H. Christensen, “Navigation for Human-Robot Interaction Tasks,” in *Int. Conf. on Robotics and Automation*, pp. 1894–1900, 2004.
- [18] G. Arechavaleta, J. Laumond, H. Hicheur, and A. Berthoz, “The Nonholonomic Nature of Human Locomotion: A Modeling Study,” in *Int. Conf. on Biomedical Robotics and Biomechatronics*, pp. 158–163, 2006.
- [19] G. Arechavaleta, J.-P. Laumond, H. Hicheur, and A. Berthoz, “An Optimality Principle Governing Human Walking,” *Trans. on Robotics*, vol. 24, no. 1, pp. 5–14, 2008.
- [20] E. Avrunin and R. Simmons, “Using Human Approach Paths to Improve Social Navigation,” in *Int. Conf. on Human-Robot Interaction*, pp. 73–74, 2013.
- [21] L. Bascetta, G. Ferretti, P. Rocco, H. Ardo, H. Bruyninckx, E. Demeester, and E. Di Lello, “Towards safe human-robot interaction in robotic cells: an approach based on visual tracking and intention estimation,” in *Int. Conf. on Intelligent Robots and Systems*, pp. 2971–2978, 2011.
- [22] P. Basili, M. Huber, O. Kourakos, T. Lorenz, T. Brandt, S. Hirche, and S. Glasauer, “Inferring the Goal of an Approaching Agent: A Human-Robot Study,” in *Int. Workshop on Robots and Human Interactive Communications*, pp. 527–532, 2012.

- [23] P. Basili, M. Sağlam, T. Kruse, M. Huber, A. Kirsch, and S. Glasauer, “Strategies of Locomotor Collision Avoidance,” *Gait & posture*, vol. 37, no. 3, pp. 385–390, 2013.
- [24] B. van Basten, S. Jansen, and I. Karamouzas, “Exploiting Motion Capture to Enhance Avoidance Behaviour in Games,” *Motion in Games*, vol. 5884, pp. 29–40, 2009.
- [25] A. Bauer, K. Klasing, G. Lidoris, Q. Mühlbauer, F. Rohrmüller, S. Sosnowski, T. Xu, K. Kühnlenz, D. Wollherr, and M. Buss, “The Autonomous City Explorer: Towards Natural Human-Robot Interaction in Urban Environments,” *Int. J. of Social Robotics*, vol. 1, no. 2, pp. 127–140, 2009.
- [26] J. Van Den Berg, S. Guy, M. Lin, and D. Manocha, “Reciprocal n-body Collision Avoidance,” *Robotics Research*, pp. 3–19, 2011.
- [27] N. Bergström, T. Kanda, T. Miyashita, and N. Ishiguro, H. anad Hagita, “Modeling of Natural Human-Robot Encounters,” in *Int. Conf. on Intelligent Robots and Systems*, pp. 2623–2629, 2008.
- [28] M. Bennewitz, W. Burgard, G. Cielniak, and S. Thrun, “Learning motion patterns of people for compliant robot motion,” *Int. J. of Robotics Research*, vol. 24, no. 1, pp. 31–48, 2005.
- [29] A. Bissacco and S. Soatto, “Hybrid Dynamical Models of Human Motion for the Recognition of Human Gaits,” *Int. J. of Computer Vision*, vol. 85, no. 1, pp. 101–114, 2009.
- [30] S. Bitgood and S. Dukes, “Not another step! Economy of movement and pedestrian choice point behavior in shopping malls,” *Environment and Behavior*, vol. 38, no. 3, pp. 394–405, 2006.
- [31] C. Breazeal, C. Kidd, A. Thomaz, G. Hoffman, and M. Berlin, “Effects of Nonverbal Communication on Efficiency and Robustness in Human-Robot Teamwork,” in *Int. Conf. on Intelligent Robots and Systems*, pp. 708–713, 2005.
- [32] K. Buchin, M. Buchin, M. Van Kreveld, and J. Luo, “Finding long and similar parts of trajectories,” *Computational Geometry*, vol. 44, no. 9, pp. 465–476, 2011.
- [33] K. Buchin, M. Buchin, M. Van Kreveld, M. Löffler, R. Silveira, C. Wenk, and L. Wiratma, “Median Trajectories,” *Algorithmica*, vol. 66, no. 3, pp. 595–614, 2013.
- [34] M. Buss and G. Schmidt, “Control Problems in Multi-Modal Telepresence Systems,” in *Advances in Control* (P. Frank, ed.), pp. 65–101, Springer London, 1999.
- [35] S. Caraian, N. Kirchner, and P. Colborne-Veel, “Moderating a Robot’s Ability to Influence People Through Its Level of Socio-contextual Interactivity,” in *Int. Conf. on Human-Robot Interaction*, pp. 149–156, 2015.
- [36] M. Caplan and M. Goldman, “Personal Space Violations as a Function of Height,” *J. of Psychology*, vol. 114, pp. 167–171, 1981.

-
- [37] C. Cassisi, P. Montalto, and A. Pulvirenti, "Similarity Measures and Dimensionality Reduction Techniques for Time Series Data Mining," in *Advances in Data Mining Knowledge Discovery and Applications*, ch. 3, INTECH, 2012.
- [38] E. Chiovetto, A. Mukovskiy, F. R. Reinhart, S. M. Khansari-Zadeh, A. Billard, J. J. Steil, and M. A. Giese, "Assessment of Human-Likeness and Naturalness of Interceptive Arm Reaching Movement Accomplished by a Humanoid Robot," in *Eur. Conf. on Visual Perception*, 2014.
- [39] Y. Chitour, F. Jean, and P. Mason, "Optimal Control Models of the Goal-oriented Human Locomotion," *J. on Control and Optimization*, vol. 50, no. 1, pp. 147–170, 2012.
- [40] J.-W. Choi, R. Curry, and G. H. Elkaim, "Path Planning Based on Bezier Curve for Autonomous Ground Vehicles," in *Advances in Electrical and Electronics Engineering - IAENG Special Edition of the World Congress on Engineering and Computer Science*, pp. 158–166, 2008.
- [41] J.-W. Choi, R. Curry, and G. H. Elkaim, "Smooth Path Generation Based on Bezier Curves for Autonomous Vehicles," in *Lecture Notes in Engineering and Computer Science: The World Congress on Engineering and Computer Science*, pp. 668–673, 2009.
- [42] J.-W. Choi, R. Curry, and G. H. Elkaim, "Piecewise Bezier Curves Path Planning with Continuous Curvature Constraint for Autonomous Driving," *Machine Learning and Systems Engineering*, pp. 31–45, 2010.
- [43] G. Csibra and G. Gergely, "Obsessed with goals: Functions and mechanisms of teleological interpretation of action in humans," *Acta Psychologica*, vol. 124, no. 1, pp. 60–78, 2007.
- [44] G. E. Cox, G. Kachergis, and R. M. Shiffrin, "Gaussian Process Regression for Trajectory Analysis," in *Annual Conf. of the Cognitive Science Society*, pp. 1440–1445, 2012.
- [45] D. R. Cox and D. V. Hinkley, *Theoretical Statistics*. Chapman & Hall, 1974.
- [46] J. Cohen, *Statistical Power Analysis for the Behavioral Sciences*. Lawrence Erlbaum Associates, Hillsdale, New Jersey, 1988.
- [47] K. Deng, A. Moore, and M. Nechyba, "Learning to recognize time series: Combining ARMA models with memory-based learning," in *Int. Symp. on Computational Intelligence in Robotics and Automation*, pp. 246–251, 1997.
- [48] A. Dragan, K. Lee, and S. Srinivasa, "Legibility and Predictability of Robot Motion," in *Int. Conf. on Human-Robot Interaction*, pp. 301–308, 2013.
- [49] A. Dragan and S. Srinivasa, "Generating Legible Motion," in *Robotics: Science and Systems*, 2013.

- [50] A. Dragan and S. Srinivasa, “Familiarization to Robot Motion,” in *Int. Conf. on Human-Robot Interaction*, pp. 366–373, 2014.
- [51] A. Dragan, S. Bauman, J. Forlizzi, and S. Srinivasa, “Effects of Robot Motion on Human-Robot Collaboration,” in *Int. Conf. on Human-Robot Interaction*, pp. 51–58, 2015.
- [52] B. R. Duffy, “Anthropomorphism and the Social Robot,” *Robotics and Autonomous Systems – Socially Interactive Robots*, vol. 42, no. 3, pp. 177–190, 2003.
- [53] B. Efron and R. Tibshirani, *An Introduction to the Bootstrap*. Chapman & Hall, 1993.
- [54] D. Ellis, E. Sommerlade, and I. Reid, “Modelling Pedestrian Trajectory Patterns with Gaussian Processes,” in *Int. Conf. on Computer Vision*, pp. 1229–1234, 2009.
- [55] A. Elnagar, “Prediction of moving objects in dynamic environments using Kalman filters,” in *Int. Symp. on Computational Intelligence in Robotics and Automation*, pp. 414–419, 2001.
- [56] A. Ess, K. Schindler, B. Leibe, and L. Van Gool, “Object detection and tracking for autonomous navigation in dynamic environments,” *Int. J. of Robotics Research*, vol. 29, no. 14, pp. 1707–1725, 2010.
- [57] L. Fahrmeir, T. Kneib, and S. Lang, *Regression*. Springer, 2009.
- [58] B. Fajen and W. Warren, “Behavioral Dynamics of Intercepting a Moving Target,” *Experimental Brain Research*, vol. 180, pp. 303–319, 2007.
- [59] B. Fajen and W. Warren, “Behavioral dynamics of steering, obstacle avoidance, and route selection,” *Experimental Psychology: Human Perception and Performance*, vol. 29, no. 2, p. 343, 2003.
- [60] G. E. Farin, *Curves and surfaces for CAD: a practical guide*. Morgan Kaufmann Publishers - Academic Press, 5th ed., 2002.
- [61] G. Ferrer and A. Sanfeliu, “Comparative analysis of human motion trajectory prediction using minimum variance curvature,” in *Int. Conf. on Human-Robot Interaction*, pp. 135–136, 2011.
- [62] P. Fink, P. Foo, and W. Warren, “Obstacle avoidance during walking in real and virtual environments,” *Trans. on Applied Perception*, vol. 4, no. 1, p. 2, 2007.
- [63] T. Flash and N. Hogan, “The coordination of arm movements: an experimentally confirmed mathematical model,” *The J. of Neuroscience*, vol. 5, no. 7, pp. 1688–1703, 1985.
- [64] A. Foka and P. Trahanias, “Predictive Autonomous Robot Navigation,” in *Int. Conf. on Intelligent Robots and Systems*, pp. 490 – 495, 2002.

-
- [65] M. Friedman, “The use of ranks to avoid the assumption of normality implicit in the analysis of variance,” *J. of the American Statistical Association*, vol. 32, no. 200, pp. 675–701, 1937.
- [66] U. Frith and C. Frith, “The social brain: allowing humans to boldly go where no other species has been,” *Philosophical Trans. of the Royal Society of London B: Biological Sciences*, vol. 365, no. 1537, pp. 165–176, 2010.
- [67] A. Garrell, M. Villamizar, F. Moreno-Noguer, and A. Sanfeliu, “Proactive Behavior of an Autonomous Mobile Robot for Human-Assisted Learning,” in *Int. Workshop on Robots and Human Interactive Communications*, pp. 107–113, 2013.
- [68] M. J. Gielniak, C. K. Liu, and A. L. Thomaz, “Generating Human-Like Motion for Robots,” *Int. J. of Robotics Research*, vol. 32, no. 11, pp. 1275–1301, 2013.
- [69] P. Glardon, *On-line Locomotion Synthesis for Virtual Humans*. PhD thesis, ECOLE POLYTECHNIQUE FEDERALE DE LAUSANNE, 2006.
- [70] R. Gockley, J. Forlizzi, and R. Simmons, “Natural Person-Following Behavior for Social Robots,” in *Int. Conf. on Human-Robot Interaction*, pp. 17–24, 2007.
- [71] E. Goffman, *Relations in public: Microstudies of the public order*. Harper and Row, New York, 1971.
- [72] C. Goerzen, Z. Kong, and B. Mettler, “A Survey of Motion Planning Algorithms from the Perspective of Autonomous UAV Guidance,” *J. of Intelligent and Robotic Systems*, vol. 57, no. 1-4, pp. 65–100, 2010.
- [73] M. Goodrich and A. Schultz, “Human-Robot Interaction: A Survey,” *Foundations and Trends in Human-Computer Interaction*, vol. 1, no. 3, pp. 203–275, 2007.
- [74] J. Gudmundsson, M. van Kreveld, and B. Speckmann, “Efficient detection of patterns in 2D trajectories of moving points,” *Geoinformatica*, vol. 11, no. 2, pp. 195–215, 2007.
- [75] E. T. Hall, *The Hidden Dimension: Man’s Use of Space in Public and Private*. The Bodley Head Ltd, London, UK, 1966.
- [76] J. Hartnett, K. Bailey, and C. Hartley, “Body height, position, and sex as determinants of personal space,” *J. of Psychology*, vol. 87, pp. 129–136, 1974.
- [77] D. Helbing and P. Molnar, “Social Force Model for Pedestrian Dynamics,” *Physical review E*, vol. 51, no. 5, p. 4282, 1995.
- [78] H. Hicheur, S. Vieilledent, M. Richardson, T. Flash, and A. Berthoz, “Velocity and curvature in human locomotion along complex curved paths: a comparison with hand movements,” *Experimental Brain Research*, vol. 162, no. 2, pp. 145–154, 2005.

- [79] H. Hicheur, Q. Pham, G. Arechavaleta, J. Laumond, and A. Berthoz, “The formation of trajectories during goal-oriented locomotion in humans. I. A. stereotyped behaviour,” *European J. of Neuroscience*, vol. 26, no. 8, pp. 2376–2390, 2007.
- [80] M. Huber, Y.-H. Su, M. Krüger, K. Faschian, S. Glasauer, and J. Hermsdörfer, “Adjustments of speed and path when avoiding collisions with another pedestrian,” *PLoS ONE*, vol. 9, no. 2, 2014.
- [81] P. Holmes, R. Full, D. Koditschek, and J. Guckenheimer, “The dynamics of legged locomotion: Models, Analyses, and Challenges,” *Society for Industrial and Applied Mathematics*, vol. 48, no. 2, pp. 207–304, 2006.
- [82] S. Hoogendoorn and P. Bovy, “Simulation of pedestrian flows by optimal control and differential games,” *Optimal Control Applications and Methods*, vol. 24, no. 3, pp. 153–172, 2003.
- [83] L. Kaelbling, M. Littman, and A. Moore, “Reinforcement Learning: A Survey,” *J. of Artificial Intelligence Research*, pp. 237–285, 1996.
- [84] S. Kajita, F. Kanehiro, K. Kaneko, K. Yokoi, and H. Hirukawa, “The 3D Linear Inverted Pendulum Mode: A simple modeling for a biped walking pattern generation,” in *Int. Conf. on Intelligent Robots and Systems*, vol. 1, pp. 239–246, 2001.
- [85] T. Kanda, D. Glas, M. Shiomi, H. Ishiguro, and N. Hagita, “Who will be the customer?: a social robot that anticipates people’s behavior from their trajectories,” in *Int. Conf. on Ubiquitous Computing*, pp. 380–389, 2008.
- [86] I. Karamouzas and M. Overmars, “A Velocity-Based Approach for Simulating Human Collision Avoidance,” in *Intelligent Virtual Agents*, vol. 6356 of *Lecture Notes in Computer Science*, pp. 180–186, Springer, 2010.
- [87] I. Karamouzas and M. H. Overmars, “Simulating Human Collision Avoidance Using a Velocity-Based Approach,” *VRIPHYS*, vol. 10, pp. 125–134, 2010.
- [88] Y. Kato, T. Kanda, and H. Ishiguro, “May I Help You?: Design of Human-like Polite Approaching Behavior,” in *Int. Conf. on Human-Robot Interaction*, pp. 35–42, 2015.
- [89] J. Kessler, C. Schröter, and H.-M. Gross, “Approaching a Person in a Socially Acceptable Manner Using a Fast Marching Planner,” in *Int. Conf. on Intelligent Robotics and Applications*, pp. 368–377, 2011.
- [90] E. Keogh and M. Pazzani, “Scaling up dynamic time warping for datamining applications,” in *Int. Conf. on Knowledge Discovery and Data Mining*, pp. 285–289, 2000.
- [91] B. Kim and J. Pineau, “Socially Adaptive Path Planning in Human Environments Using Inverse Reinforcement Learning,” *Int. J. of Social Robotics*, vol. 8, no. 1, pp. 51–66, 2015.

-
- [92] R. Kirby, R. Simmons, and J. Forlizzi, “Companion: A constraint-optimizing method for person-acceptable navigation,” in *Int. Symp. on Robot and Human Interactive Communication*, pp. 607–612, 2009.
- [93] N. Kirchner and A. Alempijevic, “A Robot Centric Perspective on the HRI Paradigm,” *Human-Robot Interaction*, vol. 1, no. 2, pp. 135–157, 2012.
- [94] H. Ko and N. Badler, “Animating human locomotion with inverse dynamics,” *Computer Graphics and Applications*, vol. 16, no. 2, pp. 50–59, 1996.
- [95] K. Koay, M. Walters, and K. Dautenhahn, “Methodological Issues using a Comfort Level Device in Human-Robot Interactions,” in *Int. Workshop on Robot and Human Interactive Communication*, pp. 359–364, 2005.
- [96] K. Koay, K. Dautenhahn, S. Woods, and M. Walters, “Empirical Results from using a Comfort Level Device in Human-Robot Interaction Studies,” in *Int. Conf. on Human-Robot Interaction*, pp. 194–201, 2006.
- [97] K. Koay, D. Syrdal, M. Ashgari-Oskoei, M. L. Walters, and K. Dautenhahn, “Social Roles and Baseline Proxemic Preferences for a Domestic Service Robot,” *Int. J. of Social Robotics*, vol. 6, no. 4, pp. 469–488, 2014.
- [98] Y. Kanayama, Y. Kimura, M. F., and T. Noguchi, “A Stable Tracking Control Method for an Autonomous Mobile Robot,” in *Int. Conf. on Robotics and Automation*, pp. 384–389, 1990.
- [99] M. van Kreveld and J. Luo, “The definition and computation of trajectory and sub-trajectory similarity,” in *Int. Symp. on Advances in Geographic Information Systems*, p. 44, 2007.
- [100] T. Kruse, P. Basili, S. Glasauer, and A. Kirsch, “Legible Robot Navigation in the Proximity of Moving Humans,” in *Int. Workshop on Advanced Robotics and its Social Impacts*, pp. 83–88, 2012.
- [101] T. Kruse, A. Kirsch, H. Khambhaita, and R. Alami, “Evaluating Directional Cost Models in Navigation,” in *Int. Conf. on Human-Robot Interaction*, pp. 350–357, 2014.
- [102] M. Kuderer, H. Kretschmar, C. Sprunk, and W. Burgard, “Feature-Based Prediction of Trajectories for Socially Compliant Navigation,” in *Robotics: Science and Systems*, pp. 193 – 200, 2012.
- [103] D. Kulic, C. Ott, D. Lee, J. Ishikawa, and Y. Nakamura, “Incremental Learning of Full Body Motion Primitives and their Sequencing through Human Motion Observation,” *J. of Robotics Research*, vol. 31, no. 3, pp. 330–345, 2012.
- [104] L. Lammer, A. Huber, A. Weiss, and M. Vincze, “Mutual Care: How older adults react when they should help their care robot,” in *Int. Symp. on New Frontiers in Human Robot Interaction - AISB*, pp. 69–76, Goldsmiths, University of London, UK, 2014.

- [105] S. Lefèvre, D. Vasquez, and C. Laugier, “A survey on motion prediction and risk assessment for intelligent vehicles,” *Robomech J.*, vol. 1, no. 1, pp. 1–14, 2014.
- [106] Z. Li, J. Deng, R. Lu, Y. Xu, J. Bai, and C.-Y. Su, “Trajectory-tracking control of mobile robot systems incorporating neural-dynamic optimized model predictive approach,” *Trans. on Systems, Man, and Cybernetics: Systems*, vol. PP, no. 99, p. 1, 2015.
- [107] Z. Li, H. Xiao, C. Yang, and Y. Zhao, “Model predictive control of nonholonomic chained systems using general projection neural networks optimization,” *Trans. on Systems, Man, and Cybernetics: Systems*, vol. 45, no. 10, pp. 1313–1321, 2015.
- [108] C. Lichtenthäler, T. Lorenz, and A. Kirsch, “Towards a legibility metric: How to measure the perceived value of a robot,” *ICSR Work-In-Progress-Track*, 2011.
- [109] C. Lichtenthäler, T. Lorenz, M. Karg, and A. Kirsch, “Increasing perceived value between human and robots – Measuring legibility in human aware navigation,” in *Workshop on Advanced Robotics and its Social Impacts*, pp. 89–94, 2012.
- [110] C. Lichtenthäler, T. Lorenz, and A. Kirsch, “Influence of legibility on perceived safety in a virtual human-robot path crossing task,” in *Int. Symp. on Robot and Human Interactive Communication*, pp. 676–681, 2012.
- [111] C. Lichtenthäler and A. Kirsch, “Towards Legible Robot Navigation – How to Increase the Intend Expressiveness of Robot Navigation Behavior,” *ICSR*, 2013.
- [112] L. Ljung, *System Identification*. Springer, 1998.
- [113] S. Lallée, U. Pattacini, S. Lemaignan, A. Lenz, C. Melhuish, L. Natale, S. Skachek, K. Hamann, J. Steinwender, E. A. Sisbot, *et al.*, “Towards a platform-independent cooperative human robot interaction system: III an architecture for learning and executing actions and shared plans,” *Trans. on Autonomous Mental Development*, vol. 4, no. 3, pp. 239–253, 2012.
- [114] J.-C. Latombe, *Robot Motion Planning*. Kluwer Academic Publishers, 1991.
- [115] S. M. LaValle, *Planning Algorithms*. Cambridge University Press, 2006.
- [116] R. McGill, J. W. Tukey, and W. A. Larsen, “Variations of Box Plots,” *The American Statistician*, vol. 32, no. 1, pp. 12–16, 1978.
- [117] R. McNeill Alexander, “Energetics and optimization of human walking and running: the 2000 Raymond Pearl memorial lecture,” *Human Biology*, vol. 14, no. 5, pp. 641–648, 2002.
- [118] E. Masehian and Y. Katebi, “Robot Motion Planning in Dynamic Environments with Moving Obstacles and Target,” 2007.

-
- [119] G. Michalos, S. Makris, J. Spiliotopoulos, I. Misios, P. Tsarouchi, and G. Chrysolouris, “ROBO-PARTNER: Seamless Human-Robot Cooperation for Intelligent, Flexible and Safe Operations in the Assembly Factories of the Future,” *Procedia CIRP*, vol. 23, pp. 71–76, 2014.
- [120] N. Mirnig, E. Strasser, A. Weiss, and T. M., “Studies in public places as a means to positively influence people’s attitude towards robots,” in *Int. Conf. on Social Robotics*, pp. 209–218, 2012.
- [121] K. Mombaur, A. Truong, and J.-P. Laumond, “From Human to Humanoid Locomotion – An Inverse Optimal Control Approach,” *Autonomous Robots*, vol. 28, no. 3, pp. 369–383, 2009.
- [122] Y. Morales, S. Satake, R. Huq, D. Glas, T. Kanda, and N. Hagita, “How do people walk side-by-side?: Using a computational model of human behavior for a social robot,” in *Int. Conf. on Human-Robot Interaction*, pp. 301–308, 2012.
- [123] M. Moussaïd, D. Helbing, and G. Theraulaz, “How simple rules determine pedestrian behavior and crowd disasters,” *National Academy of Sciences*, vol. 108, no. 17, pp. 6884–6888, 2011.
- [124] M. Nanni and D. Pedreschi, “Time-focused clustering of trajectories of moving objects,” *J. of Intelligent Information Systems*, vol. 27, no. 3, pp. 267–289, 2006.
- [125] C. Nass and Y. Moon, “Machines and Mindlessness: Social Responses to Computers,” *Int. J. of Social Issues*, vol. 56, no. 1, pp. 81–103, 2000.
- [126] N. J. Nilsson, “Shakey the Robot,” *SRI Int. Technical Note*, vol. 325, 1984.
- [127] A.-H. Olivier, R. Kulpa, J. Pettré, and A. Crétual, “A Velocity-Curvature Space Approach for Walking Motions Analysis,” in *Motion in Games* (A. Egges, R. Ger-aerts, and M. Overmars, eds.), vol. 5884 of *Lecture Notes in Computer Science*, pp. 104–115, Springer, 2009.
- [128] A.-H. Olivier, A. Marin, A. Crétual, and J. Pettré, “Minimal predicted distance: A common metric for collision avoidance during pairwise interactions between walkers,” *Gait & Posture*, vol. 36, no. 3, pp. 399–404, 2012.
- [129] A.-H. Olivier, A. Marin, A. Crétual, A. Berthoz, and J. Pettré, “Collision avoidance between two walkers: Role-dependent strategies,” *Gait & Posture*, vol. 38, no. 4, pp. 751–756, 2013.
- [130] P. Olson and M. Sivak, “Perception-response time to unexpected roadway hazards,” *Human Factors: The J. of the Human Factors and Ergonomics Society*, vol. 28, no. 1, pp. 91–96, 1986.
- [131] J. Ondřej, J. Pettré, A.-H. Olivier, and S. Donikian, “A synthetic-vision based steering approach for crowd simulation,” *Trans. on Graphics*, vol. 29, no. 4, p. 123, 2010.

- [132] E. Pacchierotti, H. Christensen, and P. Jensfelt, “Evaluation of Passing Distance for Social Robots,” in *Int. Symp. on Robot and Human Interactive Communication*, pp. 315–320, 2006.
- [133] A. K. Pandey and R. Alami, “Towards a sociable robot guide which respects and supports the human activity,” in *Int. Conf. on Automation Science and Engineering*, pp. 262–267, 2009.
- [134] A. K. Pandey, M. Ali, and R. Alami, “A Synthetic-Vision based Steering Approach for Crowd Simulation,” *Int. J. of Social Robotics*, vol. 5, no. 2, pp. 215–236, 2013.
- [135] A. V. Papadopoulos, L. Bascetta, and G. Ferretti, “Generation of Human Walking Paths,” in *Int. Conf. on Intelligent Robots and Systems*, pp. 1676–1681, 2013.
- [136] A. V. Papadopoulos, L. Bascetta, and G. Ferretti, “A Comparative Evaluation of Human Motion Planning Policies,” in *IFAC World Congress*, 2014.
- [137] M. Papageorgiou, M. Leibold (Sobotka), and M. Buss, *Optimierung: Statische, dynamische, stochastische Verfahren für die Anwendung*. Springer Vieweg, 2012.
- [138] S. Paris, J. Pettr, and S. Donikian, “Pedestrian reactive navigation for crowd simulation: a predictive approach,” *Computer Graphics Forum*, vol. 26, no. 3, pp. 665–674, 2007.
- [139] A. E. Patla and J. N. Vickers, “How far ahead do we look when required to step on specific locations in the travel path during locomotion?,” *Experimental Brain Research*, vol. 148, no. 1, pp. 133–138, 2003.
- [140] S. Pellegrini, A. Ess, K. Schindler, and L. Van Gool, “You’ll never walk alone: Modeling social behavior for multi-target tracking,” in *Int. Conf. on Computer Vision*, pp. 261–268, 2009.
- [141] J. Pettré, J. Ondrej, A.-H. Olivier, . Crtual, and S. Donikian, “Experiment-based modeling, simulation and validation of interactions between virtual walkers,” in *Eurographics Symp. on Computer Animation*, 2009.
- [142] Q.-C. Pham and H. Hicheur, “On the open-loop and feedback processes that underlie the formation of trajectories during visual and nonvisual locomotion in humans,” *J. of Neurophysiology*, vol. 102, no. 5, pp. 2800–2815, 2009.
- [143] E. Prassler, J. Scholz, and P. Fiorini, “Navigating a robotic wheelchair in a railway station during rush hour,” *Int. J. of Robotics Research*, vol. 18, no. 7, pp. 711–727, 1999.
- [144] A.-S. Puydupin-Jamin, M. Johnson, and T. Bretl, “A convex approach to inverse optimal control and its application to modeling human locomotion,” in *Int. Conf. on Robotics and Automation*, pp. 531–536, 2012.
- [145] C. E. Rasmussen and C. K. I. Williams, *Gaussian Processes for Machine Learning*. The MIT Press, 2006.

-
- [146] C. A. Ratanamahatana, J. Lin, D. Gunopulos, E. Keogh, M. Vlachos, and G. Das, *Mining Time Series Data*, pp. 1049–1077. Springer, 2010.
- [147] B. Reeves and C. Nass, *The Media Equation: How People Treat Computers, Television, and New Media Like Real People and Places*. Cambridge University Press, 1996.
- [148] B. D. Reich, “An architecture for behavioral locomotion,” *IRCS Technical Reports Series*, p. 51, 1997.
- [149] J. Rios-Martinez, A. Spalanzani, and C. Laugier, “From Proxemics Theory to Socially-Aware Navigation: A Survey,” *Int. J. of Social Robotics*, vol. 7, no. 2, pp. 137–153, 2015.
- [150] M. Rau, *Nichtlineare modellbasierte prädiktive Regelung auf Basis lernfähiger Zustandsraummodelle*. PhD thesis, Technische Universität München, 2003.
- [151] C. Reynolds, “Steering behaviors for autonomous characters,” in *Game Developers Conference*, pp. 763–782, 1999.
- [152] P. Ruijten, “On the Perceived Human-likeness of Virtual Health Agents: Towards a Generalized Measurement of Anthropomorphism,” in *Intelligent Virtual Agents – Workshop on Virtual Health Agents, At Delft*, 2015.
- [153] S. Satake, T. Kanda, D. Glas, M. Imai, H. Ishiguro, and N. Hagita, “How to approach humans? - Strategies for Social Robots to Initiate Interaction,” in *Int. Conf. on Human-Robot Interaction*, pp. 109–116, 2009.
- [154] D. Schulz, W. Burgard, D. Fox, and A. Cremers, “Tracking multiple moving targets with a mobile robot using particle filters and statistical data association,” in *Int. Conf. on Robotics and Automation*, vol. 2, pp. 1665–1670, 2001.
- [155] Z. Shiller, O. Gal, and A. Raz, “Adaptive time horizon for on-line avoidance in dynamic environments,” in *Int. Conf. on Intelligent Robots and Systems*, pp. 3539–3544, 2011.
- [156] M. Shiomi, T. Kanda, D. Glas, S. Satake, H. Ishiguro, and N. Hagita, “Who will be the customer?: A social robot that anticipates people’s behavior from their trajectories. Field Trial of Networked Social Robots in a Shopping Mall,” in *Int. Conf. on Intelligent Robots and Systems*, pp. 2846–2853, 2009.
- [157] M. Shiomi, F. Zanlungo, K. Hayashi, and T. Kanda, “Towards a Socially Acceptable Collision Avoidance for a Mobile Robot Navigating Among Pedestrians Using a Pedestrian Model,” *Int. J. of Social Robotics*, vol. 6, no. 3, pp. 443–455, 2014.
- [158] E. Sisbot, R. Alami, T. Simeon, K. Dautenhahn, M. Walters, S. Woods, K. L. Koay, and C. Nehaniv, “Navigation in the Presence of Humans,” in *Int. Conf. on Humanoid Robots*, pp. 181–188, 2005.

- [159] E. Sisbot, L. Marin-Urias, R. Alami, and T. Simeon, “A human aware mobile robot motion planner,” *Transactions on Robotics*, vol. 23, no. 5, pp. 874–883, 2007.
- [160] E. Sisbot, L. Marin-Urias, X. Broquere, D. Sidobre, and R. Alami, “Synthesizing Robot Motions Adapted to Human Presence,” *Int. J. of Social Robotics*, vol. 2, pp. 329–343, 2010.
- [161] R. Sobel and N. Lillith, “Determinant of Nonstationary Personal Space Invasion,” *J. of Psychology*, vol. 97, pp. 39–45, 1975.
- [162] R. Sommer, *Personal Space. The Behavioral Basis of Design*. Prentice-Hall, Englewood Cliffs, 1969.
- [163] W. Sparrow and K. Newell, “Metabolic energy expenditure and the regulation of movement economy,” *Psychonomic Bulletin & Review*, vol. 5, no. 2, pp. 173–196, 1998.
- [164] D. Storti and R. Rand, “Dynamics of two strongly coupled van der Pol oscillators,” *Int. J. of Non-Linear Mechanics*, vol. 17, no. 3, pp. 143–152, 1982.
- [165] S. Stuart, L. Alcock, B. Galna, S. Lord, and L. Rochester, “Re-test Reliability and Accuracy of the Dikablis Eye-Tracker when Sitting, Standing and Walking,” in *World Congress of the Int. Society of Posture and Gait Research*, 2014.
- [166] J. Su, S. Kurtek, E. Klassen, and A. Srivastava, “Statistical Analysis of Trajectories on Riemannian Manifolds: Bird Migration, Hurricane Tracking and Video Surveillance,” *The Annals of Applied Statistics*, vol. 8, no. 1, pp. 530–552, 2014.
- [167] A. Sutcliffe, J. Pineau, and D. Grollman, “Rephrasing the Problem of Robotic Social Navigation,” in *Int. Conf. on Intelligent Robots and Systems*, 2014.
- [168] M. Svenstrup, S. Tranberg, H. Andersen, and T. Bak, “Pose Estimation and Adaptive Robot Behaviour for Human-Robot Interaction,” in *Int. Conf. on Robotics and Automation*, pp. 3571–3576, 2009.
- [169] G. Taga, “A model of the neuro-musculo-skeletal system for human locomotion,” *Biological cybernetics*, vol. 73, no. 2, pp. 97–111, 1995.
- [170] L. Takayama, D. Dooley, and W. Ju, “Expressing Thought: Improving Robot Readability with Animation Principles,” in *Int. Conf. on Human-Robot Interaction*, pp. 69–76, 2011.
- [171] B. Tasthan and G. Sukthankar, “Leveraging human behavior models to predict paths in indoor environments,” *Pervasive and Mobile Computing*, vol. 7, no. 3, pp. 319–330, 2011.
- [172] S. Thompson, T. Horiuchi, and S. Kagami, “A probabilistic model of human motion and navigation intent for mobile robot path planning,” in *Int. Conf. on Autonomous Robots and Agents*, pp. 663–668, 2009.

-
- [173] E. Torta, R. Cuijpers, and J. Juola, “Design of a parametric model of personal space for robotic social navigation,” *Int. J. of Social Robotics*, vol. 5, no. 3, pp. 357–365, 2013.
- [174] P. Trautman and A. Krause, “Unfreezing the Robot: Navigation in Dense, Interacting Crowds,” in *Int. Conf. on Intelligent Robots and Systems*, 2010.
- [175] P. Trautman, *Robot navigation in dense crowds: Statistical models and experimental studies of human robot cooperation*. PhD thesis, California Institute of Technology, 2013.
- [176] A. Turnwald, W. Olszowy, D. Wollherr, and M. Buss, “Interactive Navigation of Humans from a Game Theoretic Perspective,” in *Int. Conf. on Intelligent Robots and Systems*, pp. 703–708, 2014.
- [177] A. Turnwald, D. Althoff, D. Wollherr, and M. Buss, “Understanding Human Avoidance Behavior: Interaction-Aware Decision Making Based on Game Theory,” *Int. J. of Social Robotics*, vol. 8, no. 2, pp. 331–351, 2016.
- [178] S. Vieilledent, Y. Kerlirzin, S. Dalbera, and A. Berthoz, “Relationship between velocity and curvature of a human locomotor trajectory,” *Neuroscience Letters*, vol. 305, no. 1, pp. 65–69, 2001.
- [179] M. Vlachos, G. Kollios, and D. Gunopulos, “Discovering similar multidimensional trajectories,” in *Int. Conf. on Data Engineering*, pp. 673–684, 2002.
- [180] M. Walters, K. Dautenhahn, K. Koay, C. Kaouri, R. Boekhorst, C. Nehaniv, I. Werry, and D. Lee, “Close Encounters: Spatial Distances between People and a Robot of Mechanistic Appearance,” in *Int. Conf. on Humanoid Robots*, pp. 450–455, 2005.
- [181] M. Walters, K. Koay, S. Woods, D. Syrdal, and K. Dautenhahn, “Robot to Human Approaches: Preliminary Results on Comfortable Distances and Preferences,” in *AAAI Symp. on Multidisciplinary Collaborative Socially Assistive Robots*, 2007.
- [182] C. Weinrich, M. Volkhardt, E. Einhorn, and H.-M. Gross, “Prediction of human collision avoidance behavior by lifelong learning for socially compliant robot navigation,” in *Int. Conf. on Robotics and Automation*, pp. 376–381, 2013.
- [183] R. M. Wilkie, J. P. Wann, and R. S. Allison, “Active gaze, visual look-ahead, and locomotor control,” *Journal of Experimental Psychology: Human Perception and Performance*, vol. 34, no. 5, p. 1150, 2008.
- [184] D. Wilkie, J. Van Den Berg, and D. Manocha, “Generalized Velocity Obstacles,” in *Int. Conf. on Intelligent Robots and Systems*, pp. 5573–5578, 2009.
- [185] M. Wolff, “Notes on the behaviour of pedestrians,” in *People in Places: The Sociology of the Familiar*, pp. 35–48, Praeger, New York, 1973.
- [186] N. Wolfinger, “Passing Moments: Some Social Dynamics of Pedestrian Interaction,” *J. of Contemporary Ethnography*, vol. 24, no. 3, pp. 323–340, 1995.

- [187] H. J. Woo, S. B. Park, and J. H. Kim, “Research of the optimal path planning methods for unmanned ground vehicle in DARPA Urban Challenge,” in *Int. Conf. on Control, Automation and Systems, 2008*, pp. 586–589, 2008.
- [188] S. Woods, M. Walters, K. Koay, and K. Dautenhahn, “Methodological Issues in HRI: A Comparison of Live and Video-based Methods in Robot to Human Approach Direction Trials,” in *Int. Symp. on Robot and Human Interactive Communication*, pp. 51–58, 2006.
- [189] S. J. Wright and J. Nocedal, *Numerical Optimization*, vol. 2. Springer New York, 1999.
- [190] Y. Xiong and D.-Y. Yeung, “Mixtures of ARMA models for model-based time series clustering,” in *Int. Conf. on Data Mining*, pp. 717–720, 2002.
- [191] E. Zehr and J. Duysens, “Regulation of arm and leg movement during human locomotion,” *The Neuroscientist*, vol. 10, no. 4, pp. 347–361, 2004.
- [192] M. Zhao, R. Shome, I. Yochelson, K. Bekris, and E. Kowler, “An Experimental Study for Identifying Features of Legible Manipulator Paths,” in *Int. Symp. on Experimental Robotics*, 2014.
- [193] B. D. Ziebart, N. Ratliff, G. Gallagher, C. Mertz, K. Peterson, J. A. Bagnell, M. Hebert, A. K. Dey, and S. Srinivasa, “Planning-based Prediction for Pedestrians,” in *Int. Conf. on Intelligent Robotics and Systems*, pp. 3931–3936, 2009.
- [194] T. Zielińska, “Coupled oscillators utilised as gait rhythm generators of a two-legged walking machine,” *Biological Cybernetics*, vol. 74, no. 3, pp. 263–273, 1996.
- [195] Z. Zhang, K. Huang, and T. Tan, “Comparison of similarity measures for trajectory clustering in outdoor surveillance scenes,” in *Int. Conf. on Pattern Recognition*, vol. 3, pp. 1135–1138, 2006.